Groundwater - surface water interactions on deeply weathered surfaces of low relief in the Upper Nile Basin of Uganda

Michael Owor

Presented for the degree of Doctor of Philosophy in the University College London

Department of Geography, University College London

March 2010

Declaration of authenticity

I, **Michael Owor**, confirm that the work presented in this thesis is my own. Where information has been derived from other sources, I confirm that this has been indicated in the thesis.

Abstract

Little is known of the interactions between groundwater and surface water on the deeply weathered surfaces of low relief in the Great Lakes Region of Africa (GLRA). The role of groundwater in sustaining water levels in lakes, rivers and wetlands during periods of absent rainfall is also unclear. Indeed, groundwater is commonly excluded from estimations of the surface water balances. Piezometer nests constructed on the shores of Lakes Victoria (Jinja, Entebbe) and Kyoga (Bugondo) through this study, provide the first evidence of the lithologic interface and dynamic interactions between groundwater and surface water in the GLRA. Evidence is drawn from lithological analyses (texture, lithostratigraphy), geophysical surveys (resistivity mapping, VES), hydraulic tests, borehole hydrographs and hydrochemical (major ions, δ^2H, $\delta^{18}O$) data. Groundwater interacts with surface waters primarily via preferential pathways within the coarse horizons towards the base of thick saprolite underlying relatively thin (<5 m) fluvial-lacustrine sands. Hydrological observations and hydrochemical data indicate that groundwater flows primarily into lakes; this interaction is dynamic varying by season and proximity to lake. Interactions between groundwater and Lakes Victoria and Kyoga are also influenced by changing drainage base (lake) levels that are controlled, in part, by regional, rather than local climatology and dam releases from Lake Victoria (Jinja). Groundwater levels are strongly influenced by rainfall-fed recharge that depend more upon heavy rainfall events (10 $mm \cdot d^{-1}$) during the monsoons than the total volume of rainfall; mean vertical velocities in the unsaturated zone are ~1 $m \cdot d^{-1}$. Layered heterogeneity in aquifer properties (hydraulic conductivity, storage) indicate deeply weathered rocks formed under prolonged *in situ* weathering (etchplanation) of low-relief surfaces. This layered heterogeneity in the saprolite aquifer gives rise to a two-component recession in borehole hydrographs following recharge events. A first-approximation of the proportion of the Lake Victoria's water balance supplied by groundwater is derived from new observations in this study and is in the order of 1 %.

Acknowledgements

I do gratefully acknowledge several organisations that have made this study possible. The Commonwealth Scholarship Programme (UGCA-2006-141) funded the research study at University College London. The fieldwork was supported by the International Foundation for Science (W3428-2); University of London Central Research Fund (AR/CRF/B); University College London Graduate School Research Projects Fund (1H1324); Dudley Stamp Memorial Fund; and the Department of Geography, UCL. The Directorate of Water Resources Management, Uganda (DWRM) provided access to data and logistical support during fieldwork. Makerere University granted leave of absence for study, and the Department of Geology provided field equipment, office and laboratory space during the fieldwork.

I thank all the organisations that accepted to host the field stations, namely: Uganda Railways Corporation (URC) through the Rift Valley Railways Uganda Ltd., the National Fisheries Research Institute, Jinja (NaFIRI), and the Fisheries Department, Soroti. Appreciation is extended to the local council authorities at Jinja and Bugondo for the security provided to the stations.

My sincere appreciation and gratitude go to Dr. Richard Taylor for conceiving the initiative for this research study, and for all the invaluable discussions we had, as well as the social support to make my stay in London eventful and memorable. Equally appreciated are all the guidance and time from my second supervisor Dr. Julian Thompson for making this study a success. Dr. Callist Tindimugaya facilitated and was instrumental in all the collaboration we had with the DWRM, Entebbe; Prof. Tim Atkinson for helping out with the chemical isotopic analyses.

I am grateful to Christine Mukwaya for all the help with the station permissions, data, and field logistics, and to the rest of the staff at DWRM who have helped out. Rashid Kisomoze for providing the equipment and time for the geoelectrical resistivity surveys; my field assistants and gauge readers, George Manyatta in Jinja, and Stephenson Oonyu in Bugondo for jobs well done, field staff provided and for ensuring the security of the stations and divers installed in them; James Wakyaya from the Department of Geology, Makerere University for helping out with the field and laboratory work.

I am thankful to Graham for helping out with the hydraulic tests. My appreciation also go to Shams, Lucinda, Daniel, Hoque, Becks, Raj and all the rest of the Water and Climate group at UCL for all the interactions; Janet, Tula and Ian for all the help in the laboratory at the Department of Geography, UCL.

I appreciate all the assistance from Drs. Erasmus Barifaijo and John Tiberindwa; my thanks also go to all my colleagues at the Department of Geology, Makerere University for helping out during my absence.

Finally but not least, to my family for always being there for me, I dedicate this work to you all.

Table of Contents

List of Figures

List of Tables

Chapter 1
Introduction

1.1 Groundwater - surface water interactions

Groundwater is hydraulically connected to surface waters in many regions of the world and an understanding of this interaction is fundamental to effective water resource management (Winter *et al.*, 1998; Sophocleous, 2002; Brodie *et al.*, 2007). The interaction between groundwater and surface waters influences key characteristics of aquatic environments, including the stability of water levels and water quality (Winter *et al.*, 1998). Interactions between groundwater and surface water are complex both in time and space, and are influenced by not only climate, landform, geology, and biotic factors but also human activities (Sophocleous, 2002). Interactions can occur through a range of spatial scales which include local, intermediate and regional groundwater flow regimes (Tóth, 1963). McBride and Pfannkuch (1975) observe that within isotropic and homogenous porous interface media, fluxes between surface waters and groundwater decrease exponentially with distance from the shoreline. As water moves between groundwater and surface water, important pathways for chemical transfer between terrestrial and aquatic systems exist. Repeated exchanges between surface waters and groundwater increase the contact times between the water and chemically reactive geologic materials. Additionally, the fibrous rooted vegetation in wetlands induces uptake resulting in significant interchange between surface water and pore water in the upper soil zone of wetland sediments even when there is restricted exchange at the base of the sediments (Winter *et al.*, 1998; 1999).

Worldwide, there are several examples where interactions between groundwater and surface water bodies have played a critical role in influencing surface water levels

and, by extension, lake-water balances. Within tropical Africa, this connection between groundwater and surface water has had the most considerable influence on the availability of water resources in the Lake Chad basin. The Lake Chad basin (ca. 2.3 million km^2) in the central Sahel supports the livelihoods of a population of more than 15 million over 8 countries (Cameroon, Chad, Niger, Nigeria, Central African Republic, Libya, Algeria and Sudan). Lake levels have fallen by 4 m and the area of the lake's surface has shrunk from 25,000 km^2 in the 1960s to less than 3,000 km^2 as a result primarily of rainfall deficits in the catchments supplying river flow to Lake Chad (Ngatcha *et al.*, 2008). Over 90 % of the lake's inflow derives from river discharge. Underlying the lake is a regional Quaternary aquifer composed of sandy, deltaic and lacustrine deposits with a thickness of up to 100 m close to the lake. Lake Chad is a closed basin and it is estimated that nearly 18 % of the annual water inflows leave the lake to recharge the Quaternary aquifer system (Isiorho and Matisoff, 1990). The groundwater reservoir is therefore the second largest recipient of water from Lake Chad after the atmosphere but the main repository of salt accumulation through evaporation.

The Aral Sea, an endorheic basin in Central Asia (shared by Kazakhstan and Uzbekistan) was once the world's fourth largest lake. Between 1960 and 1987, water levels fell by almost 13 m and the lake's area decreased by 40 % due to changes in climate and withdrawals of surface water for irrigation (Micklin, 1988; Jarsjö and Destouni, 2004). Associated with this change, Jarsjö and Destouni (2004) estimate groundwater inputs to Aral Sea rose as a fraction of river inflows from ~12 % in 1960 to ~100 % today (in 2004). The contribution of groundwater to other lakes in Eurasia is estimated to be ~2 % (Lakes Baikal), ~0.5 % (Balkhash) and ~30-40 % (Issyk-Kul), and ~1 % (Caspian Sea) (Zekster, 1996). Within the Great Lakes Region of North America, Grannemann *et al.* (2000) estimate that groundwater directly and indirectly contributes about 80 % of the total inflows to Lake Michigan.

1.2 Groundwater-surface water interactions in the Upper Nile Basin

Low relief (plateau) surfaces of the GLRA feature extensive areas of shallow, open surface water and both permanent and seasonal wetlands. These surface waters are particularly prominent in Uganda where Lakes Victoria and Kyoga feature wetlands (Fig. 1.1) that occupy about 18 % of the nation's land area (NWP, 2008). Regionally, surface waters provide vital developmental (e.g. hydro-electric power generation, water supply), ecological (e.g. aquatic ecosystems) and socio-economic (e.g. fishery) services (Chatterjee *et al.*; 1998; Bugenyi, 2001; Mwanja, 2004). Wetlands in the GLRA furthermore, control floods and reduce nutrient loading to adjacent surface waters (Gambrell, 1994; Balirwa, 1995; Kansiime *et al.*, 2003; Mwanuzi *et al.*, 2003; Uluocha and Okeke, 2004). The role of wetlands as geochemical barriers to the influx of elevated concentrations of aqueous and suspended contaminants (e.g. nutrients, heavy metals) to adjacent surface water bodies requires, however, further investigation (Owor *et al.*, 2007).

Changes in land use in the Lake Victoria region have occurred over the past three decades in response to population growth and rise in both commercial and subsistence agriculture (Odada *et al.*, 2004). For example, recent reports conducted on the northwestern shore of Lake Victoria reveal massive growths of blue-green algal blooms at Kitubulu Bay near Entebbe (Daily Monitor, 2007). The source of these nutrients is uncertain but has been attributed to a range of activities including deforestation, fish processing, floriculture and domestic (municipal) effluent on the lake's shores (e.g. Mwanuzi *et al.*, 2003; Kansiime *et al.*, 2003; Odada *et al.*, 2004).

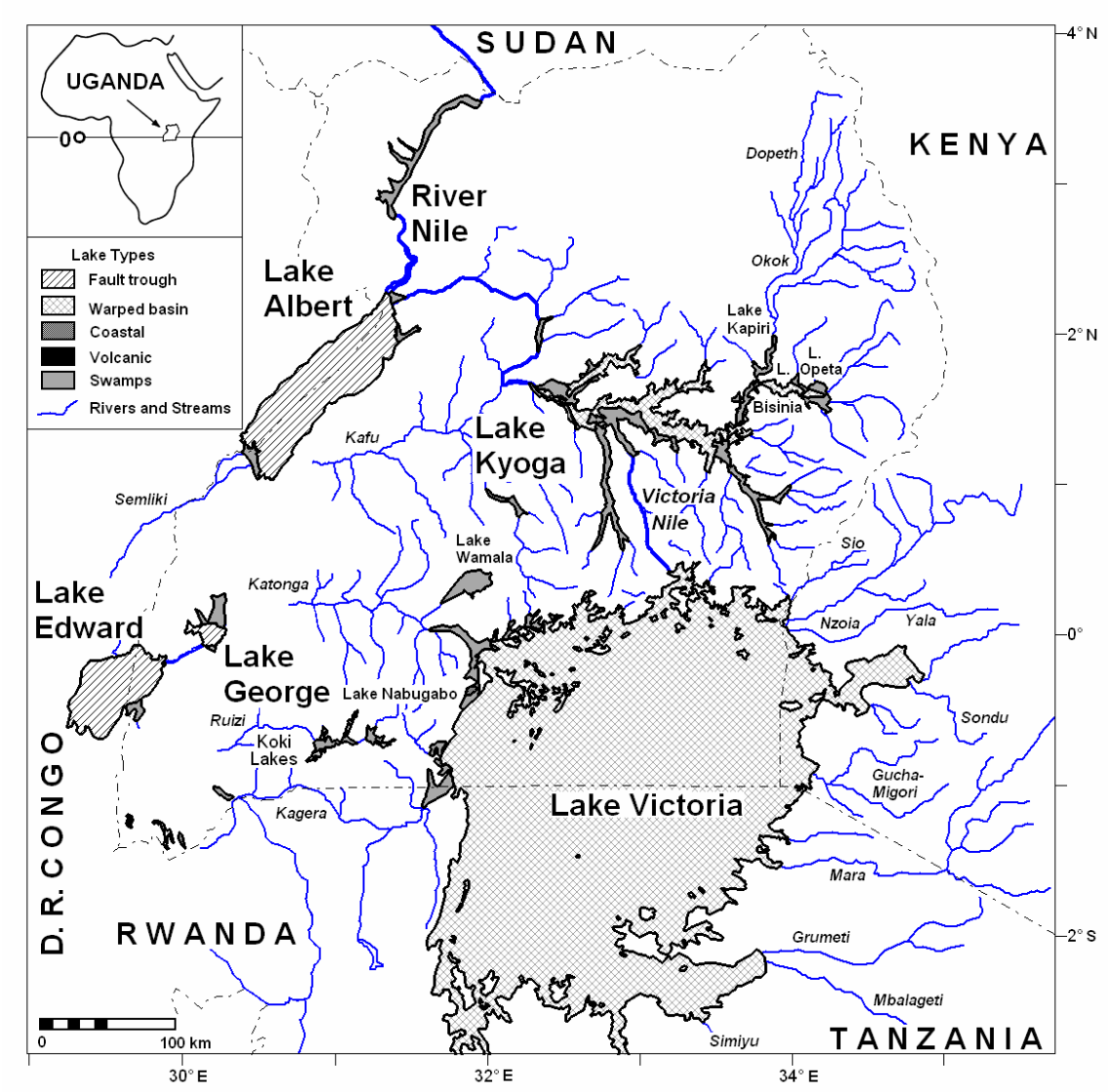

Figure 1.1 Map of the basins for Lakes Victoria and Kyoga (modified from Temple, 1970).

Water-balance studies in the Upper Nile Basin highlight the dominance of the direct input of rainfall in sustaining water levels in wetlands and surface waters (Kite, 1982, 1984; Piper *et al.*, 1986; Sene and Plinston, 1994; Yin and Nicholson, 1998; Yates, 1998; Nicholson *et al.*, 2000; Sene, 2000; Nicholson and Yin, 2001; Sene *et al.*, 2001; Tate *et al.*, 2004). Climate variability and change are therefore expected to strongly influence the balance between precipitation and evapotranspiration and consequently the depth and areal extent of shallow lakes and wetlands in the Upper Nile Basin. The role of groundwater in maintaining lake and wetland water levels during

periods of low or absent rainfall on the African plateau is unknown. Indeed, except for Swenson and Wahr (2009), all water balance studies of Lake Victoria (e.g. Kite, 1982; Piper *et al.*, 1986; Sene and Plinston, 1994; Nicholson and Yin, 2001; LVBC, 2006) and Lake Kyoga (e.g. Sutcliffe and Parks, 1999; Okonga, 2000; ILM, 2004) have, to date, either ignored the contribution of groundwater or assumed it was negligible. Neither a conceptual nor a numerical representation of the interaction between surface water and groundwater exists in the region (Taylor and Tindimugaya, 1996). Although there have been substantial changes in the level of Lake Victoria during the early 1960s and more recently (2004-2006), the interaction between groundwater and surface water in response to these extreme events remains unassessed and unclear.

Flow between groundwater and surface water transports solutes and contaminants (e.g. microorganisms, non-aqueous phase liquids) between these reservoirs. The role of these fluxes in determining the quality of groundwater and surface water in the GLRA remains unclear. Groundwater chemistry in weathered crystalline aquifers underlying the Upper Nile Basin is dominated by Ca^{2+}, Na^{+} and HCO_3^{-} and commonly features undesirable concentrations of some metals (e.g. Al, Fe) that derive from *in situ* weathering processes (Taylor *et al.*, 2004). In Uganda, groundwater abstraction is increasing as a result of rapid urbanisation in peri-urban environments and the inadequacy of centralised, surface water-fed water supplies. As it is common for domestic and municipal wastes to be neither collected nor properly managed, indiscriminate dumping of wastes constitutes an immediate risk to human health and quality of groundwater (Biryabarema, 2001; Howard *et al.*, 2003; Taylor *et al.*, 2009a). Heavy rainfall events, particularly the monsoons, have been observed to mobilise surficial contaminants into the weathered shallow aquifer system along preferential pathways (Taylor *et al.*, 2009b).

The low relief surface ("African surface") upon which surface waters reside in the GLRA derives from the long-term geomorphic evolution of the landscape and its associated drainage (McFarlane, 1976; Taylor and Howard, 1998). Rift-related, tectonic processes since at least the early Miocene are considered to have shaped the present landscape of the GLRA and strongly influenced surface hydrology (Doornkamp and Temple, 1966; Doornkamp, 1968; de Swardt and Trendall, 1969; Taylor and Howard, 1998; Trauth *et al.*, 2005). Indeed, the deeply weathered landscape has largely been shaped by the action of meteoric waters. There is, however, still no consensus about how their physiographic properties interact with those of the surrounding interfluves (von der Heyden, 2004) and thereby influence the interaction between groundwater and surface water.

1.3 Aim of study

As this study is the first to investigate the interaction between groundwater and surface waters in the Upper Nile Basin of East Africa, the overall aim of this doctoral thesis is:

to improve understanding of the interactions between groundwater and surface water on the highly weathered surfaces of low relief ("African surface") in the Great Lakes Region of Africa.

Specific research objectives include:

i) ***to characterise the lithological interface between groundwater and surface waters of Lakes Victoria and Kyoga;***

ii) ***to relate the observed interface to models of the evolution of landscape and drainage in the GLRA;***

iii) ***to assess how rainfall and dam operations influence the observed***

interaction between groundwater and surface waters in time and space; and,

iv) to quantify the hydrological fluxes between groundwater and surface water.

This research tests two operational hypotheses:

i) a temporally and spatially dynamic interaction exists between groundwater and surface waters; and

ii) groundwater contributes to the maintenance of surface water levels during dry periods.

1.4 Study design

The overall exploratory research strategy involves (i) a review of historical and current datasets; (ii) an exploratory investigation of the lithological interface between groundwater and surface water involving surface geophysics, lithologic analyses, nested piezometer construction, and chemical and isotopic analyses; and (iii) monitoring hydraulic responses of groundwater and surface water to groundwater abstraction, climate variability and dam operations.

1.4.1 Review of historical and current datasets

The analysis of existing datasets includes: (1) a network of surface water and groundwater monitoring stations proximate to Lakes Victoria and Kyoga and within the Upper Nile Basin, (2) satellite measurements of terrestrial total water storage variations using gravity anomalies (GRACE), Chambers (2006), (3) borehole logs contained in the National Groundwater Database (maintained by the Directorate of Water Resources

Management), and (4) hydrological and hydrometeorological data (daily rainfall, river flow, pan evaporation and temperature).

1.4.2 Exploratory surface surveys, drilling, station construction and hydrochemical analyses

Site selection from surface surveys together with lateral and depth relations of the lithology are ascertained from 3 geo-electrical resistivity profiles and 8 vertical electrical soundings. The lithological characteristics and texture (colour and grain size) are determined from 77 drill-bit cuttings and from well logs of 27 exploitation wells (up to 67 mbgl – metres below ground level) located within the vicinity of the study areas (Bugondo, Entebbe and Jinja). Results of the textural analysis of the drill cuttings are in addition used to estimate the hydraulic conductivity and storage of the interface. There are 8 piezometers drilled and installed into lacustrine/fluvial sands and weathered mantle (maximum depths of 48 mbgl). Physico-chemical measurements (pH, temperature and EC) and water (rainfall, lake, wetlands and groundwater) sampling enables the determination of the connectivity between groundwater and surface water using hydrochemistry (major ions and stable isotopes – $\delta^{18}O$ and $\delta^{2}H$). Samples and measurements were taken during monitoring from each piezometer during and after construction, throughout pumping tests, and on bi-monthly intervals.

1.4.3 Monitoring hydraulic responses of groundwater and surface water to groundwater abstraction, climate variability and dam operations

Continuous hourly monitoring of groundwater level and air barometric pressure and temperature variations in the stations is carried out at Bugondo and Jinja (December 2007 – July 2009), and daily measurements in Entebbe (July 1999 – July 2009). Lake levels are collected on a daily basis (January 1998 – July 2009) from the Lakes Victoria

(Entebbe and Jinja) and Kyoga (Bugondo) stations. Daily (since 1998) groundwater level variations from regional monitoring wells (10) in weathered crystalline basement aquifers are also analysed. Hydrogeological parameters are obtained from pumping tests on 6 piezometers (Bugondo and Jinja). Daily dam releases of Lake Victoria at the Jinja outlet are analysed from January 1999 to September 2009.

1.4.4 Conceptual framework

Assessments of the interactions between surface water and groundwater commonly employ a wide range of methods (Winter *et al.*, 1998; Sophocleous, 2002; Hayashi and Rosenberry, 2002; Kalbus *et al.*, 2006; Brodie *et al.*, 2007). These include: hydrographic analysis, hydrogeological mapping, modelling, ecological indicators, field indicators (e.g. springs), artificial tracers, geophysics and remote sensing, hydrochemistry and environmental tracers, hydrometrics, seepage measurements, temperature monitoring, and water budgets. Brodie *et al.* (2007) note that simple methods (e.g. field observations, chemical surveys or stream flow measurements) provide a catchment-scale perspective on connectivity and show target areas for more detailed investigations. In contrast, site-specific investigations (e.g. seepage meters, piezometers, temperature loggers or environmental tracers) provide more detailed understanding and quantify key processes.

Assessments of the interaction between groundwater and surface water therefore commonly require a combination of approaches in order to extrapolate findings in time and space. Since the number of field measurements is limited for a complete understanding of the connectivity between groundwater and surface water, modelling, both conceptual and numerical, provides a valuable tool for integrating information obtained from other methods (Brodie *et al.*, 2007). Table 1.1 summarises the spatio-temporal scales, cost, limitations and outcomes of the methods used to determine the

connectivity between surface water and groundwater. Site-specific field methods like borehole transects, resistivity, water chemistry and well hydraulics provide a catchment-scale perspective as well as the understanding and quantifying of the key processes. Differences in spatial and temporal scales of the methods form an overall assessment strategy which is then used to develop a conceptual model for groundwater - surface water interactions. It is expected that through a sustained monitoring process, this conceptual model can, in future, inform predictive models through an iterative process which identifies information gaps and requires further data gathering and evaluation to keep the model viable.

Table 1.1 A summary of the methods used to assess groundwater-surface water interactions highlighting the spatio-temporal issues (adapted from Brodie *et al.*, 2007).

Method	**Spatial scale**	**Temporal scale**	**Cost**	**Limitations**	**Outcomes**
Hydrometrics	Local borehole transects	Short to medium-term	Low to medium, costly drilling wells	Require *K* estimates; complex groundwater flow conditions; it is a point measurement	Simple guide to flow amounts and direction; comparisons of groundwater and lakes hydrographs; recharge estimates
Geo-electrical resistivity	Local to intermediate	Short to long-term	Medium	Complex data processing and calibration; prone to cultural obstacles	Provides rapid, subsurface information
Hydraulic tests	Local to intermediate	*T* and *S* are time-insensitive	Medium to high	Limited borehole data can lead to misinterpretation	Conceptual model of groundwater systems around lakes and hydrogeological controls on connectivity
Major chemistry and stable isotopes	Local to regional	Short to medium-term	Medium to high	Can have long lead times between sample collection and final analytical results	Seepage flux, mixing and defines key hydrological processes (i.e. groundwater recharge and discharge)
Water Budget	Intermediate to regional	Short to medium term	Low to medium, expensive collecting all data	Measurement errors; accounting for all water balance components	Estimates of groundwater contributions to lake water balances
Modelling	Local to regional	Medium to long-term	Low to high	Simple models are not adequately robust; complex ones are data hungry, costly and time-consuming	Predictive tool for management and policy; helps define information gaps

1.4.5 Re: Objective (i) to characterise the lithological interface between groundwater and surface waters of Lakes Victoria and Kyoga, and (ii) to relate the observed interface to models of the evolution of landscape and drainage in the GLRA

Hydrostratigraphic characteristics of the interface between groundwater and surface water were shaped by the evolution of landscape and drainage in the GLRA. Vertical electrical sounding and resistivity mapping is commonly used to detect zones of deep weathering (saprolite) in the crystalline basement for groundwater development in the GLRA, as well as profiles of the stratigraphy (Batte *et al.*, 2008). Well logs provide lithological, colour, texture (estimates of hydraulic conductivity, K and specific yield, S_y) determinations and stratigraphy of the weathered profiles (McFarlane, 1992; Chilton and Foster, 1995; Taylor and Howard, 1999a). Both these sets of measurements provide local scale, long-term information for quantifying key interaction processes involved within the interface (Table 1.1). Borehole transects determine the hydraulic gradients (i) between groundwater and surface waters (McFarlane, 1992; McCartney and Neal, 1999), which indicate local scale, short to medium term interaction processes. Water chemistry provides information on the interconnection of the subsurface interface (Chilton and Smith-Carington, 1984; Lloyd and Heathcote, 1985; Chilton and Foster, 1995) that shows local to catchment scale, short to medium term perspective on the connectivity of the interface. Stable (δ^2H and δ^{18}O) isotopes show groundwater recharge and discharge fluxes in time and space into surface waters (e.g. Lloyd and Heathcote, 1985; McFarlane, 1992; Taylor and Howard, 1996).

1.4.6 Re: Objective (iii) to assess how rainfall and dam operations influence the observed interaction between groundwater and surface waters in time and space

Borehole and surface water high frequency monitoring is used to determine the temporal and spatial hydraulic gradients between groundwater and surface waters

(McCartney and Neal, 1999). Temporal and spatial rainfall patterns are used to assess changes/variations that influence groundwater levels (Taylor and Howard, 1996; Butterworth *et al.*, 1999). Both these sets of measurements provide local scale, short to medium term estimates of the key interaction processes (Table 1.1).

1.4.7 Re: Objective (iv) to quantify the hydrological fluxes between groundwater and surface water

Hydraulic tests is used to estimate transmissivity, *T* and storativity, *S* values that can be used to depict hydrogeological characteristics within the vicinity of surface waters (e.g. Chilton and Smith-Carington, 1984; Chilton and Foster, 1995; Taylor and Howard, 1996), which provides local to intermediate scale, long-term estimates (Table 1.1). Surface water and groundwater hydrographs provide discharge estimates and groundwater storage variations (e.g. Chilton and Smith-Carington, 1984). Groundwater recharge responses are compared with rainfall inputs and surface water influences (e.g. Taylor and Howard, 1996; Butterworth *et al.*, 1999). Both these sets of analyses provide local scale, short to medium term interaction processes. Water budgets highlight the contribution of groundwater to surface waters (e.g. McCartney and Neal, 1999; McCartney, 2000). This set of analyses show local to catchment scale, short to medium term interaction perspective.

1.5 Thesis structure

The thesis follows a logical progression of chapters that begins with a broad review of the evolution of the low relief surface in the GLRA, followed by detailed site observations, and then finally scales up the findings over the Upper Nile Basin. Chapter 2 presents a review of the evolution of the drainage on the low relief surfaces (e.g. African surface) and the physical interface between groundwater and surface waters.

Chapter 3 characterises the litho-stratigraphic interface between groundwater and surface waters at the Bugondo, Jinja and Entebbe stations. Chapter 4 evaluates temporal and spatial hydrodynamics between groundwater and surface waters under the influence of regulated outflow on these stations. Chapter 5 describes seasonal climatic influences on groundwater level and lake storage variations for several monitoring stations in the Upper Nile Basin. Chapter 6 estimates the scaled out regional groundwater discharges into Lake Victoria. Chapter 7 synthesizes and summarises the findings and contributions that have been made in improving the conceptual understanding of groundwater-surface water interactions in the region.

Chapter 2
Evolution of drainage on low relief surfaces in the Upper Nile Basin: implications for the groundwater – surface water interactions

2.1 Introduction

This chapter reviews the chronology of rift-related, tectonic processes that have shaped the present landscape of the GLRA and determine the interface between groundwater and surface waters on its low relief surfaces (i.e. the African surface). The underlying hypothesis is that the hydrological relationship between groundwater and surface water is a function of the long-term geomorphic evolution of the landscape that has been driven by the movement of meteoric water. Current conditions are a "snapshot" of subaerial processes that have shaped the landscape of the GLRA. An analysis is made of changes to Lakes Victoria and Kyoga from the late Cenozoic era to the contemporary regional hydrology. Insight is finally drawn from existing geomorphic models for the evolution of dambos, waterlogged surface depressions.

2.2 Regional geology and deeply weathered landscapes

2.2.1 Synopsis of the regional geology of Uganda

Most of Uganda is underlain by Precambrian rocks though not all various facies have been exhaustively mapped and stratigraphically correlated. The Archaean Gneissic-Granulitic Complex (AGGC) coined by Schlüter (1997) covers most of northern and central parts of the country and comprises high-grade metamorphic facies rocks (Fig. 2.1). It is suggested that the oldest of these units is the Watian Group that is

of about Meso-Archaean age (ca. 2.91 Ga) found in the northwestern region of West Nile (Goodwin, 1991, Schlüter, 1997). A suite of rocks of similar age have been identified to the northeast of Uganda which comprise such rocks as acid and intermediate granulites and charnockites, quartz diorites and quartz-feldspathic varieties (Schlüter, 2006). Next in the succession to the Watian Group is believed to be the Aruan Group that also outcrops close to the Watian Group in West Nile region. This Aruan Group comprises biotite gneisses, banded, migmatitic and granite gneisses with lesser quantities of hornblende gneisses, amphibolites, quartzites and very few ultrabasic pods (Schlüter, 2006). The Mirian Group also outcrops in the West Nile region and is postulated to be the next in age, with similar lithology as the Aruan group (Schlüter, 2006). More common in western Kenya and ascribed to the Neo-Archaean era (2.8-3.2 Ga) are pockets of the Nyanzian System found in the southeastern region of Uganda and are made up of rhyolites, porphyries, tuffs and basalts.

Next in succession to the AGGC is the Buganda-Toro System (BTS), also known as the Rwenzori Fold Belt, that is reputed to be of Palaeo-Proterozoic age (ca. 2.5-1.85 Ga, Cahen *et al.*, 1984). The BTS covers most of the western and south-central areas and comprises argillites, basal arenites, and locally amphibolites (e.g. Jinja area). It is also highly granitised with phyllites underlying areas proximate to Lake Victoria (Schlüter, 2006). Structures include tight folds on ENE axes in the east which varies to the west, with a decrease in intensity and a lowering of the metamorphic grade to the south. The BTS extends westwards where it was uplifted and prominently exposed on the Rwenzori Mountains. The Toro Supergroup comprise (stratigraphically upwards): quartzites and conglomerates, metamorphosed tholeiitic lavas (sometimes pillowed) and sills, andalusite-cordierite and sillimanite muscovite metapelites; less common rocks are biotite schists, banded epidote-amphibole rocks and dolomitic marbles (Cahen *et al.*,

1984). Toro rocks are characterised by a higher grade of metamorphism (grade increases westwards) than the Buganda Group, and often more complex structure.

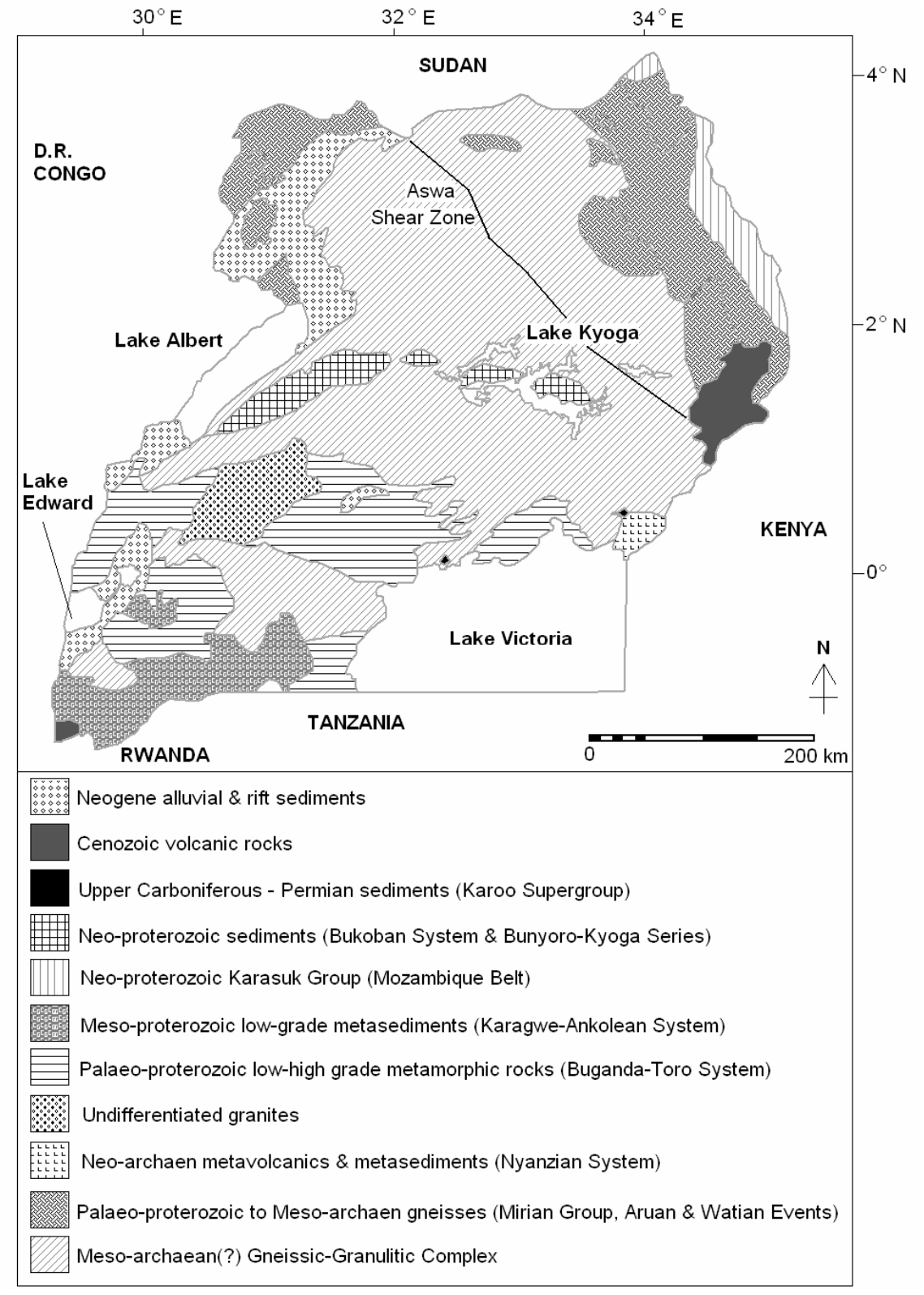

Figure 2.1 Simplified regional geology of Uganda (modified from Schlüter, 2006).

To the southwest, the Karagwe-Ankolean System (KAS) (part of the Kibaran Belt of central and eastern Africa) is considered to be of Meso-Proterozoic age (ca. 1.2-1.6 Ga) and unconformably overlies the Buganda System (Schlüter, 2006). Rocks from this KAS include mainly argillites, as well as arenites and silty rocks, with metacalcareous rocks at the base of the system. It also has a lower grade of metamorphism than the former, open folds that primarily trend to the northwest and northeast. These can, however, be more complex in the lower parts where there are isoclinal structures.

Other units like the Madi Series in the northwest together with the Bunyoro Series of the central region comprise argillaceous rocks, but are of indeterminate ages (Schlüter, 2006). The south- and west-central areas feature the Singo and Mityana Series that are both arenaceous and unmetamorphosed consisting of mainly mudstones. To the northeast along the border between Uganda and Kenya, the Karasuk Group form an elongate band which comprises gneisses, amphibolites, marbles, quartzites and ultramafic rocks, reckoned to be part of the Meso-Proterozoic (ca. 1.2-1.6 Ga) high-grade metamorphic Mozambique Belt (Leggo, 1974; Cahen *et al.*, 1984; Goodwin, 1991). Within central Uganda, detailed geologic mapping has not been completed and inhibited by a paucity of exposures. Inselbergs possess a quartzofeldspathic composition consistent with Archaean gneisses observed in northern and south-central areas (Taylor and Howard, 1998). There are also several undifferentiated intrusive rocks considered to be of Precambrian age scattered in several parts of the country. Exposures of Karoo age shales thought to be of Ecca age (ca. 250-300 Ma) from the fossil plant remains, are found in areas of Entebbe, Bugiri and Dagusi islands on and off the north-central shore of Lake Victoria, respectively (Schlüter, 1997).

Volcanic tuffs extruded during the Early Miocene to cover the stripped surface in eastern and western Uganda (Bishop and Trendall, 1967). Carbonatite ring complexes (ca. Cretaceous, Schlüter, 1997) are found in the eastern to northeastern areas where they form prominent topographic highs. Similar volcanic rocks are also scattered in the southwestern region extending into Rwanda and D.R. Congo. Within the western arm of the East African Rift System (EARS), narrow, deep and stratified lakes and downfaulted rift troughs have accumulated organic-rich, fossiliferous sediments that are over 4,000 m thick. Towards the northeast, the Aswa shear zone (>300 km long) forms the most prominent structure trending northwest-southeast within the Precambrian rocks.

The region around Lake Victoria has quite varied geology (Fig. 2.2). The western part in Tanzania is underlain by rocks of the Neo-Proterozoic Bukoban system comprising conglomerates, sandstones, quartzites, greywackes, shales, dolomitic limestones and basalts and the BTS (Temple, 1966; Schlüter, 1997; Schlüter, 2006). The northern area of the lake features the AGGC as well as the Archaean Nyanzian-Kavirondian System comprising quartzites, graphitic shales, banded iron formations, lava, tuff and amphibolites. The eastern sections of the lake are underlain by undifferentiated granites, Nyanzian-Kavirondian system, and Cenozoic sediments and volcanics whereas the southern regions are underlain by granitoid rocks of the Archaean Dodoma schist belt and pockets of the Nyanzian-Kavirondian System.

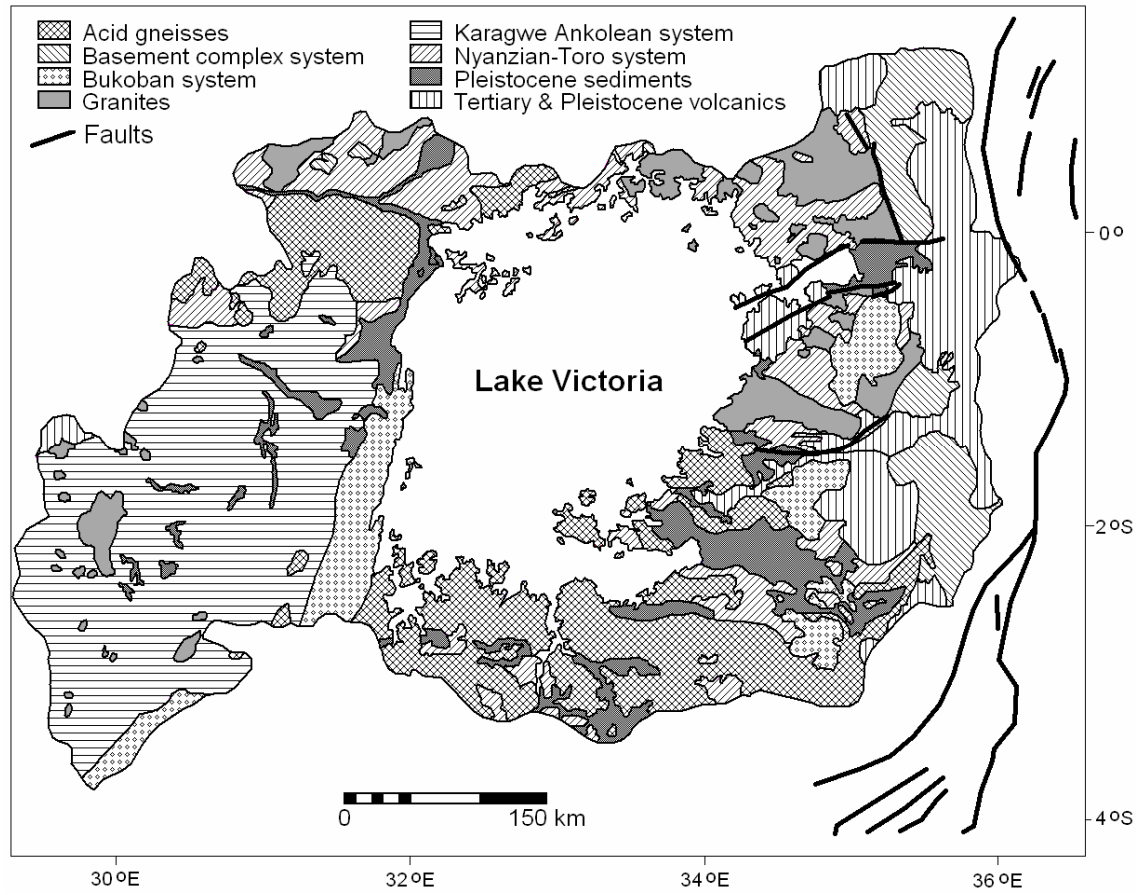

Figure 2.2 Regional geology of the Lake Victoria catchment (adapted from Temple, 1966).

2.2.2 Weathering and saprolite formation

The African surface has undergone alternating cycles of deep weathering and stripping that have produced a highly variable regolith. This *in situ* weathered regolith (saprolite) features a variable transmissivity (T = 5-20 $m^2 \cdot d^{-1}$, Taylor *et al.*, 2004) which regionally is an important source of groundwater. Two fundamentally different models have been put forward for the origin of the African erosion surface (McFarlane, 1992). In Malawi, King (1962) ascribed the low relief which was supposed to be applicable to all parts of Africa, to a mechanism of stripping associated with the process of *pediplanation* which was a result of direct surface runoff. King's model is based in regions that are arid with limited fluvial action. Alternatively, Wayland (1934) had earlier attributed the surface to *etchplanation* which involves differential weathering and

leaching. *In situ* rock weathering produces a thick surficial residuum (saprolite) which is relatively resistant to leaching that is locally redistributed to even out the irregularly lowered surface by weathering (McFarlane, 1992). Relief is subdued by downcasting that includes the slow subsidence and transport of residual materials downslope towards the bottomlands. The erosion surface is thus regarded to be shaped by the action of recharge. Tectonic activity is believed to control geomorphic processes (etchplanation vs. pediplanation) in the region (Taylor and Howard, 1998) and likely has also influenced the palaeoclimatic variability (Sepulchre *et al.*, 2006; Maslin and Christensen, 2007) which, in turn, may have impacted on the dominance of etchplanation over pediplanation and vice versa.

2.2.3 Lateritic weathering profiles

2.2.3.1 Definitions

Deeply weathered surfaces within the tropical regions like the GLRA are usually capped by a variety of iron-rich to alumina-enriched residua horizons. They are broadly known as laterite but their genesis and evolution are ambiguous. Schellmann in 1983 made a new formulation of laterites initially coined by Buchanan in 1807 in order to distinguish between the highly weathered (laterites) and less strongly weathered residual rocks (saprolites), and also from surficial ferruginous deposits of planation surfaces or at the bottom of local slopes (Aleva, 1994). This usage defines *laterites* as products of intense subaerial rock weathering that consist mainly of mineral assemblages of goethite, hematite, aluminum hydroxides, kaolinite minerals and quartz. The SiO_2:(Al_2O_3+Fe_2O_3) ratio of the laterite must also be lower than that of the kaolinized parent rock in which all the alumina of the parent rock is present in the form of

kaolinite; all the iron should be in form of iron oxides, additionally with the silica only from the kaolinite and the primary quartz.

There are a few other common terminologies used to describe lateritic horizons. *Cuirass* also known as the *hardcap* forms the upper, hard part of the Fe-Al accumulation zone, whereas the *carapace* is the softer part of the laterite that commonly underlies the cuirass. *Ferricrete* is considered to be a conglomerate bound by iron oxides whereas *alcrete* is bound by gibbsite both of which are externally sourced from outside the area of interest, i.e. allochthonous rock. *Duricrust* is broadly used for the indurated surficial material which may be ferruginous, aluminous, siliceous or calcareous, or a combination of these, i.e. autochthonous rock.

The common essential minerals in laterites and related rocks are iron minerals, hematite (Fe_2O_3) and goethite (α-FeO(OH)), the aluminium minerals, gibbsite ($Al(OH)_3$) and boehmite (AlO(OH)), and the clay mineral kaolinite ($Al_2Si_2O_5(OH)_4$). From a triangle formed by connecting the points for hematite, gibbsite and kaolinite, a ternary plot was derived which highlights the central position of laterites as an admixture of ferruginous, bauxitic and kaolinitic materials (Aleva, 1994). Laterite formation concentrates some, less mobile elements such as Fe, Al, Mn, Ni, Ti and Cr giving rise to a suite of different types of laterites.

2.2.3.2 Theories of laterite genesis

Several diverse theories have been postulated to explain the processes leading to laterite formation, cited and summarised by Aleva (1994). D'Hoore in 1954 considered *subtractive* or *relative enrichment* by selective surficial removal of elements, against *additive* or *absolute* enrichment by accumulation of materials from other parts of the regolith. Later, Millot and Bonifas in 1955 realised that relative accumulation of Fe_2O_3 and Al_2O_3 was the main process of enrichment in the weathering profile with iron being

commonly accumulated in the upper parts, whereas solution removed bases (largely Na, K, Mg and Ca) and silica. Much later in 1983, Pedro and Melfi suggested a suite of successive minerals as well as environmental requirements necessary for the formation of laterite minerals. Ultimately, Boulange in 1984 proposed the theory of *isovolumetric* transformation, where there is relative accumulation of Al and Fe, through the removal in solution of other elements (e.g. bases and silica) which commonly result in relict fabric and structures, e.g. feldspars altered to gibbsite without loss of shape or cleavage, whereas iron appears as goethite. Alternatively, it is contended that *allovolumetric* change can also take place where there is absolute enrichment of Al and Fe through filling of voids formed when other elements (e.g. bases and silica) are leached out, with the gibbsite mainly formed from desilification of earlier weathering products, e.g. kaolinite. Swartz in 1992 showed that it is possible for residual and transported ferruginous deposits with an oolitic fabric to occur together. It was therefore proposed that the generic requirements for laterite formation include: parent rock composed of weatherable minerals (e.g. alkali- and calc-alkali silicates), warm and humid climate to accelerate reaction speed, sufficient rainfall to provide abundant recharge to flush out solutes, abundance of bacteria and other micro(organisms), geomorphic positions that promotes the free flow of recharge, and sufficient time in the order of at least several million years.

2.2.3.3 Laterite-capped weathering profiles

The *regolith* also known in the past as the overburden and coined by Merill in 1897 represents all the unconsolidated and possibly secondary re-cemented cover that overlies the more coherent bedrock and that has been formed by weathering, erosion, transport and/or deposition of older material (Aleva, 1994). A typical lateritic profile is defined in this perspective as a stratigraphic model of all the main possible widely

accepted horizons from the soil zone to the parent bedrock, which is likely to differ from a natural profile that usually lacks one or more of these zones. Successive interfaces can reach thicknesses of several tens of metres, and may laterally vary in thickness within one deposit.

The stratigraphic zones of typical laterite-capped profiles are however often influenced by local conditions (Fig. 2.3) which make it difficult to make objective descriptions. McFarlane (1992) for example, views the saprolite to constitute the whole region underlying the laterite, arguing for relative accumulation from within the underlying saprolite zone. Ollier and Galloway (1990) have a ferricrete cap overlying the mottled and pallid (Fe-depleted) zones both considered as part of the saprolite being formed by the absolute accumulation of iron. McFarlane (1969) contends that there is no adequate mechanism for the upward removal of iron from the pallid zone. The Geological Society Engineering Group Working Party (GSEGWP, 1977) assigned a weathering grade where a progressive modification of a consistent parent rock is assumed and also implicit therein is the conservation of the different weathering grades during development. Both notions are difficult to support (McFarlane, 1991). Aleva in 1986 adapted two earlier schemes from Millot in 1964 and Lelong in 1969 (cited in Aleva, 1994), where saprolite was apportioned into unstructured saprolite zones where intensive weathering had occurred, overlie a structured saprolite horizon which grades into a transition zone just above bedrock. From the definition saprolite (Bates and Jackson, 1987) it is apparent that the extent of this saprolite zone is based on the prevailing understanding of the genesis of laterites.

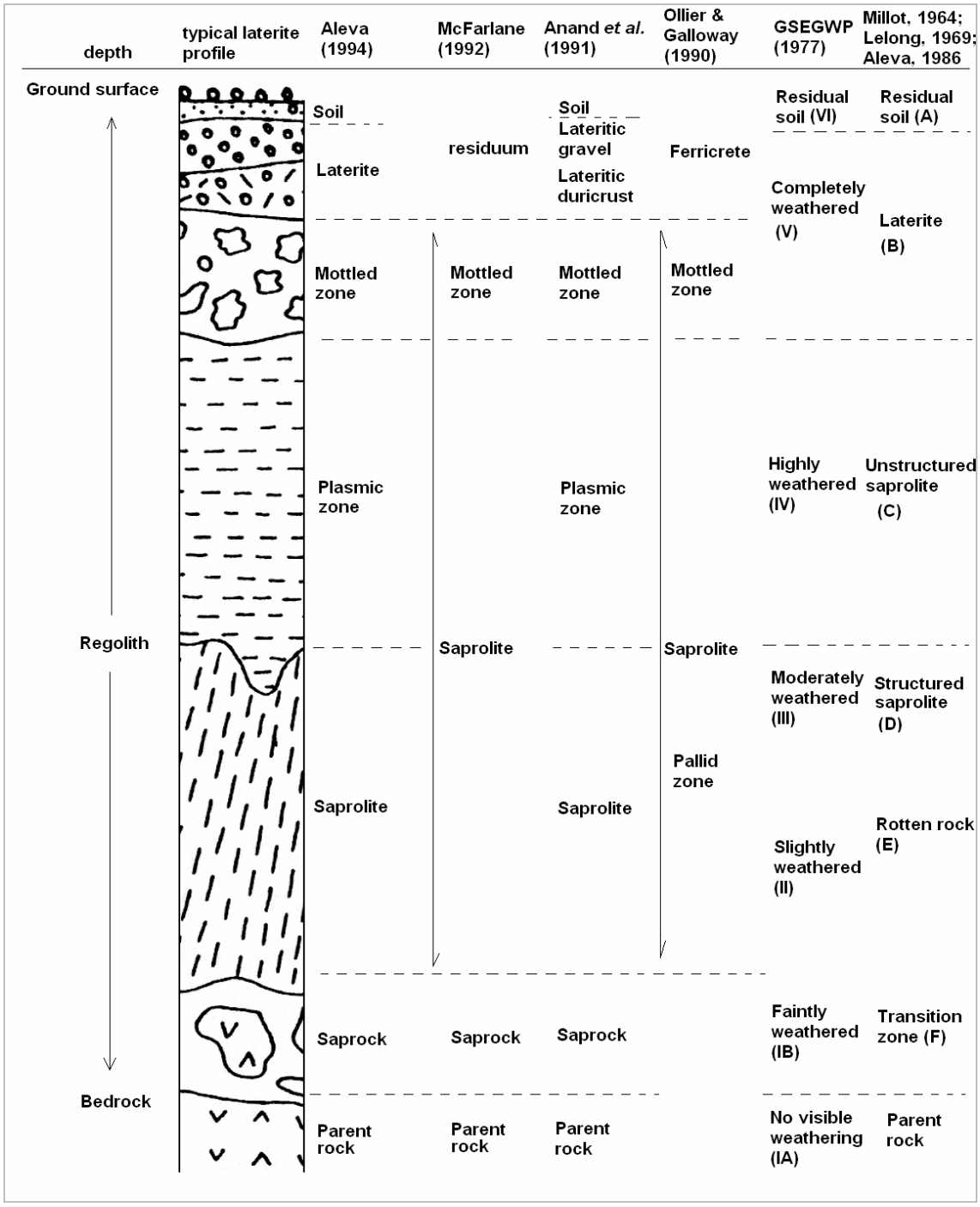

Figure 2.3 Stratigraphic profiles showing different perspectives of the weathering horizons (modified from Aleva, 1994).

2.2.3.4 Laterites within the Upper Nile Basin

Earlier studies cited by McFarlane (1976) on the northern shore of Lake Victoria (due west of Jinja) showed that laterites occur at all levels from 1,341 m above sea level (masl) to below the level of the lake (1,134 masl). Within the metasediments of the Buganda series of the BTS, the laterites overlie phyllitic mudstones. Laterites were, as a result, thought to be more topographically controlled and indirectly influenced by local lithological changes. Johnson (1960) mapped profiles of pisolithic and vermiform laterites (up to 3 m thick) and murram (lateritic gravel) in western central parts of Uganda around the Lake Wamala area (Fig. 1.1). Although there was an ubiquitous formation in all rock types, they were better developed on amphibolites and shales, schists, sandstones and quartzites. There were variations in the dolerites, and they also masked the dip slopes of the Mityana Series. Trendall (1965) noted that the laterites (up to 2.5 m thick) of the Teso Catena that underlie the region east of Lake Kyoga were concealed beneath the soils (up to 3 m thick) except at points where there was a positive break in the slope of the undulating landscape. This view is similarly held by McFarlane (1976) who found out that groundwater laterites were not commonly exposed but were often overlain by soil within which patches of pedogenetic laterite was developed. Maignien (1966) noted that indurated lateritic horizons could form excellent storage reservoirs for groundwater with high permeability when they were strongly jointed. It was also suggested that where there was sufficient development of interconnected secondary openings after the soluble solutions had been washed out from the formation, circular or linear crumbling could occur levelling the line of water flow. Adjacent stream water courses could then converge into these depressions and interact with the jointed formation which could influence the discharge of the streams along their courses.

According to Jones (1985), the main aquifer within the AGGC saprolite derives from the base of the profile below the upper clayey horizons where selective mineral decomposition has produced a coarse-grained, gravelly material. Way (1939) exploring for groundwater in Central Uganda found that weathered crystalline basement rocks which were capped by lateritic profiles had significant water-bearing horizons often either in the leached lateritized zone under the cuirass or in the decomposed zone (saprolite/saprock) just above the solid rock. The cuirass was found to be usually unreliable and subject to extreme fluctuations, whereas the saprolite/saprock was likely to prove more sustainable.

2.3 Tectonically controlled cycles of deep weathering and stripping and the evolution of the regional drainage and landscape

Rift-related, tectonic processes since about early Miocene are considered to have shaped the present landscape of the GLRA and thus influenced surface hydrology through the development of landscape features (Taylor and Howard, 1998; Taylor and Howard, 1999a; 2000; Trauth *et al.*, 2005). As a consequence, there have been debates over the evolution, nature, relationship and number of the resultant landforms. However, there is general consensus about three broad categories of landscape elements of the low-relief surface (Doornkamp and Temple, 1966; Doornkamp, 1968; de Swardt and Trendall, 1969; Taylor and Howard, 1998):

(i) Upland (laterite) landscape and high surface of eastern Uganda, a dissected erosion surface with residuals (Jurassic / mid-Cretaceous surface).

(ii) Lowland (laterite) landscape, with a less defined character (Miocene / Recent surface).

(iii) Depositional or infill landscapes which occur along valleys on the plateau, on the margins of Lake Victoria, and in the western rift valley.

Doornkamp and Temple (1966) established that the tectonic events which culminated in the formation of the present-day EARS brought about a regional uplift in a series of marked stages (Fig. 2.4). Based on the morphoclimatic evolution of the African surface from the end of Palaeozoic, Taylor and Howard (1998) identified six broad cycles of stripping (pediplanation) and deep weathering (etchplanation) within the African surface that have shaped the weathered land surfaces. A summary is made of the sequence of Post-Palaeozoic events and the ensuing landforms and drainage based on the models of Doornkamp and Temple (1966) and Taylor and Howard (1998).

2.3.1 Regional tectonic quiescence during the Pre-Neogene period

Following the Precambrian orogenic events, the Palaeozoic era is considered to be characterised by prolonged tectonic quiescence where sustained exposure to sub-aerial denudation resulted in a general planing down to almost a common level forming the Gondwana surface, precursor of the African surface (Groves, 1934). Around Jurassic to Mid-Cretaceous, it is posited that humid conditions, following deglaciation at the end of the Palaeozoic, enhanced deep weathering of the Palaeozoic landscape to form an extensive, almost featureless plain (King, 1962). This ancient upland landscape had, in general, developed to a stage of late-maturity with wide, open valleys, meandering streams and rounded, gently undulating watersheds (Doornkamp and Temple, 1966). Relative relief may have ranged from 30 m to 275 m depending on local physiographic conditions during the Mid-Cretaceous, when the Congo drainage was instigated across equatorial Africa along a failed rift that induced an eastward incision. Incision occurred through to the Early Miocene causing extensive stripping of the saprolite in the region (Bishop and Trendall, 1967; de Swardt and Trendall, 1969; McFarlane, 1976).

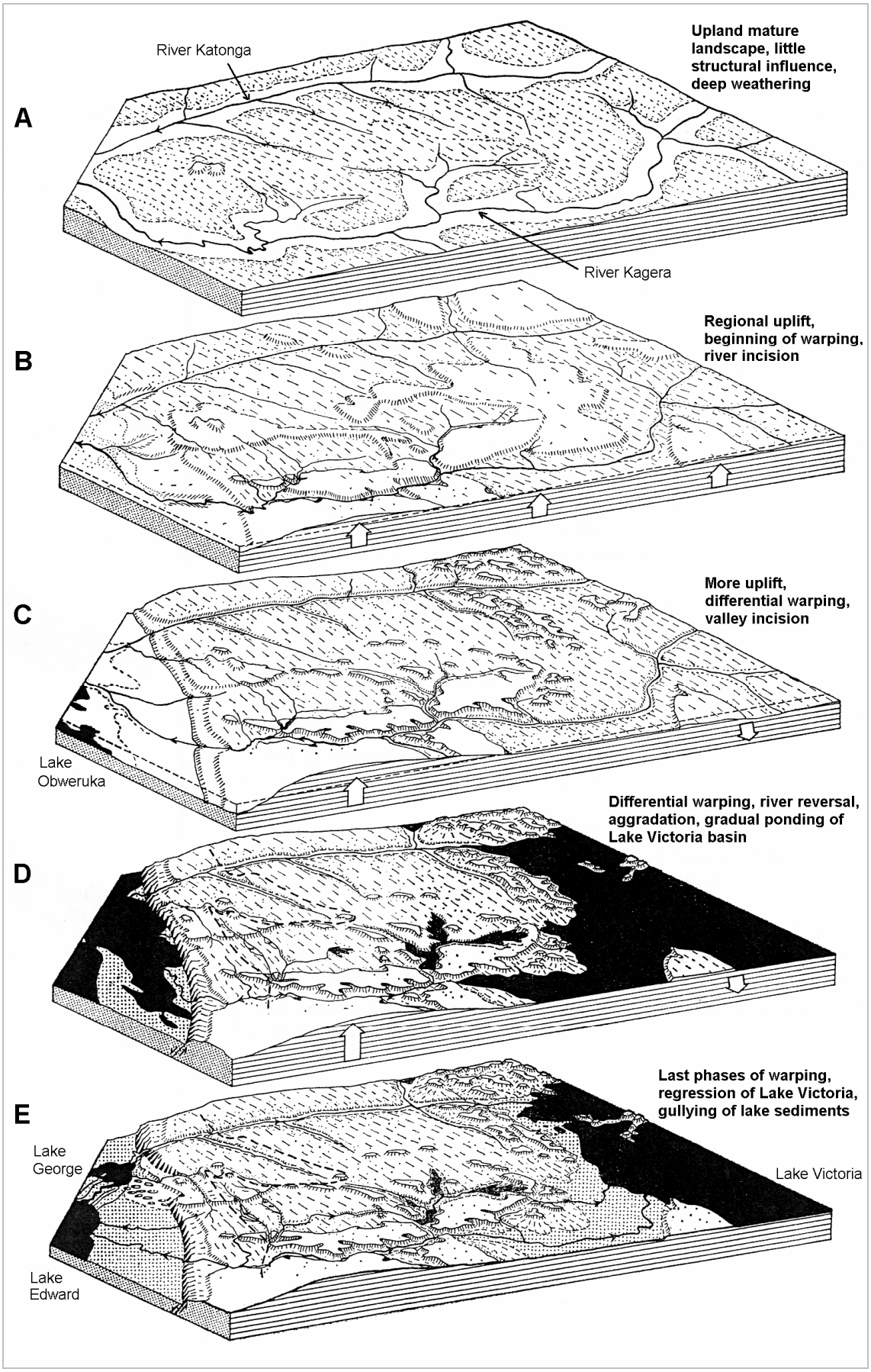

Figure 2.4 Three-dimensional illustrations of the major stages in the evolution of the low relief surface of southern Uganda (adapted from Doornkamp and Temple, 1966).

Rivers Kafu, Katonga and Kagera formed headwaters of the Congo basin in western Kenya (Fig. 2.4a) and had east-west drainage (Temple, 1970) (Fig. 2.5). Ojany (1970) proposes that the eastern boundary of these headwaters, found in the present eastern rift valley in Kenya, was a topographically low region flanked by old upland massifs, which favoured drainage into this area of negative relief with outlets either/both to the north or south. Remnants of the Jurassic to Mid-Cretaceous surface are confined to ferricrete-capped mesas underlain by the quartzites of the BTS and KAS suites (Doornkamp and Temple, 1966; de Swardt and Trendall, 1969), along the shore of Lake Victoria and southwestern Uganda. Inselbergs crop up below the upland landscape but rise, in the west, to considerable heights above the lowland landscape. The greater development of hill-crest inselbergs in the west, compared to the east, is probably related to the greater degree of stream incision and relative relief (Doornkamp, 1968).

2.3.2 Regional tectonic uplift from the Early Neogene period

Trauth *et al.* (2005; 2007) and Maslin and Christensen (2007) together with previous works quoted therein suggest that the volcanism of the EARS started in the Ethiopian Rift, between about 45 and 33 Ma (Eocene). This volcanism continued to northern Kenya in ~33 Ma (Oligocene) and was followed in the central and southern segments of the rift in Kenya and Tanzania between about 15 and 8 Ma (Miocene). Major faulting alternatively, is proposed to have begun in Ethiopia from around 20 to 14 Ma (Miocene) and was followed by the evolution of the Turkana Rift zone in northern Kenya that proceeded southwards and eventually developed into the central Kenya rift by ~2.6 Ma (Pliocene). Within Tanzania, the present-day rift escarpments were thought have been produced by a major phase of rifting that took place around 1.2 Ma (Pleistocene). On the western branch of the EARS, development is considered to have

commenced at about 12 to 10 Ma (Middle-Late Miocene), within the central Tanganyika Basin. More recent phases of major uplift occurred between 5 and 2 Ma in the Tanganyika and Malawi rifts (Sepulchre *et al.*, 2006). Major Tanzanian escarpments are thought to have been present by about 3 Ma (Pliocene) which led to a 6,000-km-long elevated area, mostly oriented north-south and bordered by crests culminating between 1,500 and 5,100 m (Sepulchre *et al.*, 2006).

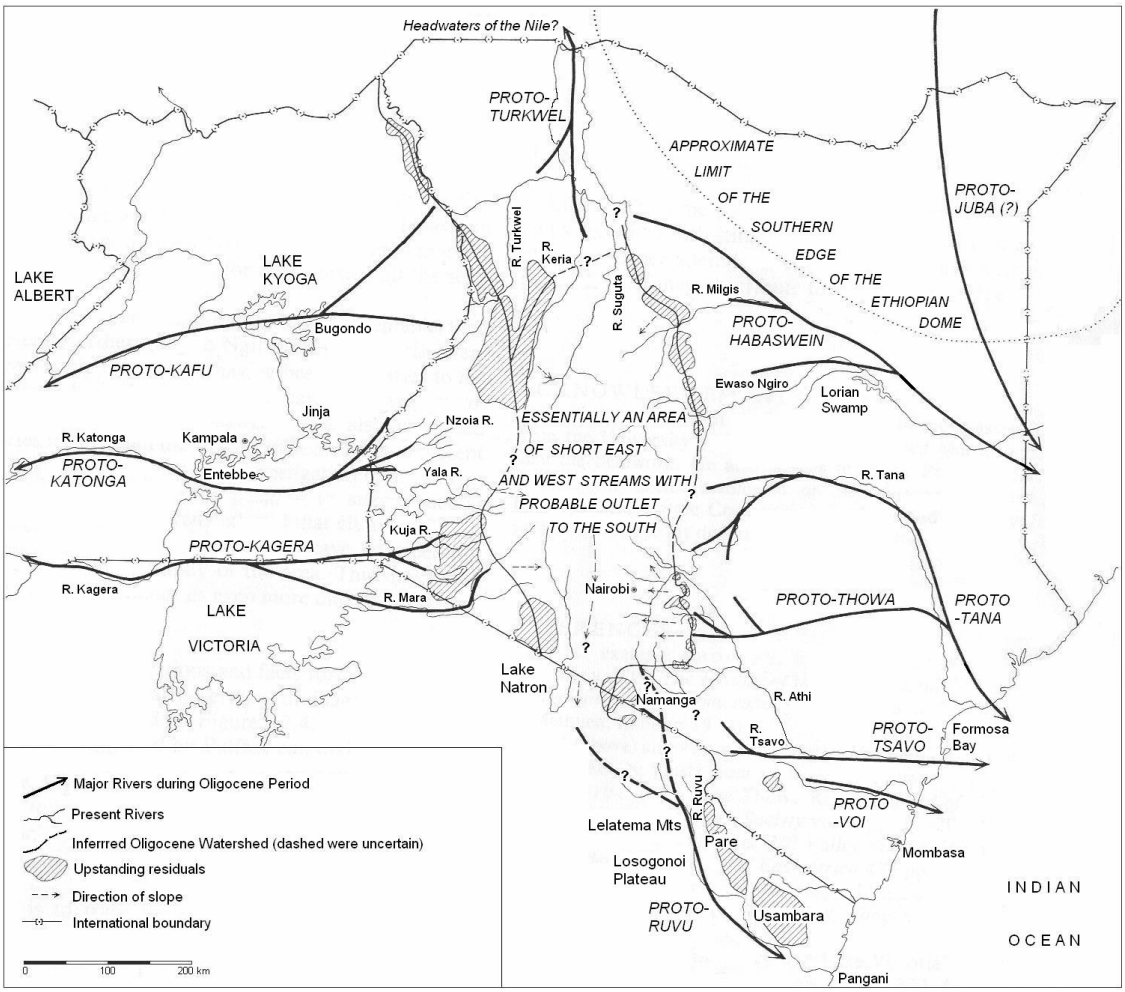

Figure 2.5 Suggested drainage pattern in eastern Africa in the early Tertiary period (reproduced from Ojany, 1970).

During the Early Miocene, climatic conditions are considered to have favoured rainfall-fed groundwater recharge that induced deep weathering with humid conditions capable of sustaining rainforest cover in eastern Africa (Pickford, 1995; Taylor and Howard, 1998). By about Mid-Miocene, western rifting produced a shallow downwarp and induced local stripping of the upland surface which evolved into the lowland surface (Fig. 2.4b). Incision of streams rapidly opened up weaker zones within the less resistant granites and mica-schists bringing about their present superimposition (Doornkamp and Temple, 1966). Drainage was partly antecedent indicating that warping must have been weaker and initially slower than the rate of downcutting (Combe, 1932). From approximately the Late Miocene, increased uplift and differential warping led to a relative depression producing a deep graben that formed the palaeo-Lake Obweruka in the western rift zone and the proto-Lake Victoria basin (Doornkamp and Temple, 1966) (Fig. 2.4c). Remnants of the upland became more isolated as the depression broadened. Antecedence was exaggerated through further faulting, as the lowland and upland surfaces became progressively divergent. This period was terminated by a new phase of valley stripping and incision. The rising warp progressively reduced the competence of the drainage network to carry load inducing aggradation which continued during and after the period of actual reversal. Palaeo-Lake Obweruka was then cut into half by the upthrusting of the Rwenzori horst gradually initiating the formation of Lakes Edward and Albert during the Late Pliocene (Doornkamp and Temple, 1966; Taylor and Howard, 1998). Differential warping and uplift parallel to the western rift escarpment overcame westward river incision and direction which after progressive aggradation was reversed (Fig. 2.4d). This differential warping would appear to have been slowly taking place throughout the evolution of the lowland surface. Had the adjustment to the large amount of tectonic deformation been sudden, the drainage could not have maintained its westward flow but would have been

rapidly ponded back on the upland landscape (Doornkamp and Temple, 1966) (Figs. 2.4c and d).

In areas east of the axis of the western uplift, a reduction in relief led to the ponding of surface water in the wide drainage channels linked with the former west-flowing headwaters (Kagera and Katonga) of the Congo basin. This led to the gradual ponding up of the proto-Lake Victoria basin, as tributary valley heads were converted into satellite lakes. Bishop (1969) proposed that the proto-Lake Victoria with long inlets towards the west in Kagera and the Katonga rivers possibly continued to flow via the site of the present Katonga swamp-divide (base of sediments are presently 55 m above lake). In the western rift, the northern part of Lake Obweruka started to dry up as it is suggested to have found a northward outlet to the Nile that was initiated during the Late Pleistocene (Livingstone, 1980). Between the axis of uplift and the western rift escarpment, increased gradients led to incision and stripping of narrow drainage channels within the wide basin topography. Where the three great through valleys (Kagera, Katonga and Kafu) have their rivers reversed, there is a zone of several kilometres of papyrus swamp in which the direction of flow is almost indeterminate (Groves, 1934). Each of these river-reversals is about 40 km from the nearest flexure zone of the western rift scarp.

The eastern rifting that may have coincided with a pluvial period (Trauth *et al.*, 2005; 2007) rejuvenated west-bound rivers (e.g. Nzoia, Yala, Kuja and Mara) that had developed broad graded valleys east of the proto-Victoria depression, as earlier postulated by Stockley and Williams in 1938 (cited in Ouma, 1970). Ouma (1970) noted that whereas the formation of the western rift valley decreased stream profiles down to the point of reversal of flow direction, the rising shoulders of the eastern rift exaggerated the gradients of the west-bound streams (Fig. 2.6). Furthermore, McCall in 1958 suggested that to the east of the proto-Victoria depression, the Sub-Miocene

surface was tilted westward and northwestward (Ouma, 1970). As a result, present-day rivers flowing into Lake Victoria drain a landscape of considerably varied morphological texture whose altitudes ranges from 1,134 masl at the lake shore to over 2 438 masl in western Kenya, and even reaching 4,267 masl on Mount Elgon in eastern Uganda, with Karagwe in northern Tanzania also exhibiting a high relief (1,189 – 1,900 masl). Periodic falls in the levels of Lake Victoria (Temple, 1970) rejuvenated all the rivers and affluents into the lake, like the Kagera which has several river terraces (>60 m above Lake Victoria level) in its valley (Combe, 1932). It is argued that due to the reduced discharge following the end of the latest pluvial episode of Pleistocene (~1.1-0.9 Ma, Trauth, 2005), all the rivers east of the lake are underfits, whereas those to the west of the lake are partly or wholly superimposed on the dip-slopes (Ouma, 1970). Thus, since Mid-Pleistocene, stream gradients were slightly decreased by back-tilting in northern Tanzania, whereas in western Uganda there was reversal of flow direction towards the proto-Victoria depression (Fig. 1.1). In Kenya and the northern half of the lake region of Tanzania stream profiles were significantly steepened (Fig. 2.6).

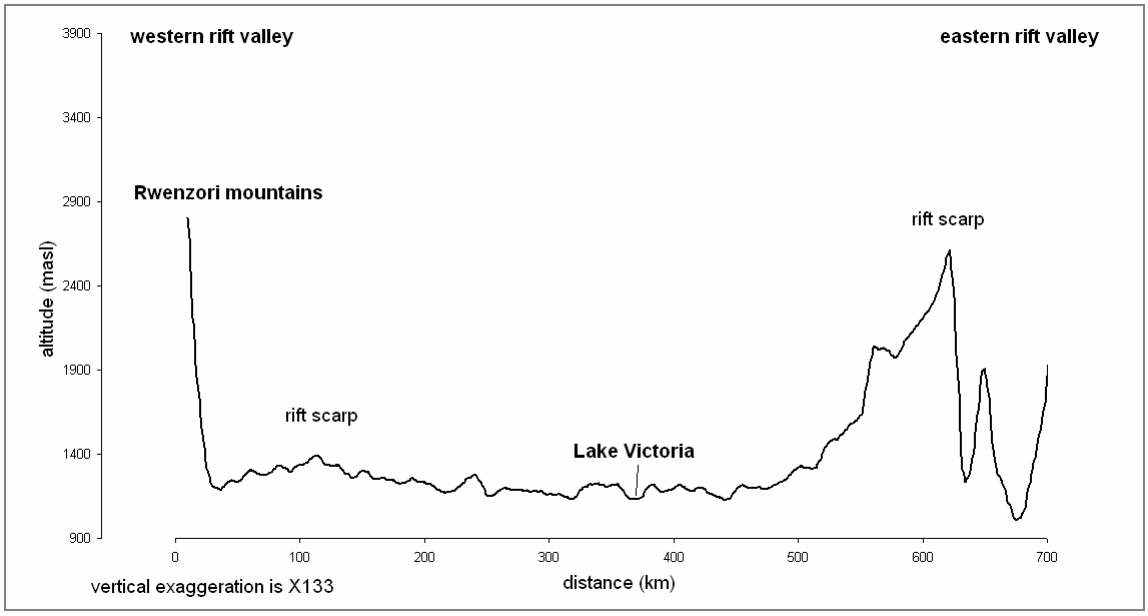

Figure 2.6 West-East profiles of the topographic gradients towards Lake Victoria from the western to eastern arms of the EARS along approximately the 0°24' N latitude (from 90-m SRTM, 2009 digital terrain model).

2.4 Influence of Recent (Late Cenozoic) tectonic and climatic events on drainage and sediment stratigraphy

2.4.1 Regional warping and climatic changes on regional drainage

Trauth *et al.* (2007) propose that the late Cenozoic climate of East Africa is punctuated by episodes of short, alternating periods of extreme wetness and aridity, superimposed on a regime of subdued moisture availability exhibiting a long-term drying trend. Of the three main forcing factors thought to be significant for regional and global climate changes, i.e. local tectonics, regional orbital forcing, and global climate changes, uplift associated with the EARS formation is considered to have altered wind flow patterns from a more zonal to more meridinal direction (Maslin and Christensen, 2007). Sepulchre *et al.* (2006) suggest from palaeoenvironmental records that tectonic uplift within the eastern rift caused a rain shadow effect which reduced the moisture available for rain on the eastern sides of the mountains/valleys, and thus generated a strong aridification in the region. Trauth *et al.* (2005; 2007) assert that the deep lakes of the EARS are synchronous with major global events dated by radiometric age determinations, at ~2.7-2.5 Ma (intensification of Northern Hemisphere Glaciation), ~1.9-1.7 Ma (onset of Walker Circulation - east-west zonal atmospheric circulation), and ~1.1-0.9 Ma (Mid-Pleistocene Revolution - shift from glacial/interglacial cycles every 41 ka to every ~100 ka), and that their appearance was dictated by precessional forcing of moisture availability in the tropics. There was also limited evidence for lake phases around ~4.7-4.3 Ma, 4.0-3.9 Ma, ~3.4-3.3 Ma, and ~3.20-2.95 Ma (Trauth *et al.*, 2007).

A shift towards drier conditions is considered to have occurred around 25 ka (Taylor and Howard, 1998) (Fig. 2.4e). This shift coincided with the last phases of

downwarping along a north–south transect that created the saucer-like depressions, and led to the regression of Lake Victoria margins eastwards, and formed present lakes Kyoga and Victoria. There was as a result an increase in the surface gradient of the low relief surface towards the axis of upwarp in western Uganda. Exposure of lacustrine deposits ensued as the lake levels fell in stages, followed by the gullying of lake sediments. Lacustrine deposits have been traced down the Kagera River (as the Nsongezi Formation) along which at one point they outcrop 35 m above the modern lake shore (Kendall, 1969). This period of desiccation caused a considerable reduction in the size of the great lake and the withdrawal of Lake Victoria to an area probably smaller than its present one, accompanied by an almost complete disappearance of Lake Kyoga (Groves, 1934). Ensuing development of wet and warm climatic conditions around 12.5 ka (Kendall, 1969), filled the Victoria and Kyoga depressions. An outlet for Lake Victoria at Jinja was subsequently routed by the later capture along an old tributary of the Kafu-Lake Kyoga drainage system, when according to Bishop (1969) upwarp caused the original western outlet of Lake Victoria to reach similar base levels with the eastern-lying section. Temple (1966) on the other hand argues that it was overflow rather than capture that formed the river, since the area was especially favourable. At the Jinja outlet, there are dykes of amphibolite dolerite which gave rise to the Ripon Falls, now drowned when the Owen Falls hydroelectric power station (Nalubale Dam) was constructed in 1954. The Victoria Nile gorge of this overflow channel just below Jinja manifests youthfulness and still runs at the same level as the old south-flowing river whose course it occupied (de Swardt and Trendall, 1969).

Between the Albert and Victoria Nile basins there is a north-south trending basin divide from which streams flow both to the east and west that lies on the apex of the upwarped zone and is morphologically evidenced by the presence of major through-valleys (Wayland, 1929). The main valleys east of the upwarp are invariably choked

with an infill of alluvium or vegetation (papyrus) or standing water (Doornkamp and Temple, 1966) which has obscured the final phase of incision of the lowland landscape cycle. Generally, the incompetence of the east-west trending valleys inevitably affected the local base level and competence of the north-south tributaries, silting up the whole valley system. Rivers that were reversed formed lakes including many of the east-west tributary heads. East of the Upper Nile Basin of Uganda, Temple (1970) used a genetic approach to classify two major types of lakes. The first set is lakes formed by warping and back-tilting of pre-existing basins forming a connected series of major lakes in central and southern Uganda (Fig. 2.7), and comprise mainly Lakes Victoria and Kyoga, as well as Wamala and the Koki lakes (Lakes Nakivali, Mburo, Karunga, Kachira and Kijanebalola). The second set are shoreline lakes which have been most readily identified along the western shoreline of Lake Victoria, and are particularly well developed in the area around Lake Nabugabo which is over 3 m above Lake Victoria level (Bishop, 1959) (Fig. 2.7). The eastward regression of Lake Victoria under the influence first of tilting and later of eustatic fall in lake level from the late Middle Pleistocene exposed extensive lacustrine zones comprising cliff-lines, sand-bars and lagoons (Temple, 1970).

The Kyoga-Kwania complex is a shallow palmate system with long narrow branches spread out commonly eastwards becoming even smaller into the inflow streams with a shoreline which follows a contour on the drowned landscape and receives the overflow of Lake Victoria (Fig. 2.7) (Trendall, 1965). It is evidently an inundated portion of the reversed River Kafu together with a number of its tributaries (Groves, 1934). This is thought to have assisted in its capture of a Lake Albert feeder currently comprising the lower portion of the Victoria Nile, when its original westward outlet was raised to the lowest base level separating the proto-lake from the western rift scarp streams (Bishop, 1969). It is also suggested another river capture of the Kyoga

system took place by the northeastern rivers where a swampy divide and the form of the watershed is considered to have been the old headwaters of the Aswa River.

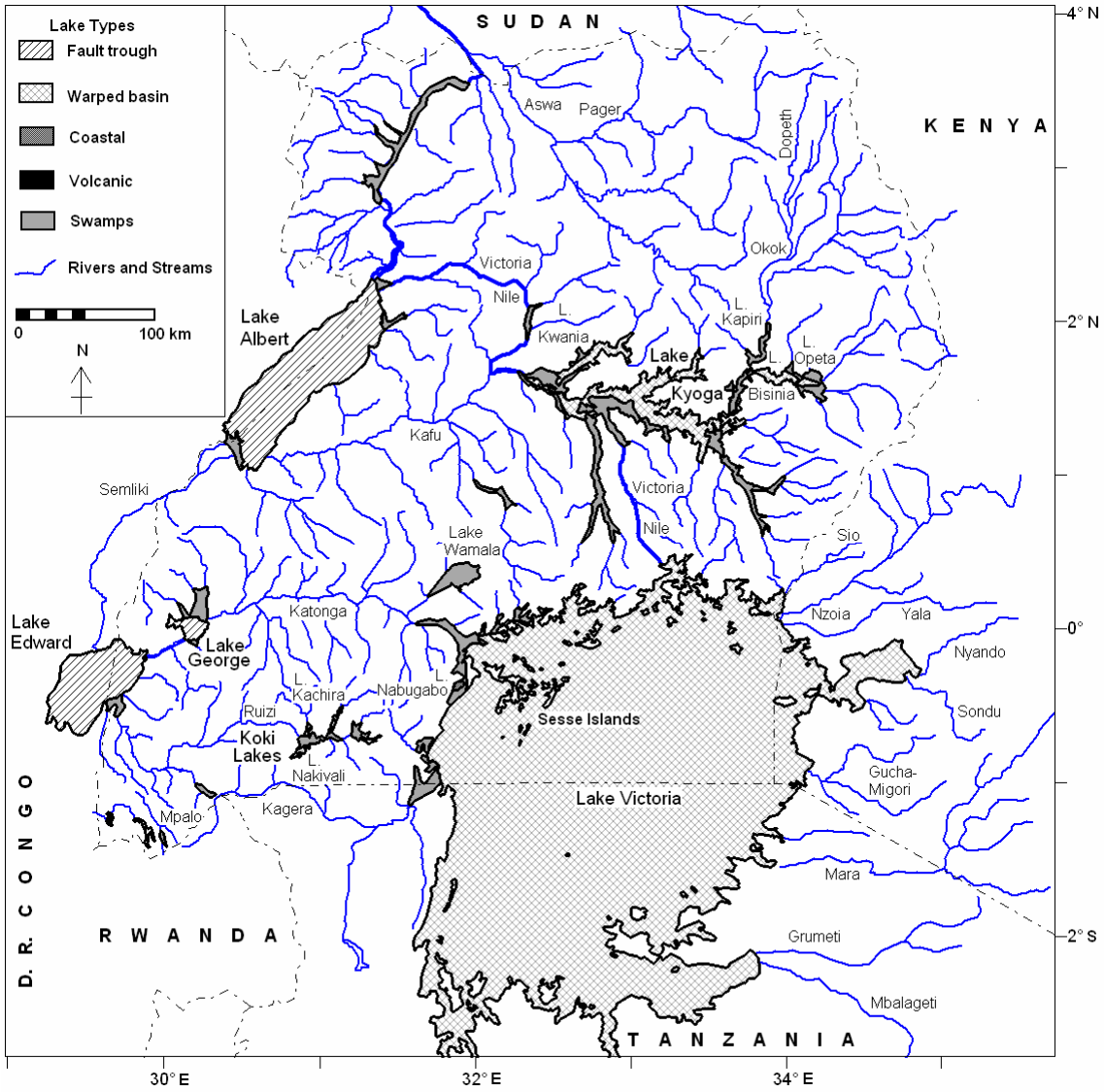

Figure 2.7 The contemporary drainage of Uganda showing the categories of lake formation (adapted from Temple, 1970).

Lake Victoria has rectangular appendages of Kavirondo and Speke gulfs on the eastern side (Fig. 2.8) that are speculated to be faulted basins whose origins may pre-date (Pre-Tertiary) the main water body (Doornkamp and Temple, 1966) which covers the drowned middle course of two major ancient river systems, the Katonga and the Kagera-Rufua (de Swardt and Trendall, 1969). The main body of the lake, an enormous oval saucer, is thought to be a result of warping of a former plateau surface and its

associated drainage network. The present lake (Post-Miocene) occupies a position of relative and probably absolute downwarp between swells or dome structures associated with the eastern and western rifts (Temple, 1970). Along much of the lake's perimeter, particularly in the north and south, the shoreline is highly irregular and appears partially drowned. Even coastlines in the southwest and east are associated with old fault zones, strike of resistant rocks, or show characteristics of upwarp (Kendall, 1969). Kavirondo Gulf is bounded by fault scarps forming a miniature rift associated with the eastern rift (Groves, 1934). Where the Katonga River flows into Lake Victoria, its former course is marked by a deep channel passing between the Sese Islands (Fig. 2.8) (Temple, 1970). Accordingly, the headwaters of the Katonga are thought to have arisen at the eastern end of Kavirondo Gulf and are now represented by the River Nyando, which is still flowing in a westerly direction (Groves, 1934).

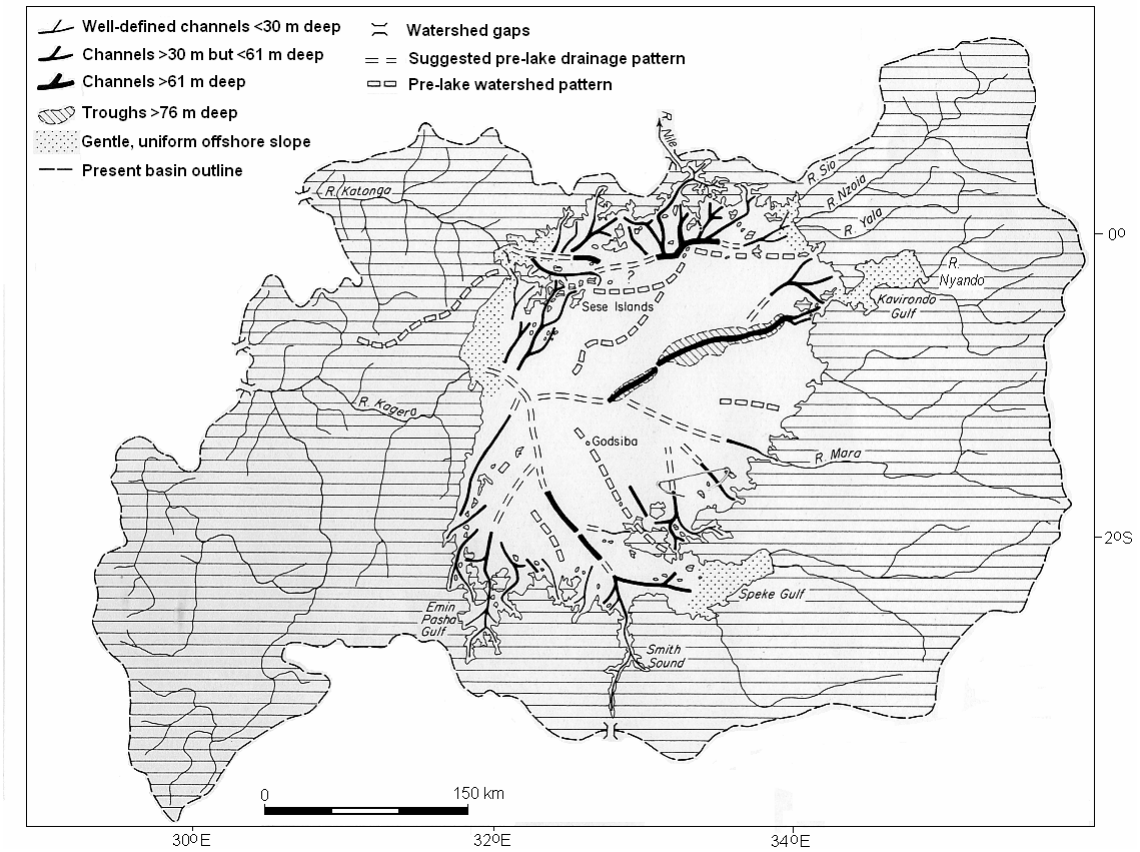

Figure 2.8 The postulated Pre-lake drainage over Lake Victoria basin (adapted from Temple, 1970).

Remnants of the lowland surface (Miocene-Recent) that are suggested to have resulted from these latest episodes of rift-related, volcano-tectonic processes, occupy areas with more resistant rocks. Erosion has washed away the less resistant rocks, like granites, gneisses and mica schists of the Katonga valley, and large areas of central and southern Ankole (Doornkamp and Temple, 1966). To the east the lowland surface is represented on the present lacustrine margins by a slope of low inclination above the valley floors; in the central and south by lowland embayments between the mountains, and in the north by a low, mature landscape.

2.4.2 Stratigraphy and drainage of Lakes Victoria and Kyoga during the Late Cenozoic era

A chronology of the east African climatic changes over the last 50 ka has been developed from the radiocarbon dating of diatom assemblages within the lakebeds (Crul, 1995). Kendall (1969) earlier proposed that ~14.7 – 12 ka B.P. was dry, with ~12 – 10.5 ka B.P., being moderately wet however, whereas ~10.5 – 9.5 ka B.P. became moderately dry, and after ~6.5 ka B.P., the climate got slightly drier and/or more seasonal. Before ~42 ka B.P. (Middle Pleistocene), there were similar climatic conditions to the present, whereas ~42 – 32 ka as well as ~21 – 12 ka B.P. was considered to be colder and drier, according to Taylor (1990). Stager *et al.* (1997) on the other hand distinguished four climatic phases bounded by sudden transitions during Holocene where there was a variably dry period (~11.4 – 10 ka B.P), followed by a humid period (~10 –7.2 ka B.P.), then a more seasonal period (~7.2 –2.2 ka B.P.), and finally there was a more arid period (~2.2 – 0 ka B.P.), with a dry ‘‘Little Ice Age’’ event (~0.6 – 0.2 ka B.P), which is considered to have affected the southern hemisphere. A general drying up or seasonality is posited, which is reiterated by the Trauth *et al.* (2007) theory of a long-term drying trend since the last lake phase periods. Verschuren *et al.* (2000) however, indicates that during the last 1.1 ka, equatorial east Africa had

significantly drier climate than today during the “Medieval Warm Period” (~AD 1000 – 1270) and a relatively wet climate during the “Little Ice Age” (~AD 1270 – 1850) which was interrupted by 3 (~AD 1380 – 1420, 1560 – 1620 and 1760 – 1840) prolonged dry episodes.

Johnson *et al.* (1996) interpreted seismic reflection profiles to show that the eastern two-thirds of the Lake Victoria basin contains a relatively thin (~40 m) sediment cover consisting of about four sequences separated by erosional unconformities. The top unit is almost 8 m thick consisting of dark, organic-rich, diatomaceous muds underlain by a stiff silty clay. Beneath this unit are two units that are highly stratified with a total thickness of about 23 m, probably with a similar composition. The lower, substantially older unit is believed to correspond to the ~15-Ma Miocene lacustrine, fluvial, and volcaniclastic rocks that crop out on islands on the northeastern part of the lake. These highly stratified sequences were interpreted as lacustrine sediments deposited since Lake Victoria formed as a result of ponding of the pre-existing river drainage system. A fourth distinctly stratified sequence observed on the western third of the lake is up to 35 m thick. It tilts upward to the west and lies stratigraphically between the old, indurated sequence and the overlying stratified units in the region to the east. A total sediment thickness of not more than 60 m was estimated within the lake.

Several authors argue that during the last glacial maximum (ca. 20 ka) most of the major lakes in the region were hydrologically closed water bodies (e.g. Kendall, 1969; Talbot *et al.*, 2000). Johnson *et al.* (1996) proposed that Lake Victoria was at least 65 m below its present level at the end of the last glaciation (15-17 ka), which supports the detection of the chemical concentration of calcite in lakebed sediment cores that characterises a closed or shallow basin prior to ca. 12.5 ka (Kendall (1969). Palaeoenvironmental indicators preserved in lake sediments suggest rapidly rising lake levels during the late Pleistocene, and both Lakes Victoria and Albert were filled up by

ca. 10-12 ka (Talbot *et al.*, 2000). By 11.5 ka, it is considered by Talbot *et al.* (2000) from oldest fossil remains that an integrated drainage network similar to the present one was already in existence, and from $^{87}Sr/^{86}Sr$ isotopic data, Lake Victoria must have overflowed no later than this period. Kendall (1969) and Beuning *et al.* (2002) place the transition from closed to open basin conditions following the desiccation of the last glacial maximum at ca. 12.5-13 ka. Further evidence for a short period of Lake Victoria fall and low flow in the White Nile just before ca. 10 ka suggests that the network has almost certainly been episodically disrupted; its level has been controlled largely by downcutting of the Victoria Nile outlet (Kendall, 1969; Talbot *et al.*, 2000).

Groves (1934) earlier observed that the receding levels of Lake Victoria resulted into levels of high terraces from 4-15 m above the present level around Entebbe. Bishop (1959) and according to Kendall (1969), Temple in 1964 documented 5 horizontal raised fossil beaches. The upper 2 strandlines, 61-67 m and 33-38 m above the lake level, were tilted upward (warped) to the west and thought to represent the period before the drainage reversal. Along the northern and southern shores, are the lower 3 horizontal strandlines at 18-20, 12-14 and 3-4 m above the lake level, considered to post-date the tectonic events. Bishop (1969) noted that similar heights have also been mapped along the northeastern shore and the southern Tanzanian shore and suggested that the 18-m strandline denoted a stable basin environment since its development. Only the 3-m beach level near Entebbe was dated in absolute terms at ca. 3 720 ^{14}C yr B.P. (Kendall, 1969). Kendall also described a hinge line of the basin which appears to run north-south through the Jinja area, almost bisecting the lake, with a watershed which is of low relief and close to the lake both to the north and south. On the south side of the hinge line, several authors have noted a water gap at the 18-21 m strandlines above the lake level and to the north are gaps ~21 m above lake level (Kendall, 1969). They suggest that there may have been a brief southward drainage, although these breaches would have

kept the lake level from rising over the 18-m strandline. Kendall argued that whereas the 3-m beach is indicative of climatic changes, the 12-m and 18-m strandlines could not have formed during a pluvial period with the outlet at its present level. As a result, they are most likely related to stages in the erosion of the Nile gorge. This assertion follows the findings of Bisset (1949) who mapped the amphibolites through which the upper gorge had been cut and found that they were highly weathered and broken to depths approximating the present river bed.

Regarding the occurrence of extreme pluvial events following the drainage reversal in the GLRA during the Late Cenozoic era, the areal extent of Lakes Victoria and Kyoga for a 20-m rise in lake levels is simulated. The catchment surface physiography and lake levels are generated using SRTM (2009) altitude data (Fig. 2.9). The present average levels of Lakes Victoria and Kyoga are 1,134 and 1,034 masl, respectively. Figure 2.9a shows that the spatial extent of Lake Victoria would have flooded mainly the inflow river points (especially the Kagera River) as well as southern part of the low lying, north-south hinge line zone. The Kyoga system on the other hand may well have coalesced all the small isolated lakes and wetlands into a broad lake basin that buffered most of the flow from Lake Victoria (Fig. 2.9b). A longitudinal profile to the Victoria Nile of the gradient between Lake Victoria (longitude, $33^{o}12'$ E) at Jinja and Lake Kyoga at Bugondo (longitude, $33^{o}16'$ E) is about 0.7 $m \cdot km^{-1}$. There is relief on the northern shore of Lake Victoria that is capable of ponding the waters and separating the northern part of the Victoria catchment from the Kyoga catchment. Most of the intervening region is hilly, low-relief country which culminates into the wetlands of Lake Kyoga. It is apparent that most of these wetlands would have been submerged in this event. Any fluvial-lacustrine sediments deposited during these events are likely have been swept away or thinly spread out over wide areas by wave action during the recession to current lake levels.

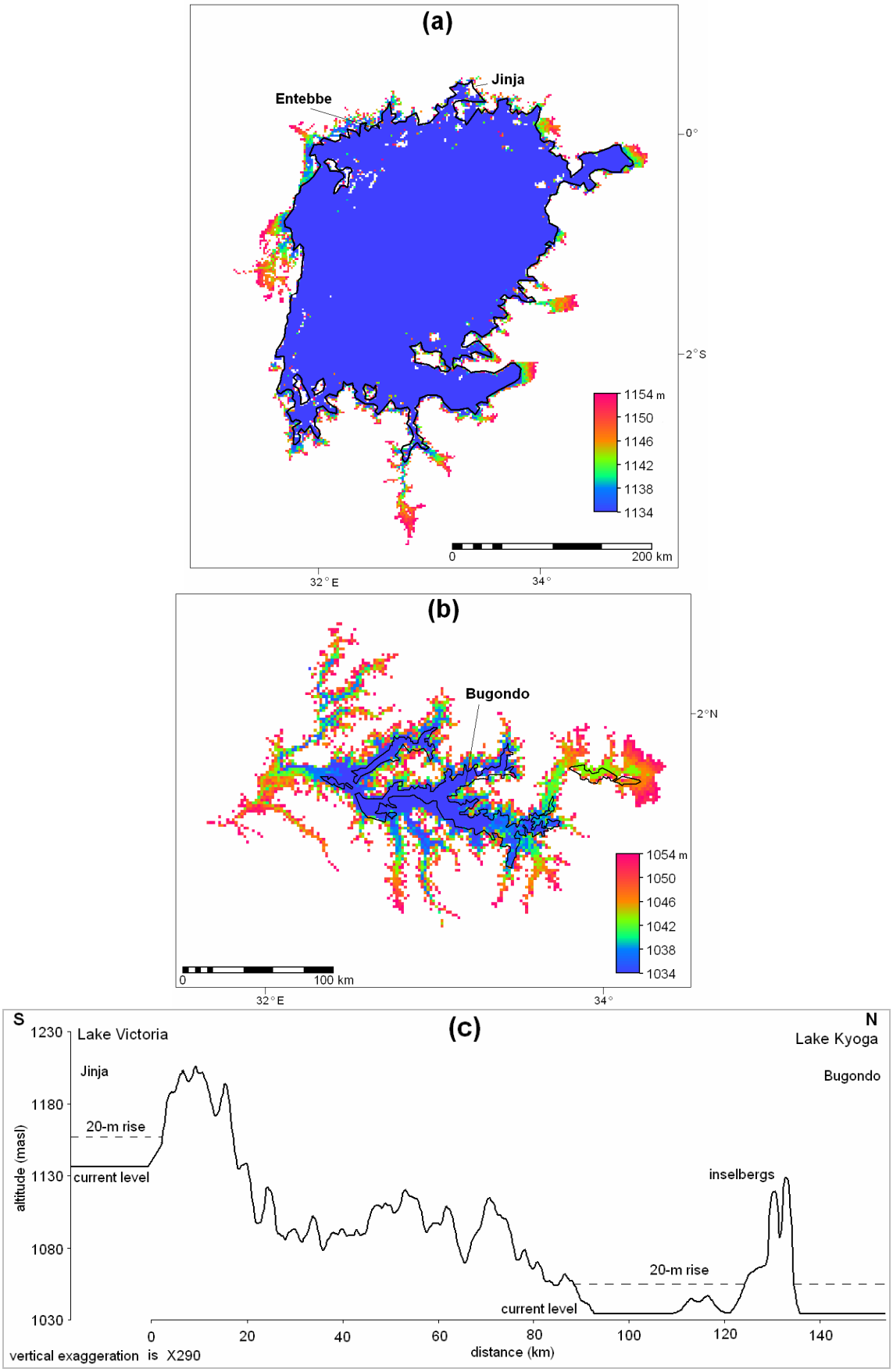

Figure 2.9 Estimated areal extents for the present to a 20-m rise in lake levels for (a) Lake Victoria spatial extents from 1,134 to 1,154 masl (b) Lake Kyoga from spatial extents from 1,034 to 1,054 masl, and (c) longitudinal (S-N) profile (along longitude, 33°14' E) to the Victoria Nile between Lakes Victoria and Kyoga.

2.5 Contemporary regional hydrology of the Upper Nile Basin

The contemporary hydrology of the Upper Nile Basin is dominated by catchments of Lakes Victoria and Kyoga drained by the Victoria Nile (Fig. 2.7). Lake Victoria has a surface area of 69,000 km^2, 4 % of which is occupied by islands, giving a volume of about 2,750 km^3. North and south of the lake the watershed is less than 25 m above lake level (Kendall, 1969). Lake Victoria has an average depth of 40 m and a maximum of 84 m in the northeastern part. The lake is monomictic and its overturn coincides with the onset of the southeast trade winds in the cooler period between May and August, according to Talling in 1966 (cited in Schlüter, 1997). Depths of less than 50 m (typically 4-7 m) are typical of the western and northwestern parts of the lake. Main inflows are from the Rivers Kagera (ca. 30%) to the west, and Nzoia and Gucha-Migori to the east (Sene and Plinston, 1994). The Kagera River rises from over 1,600 masl and is fed by a complex of streams of varying order (Shahin, 1985). The northern lakeshore provides the main outlet, the Victoria Nile that discharges northwestwards through Lake Kyoga with a gradient of about 105 m over a distance of 130 km. It has a water surface width on its upper part that varies between 300 and 600 m. A watershed lies a few kilometres from the northern shore of the lake beyond which the land slopes gently northwards for about 80 km into Lake Kyoga (Carter, 1956). East of Lake Victoria in Kenya is a large drainage network although only a few are perennial streams. The main rivers are simple consequent streams that either radiate from the central highlands or from the Ethiopian foothills to the north (Ojany, 1970). A majority of rivers flowing westwards into Lake Victoria are generally still fast-flowing with waterfalls, rapids, and incision. The lakeshore fringing swamps show a distinct succession of zones associated with the water depths, which include, water-lily zone, fern and sledge zone, papyrus zone, palm swamp, and a fringing forest (Carter, 1956).

Lake Kyoga system has a catchment area of about 60 000 km^2, comprising mainly Lakes Kyoga (1,800 km^2), Kwania (783 km^2), Bisina (130 km^2) and Nakuwa (83 km^2), and about 30 other minor lakes, all totalling about 4,222 km^2 (ILM, 2004). The lake volume has varied with lake level changes since 1962 resulting in an average of 12 km^3 (ILM, 2004). Lake Kyoga has both a lake zone and a flow-through conduit which channels the main upper Victoria Nile waters. It has average depths of 3.5-4.5 m with a maximum of 5.8 m in the lake zone (Temple, 1970), whereas the flow through zone has depths that reach 7-9 m (ILM, 2004). Main inflows apart from the Victoria Nile include Mpologoma, Awoja, Omunyal, Abalang, Olweny, Sezibwa and Enget. Bishop (1969) notes that the Victoria Nile both above and below Lake Kyoga is extremely juvenile and down-cutting its channel at a rapid rate, together with sedimentation has contributed to the lowering of its level. The lake itself comprises a system of shallow lakes frequently filled with swamp vegetation. A dense cover of water lilies (*Nymphaeaceae*) exists over much of the water surface in addition to extensive fringing swamps of abundant papyrus (*Cyperus papyrus L.*) (Carter, 1956). These papyrus beds, floating suds, and water hyacinth mats have been mapped to block the lake outlet especially during heavy rainfall events thus leading to even higher water levels (ILM, 2004). Most of the catchment is largely characterised by a series of low hills and flat valleys with impeded drainage (Shahin, 1985). The majority of the rivers and streams in this northern and northeastern parts of the Victoria Nile basin are seasonal or intermittent. Regionally, drainage is largely dominated by simple consequent steams that have been shaped by the regional tectonic activities. After widening to form Lake Kyoga, the Victoria Nile captures the Kafu River from the west before flowing north to Lake Albert. There is a large fall in base level from about 1,036 masl on Lake Kyoga through a series of rapids and Murchison Falls to about 619 masl into Lake Albert (Bishop, 1969). A late reversal is reputed to account for the shallow Kafu River which joins Lake Kyoga close to the

mouth and for the extensive low-level floodplain flats underlain by grey swamp deposits that border the Kafu and western Lake Kyoga (Bishop, 1969).

2.6 Synthesis of the hydrogeological characteristics of the interface between groundwater and surface waters

2.6.1 Implications of drainage evolution on the groundwater – surface water interface

Within the low-relief surface of the GLRA, the evolution of drainage by rift-related, tectonic processes has generally resulted into landscape features that range from dissected high surfaces dominated by stripping (pediplanation) through depositional landscapes characterised by deep weathering (etchplanation) processes (e.g. Doornkamp and Temple, 1966; Doornkamp, 1968; de Swardt and Trendall, 1969; Taylor and Howard, 1998; Trauth *et al.*, 2005). Upland landscapes feature a majority of swift-flowing rivers that are still youthful with waterfalls, rapids, and incision. Intermediate in altitude, are lowland landscapes made of less defined character forming hilly, low-relief country with generally youthful rivers which culminate into lakes and wetlands. At the bottom, depositional or infill landscapes which occur along valleys on the plateau are occupied by swampy, waterlogged; shallow lakes and wetlands with rivers whose direction of flow is almost indeterminate. These low-relief surfaces in the Upper Nile Basin are dominated by Lakes Victoria and Kyoga, with numerous smaller open surface water and waterlogged depressions at or near the head of the drainage network. Of the surface water bodies within the low-relief surface, dambos are the most ubiquitous and thus studied due to their role in agriculture and water supply to downstream river networks (von der Heyden, 2004). Seasonally waterlogged depressions, known as dambos or locally *mbugas* occur as headwaters of most ephemeral and perennial

streams in subtropical and tropical Africa, like the GLRA (McFarlane, 1992; McCartney and Neal, 1999; McCartney, 2000; von der Heyden, 2004).

2.6.2 Geomorphic evolution of low relief dambos

Dambos have been for long perceived to act as regulators of flow, storing water during the wet season and releasing it during the dry season (Mackel, 1974). Retaining soil moisture during the dry season is critical for agriculture (McCartney, 2000). Generally, dambos are associated with the African crystalline Basement Complex (Acres *et al.*, 1985; Whitlow, 1985; McFarlane 1992). Granite and quartzite commonly weather to sandy soils, whereas the clay soils usually overlie gabbros, basement schists, dolerites, basalts and argillaceous sedimentary rocks (Boast, 1990). Bullock (1992) argues that dambos have shallow, poorly drained, clayey soils with low hydraulic conductivity and permeability that largely form an impenetrable barrier to vertical flow of water between the dambo surface and the underlying regolith. There is still however little consensus of how physiographic properties of dambos interact with those of the surrounding interfluves to influence the hydrology of surface waters.

2.6.3 Hydrology implied by dambo formation

McFarlane (1992) identified two differing models for the origin of dambos. One, known as the *fluviatile model* (Fig. 2.10a), considers dambos as ancient river systems whose valleys have been excavated by direct surface runoff and, subsequently infilled under conditions of progressively reducing flow energy resulting in a succession that fines upwards (gravel and sand at the base and clay at the top). The other, an *in situ model* (Fig. 2.10b) suggests that dambos are bottomlands that occur in areas lowered through the differential leaching of saprolite by chemical and biochemical weathering.

In the fluviatile hypothesis, direct surface runoff or shallow throughflow from the interfluves recharges the groundwater system via the sandy base of the dambo infill. Alternatively, according to the *in situ* weathering model a 'palaeodambo' clay wedge prevents groundwater recharge but throughflow from the interfluves discharges in the sand at the margins of the dambo floors. Thus, the *in situ* weathering model supports shallow aquifer flow into the dambo, with little recharge or no communication between perched aquifer and the underlying regolith aquifer. In contrast, the fluviatile model backs recharge of the deeper aquifer from flow within the perched aquifer, with little groundwater entering the surface water system through the dambo verges. Consequently, the fluviatile model limits groundwater interaction with the dambo.

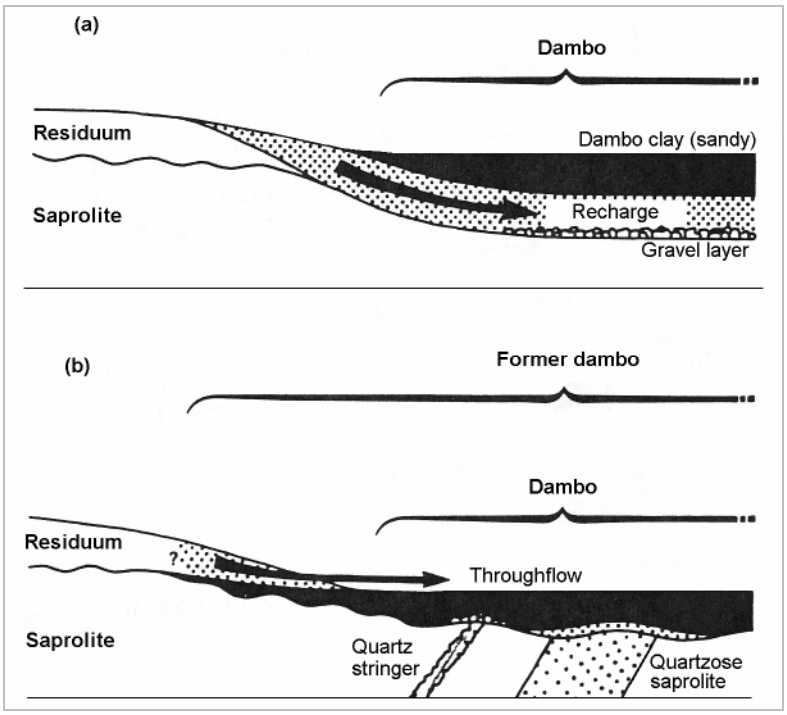

Figure 2.10 Hypothetical stratigraphical profiles for (a) fluviatile (b) *in situ* dambo models (adapted from McFarlane, 1992).

McCartney and Neal (1999) put forward a modification of the McFarlane models. In this model a thick clay wedge separates the dambo from the saprolite. Additionally, there is no support for the perforations in the clay wedge that would allow

upwelling of groundwater from the saprolite to the surface water. Catchment flows are instead derived mostly from shallow water sources. The dambo dries up when the water level in the shallow recharging system falls below the clay layer underlying the dambo. Thus, there are no fluxes between the dambo and the deeper regolith/saprolite layer whose discharge is supposedly linked to an adjacent regional groundwater system.

An earlier model proposed by Bell *et al.* in 1987 (cited in von der Heyden, 2004) is based on an impermeable bedrock/laterite layer underlying shallow interfluve and dambo soils. This model has three groundwater reservoirs due to the variations in the depth of the shallow soils, i.e. the interfluve, upper dambo zone, and lower dambo zone. There is hydrologic connectivity through the three zones during the rain season. When the water table in the interfluve falls, a decline in the hydraulic gradient drives less water into the lower dambo zone, with the seepage zone between the upper and lower dambo layers losing most of the water to evapotranspiration. Consequently, the upper dambo zone remains saturated as the lower dambo zone, dambo bottom and channel all dry up.

Models of the origins of the erosion surface and the dambos are genetically linked. The pediplanation and a fluviatile dambo origin involve similar hydrological and hydrogeological processes. This is markedly different from those of the etchplanation model, which attaches both the origin of the erosion surface and the origin and evolution of the dambos to the infiltration of surface water and its role as a subsurface agent. Consequently, the fluviatile hypothesis is not well connected to the evolution of the rest of the landscape (interfluve) and it does not explain the destination of the large groundwater influx. Conversely, etchplanation is not well connected to the subsequent (later) history of the landscape. The fact that the clay barrier extends throughout the *in situ* weathered regolith requires high regolith permeability to transmit the huge recharge waters to the dambos. These prevailing hypotheses will be tested in this thesis.

2.7 Summary

Deeply weathered surfaces (saprolite) within the Upper Nile Basin are usually capped by a variety of iron-rich to alumina-enriched residua horizons (laterite). Indurated laterites can form considerable storage reservoirs for groundwater with significant permeability when they are strongly jointed. Weathered crystalline basement rocks capped by lateritic profiles often have substantial water bearing horizons within the leached lateritized zone under the cuirass or in the decomposed zone (saprolite/saprock interface) just above the solid rock.

A sequence of rift-related, tectonic processes since early Miocene is considered to have shaped the present landscape of the GLRA and thus influence surface hydrology. In northwestern Tanzania and western Uganda, stream gradients were slightly decreased by back-tilting that resulted in reversal of flow direction towards the Victoria and Kyoga depressions, whereas in Kenya and the northern half of the lake region of Tanzania, stream profiles were significantly steepened.

Two lake types dominate the Upper Nile Basin, those produced by tectonic forces (chiefly Lakes Victoria and Kyoga) and the rest created by coastal or shoreline processes (e.g. Lake Nabugabo) as Lake Victoria receded. Fluvial-lacustrine sediments underlying Lake Victoria show four to five main sequences separated by erosional unconformities totalling up to 60 m thick (Johnson *et al.*, 1996). A diatomaceous sapropel (mud) layer of variable thickness is underlain by stiff silty clay (~8 m thick), followed by a highly stratified layer of suspected similar texture that is tilted upward to the west (~23-35 m thick) which, overlies an old, indurated sequence (related to regional bedrocks).

At the headwaters of most ephemeral and perennial streams in the region are seasonally waterlogged depressions (dambos). McFarlane (1992) put forward two

differing models for the origin of dambos, a '*fluviatile model*' formed by infilling during the progressive reduction in the flow energy of surface runoff (pediplanation), and an '*in situ model*' formed through the differential leaching of saprolite by infiltrating groundwater (etchplanation). These models are considered to be genetically linked to the origins of the erosion surface.

Chapter 3
Hydrostratigraphy of the interface between groundwater and surface water on Lakes Victoria and Kyoga

3.1 Introduction

This chapter provides the first, direct analysis of the lithologic interface between groundwater and surface water within the Upper Nile Basin. This exploratory research enables competing conceptual models for long-term evolution of the landscape and its associated drainage (reviewed in chapter 2) to be tested. The investigation centres around the construction of piezometer nests on the shores of Lake Kyoga at Bugondo and Lake Victoria at Jinja. Lithological and geophysical characterisations of the interface derive from drill cuttings and geo-electrical resistivity profiles and vertical electrical soundings. The deduced hydrostratigraphy includes depth variations in hydraulic conductivity and specific yield estimated from lithologic textural analyses. The hydraulic gradient between groundwater and surface water is determined from a triangulation of initial static water levels in nested piezometers. Hydrochemical (physico-chemistry, major and stable isotope chemistry) observations are used to investigate the connectivity between groundwater and surface waters. Finally, the relationship between the observed lithologic interface and prevailing geomorphic models for the evolution of the interface between groundwater and surface water in the GLRA is reviewed.

3.2 Methods

Combined groundwater-level and lake-stage monitoring stations were constructed on the shores of Lakes Victoria and Kyoga (Fig. 3.1) in areas of contrasting

land use and remote from groundwater abstraction. The Jinja station is next to a busy railways pier on Lake Victoria whereas Bugondo is in a rural farming district, close to a fish-landing station on Lake Kyoga. Reference is also made to an existing piezometer at Entebbe that is situated within the compound of the Directorate of Water Resources Management (DWRM).

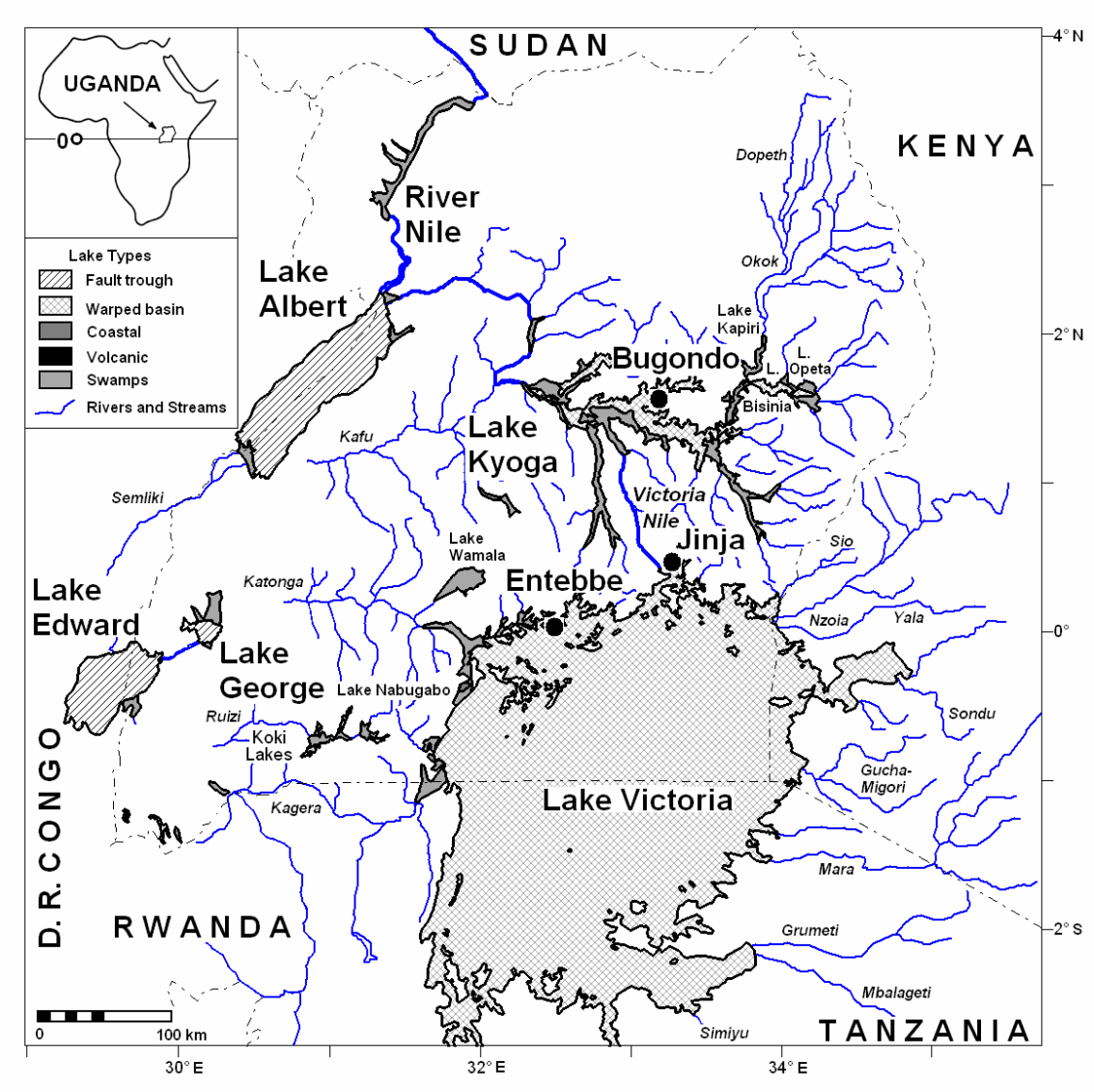

Figure 3.1 Map of regional drainage networks for Lakes Victoria and Kyoga showing the location of study stations at Bugondo, Jinja and Entebbe (modified from Temple, 1970).

3.2.1 Exploratory drilling, lithological sampling and nested piezometer installation

At each monitoring station, a nest of 3 piezometers was constructed to triangulate the direction of groundwater flow (Brassington, 1998) adjacent to surface waters. The installation of each piezometer enabled direct physical (lithological) investigations of the interface between groundwater and surface water. Construction of the network of piezometers at each station was carried out from 10-17 November (Jinja) and 21-25 November 2007 (Bugondo). Station construction and development was done by the AQUATEC Enterprises (U) Ltd. under direct supervision. The first station is located in the Old Boma, Jinja Municipality, Jinja District (Fig. 3.2), whereas the second one is in Opucet village, Bugondo Sub-county, Soroti District (Fig. 3.3).

Each piezometer was drilled with a direct rotary drag drill bit powered by a petrol-driven motor (Honda GXV 120, 4.0 HP, 3.0 KW, 118 cm^3) and facilitated by mud pumped under pressure by a diesel-driven motor (PAT-self priming pump, model KND-40, 6-9 HP, 2,000 rpm). Mud loosened the materials, lubricated the drill bit and ensured a stable borehole. Each drilling pipe flight was 1.5 m long. Drilling was done with a 6-inch (15.2 cm) diameter bit, except where the formation was hard when a 4-inch (10.2 cm) diameter bit was used. Several m^3 of drilling mud were required to facilitate the drilling process. On reaching required depths, an 8-inch (20.3 cm) diameter bit was used to ream the borehole in order to create adequate annular space for the gravel pack. The drilling rig was slow to penetrate the duricrust and, in one case, a borehole (BP03) was abandoned after drilling up to a depth of ~10 m. Lithological descriptions were made whenever a change in the texture and colour of the materials occurred and at least every 1.5 m intervals with a change in the drilling pipe flight lengths. Changes in lithology were also deduced from the rate and steadiness or jerkiness of the drilling penetration. Formation cuttings (0.5 kg) were sampled after excess water was removed.

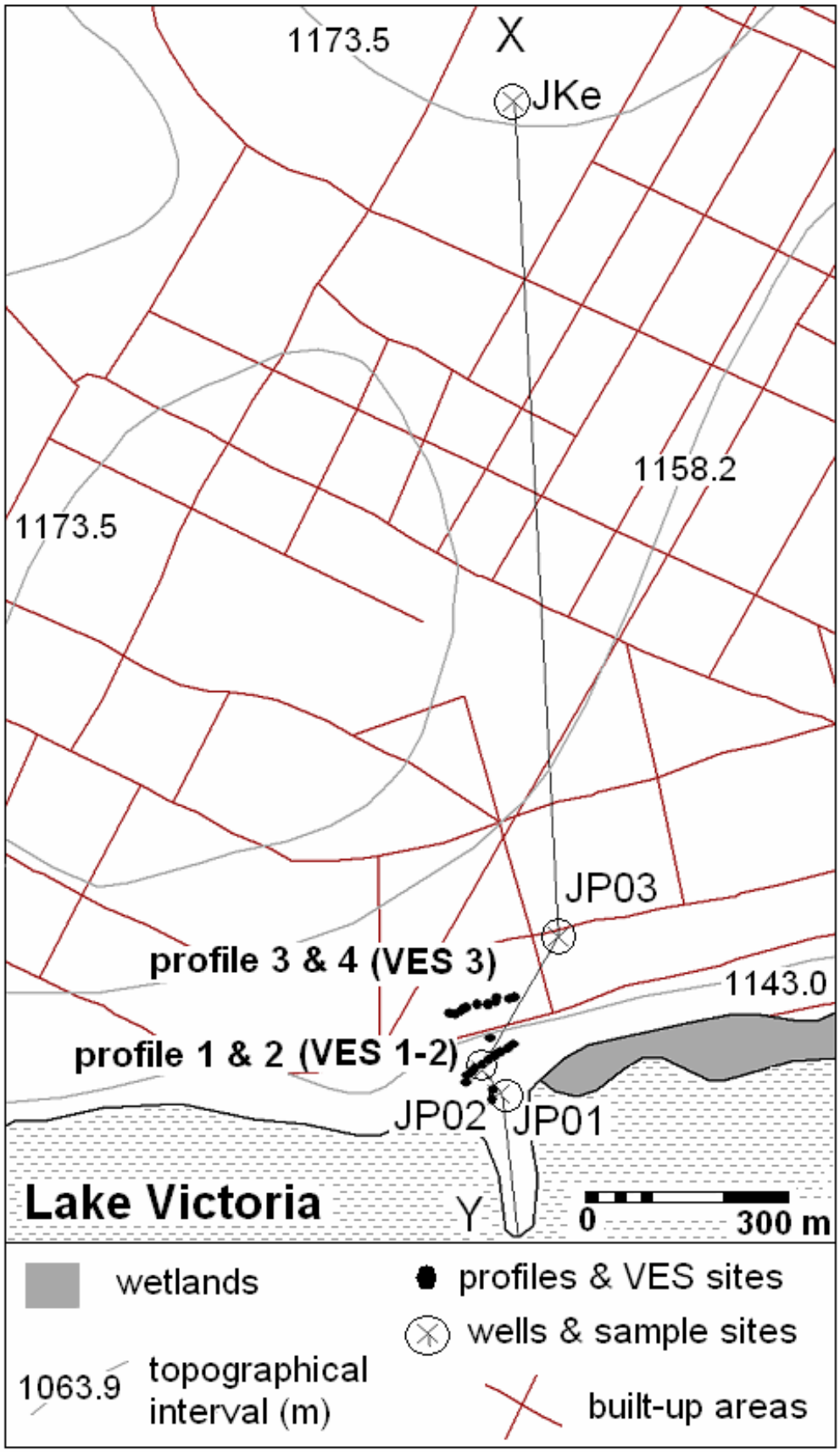

Figure 3.2 Constructed piezometer nest on the shore of Lake Victoria at Jinja.

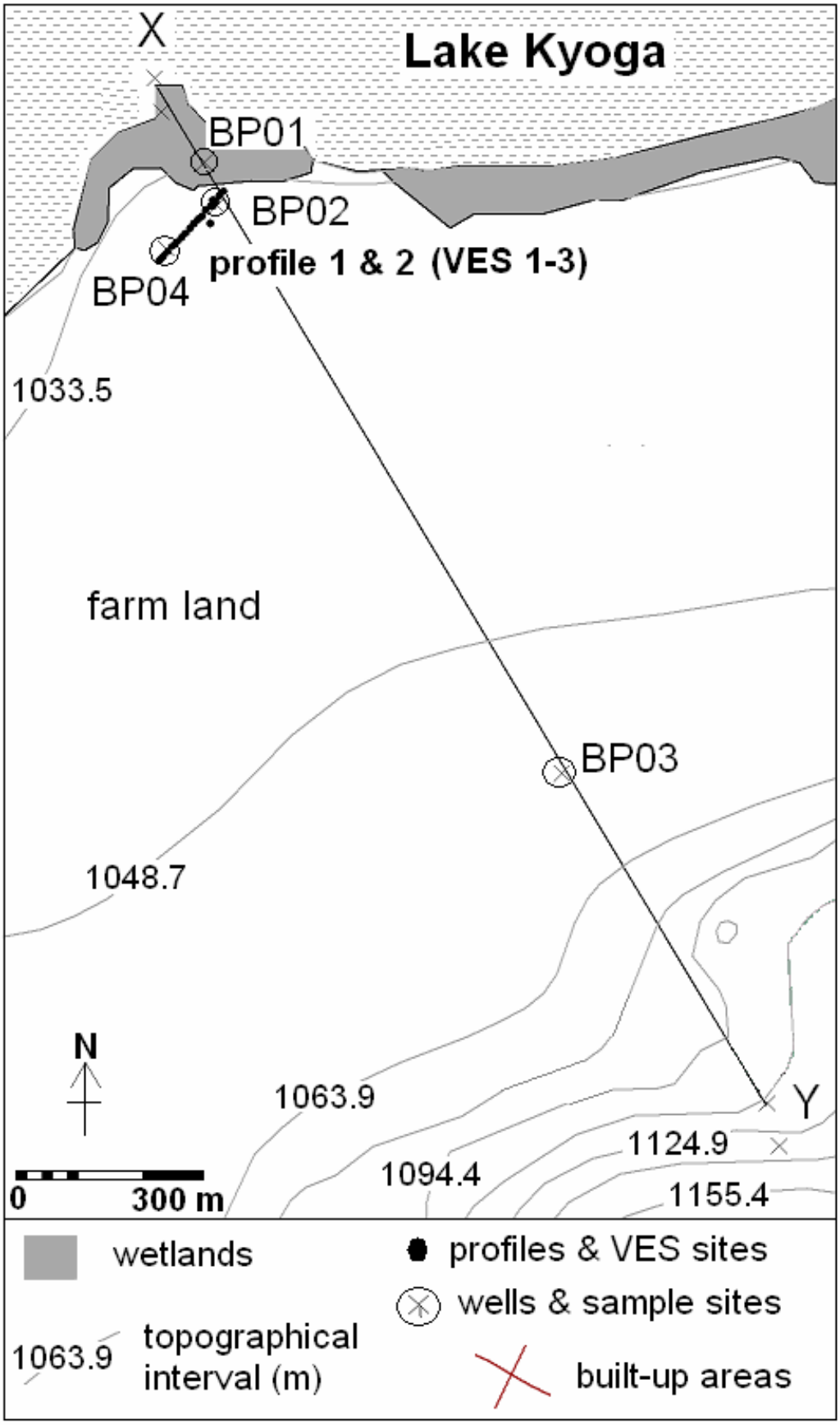

Figure 3.3 Constructed piezometer nest on the shore of Lake Kyoga at Bugondo.

Aller *et al.* (1989) list the limitations to mud drilling which include *inter alia*: (1) hampering the identification of water-bearing zones; (2) difficulty in removing drilling mud and wall cake from outer perimeter of filter pack during development; (3) the influence of drilling fluid additives on quality of groundwater samples; (4) circulated (ditch) samples being poor for monitoring well screen selection; and (5) the possibility that drilling fluids invaded permeable zones which can compromise subsequent sampling. Since it was difficult to follow the mud maintenance procedures during drilling, there is some uncertainty about the precise depth intervals of retrieved samples; mixing from different depths could have occurred and a portion of the fines (clay and silt) may well have been washed out. Accordingly, borehole logs are further tested against lithological profiles deduced from surface geophysics in order to estimate the depth of the weathered zone.

At Jinja, piezometer JP01 was drilled to 12 mbgl (Fig. 3.2). Two water-bearing horizons were struck between 0.5-3 (low yield) and 7.5-12 mbgl, and both zones were screened. Site JP02 reached 21 mbgl, with two water-bearing zones, from 0.5-3 (low yield) and 12-21 mbgl; both layers were screened. Site JP03 was drilled up to 24 mbgl and yielded a single water-bearing horizon (15-24 mbgl) which was screened. At Bugondo, piezometer BP01 reached 15.5 mbgl, the bottom 2 m of the well collapsed before the installation of the well casing (Fig. 3.3). Two water-bearing formations from 0.5-3 (low yield), and 9-15 mbgl were encountered and both of these horizons were screened. Piezometer BP02 was up to 19.5 mbgl but similarly the deepest 2.5 m of the borehole collapsed. Two water-bearing zones from 0.5-4.5 (low yield) and 13-19.5 mbgl were encountered but it was only possible to install a screen through the deeper groundwater layer to 16.5 mbgl. Conversely, piezometer BP03 reached 10 mbgl but was abandoned because the drilling bit could not penetrate the duricrust. Piezometer BP04 was drilled up to 14 mbgl when again drilling failed to penetrate the cuirass. There were

several duricrust levels (6.2-7.5, 8.5-9, 11.5-12.5, and from 12.8 mbgl) with water-bearing zones realised at 1-3 (low yield) and 8.5-12 mbgl. It was not possible to ream the borehole to the 8-inch (20.3 cm) diameter beyond 13.2 mbgl, owing to the occurrence of several lenses of duricrust, and so both water-bearing zones were screened.

3.2.2 Lithological analyses

Lithological characterisations included the colour of collected drill bit cuttings which was assessed in relation to the Munsell soil colour charts (2000 edition). Sediment samples were wet-sieved using nylon sieves. Size ranges were weighed after drying (60^{o}C) in an oven overnight within the Department of Geography, UCL laboratories. Sieve mesh sizes followed the Wentworth (1922) classification that included <0.004 mm (clay), <0.063 mm (silt), <0.125 mm (very fine sand), <0.25 mm (fine sand), <0.5 mm (medium sand) and >0.5 mm (coarse sand and gravel). Clay and silt particles were distinguished from the <0.063 mm sediment fraction using a Micromeritics Sedigraph III particle-size analyzer with a MasterTech 52 autosampler. Sediments were considered to be free of organics except for the top 50 cm of the wetland soils and sediments, and therefore not removed by pre-treatment. It is conceivable that drying may have altered the properties of these weathered sediments so that the grain size distribution may have been slightly modified from that which occurs under natural field conditions. The clay fraction in the lateritic sediments may also be much higher than detected due to the influence of accumulated iron oxides in binding particles to form larger aggregates in these weathered mantle materials (Taylor and Howard, 1999a).

3.2.3 Major and isotope water chemistry

Hydrochemistry provides information about the aquifer environment and the history of groundwater movement enabling flux rates and the travel times as well as mixing of different water types to be described (Lloyd and Heathcote, 1985). Analysis of physico-chemical parameters in groundwater was conducted *in situ* (procedures certified by the International Organisation of Standardisation,) after well development and during hydraulic tests by pumping water from the piezometers via a flow-through cell. Physico-chemical parameters include Dissolved oxygen (DO), pH and temperature, and electrical conductivity (EC) (Table 3.1). All these field meters were calibrated with standard buffers prior to use in the field. Water samples (1 litre for major chemical and 25 ml for stable isotopic analyses) were collected into capped PVC bottles, placed in coolers and out of sunlight while in transit to laboratories. Determinations in the laboratory include major ions (K^+, Na^+, Mg^{2+}, Ca^{2+}, HCO_3^-, SO_4^{2-}, Cl^-) and trace elements and ions (total Fe, F^-, PO_4^{3-}, NO_3^-). Analyses were carried out at the Water Quality Control Laboratory, Entebbe, Uganda, where quality control procedures were followed based on ISO 17025 after the analytical procedures of Eaton *et al.* (1995).

Table 3.1 The parameters, methods and tools used for the *in situ* and laboratory hydrochemical analyses.

parameter	Method/tool
DO	Hanna HI 9146 dissolved oxygen meter (ISO 5814: 1990)
pH and temperature	Hanna HI 991003 pH/ORP/temperature meter (ISO 10523: 2008)
EC	Hanna HI 9835 EC/TDS/NaCl/^{0}C meter (ISO 284: 2003)
Major ions (K^+, Na^+, Mg^{2+}, Ca^{2+}, HCO_3^-, SO_4^{2-}, Cl^-)	Photoelectric flame photometry and atomic absorption spectrometry
total Fe	Calorimetry
PO_4^{3-} and NO_3^-	Photometry
F^-	Ion selective electrodes
Isotopes (δ^2H, $\delta^{18}O$)	Thermo-Finnigan isotope ratio gas-source mass spectrometers (MAT253, Delta V Advantage, Delta Plus XP)

In addition to these conventional methods, investigations included analysis of stable isotopic tracers (δ^2H, $\delta^{18}O$) in water samples. Hydrogen is omnipresent in terrestrial environments in different oxidation states (e.g. H_2O) and plays a major role in a wide variety of geological processes (e.g. hydrolysis). Oxygen is the most abundant element in the earth's crust and occurs in several phases which are thermally stable over large temperature ranges. Stable isotope ratios of hydrogen ($^2H/^1H$) and oxygen ($^{18}O/^{16}O$) in the collected water samples were analysed and reported as deviations from the standard, VSMOW (Vienna Standard Mean Ocean Water standard), according to equation 3.1 (Lloyd and Heathcote, 1985; Coplen, 1993; Hoefs, 1997) where δ, is the deviation from the standard expressed as per mille ($^o/_{oo}$).

$$\partial^{18}O_{sample} = \frac{(^{18}O/^{16}O)_{sample} - (^{18}O/^{16}O)_{VSMOW}}{(^{18}O/^{16}O)_{VSMOW}} \times 1000 \qquad (3.1)$$

Hydrogen and oxygen isotopes in precipitation fractionate in proportion as a function of largely ambient temperature (Craig, 1961; Mazor, 2004). Lower temperature supports more fractionation due to lower vapour pressure exerted by heavy isotopes which leads to their depletion. The two isotopes in global precipitation regress along the global meteoric water line (GMWL) with a slope of 8 (Craig, 1961), i.e. $\delta^2H = 8*\delta^{18}O + 10$. Deviations from the GMWL are considered to be due to other isotopic processes, such as, evaporation from open water (slope of ~5, Craig, 1961), exchange with rock minerals, or CO_2 exchange (Fig. 3.4). Groundwater - surface water interactions often lead to depleted ^2H and ^{18}O in groundwater relative to surface water due to the fact that rainfall-fed, groundwater recharge is more depleted in heavy isotopes than surface waters (Coplen *et al.*, 2000). Seasonal variability of ^2H and ^{18}O in lake water can be

used to determine relative quantities of recharge or even recharge velocities if dispersion does not mask these variations (Coplen, 1993).

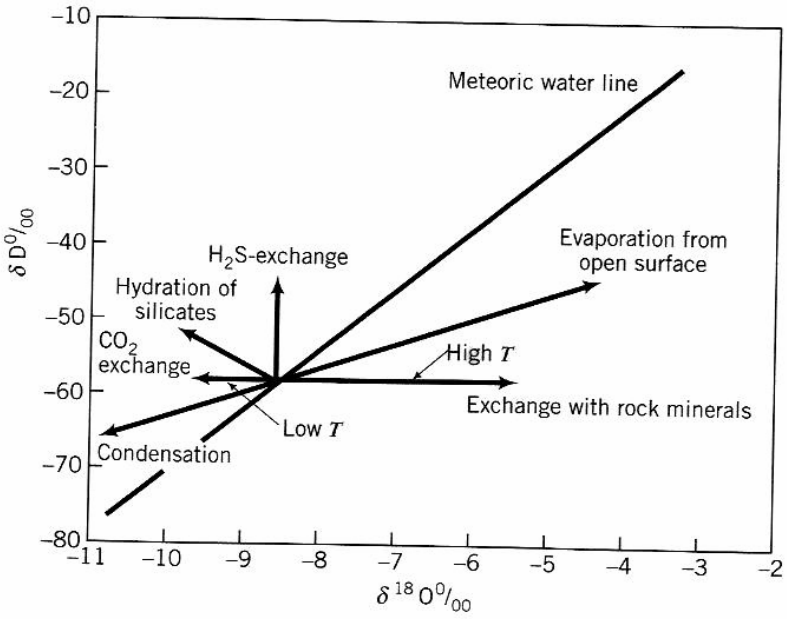

Figure 3.4 The deviations of the isotopic (δ^2H and $\delta^{18}O$) from the GMWL as a result of the influence of various processes (adapted from Domenico and Schwartz, 1998).

Stable isotope analyses were carried out at the Bloomsbury Environmental Isotope Facility in UCL using a gas-source mass spectrometer (Table 3.1). Uncertainty in the $\delta^{18}O$ analyses was ±0.05 $^{o}/_{oo}$ based on three lines of evidence, (i) 20 repeat analyses of a lab standard had this standard deviation, (ii) analysis of the differences between duplicated analyses of 68 water samples carried out in different runs gave 0.044 $^{o}/_{oo}$ as the standard deviation for a single analysis by the Method of Replicates, (iii) 5 analyses of the IAEA (International Atomic Energy Agency) standard water GISP (Greenland Ice Sheet Precipitation) gave mean -24.81 VSMOW $^{o}/_{oo}$ with standard error of 0.023, whereas the accepted value for this standard is -24.8±0.05 VSMOW $^{o}/_{oo}$. Monthly variations in the stable isotopic ratios (δ^2H and $\delta^{18}O$) for precipitation at Entebbe (1961-1974) were obtained from the IAEA (ISOHIS-WISER) website (Taylor and Howard, 1999b) and combined with more recent data (1998-2004) provided by DWRM. Additionally there were spot measurements for Lake Victoria, groundwater

(boreholes, springs, shallow wells) and rivers flowing into Lake Victoria, and from Taylor and Howard (1999b) in the Upper Nile region.

3.2.4 Piezometer installation

Each piezometer was developed by the air-lift method (Table 3.2). High pressure provided by a diesel-driven pump (Yanmar CAGIVA S.p.A., L100AE-DTMRYC; 7.4 KW - 10 ps/3,600 rpm), was used to remove fine materials from the vicinity of the piezometer. Injection of compressed air at a point below the water level in the piezometer results in a mixture of air bubbles and water, which being lighter in weight than water outside the discharge pipe, forces the air/water mixture out of the well. The process served to remove any mud 'cake' that resulted from drilling. Static groundwater levels were measured using an Eijelkamp groundwater level meter after the stabilisation of water levels upon completion of well development (Table 3.2). A flight of casing (4-inch or 10.2 cm diameter) was then installed to the bottom of the piezometer. Continuous casing comprises reinforced PVC in 2.84-m lengths; well screens include horizontal slots (~1-mm sized openings) cut into 2.84-m PVC pipes. A sand trap (0.5-m depth) made up of continuous PVC casing was placed at the bottom of each piezometer. Well design was determined by the depth and number of the groundwater-bearing zones. Silicic gravel (sieved lake bottom gravel, >0.5 mm diameter) was packed around the well annulus to enable free water inflow from water-bearing zones. The top of the gravel pack was then sealed with cement (Portland cement mixed with sands) and the annular space above it backfilled with the formation materials. Around the top of the wells, a cement sealing was cast about the well rim area to prevent infiltration of contaminants and flood waters. Metallic casing (8-inch or 20.3 cm diameter) of 1-m depths enveloped the top of the piezometers and was padlocked. Piezometers were surveyed relative to the lakes datum using a Kern dumpy level theodolite and a

measuring staff. An existing monitoring well in Entebbe was constructed in 1999 at a distance of about 140 m from Lake Victoria shore. It was drilled to a depth of 48 mbgl with the water struck from 21 mbgl, and was screened from 18 mbgl.

Table 3.2 Monitoring well construction (2007) parameters in Jinja and Bugondo, including the long-term (1999) monitoring well at Entebbe.

Site	Altitude (m)	Depth (mbgl)	Screen length (m)	SWL (mbgl)	Airlift discharge ($m^3 \cdot h^{-1}$)	Development (h)
JP01	1,135.96	12.0	5.68	0.0	0.7	8
JP02	1,136.55	21.0	8.52	0.0	0.8	2
JP03	1,149.30	24.0	8.52	11.9	1.7	8
BP01	1,033.90	13.6	5.68	0.0	2.4	4
BP02	1,035.92	17.0	8.52	2.1	2.2	2
BP03	1,079*	-	-	-	-	-
BP04	1,035.87	13.2	8.52	1.67	2.0	4
DWRM	1,141.26	48	n/a	5.26	8.8	n/a

*Handheld Garmin® etrex summit GPS receiver reading; n/a: not available.

3.2.5 Surface geo-electrical resistivity surveys

Rocks and minerals exhibit large variations in electrical conductivity. It is thus possible to measure potentials, currents, and electromagnetic fields that occur naturally or are artificially introduced. Of the several electrical properties of rocks and minerals, electrical conductivity (or the inverse, electrical resistivity) is by far the most important (Telford *et al.*, 1990; Binley and Kemna, 2005). Since the earth is inhomogeneous, measured potentials can differ, when current is introduced into the ground, from those calculated under the assumption that the ground is homogenous (Parasnis, 1997). Most geological formations contain interstitial water with dissolved salts which provide ionic conductivity. This ionic conductivity then depends on the moisture content, nature of the electrolytes and degree to which voids (pores, microfissures, cracks, fractures, etc) are saturated with water (Parasnis, 1997). Groundwater commonly has resistivity values of 10-100 ohm·m depending on the concentration of dissolved salts. Furthermore,

saturated fractured rocks normally have relatively low resistivities whereas the resistivity of clay-rich formations depends upon the proportion of clay minerals to other materials (Parasnis, 1997).

Schlumberger arrays were used to determine the variation of electrical conductivity with depth and estimate the thickness of the weathered overburden (saprolite) assuming minimal lateral variations (Telford *et al.*, 1990; Parasnis, 1997; Binley and Kemna, 2005; Cassiani *et al.* 2006). The approximate depth of penetration at each specific electrode spacing was estimated from the empirical relation devised by Edwards (1977) where there is an effective depth of penetration for each array configuration yielding a specific apparent resistivity. Effective depth is defined as the depth at which exactly half the total resistivity signal originates from above and the other half from below and is, in effect, the median depth of investigation. Considering that there are always lateral variations, electrical resistivity profiling was also conducted to detect local, relatively shallow heterogeneities, such as the boundary between the fluvial-lacustrine sands and the saprolite. Instrument noise, site cultural features (e.g. power lines, buildings), and telluric currents (e.g. naturally occurring earth currents, self potentials, magnetotelluric currents) can all influence observed resistivities.

Vertical electrical soundings (VES) and resistivity profiles (Binley and Kemna, 2005) were carried out at Jinja (Fig. 3.2) and Bugondo (Fig. 3.3) monitoring stations initially in August 2007 and again in July 2008. Hand augers which were also dug next to each of the profiles and VES sites closest to the lakes struck the groundwater zone at shallow depths (0.5 - 2 mbgl) from which lithologic samples were also collected in August 2007. The VES arrays involved keeping the inner electrodes fixed (1 m apart) while moving outer electrodes outwards symmetrically in specified steps from 3 m to a maximum of 116 m apart. This electrode array spacing was designed to ensure that the lithological changes at shallow penetration depths were identified based on the available

borehole logs. From an outer electrode distance of 26.4 m, an overlap of measurements was taken for an inner electrode distance of 10 m in order to maintain the reading accuracy of the resistivimeter (ABEM Terrameter SAS 300C). In Jinja, VES were made about 50 m apart and from Lake Victoria shore (Fig. 3.2). Another VES was conducted about 100 m from the other two at a higher altitude along an old shoreline of Lake Victoria. Three VES were carried out in Bugondo at about 50 m apart and from the Lake Kyoga shore (Fig. 3.3).

Resistivity profiling maintained a fixed spacing between the electrodes as the entire array was moved along a straight line at 10-m intervals. In Jinja, four profiles both generally trending northeast-southwest were measured at two locations (Fig. 3.2). The first two profiles spanned VES 2, whereas the second two profiles were astride the VES 3 site. Two resistivity profiles trending northeast-southwest were mapped on one location in Bugondo for outer electrode distances of 8.8 m and 55 m, respectively (Fig. 3.3). At each of the two Jinja sites, the profiles were mapped at outer electrode distances of 8.8 m and 38 m, for inner electrode spacing of 1 m and 10 m, respectively.

A one-dimensional simple inversion model of the subsurface (Loke, 2004) was used to interpret VES data. These models simulate actual ground resistivity using the apparent resistivity data measured with the array configuration. Assumptions include the presence of horizontal layers in the subsurface where resistivity changes only with depth but remains constant laterally. Important limitations with this approach include non-linear (i.e. complex relation between data and model) and non-unique (i.e. more than one model fits data) nature of solutions (e.g. Binley and Kemna, 2005). Constraints therefore are imposed and based upon observed lithologic layers, i.e. fluvial-lacustrine sands, saprolite and saprock/bedrock. Indeed, there is a danger of over-interpreting the results that includes the unsubstantiated assignment of multiple lithologic layers. The software, RES1D.EXE was used as it has been found to provide sensible results in

geological situations where the one-dimensional model is appropriate (Loke, 2004). The number of model input layers was constrained by the well logs that were obtained during the construction of the observation stations.

3.2.6 Estimates of hydraulic properties from lithologic texture

Saturated hydraulic conductivity (K) of the sediments with depth was estimated from particle-size analyses using the empirical relationships devised by Hazen and modified by Shepherd (Cronican and Gribb, 2004) (equation 3.2), where K_s is expressed in cm·s^{-1}, c is a constant from 0.05-1.18 but can reach a value of 9.85, with an average value of 0.625 applied, and e is an exponent from 1.11-2.05 with an average of 1.72 which was used, D_{10} is the particle diameter (mm) for 10% of all particles finer by weight.

$$K_s = cD_{10}^{e} \qquad (3.2)$$

Both values of c and the e are typically higher for well-sorted samples with uniformly sized particles and highly spherical grains (Cronican and Gribb, 2004). Sobieraj *et al.* (2001) suggest that it is inadequate to estimate K_s derived from empirical relationships consisting of particle size distribution, bulk density and saturated moisture content information, due to the controlling influence of soil macroporosity (e.g. from high fine plant root density) on K_s in the top horizons (0.4 m depths). Macropores were not observed and are not considered to exert a dominant influence over lithological depths that have been logged.

Kasenow (2008) carried out 2,000 laboratory tests on undisturbed samples of all soil types, as well as 100 *in situ* hydraulic conductivity tests to estimate specific yield from hydraulic conductivity. The relationship that was developed is applicable for sediments with a texture that is finer than coarse-grained sand with K values less than

61 $m \cdot d^{-1}$. All sediments sampled satisfy these requirements. It is however possible that bimodal particle-size distributions commonly encountered in weathered soils (Taylor and Howard, 1999a) introduces uncertainty in the relationship between particle size and both K and S_y.

3.3 Groundwater – surface water monitoring stations

3.3.1 Soils and geology on Lake Kyoga station at Bugondo

The monitoring station at Bugondo is located along the southern shore of the main northeasterly arm of Lake Kyoga (Figs. 3.1 and 3.3). The depth of Lake Kyoga near Bugondo is 3-4 m but reduces towards the narrower arms. Wider parts of the lake are largely open water fringed by papyrus and perhaps water-lilies. Often the narrower arms are completely covered with water-lilies and papyrus (Hurst, 1925). To the southeast of the Bugondo station a gentle gradient gradually rises for about 1 km to the NE-SW trending amphibolite ridges that form a pronounced physical boundary (Fig. 3.3). On the Bugondo hills, upslope soils have developed on resistant rock features, which form skeletal (shallow) soils on steep rocky slopes (leptosols), with no laterite from the parent AGGC quartzites (Cheney, 1960). Along the shore of Lake Kyoga in Bugondo, there are soils comprising peat, peaty sands and clays (histosols). Interfluves have shallow grey brown sandy loams over laterite (petric plinthosols - acric). These soils supported cotton growing in the past but have since been diversified to include a wider range of crops, such as millet, sorghum, cassava and sweet potatoes. The geology of Bugondo forms part of the largely unmapped regions that are considered to constitute Precambrian (Bunyoro-Kyoga Series) mudstones, sandstones, arkoses, conglomerates and silicified rocks. Low-lying areas adjoining Lake Kyoga form part of the study area and are covered by lateritised fluvial-lacustrine sediments.

3.3.2 Soils and geology on Lake Victoria station at Jinja

The monitoring station at Jinja is located on the northern shore of Lake Victoria close to its outlet (Figs. 3.1 and 3.2). It forms a narrow <400 m shoreline that sharply rises to form a shelf that runs parallel to the lakeshore and is considered to make a former shoreline (Temple, 1966) (Fig. 3.2). Papyrus swamps line the shore between the monitoring station and the lake. Carter (1956) describes finding similar habitats for both the lakeshore swamps on Lake Kyoga and the northern shore of Lake Victoria. The littoral regions of the lakes, fringed by papyrus, show a succession of zones between the open water and the shore, each with its own plant community. This succession is variable, but generally includes from the open water the water-lily, fern and sedge (often absent), papyrus (*Cyperus papyrus*), to grass swamp zones on the shore side.

Jinja is the second largest commercial centre in the country with a population of over 100,000, lying on the northwestern edge of the Napoleon Gulf which leads to the outlet of the Victoria Nile (Fig. 3.2). It was the old industrial centre of the country which hosted several agricultural and metal processing industries due to the proximity of the Nalubale hydroelectric power station at the outlet of Lake Victoria. The station is found in a low-lying swampy strip that is bounded by a northwest trending platform (~8m high) that gradually rises eastwards through the town where it forms a broad relatively flat surface. Further north and eastwards, the landscape features several laterite-capped mesas and inselbergs. Soils in Jinja comprise dark red clays that are lateritic and ferruginous (Carter, 1956) (nitisols), developed on amphibolite and phyllite which uniformly cover the interfluves from the lakeshore, and support cotton and sugar with a high productivity (Cheney, 1960).

The geology of the Jinja region is considered to be part of Buganda group of the BTS (section 2.2.1). Lithologies within this group include basal quartzites separated by

pelitic rocks, which are overlain by slates, some phyllites, schists, and shales, succeeded by basal volcanics, amphibolites and tuffs with some ultrabasic rocks (Schlüter, 2006). Massive actinolite-bearing local amphibolites occur along both banks of River Nile. These amphibolites grade into sediments where intercalated tuffs derived from a basic volcanic sequence is indicated (Schlüter, 2006). Thicknesses of the Buganda group are variable. Near Jinja, the BTS is estimated to be up to 1 km and elsewhere may reach 7 km (Pallister, 1959). Bisset (1949) summarised the local geology of the Jinja area. Mica schists occupy a belt trending northeast-southwest running beneath the Napoleon Gulf, which is highly eroded to form the Napoleon Gulf and is considered to have aided in the formation of the outlet of the Victoria Nile. Shales dominate the north and northeastern parts of the town, and are of variable resistance forming a few hills downstream of either sides of the Victoria Nile. Amphibolites underlie the southern, eastern and western parts of the town as well as the bed of the Victoria Nile. These rocks are consolidated, hard and resistant on the interfluve but are highly weathered on the banks of the lake and river. At the outlet of the Victoria Nile, except for the quartzite ridges and a few amphibolite outcrops, the area is covered by an extensive weathered zone normally capped by laterite (Way, 1939; Bisset, 1949). Generally, the thickness of the weathered zone adjacent to the Victoria Nile is on average 6-15 m on the western bank compared to 6-27 m on the eastern bank (Brown and Gittins, 1959).

3.3.3 Soils and geology on Lake Victoria station at Entebbe

The monitoring station at Entebbe lies within a peninsula that runs approximately NE-SW on the northwestern shore of Lake Victoria (Figs. 3.1 and 3.5). Shallow swampless bays on the eastern shore exhibit similar orientation; longer axes of papyrus-choked indents of the western coast are at right angles to this direction (UGS, 1921). Papyrus swamps west of Entebbe fill some of the indentations along the coast

(Hurst, 1925). The action of prevalent winds which blow from the lake is to bank up fine sand in the eastern bays, and it is for this reason that indentations of the east coast are swampless and much less marked than those of the west (UGS, 1921). The peninsula has a southwesterly extension from the northern shore of Lake Victoria to the Nsamizi hill in the northeast (Fig. 3.5). An airport occupies the low-lying expanse of land that separates this hill from the two smaller hills to the southwest. All these hills form an undulating terrain sloping to the lakeshore in a marked series of platforms or low steps, which give rise to shoreline cliffs (pronounced on the southeastern coast) as well as low-lying swampy areas (Du Bois and Jeffery, 1955). Low-lying swampy fringes of the peninsula have gleysols whereas the higher areas are dominated by reddish brown sandy loams on red clay loams (acric ferralsols) (Cheney, 1960).

The tip of the Entebbe peninsula is underlain by undifferentiated (migmatic and grandioritic) gneisses of the AGGC. A local strip of Karoo (Ecca age from fossil plant remains) shales covers about 2 km wide in an infaulted east-west trend across the southern end of the peninsula with schists and quartzites on the north side and gneissose granite on the south (Schlüter, 2006). Within the Karoo beds, Brown (1950) determined thicknesses of 415 m in the west increasing to 470 m in the east by gravimetric surveys. Well logs to 357 m depth yield white, buff and red-brown shales that grade to grey to black with depth, with many pyritic horizons and traces of carbonaceous matter, as well as some sandy and calcareous beds (Schlüter, 1997). It is believed that the interbedded sandy and calcareous members form the water-bearing zones. Small lenses of BTS quartzites are also present in the region, which are also associated with phyllites to the south. Within the lower relief areas next to Lake Victoria are fluvial-lacustrine sediments (mainly on the northwestern side of peninsula), which constitute gravel and sand found at several points along the shoreline. In some of these places, they have been severely lateritised and form pavements of surface ironstone (Pallister, 1959).

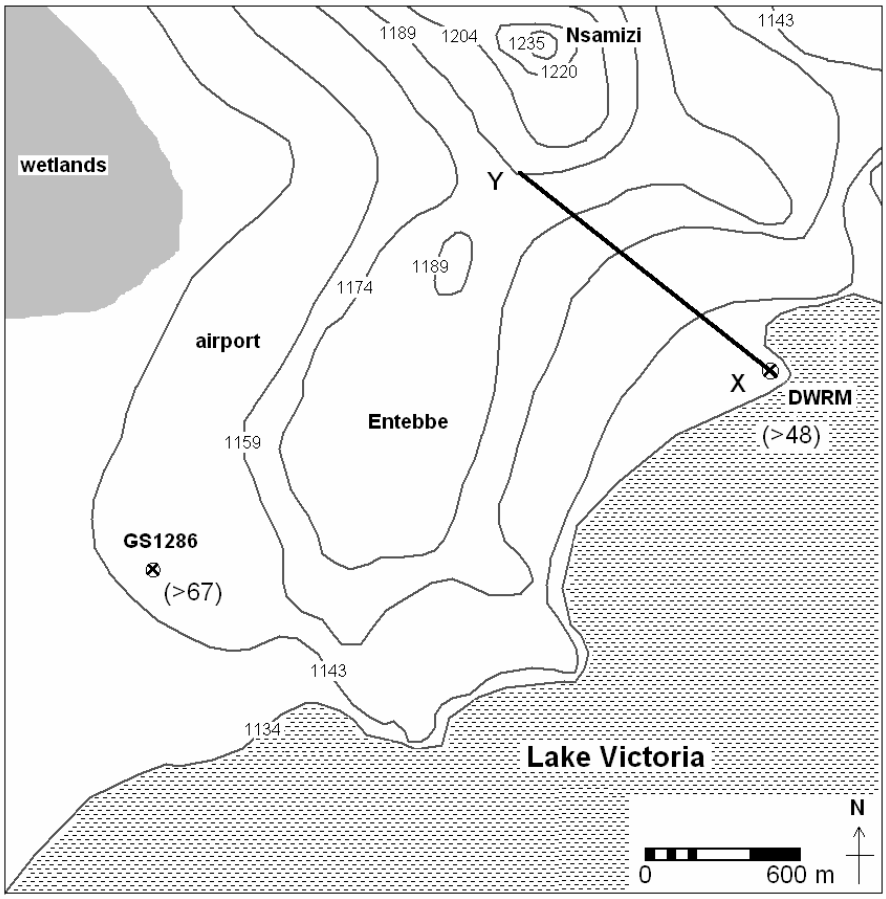

Figure 3.5 The piezometer (DWRM) on the shore of Lake Victoria and also showing the depth (mbgl) of the two wells into the fractured bedrock (saprolite/saprock) at the Entebbe peninsula.

3.4 Results and discussion

3.4.1 Sediment lithological characteristics

Borehole logs and textural data along with storage (S_y) estimates derived from lithologic textural data at Bugondo (BP01, BP02, BP03 and BP04) are displayed in figure 3.6. Several classification systems of weathered mantle profiles were discussed in section 2.2.3.3. A complexity earlier raised by Taylor and Howard (1999a) is that all these schemes imply a genesis beyond their simple description and yet this is still

contentious. Similar to Taylor and Howard (1999a), this study has used graphical logs to objectively describe weathered profiles.

In Bugondo, at BP01 piezometer (Fig. 3.6), beneath the peaty sands and clays, hydrostratigraphic units range with depth from light grey, fluvial-lacustrine sands (~2 m thick), through a light brown, vesicular and pisolithic duricrust (~2 m thick), to yellowish and pale brown saprolite. The dominant sandy (>0.063 mm grain size fractions) texture is consistent with depth (>80 % mass), subtly reducing between 6 and 9 mbgl where the fine (clay and silt) fractions are more pronounced (~20 % mass) (Fig. 3.7). The lower proportion of the fine fractions (~15 %) within the upper and lower zones suggest that the two water strike zones (0.5-3 and 9-15 mbgl) realised during drilling are likely to transmit the most groundwater. Higher proportion of the fine fractions at the bottom of the stratigraphic profile is attributed to the drilling mud and collapse of the upper sediment horizons.

The hydrostratigraphy at piezometer BP02 varies with depth from light brownish grey fluvial-lacustrine sands (~5 m thick), through a hard, pale to light brown duricrust (~2 m thick), to yellowish to pale brown saprolite (Fig. 3.6). Dominant sandy fractions are consistent with depth (>80 % mass) and slightly decrease at the bottom of the saprolite (Fig. 3.7). On the other hand, the fine fractions are similarly consistent (<10 % mass) with depth but show a slight increase at the bottom of the profile (~20 % mass). These coarse textural horizons support the water strike zones (0.5-4.5 and 13-19.5 mbgl) realised during drilling. The higher proportion of the fine fractions at the bottom of the stratigraphic profile is attributed to the drilling mud and collapse of the upper sediment horizons.

The lithology at piezometer BP03 has a uniform, pale to light brown lateritic gravel and clay with a duricrust from about 9 mbgl (Fig. 3.6). There is a decrease with

depth (80 to 70 % mass) of the sandy textural fraction (Fig. 3.7). Conversely, the fine fractions increase (20 to 30 % mass) with depth. This provides poorly sorted textural horizons, which suggest lower permeability media due to smaller grains filling up openings created by the larger grain sizes. This area is situated at a higher altitude relative to the lakeshore and provides an indication of the depth of the saprolite upslope.

The hydrostratigraphy of piezometer BP04 at shallow depths features light grey sands that are mixed with peaty soils (~3 m thick), below which are light yellowish brown, lateritic gravel horizons interspersed by several thin lenses of very pale brown lenses of duricrust (Fig. 3.6). The duricrust dominates the formation from about 12 mbgl. There is a consistently high (>75 % mass) sandy grain size fraction with depth that exhibits a slight decrease from 4 to 8 mbgl (Fig. 3.7). The fine fractions on the other hand, fluctuate with depth, elevated proportions (~20 % mass) coinciding with the top, middle and bottom parts of the stratigraphic profile. Coarse textural zones correspond to the two water strike zones (1-3 and 8.5-12 mbgl) obtained during drilling, suggesting that the deeper coarse-grained horizons form a more permeable water-bearing zone (saprolite).

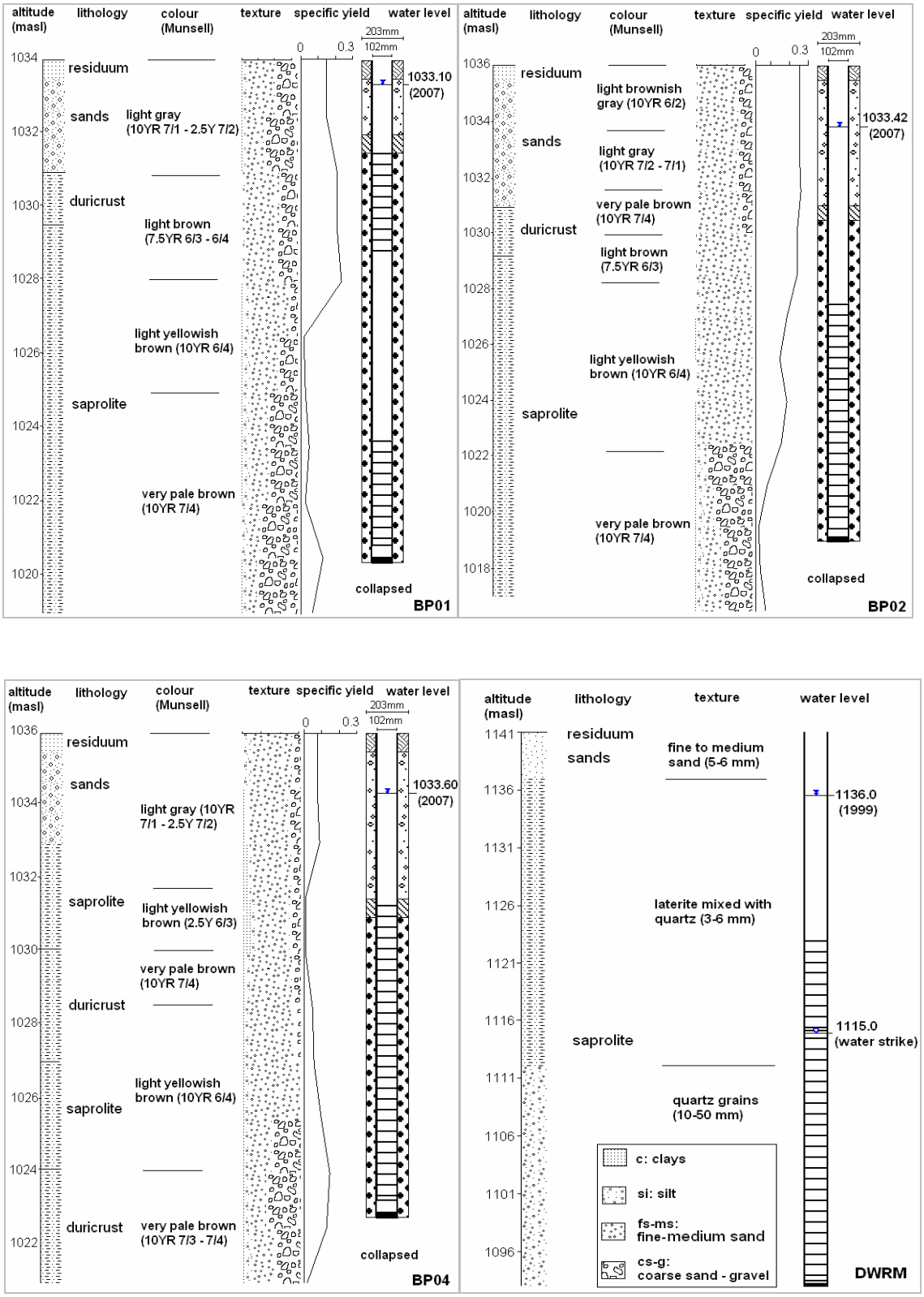

Figure 3.6 Graphical well logs showing lithology, colour, texture, indicative specific yield and static water levels on well completion at Bugondo.

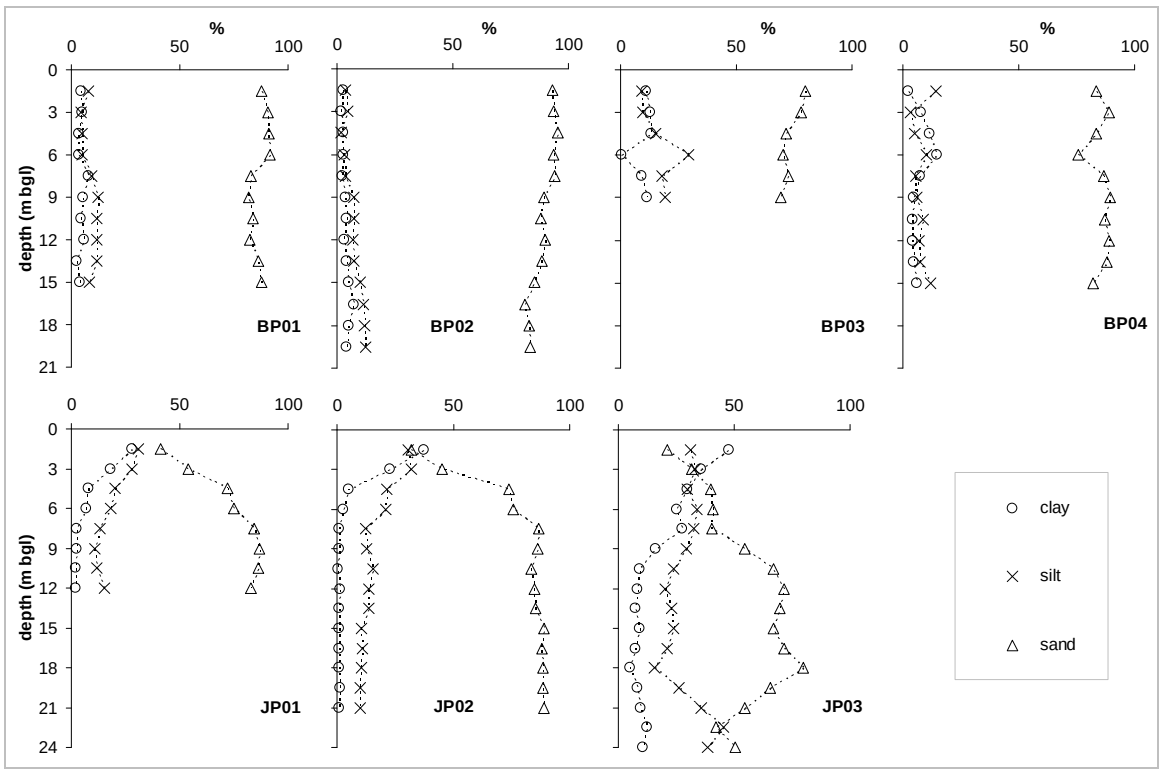

Figure 3.7 Particle-size depth distributions for dominant particle-size modes of sediment well logs from Bugondo (BP) and Jinja (JP). The symbols indicate the bottom of depth ranges which were sampled.

Observations of borehole logs and textural data along with S_y estimates derived from lithologic textural data for piezometers in Jinja (JP01, JP02 and JP03) and Entebbe (DWRM) are shown in figure 3.8. At Jinja, the hydrostratigraphy of the top of JP01 piezometer, include dark red clays, and strong to dark yellowish brown infill mixed lateritic gravel (~4 m thick) (Fig. 3.8). This is followed with depth by light yellowish brown to olive coloured texture as the material grades into lithic fragments of weathered amphibolite (saprolite). With depth, the dominant sandy sediment fraction increases (~40 to ~90 % mass) whereas the fine fraction decreases (~60 to ~10 % mass) through the saprolite (Fig. 3.7). Thus, even if there are two water-strike zones (0.5-3 and 7.5-12 mbgl), it is apparent that the lower zone with least fine fractions is likely to be the main water-transmitting layer (saprolite) whose permeability increases with depth.

The hydrostratigraphy at piezometer JP02 has a thin layer (<3 m thick) of brown to dark brown mixed sands and lateritic infill, beneath which the material grades into

light to pale olive lithic fragments of weathered amphibolite (saprolite) (Fig. 3.8). A similar dominant sandy textural profile to JP01 is evident, increasing with depth (~30 to ~90 % mass) whereas the fine fraction decreases with depth (~70 to ~10 % mass) through the saprolite (Fig. 3.7). This profile also suggests increasing permeability with depth which indicates that the latter of the two water strike zones (0.5-3 and 12-21 mbgl) has the potential to transmit more groundwater fluxes than the upper horizon.

The hydrostratigraphy at piezometer JP03 is a dark red to red, fairly consolidated lateritic gravel and clay (~6 m thick) beneath which there is a strong to light yellowish brown saprolite (Fig. 3.8). Dominant sandy fractions occur from ~9 mbgl and increase (~50 to 70 % mass) with depth (Fig. 3.7). Fine textural fractions are generally high and conversely, dominate the top 9 mbgl (~80 to 50 % mass) and then decrease (~20 % mass) with depth until ~18 mbgl, where there is an increase (~50 % mass) again up to 24 mbgl. This large proportion of fines at the bottom of the well is attributed to the drilling mud and collapse of the upper sediment horizons. It is the lower zone with the least fine fractions that provides the sole groundwater-transmitting zone (15-24 mbgl).

At Entebbe, the stratigraphy of the DWRM piezometer is reported to be fine to medium fluvial-lacustrine sands (~5 m thick), overlying a zone that is composed of lateritic gravel and sands (Fig. 3.8). Beneath this horizon is the saprolite layer dominated by unconsolidated quartz grains which provides the main groundwater-transmitting zone (21-48 mbgl).

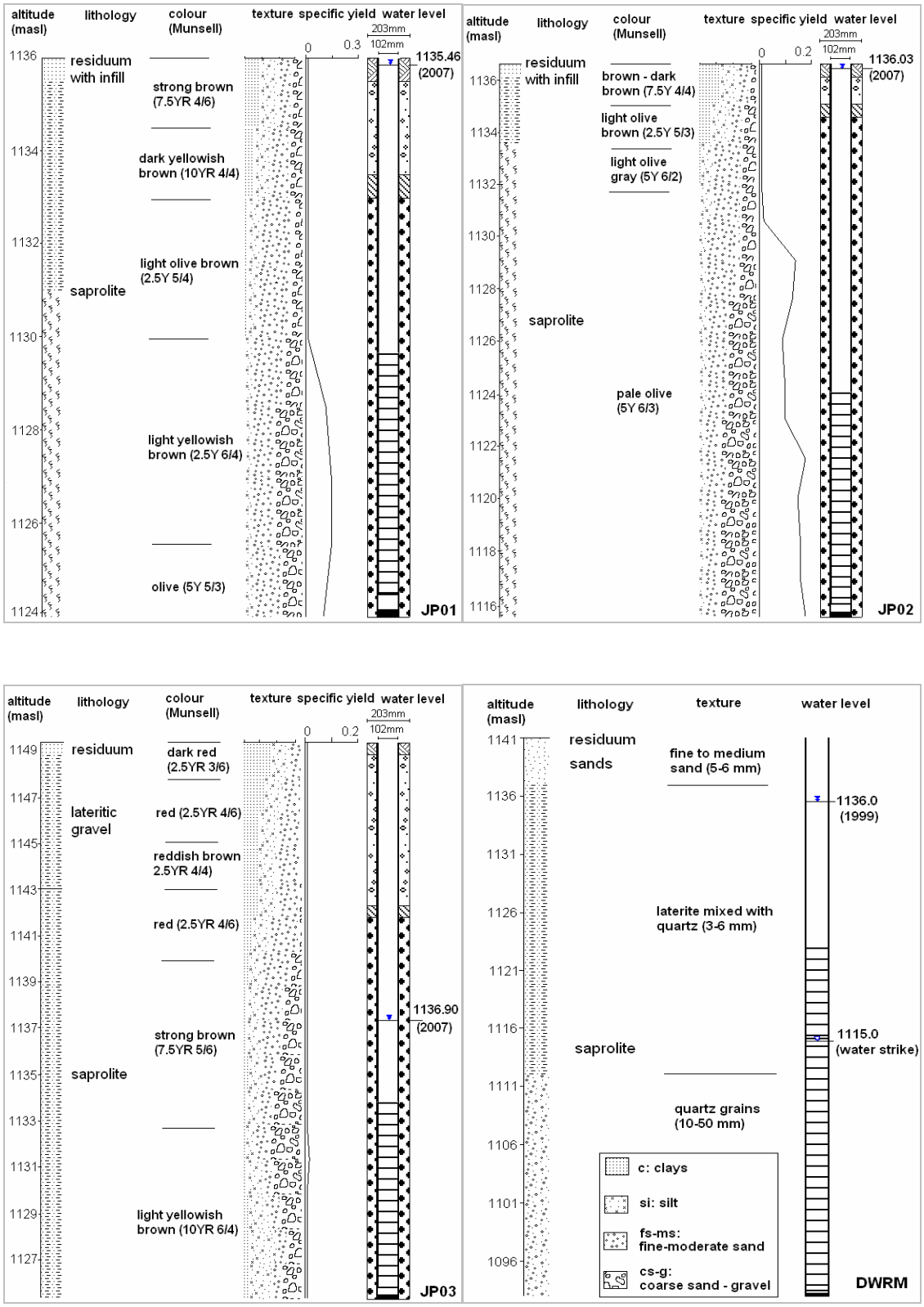

Figure 3.8 Graphical of well logs showing lithology, colour, texture, indicative specific yield and static water levels on well completion at Jinja (JP) and Entebbe (DWRM).

As noted by Taylor and Howard, (1999a) and consistent with previous research, there is a paucity of silt-sized particles in shallow (<2 m depth) soils from all the profiles, a condition which have been attributed to rapid and intense alteration of sand-sized, feldspars and mica into clays. It is apparent from all these stations that fluvial-lacustrine and/or lateritic horizons have mixed (fines to coarse sand and gravel) textural distributions. These lithologies overlie a saprolite zone dominated by a coarse (fine sand to coarse sand and gravel) textural fraction with depth. On the basis of textural classes alone, it is evident that the deeper parts of the saprolite zone have a greater potential to transmit higher groundwater fluxes than the overlying mixed fluvial-lacustrine horizons.

3.4.2 Stratigraphy of monitoring stations deduced from surface resistivity modelling

The lithostratigraphy of constructed monitoring stations deduced from drilling logs is compared here to those determined by inverse modelling of Schlumberger VES arrays (Edwards, 1977). In Bugondo, two VES (2 and 3) display a similar narrow, concave-upwards pattern whereas VES 1 shows an upward trend (Fig. 3.9). A comparable trend to the aforementioned two VES at Bugondo is evident in the three Jinja VES results albeit with shifts and slightly wider curvature (Figs. 3.10 and 3.11). The overall shape of the middle portion of the profile gives an idea of the character of the beds between the surface and the basement (Telford *et al.*, 1990). These shapes have a definite minimum and maximum resistivity, indicative of beds at middle depth of anomalously low resistivity. These curves suggest that layer two is thicker than layer one, with a resistivity in layer three that is greater than that of layer one. On the other hand, VES 1 at Jinja reveals a fairly uniform increase in resistivity with depth (Fig. 3.10) and indicates that layer two is thicker than layer one; the bedrock has a much larger resistivity than that of layer one.

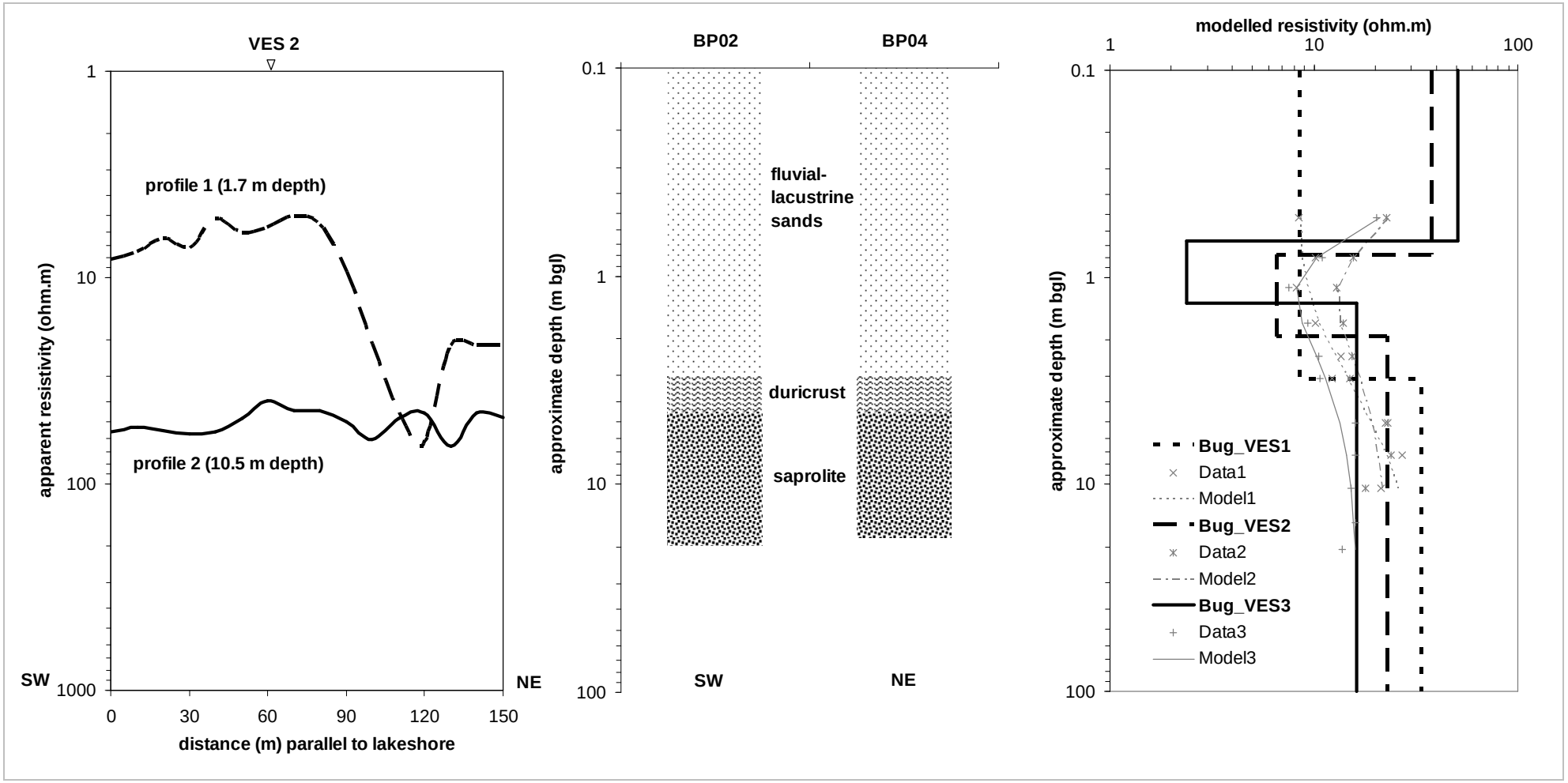

Figure 3.9 Depth resistivity profiles with the corresponding multiple layer inversion models between piezometers BP02 and BP04 at Bugondo on the shore of Lake Kyoga.

Recognising that lateral variations occur in heterogeneous saprolite, apparent resistivity profiles were measured across the areas where VES arrays had been conducted. Profiles at Bugondo were carried out along a transect between the BP02 and BP04 piezometers (Fig. 3.3). Using an outer electrode spacing of 8.8 m (profile 1, ~1.7 mbgl depth), consistent resistivity of <1 ohm·m is recorded until a positive anomalous boundary at the northeastern edge is observed where there is a lateritic gravel road leading to the pier (Fig. 3.9). The deeper profile 2 within the same area from an outer electrode spacing of 55 m (profile 2, ~10.5 mbgl depth), gives apparent resistivity similar to the gravel road (10-100 ohm·m) in the upper section which is even throughout its extent signifying uniform material. Conversely, in Jinja for the piezometer closest to the lake, profiles (1 and 2) conducted with outer electrode spacing of 8.8 m (~1.7 mbgl depth) and 38 m (~7.3 mbgl depth) show similar apparent resistivities at just under 10 ohm·m (Fig. 3.10). These profiles were conducted along a transect between and orthogonal to JP01 and JP02 piezometers (Fig. 3.2). The second profile (outer electrode spacing of 38 m, ~7.3 mbgl depth) at the higher elevation (~6 m below JP03) is similarly uniform in extent and comparable to the deeper profile on the first piezometer whereas the shallow profile (outer electrode spacing of 8.8 m, ~1.7 mbgl depth) reveals a consistent but higher apparent resistivity of over 10 ohm·m (Fig. 3.11).

Model results from Bugondo VES generally concur with lithological data and produce three layers except for VES1 that combine layers 1 and 2 (Fig. 3.9). Between the VES data and inverse model estimates at Bugondo, the root mean square error (rmse) is 7.6 to 13.6 %. The uppermost layer is ~1 m thick and is associated with fluvial-lacustrine sands. The thickness of this layer is less than observed in BP01 (~3 m), BP02 (~5 m) and BP04 (~3 m). The intermediate layer of variable thickness (~3 m) is likely to be a fairly compact, saturated clay layer interspersed by duricrust. Clays naturally have high cation exchange capacity resulting in low resistivity due to the

surface conductivity operating in the vicinity of the pore water/mineral interface within the electrical double layer coating the mineral-water interface (Revil and Leroy, 2001). This layer is found at different depths in BP01 (~2 m thick), BP02 (~2 m thick) and BP04 (totalling ~4 m thick). At the bottom end of this system is saprolite with low clay contents. Apparent resistivity of profiles mapped across the area at median depths of approximately 2 and 10 m, respectively, point to a distinct interface between those two depths (~3 m depth). On the other hand, piezometers BP01 (~ 4 m), BP02 (~ 5 m) and BP04 (~3 m) all show variable depths to the top of the saprolite. The fractured bedrock or basement (saprock) which is at depth is not possible to be discerned from the shallow depth of penetration that was realised during the VES surveys.

At Jinja, three model layers are also defined next to the lakeshore (Fig. 3.10). Between the VES data and inverse model estimates at these sites, the rmse is 7.7 to 10.2 %. The most shallow layer (~3 m thickness) is saturated and composed of mixed fluvial-lacustrine sands with infill. An intermediate layer of lateritic gravel with clay-rich layer is again apparent (~4 m thick). The mixed top layer has a similar composition to the intermediate layer as shown by the profiles taken at about 2 and 7 m depths. The thicknesses of these top two layers vary for both JP01 (~5 m) and JP02 (~2 m). Below this, the saprolite features fragments of weathered amphibolite minerals (also in both JP01 and JP02). VES 1 has higher resistivity signifying the close proximity of the fractured amphibolite bedrock (saprock) at this location (at ~10 m depth from JP01). At the higher elevation shoreline closer to JP03, three layers are apparent (Fig. 3.11). Between the VES data and inverse model estimates at this site, the rmse is 11.5 %. A mixed residuum top layer of ~2 m thick, followed by the variable lateritic gravel with clay-rich layer (~6 m depth), beneath which is the thick saturated saprolite. At JP03 which is around 6 m above this VES4 site the saprolite is ~6 m below the lateritic gravel layer.

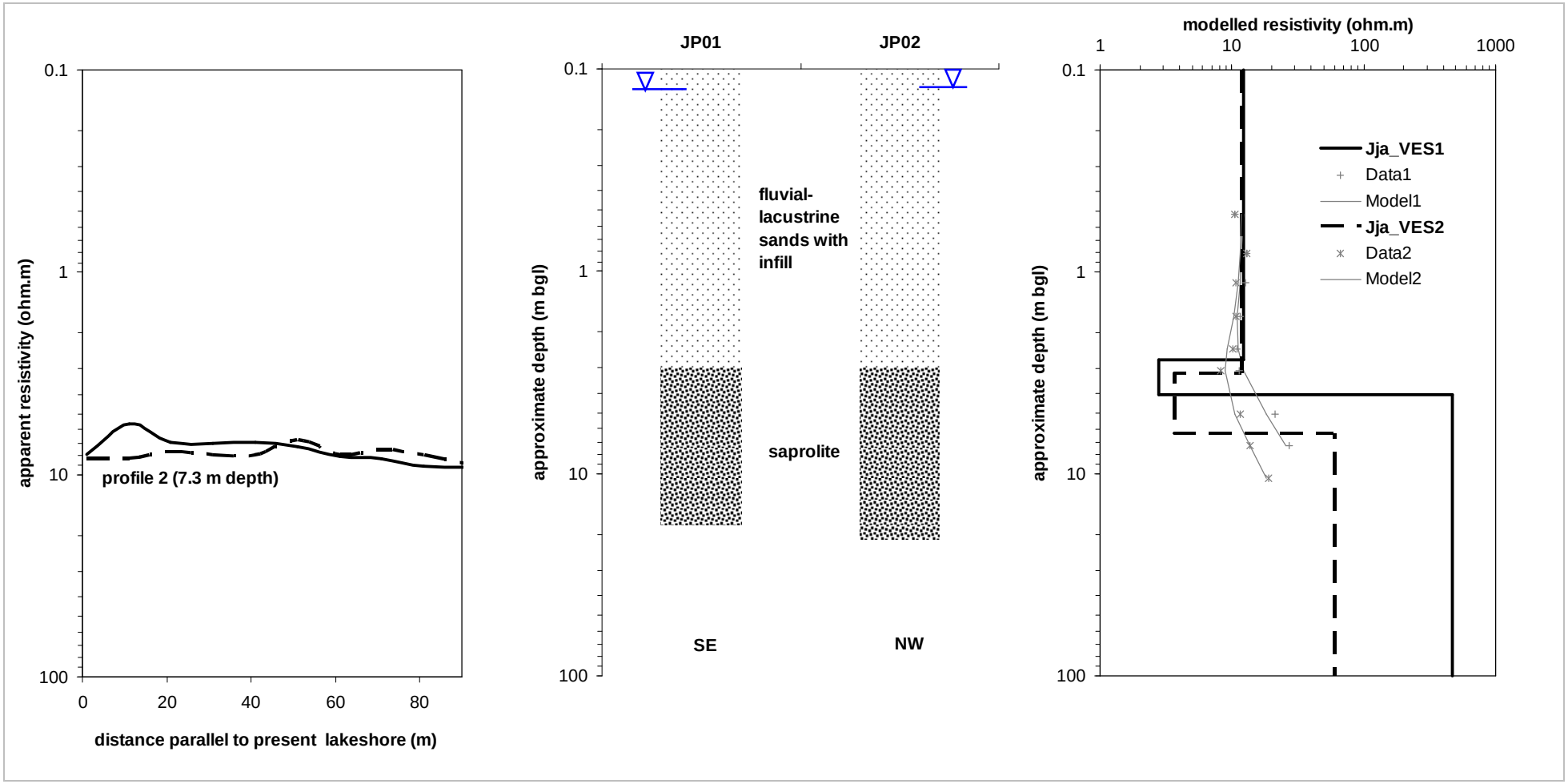

Figure 3.10 Depth resistivity profiles with the corresponding multiple layer inversion models taken orthogonal to piezometers JP01 and JP02 at Jinja on the shore of Lake Victoria.

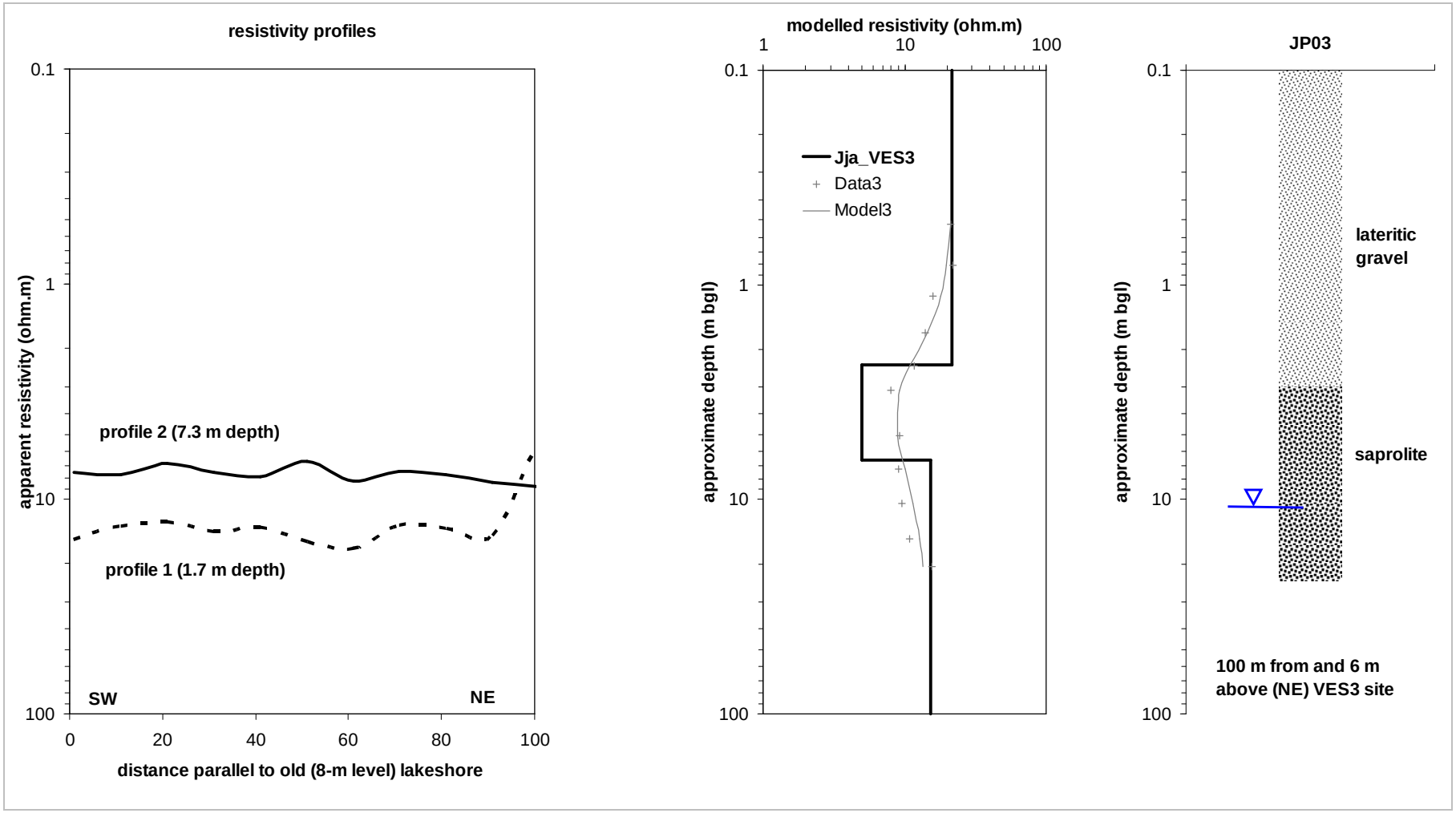

Figure 3.11 Depth resistivity profiles at old elevated shoreline with the corresponding multiple layer inversion models taken 100 m NE and about 6 m above the JP03 piezometer at Jinja on the shore of Lake Victoria.

The VES together with resistivity profiling complement the lithologic logs at Bugondo in identifying a consistent litho-stratigraphic sequence: mixed fluvial-lacustrine sediments that overlie a duricrust of lateritic gravel which in turn, is succeeded with depth by saprolite. The relative depths of the interfaces and thicknesses of these layers vary slightly. At Jinja, VES data together with resistivity profiling recognise a sequence of 3 lithostratigraphic units: mixed fluvial-lacustrine sediments, that overlie a middle transition zone which is succeeded with depth by saprolite close to the lakeshore. Drilling logs only distinguish between mixed fluvial-lacustrine sediments overlying a thick saprolite. All the three methods at this location generally indicate a mixed fluvial-lacustrine layer with infill (~2-7 m thick) overlying a thick saprolite of variable thickness (from ~10 m depth). Along the former shoreline at higher elevation in Jinja, VES together with resistivity profiling again identify 3 distinct horizons, i.e. lateritic gravel with a middle zone separating it from saprolite, whereas the lithologic logs show only lateritic gravel overlying a thick saprolite. Generally, this elevated location has fairly thick lateritic gravel (~6 m thick) above thick saprolite.

3.4.3 Hydraulic gradient between groundwater and surface water

Static water levels recorded in all constructed piezometers rest above the main water strike zones detected during drilling. This difference is considered to reflect either the existence of leaky or confined aquifer conditions or imprecision in sampling during well construction. At Jinja, apart from JP03 piezometer, located on an embankment associated with an old drainage level of Lake Victoria with a static water level of ~12 mbgl, the other two (JP01 and JP02) piezometers both have water levels close to the surface. Similarly at Bugondo, all the three (BP01, BP02 and BP04) piezometers have static water levels ranging from ~0 to 5 mbgl. Well yields estimated using the airlift method during the development process, range from 0.7 to 2.4 $m^3 \cdot h^{-1}$ except for the DWRM piezometer at Entebbe which has a much higher yield of 8.8 $m^3 \cdot h^{-1}$. These are characteristic yields of aquifers that have low to moderate groundwater potential (MacDonald *et al.*, 2005) typical of highly weathered crystalline rock.

Comparison is made between static groundwater levels and lake stages for Lakes Kyoga (Fig. 3.12) and Victoria (Fig. 3.13) to ascertain the hydraulic gradient (*i*) following well completion. Assuming a relatively homogeneous saprolite groundwater flow system triangulated by the three piezometers there is a *i* of about 0.004 $m \cdot m^{-1}$ in a northwest direction towards the lake at Bugondo. At Jinja, similarly all the three piezometers have a *i* of about 0.01 $m \cdot m^{-1}$ southeastwards in the direction of the lake. Barring significant geological controls (e.g. a dyke or fault gouge), these *i* recorded after construction indicate groundwater flow from the piezometers into both lakes. Individual piezometer *i* towards Lake Kyoga at Bugondo range from 0.003 to 0.01 $m \cdot m^{-1}$ whereas gradients towards Lake Victoria at Jinja vary from about 0.01 to 0.1 $m \cdot m^{-1}$. At Entebbe there is a *i* from the groundwater of about 0.006 $m \cdot m^{-1}$ eastwards towards Lake Victoria (Figs. 3.5 and 3.14).

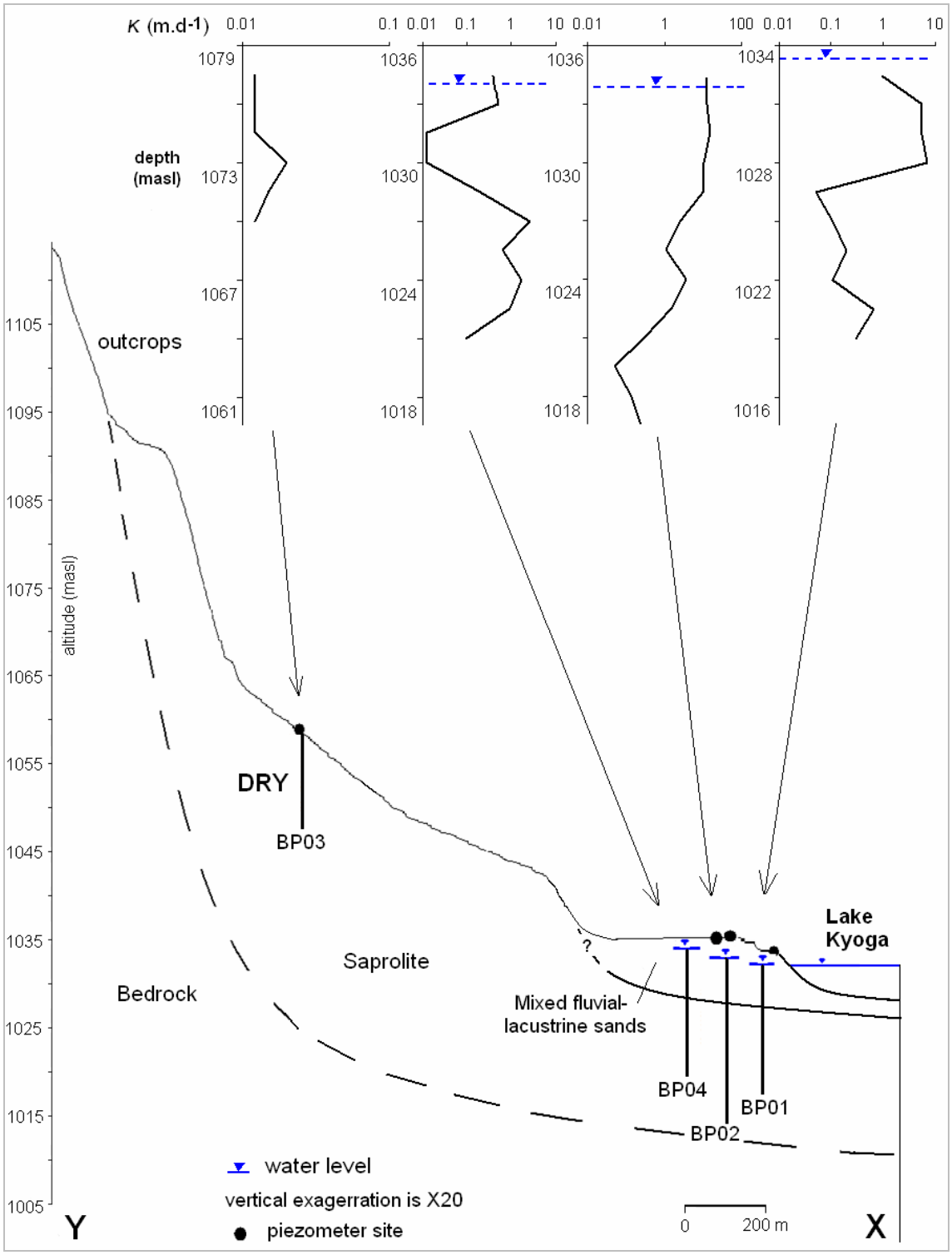

Figure 3.12 An initial (November 2007) static hydraulic gradient between groundwater and Lake Kyoga and also showing depth profiles of indicative saturated hydraulic conductivity values at Bugondo.

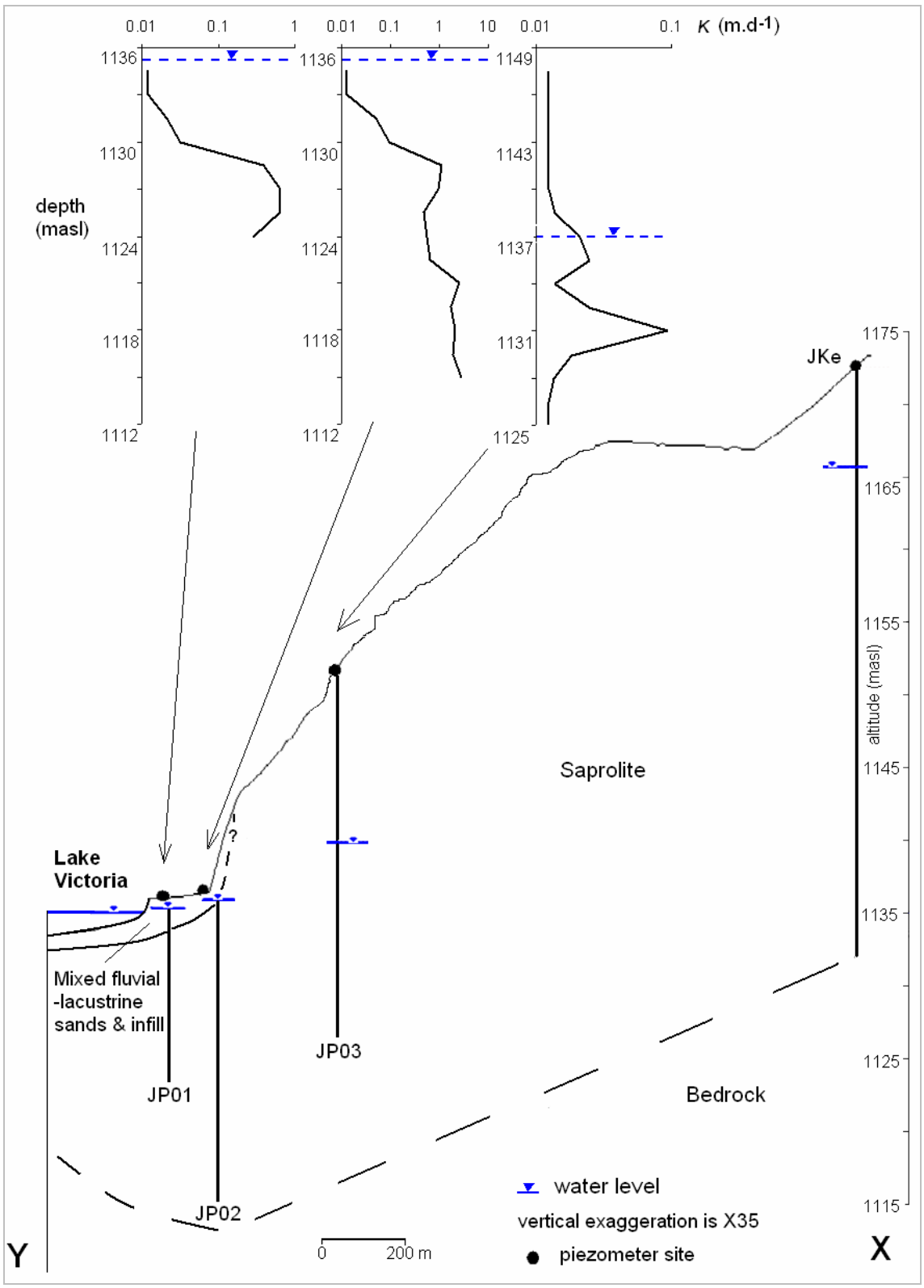

Figure 3.13 An initial (November 2007) static hydraulic gradient between groundwater and Lake Victoria and also showing depth profiles of indicative saturated hydraulic conductivity values at Jinja.

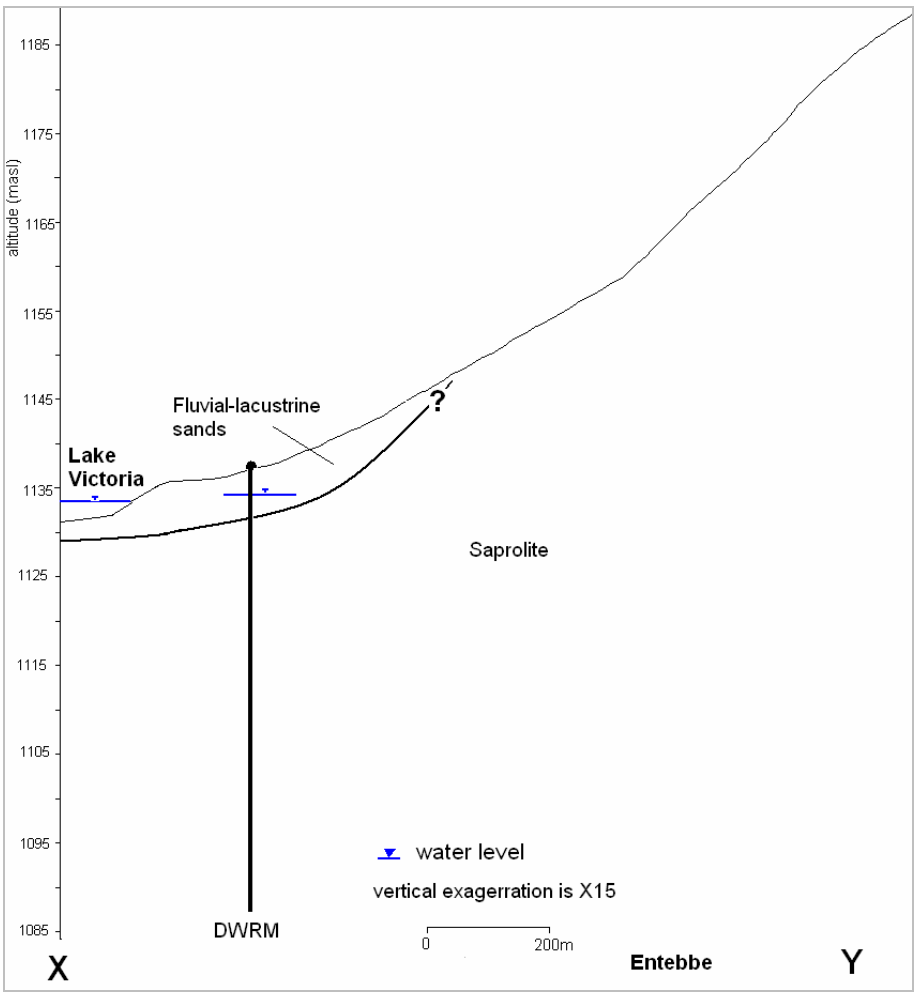

Figure 3.14 An initial (July 1999) static hydraulic gradient between groundwater and Lake Victoria at Entebbe.

3.4.4 Depth profiles from lithologic textural estimates of hydraulic conductivity (*K*) and specific yield (S_y)

At Bugondo all the litho-stratigraphic layers at the three piezometers are saturated except for the top ~2 mbgl of BP02 and BP04; BP03 is dry throughout its ~10 mbgl depth. Next to the lake (BP01), estimated values of *K* values in the upper fluvial-lacustrine sands (1 $m \cdot d^{-1}$), increase with depth in the lower sands above the saprolite (6-7 $m \cdot d^{-1}$) as a result of a reduction in the proportion of clays. Estimated *K* reduces in the underlying saprolite but rises again within the deeper saturated domain (0.05-1 $m \cdot d^{-1}$) (Fig. 3.12). Specific yield (S_y) estimates follow similar *K* patterns with values varying from 0.15 to 0.24 in the fluvial-lacustrine sands and declines to 0.02 in the saprolite

(Fig. 3.6). The higher S_y values are characteristic of unconsolidated fine to coarse sand material (Freeze and Cherry, 1979). The value for S_y of 0.02 in saprolite concurs with that of Taylor *et al.* (2009b) derived from volume-balance calculations based on tracer experiments on the gneiss saprolite in eastern Uganda. However, the middle piezometer from the lake (BP02) has high *K* values (13-15 $m \cdot d^{-1}$) in the unsaturated sands reducing slightly within the underlying saturated saprolite (0.4-10 $m \cdot d^{-1}$), and reduces significantly with depth to about 0.05 $m \cdot d^{-1}$ (Fig. 3.12). Specific yield values drop from 0.25 in the sands to about 0.02 in the saprolite (Fig. 3.6). The third piezometer from the lake (BP04) has a thin sandy layer with a quite low *K* (0.4-1 $m \cdot d^{-1}$) which rises within the underlying saturated saprolite layer interspersed with vesicular and pisolithic duricrust (1-3 $m \cdot d^{-1}$) (Fig. 3.12). Specific yield estimates range from 0.08 to <0.01 before rising to about 0.1 indicating a physical barrier at intermediate depths (Fig. 3.6). The furthest borehole from the lake (BP03) is dry. Lateritic gravel occurs up to a depth of 10 mbgl at which level is duricrust exhibiting very low *K* values (<0.02 $m \cdot d^{-1}$) (Fig. 3.12). Specific yield values in this unsaturated zone are all <0.01 which characterises this clay-rich medium (Fig. 3.6).

At Jinja, the litho-stratigraphic layers sampled at the three (JP01, JP02 and JP03) piezometers are saturated except for the top ~12 mbgl at piezometer JP03. Next to the lake (JP01) the infill mixed with the fluvial-lacustrine sands substantially affects the *K* values (<0.02 $m \cdot d^{-1}$) which increase with depth into the underlying saprolite (1-3 $m \cdot d^{-1}$) (Fig. 3.13). Specific yield estimates start at <0.01 before gradually rising to 0.1 in deeper saprolite horizons (Fig. 3.8). The middle piezometer (JP02) exhibits similar *K* values to JP01 within the top layer, but has a significant increase in the underlying saprolite (0.5-3 $m \cdot d^{-1}$) (Fig. 3.13). Again S_y values gradually rise from <0.01 in the mixed sands to about 0.18 in the permeable saprolite (Fig. 3.8). The furthest wholly lateritic gravel and clay to saprolite aquifer (JP03) has low *K* values (<0.02 $m \cdot d^{-1}$) until

the water-bearing zone when K improves slightly (up to 0.1 $m \cdot d^{-1}$) (Fig. 3.13). Here the S_y is uniformly low at <0.01 except for the water-bearing zone where it rises to 0.02 which typifies a consistently weathered saprolite profile (Fig. 3.8). Nonetheless, the indicative K and S_y values based on empirical relationships from lithologic texture are highly tentative.

3.4.5 Variations in major-ion chemistry

Groundwater temperature variations indicate the depth of circulation and mixing of different water types. These changes reflect, in turn, recharge and discharge processes that are associated with EC and pH changes (e.g. Mazor, 2004). Lake Victoria is relatively homogeneous from the surface to a depth of 60 m, with a mean value of 3.40 ± 0.07 for $\delta^{18}O$ and 25.18 ± 0.86 for $\delta^{2}H$ (IAEA, 2004), which provides relatively steady state conditions. Temporal changes in the temperatures of Lakes Kyoga and Victoria are fairly stable from 25.0 to 30.1 ^{o}C. In contrast, the groundwater temperatures at both Bugondo and Jinja stations range from 20.1 to 29.4 ^{o}C. Average EC of waters from Lake Victoria is 145 $\mu S \cdot cm^{-1}$ whereas for Lake Kyoga it is 331 $\mu S \cdot cm^{-1}$. The average pH of lake waters also differ slightly: 7.8 (Lake Victoria) and 8.1 (Lake Kyoga) (Fig. 3.15). The slightly higher pH of Lake Kyoga is attributed to the consumption of aqueous inorganic carbon (i.e. H_2CO_3, CO_3^{2-}, HCO_3^{-}) for photosynthesis by aquatic plants in wetlands that lie around the fringe of Lake Kyoga (Kattan, 2006). The reduction in dissolved CO_2 raises the lake's pH. Distinct hydrochemical differences occur among groundwater sources. In Bugondo, whereas BP01, BP02 and BP04 have average pH of 7.3 to 7.4, the average EC decreases along the flow path from BP04 (3,232 $\mu S \cdot cm^{-1}$) through BP02 (1,605 $\mu S \cdot cm^{-1}$) to BP01 (1,543 $\mu S \cdot cm^{-1}$) next to the lakeshore. Within Jinja, a similar trend is encountered. Piezometers JP01, JP02 and JP03 have an average pH of 6.4 to 6.9 but the EC reduce from JP03 (2,528 $\mu S \cdot cm^{-1}$)

through JP02 (1,919 $\mu S \cdot cm^{-1}$) to JP01 (689 $\mu S \cdot cm^{-1}$) adjacent to the lakeshore. Since there is limited anthropogenic activity in the region the chemistry of the groundwater is likely to be determined primarily by water-rock interactions. Chilton and Smith-Carington (1984) from a study of the weathered basement aquifers in Malawi found EC ranging from <750 up to 7,000 $\mu S \cdot cm^{-1}$ over distances of a few hundred metres. These differences in hydrochemistry were consequently attributed to the slow movement of groundwater and incomplete mixing, affirming the typically low permeability of the aquifers suggested by hydraulic tests and estimates from lithologic texture. Heterogeneity in groundwater flow is also noted by Taylor and Howard (1996) in northern Uganda where the regolith transmit at significantly higher rates than the underlying fractured-bedrock aquifers. At Entebbe piezometer DWRM conversely, has an average EC of 105 $\mu S \cdot cm^{-1}$ and pH of 5.3, typical of recently recharged waters in a shallow environment where there is close proximity to the soil horizon for CO_2 dissolution from organic matter (Alagbe, 2002).

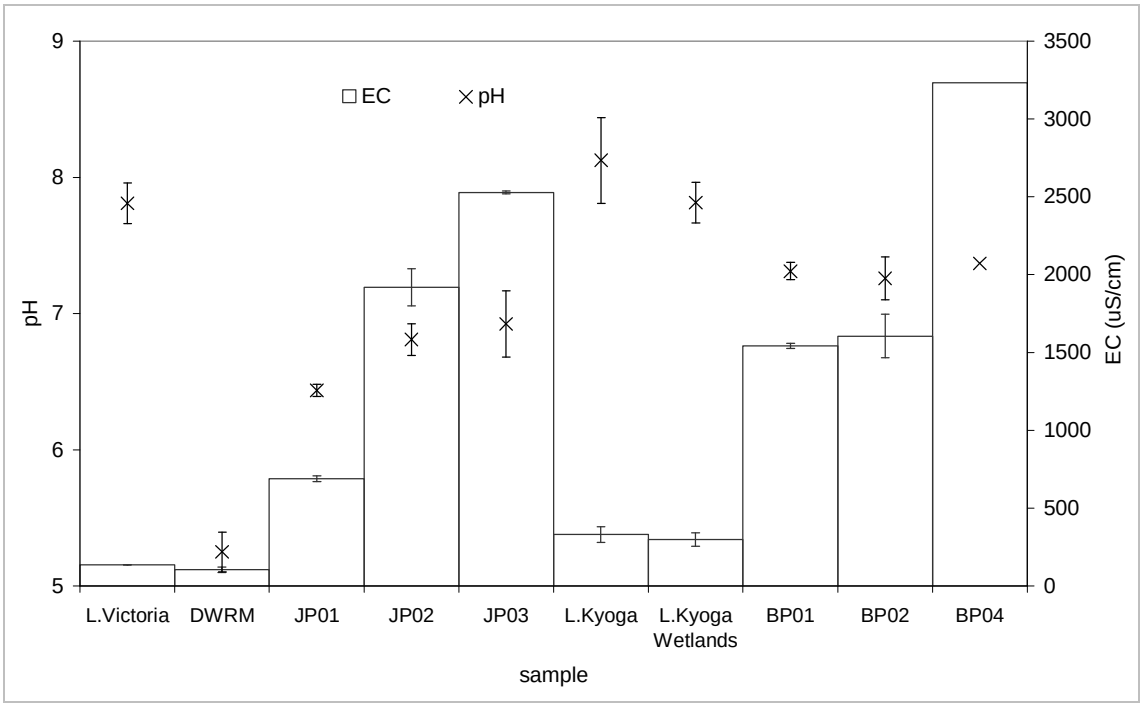

Figure 3.15 Variations in pH and EC of all the water sample stations in Bugondo (BP) on Lake Kyoga, and Entebbe (DWRM) and Jinja (JP) on Lake Victoria. The bars indicate the standard error of the mean.

Major-ion chemistry shows a broad variation of up to three orders of magnitude with cations along flow decreasing in the order from $Na^+ > Ca^{2+} > Mg^{2+} > K^+$, and anions reducing in the order from $HCO_3^- > SO_4^{2-} > Cl^-$ for all the samples. The charge balance error for all ion concentrations measured in water samples is less than 10 %. Most waters are dominated by Na^+ and HCO_3^- (Fig. 3.16). Two piezometers at Jinja (JP02 and JP03) which are furthest from Lake Victoria, together with a lake sample from Entebbe, are not dominated by a specific anion or cation, which suggests waters exhibiting simple dissolution or mixing (Lloyd and Heathcote, 1985). Groundwater at Entebbe (DWRM) is a Ca^{2+}/Cl^- water type and may reflect reverse ion exchange of $Na^+ – Cl^-$ waters. There is also a broad range of secondary ions and elements from very low contents in surface water to elevated quantities in the groundwater, e.g. total Fe (0.08 - 74 $mg \cdot l^{-1}$), F^- (0.3 - 5 $mg \cdot l^{-1}$), PO_4^{3-} (0.1 - 0.2 $mg \cdot l^{-1}$), and NO_3^- (0.02 - 0.6 $mg \cdot l^{-1}$).

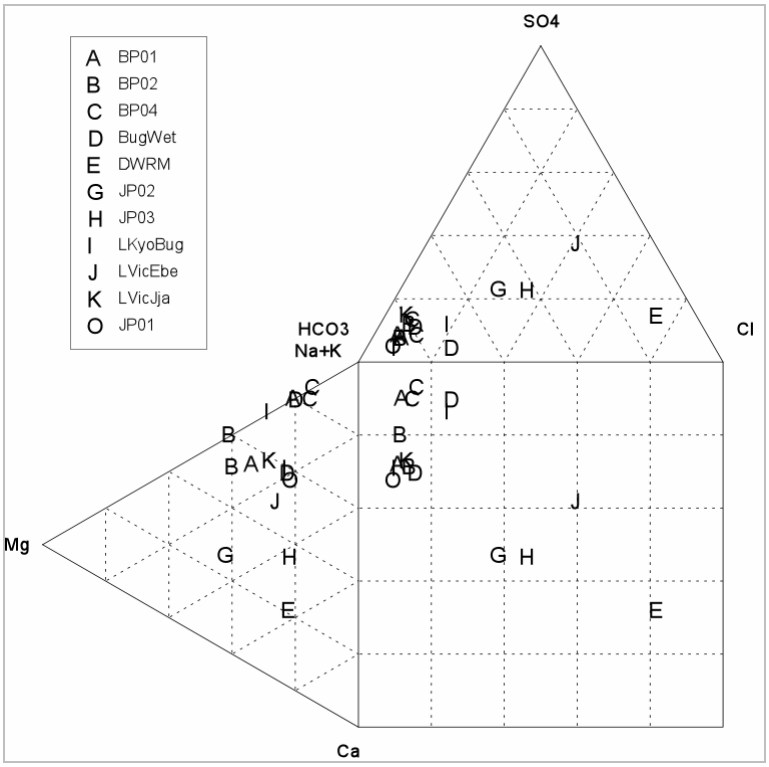

Figure 3.16 Durov plot ($meq \cdot l^{-1}$) of the major ion hydrochemistry showing water types.

Total dissolved ions (TDI) in waters are commonly plotted against the major ions e.g. K^+, Na^+, Mg^{2+}, Ca^{2+}, HCO_3^-, Cl^- and SO_4^{2-} as an indirect verification of the hydraulic connections between groundwater and surface water (Mazor, 2004). Similar data clusters formed by several major ions of water samples indicate a related source of water. Linear correlations between individual ions and TDI depict intermixing of various proportions of water from two end members. When the mixing line extrapolates to the zero points, it indicates mixing between mineralised water and dilute water with negligible ion concentrations. Accordingly, a mixing line that extrapolates to a point on the TDI axis indicates a fresh end member that contains significant concentrations of other ions, whereas the line that extrapolates to the ion axis suggests that both intermixing waters contain significant concentrations of the ion. Conversely, random distributions may indicate non-related water sources of different compositions or poor analytical data quality.

Figure 3.17 shows the major chemical interrelations of the Lake Kyoga, wetlands together with the Bugondo monitoring stations. Samples collected for major chemical analyses include: 2 (wetlands), 2 (BP04), 3 (Lake Kyoga), 3 (BP02) and 3 (BP04). Apart from Ca^{2+} which suggests non-related water sources, the rest of the ions (Na^+, Mg^{2+}, HCO_3^- and SO_4^{2-}) show fairly linear mixing lines between Lake Kyoga and wetlands with groundwater at stations progressively further away from the surface water. The Ca^{2+} mixing line extrapolates to points on the TDI axis which suggest that the fresh end member contains significant concentrations of major ions other than Ca^{2+}. A slightly different scenario is seen on the shore of Lake Victoria at Jinja (Fig. 3.18). A single sample was collected from each of the 6 sample sites. Here, Na^+, Mg^{2+} and HCO_3^- indicate mixing between the lake and groundwater at the stations progressively further away from the surface water. However, Ca^{2+}, Cl^- and SO_4^{2-} exhibit two clusters

of distinct water types, one involving the lake, wetlands and JP01, and a second of JP02 and JP03.

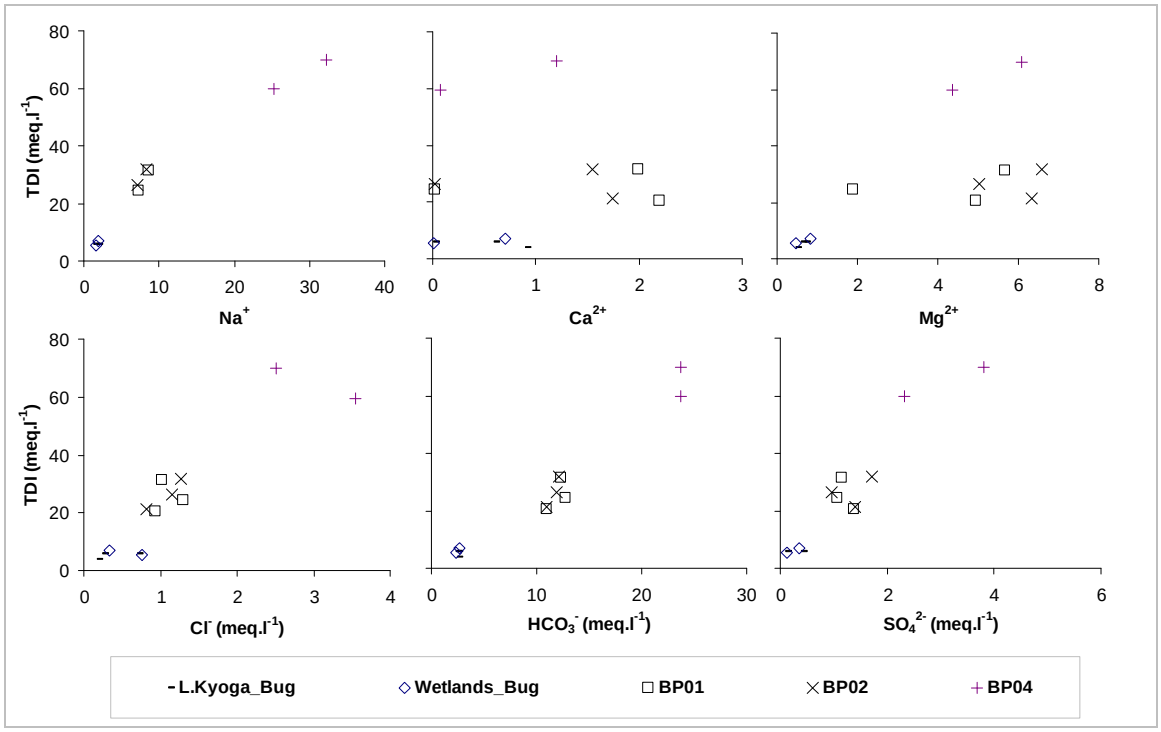

Figure 3.17 Cross plots of TDI (total dissolved ions) vs. major chemical ions (Na^{+}, Ca^{2+}, Mg^{2+}, Cl^{-}, HCO_3^{-}, SO_4^{2-}) in meq·l^{-1} for the Lake Kyoga, wetlands and the Bugondo groundwater monitoring stations.

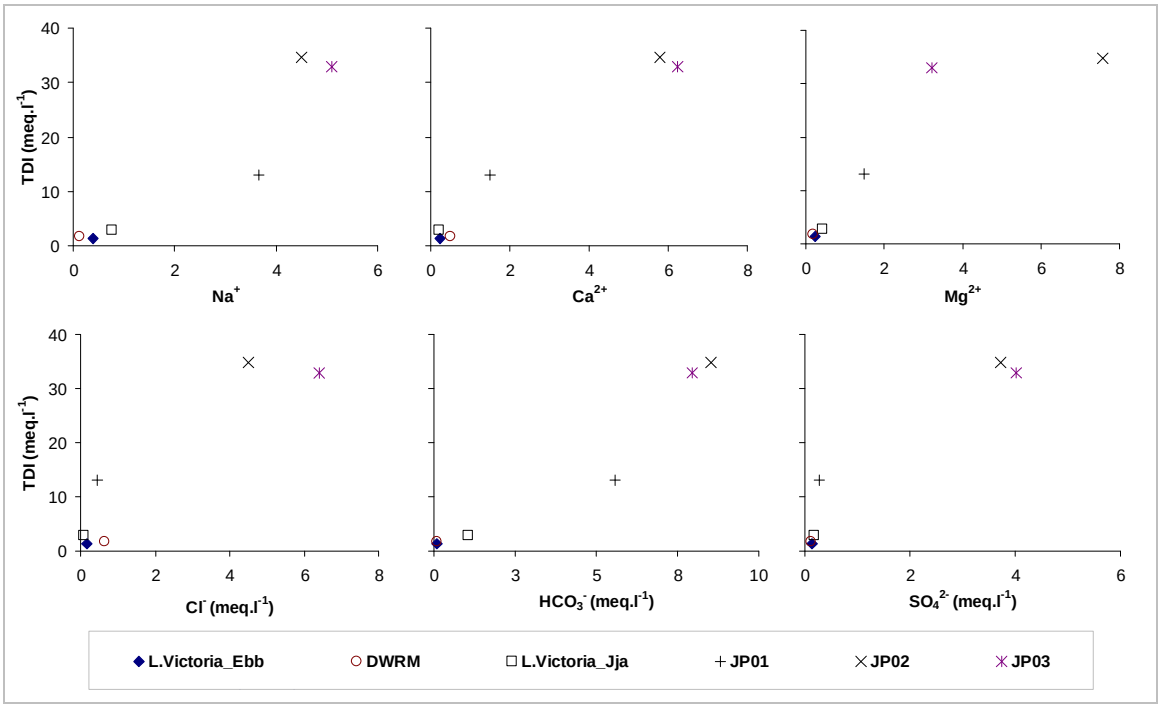

Figure 3.18 Cross plots of TDI (total dissolved ions) vs. major chemical ions (Na^{+}, Ca^{2+}, Mg^{2+}, Cl^{-}, HCO_3^{-}, SO_4^{2-}) in meq·l^{-1} for the Lake Victoria at Entebbe and Jinja, DWRM and the Jinja groundwater monitoring stations.

In general, it is thus hypothesised that, as mineralised groundwater within the interfluve upwell from saprolite into the lakes, local diffuse recharge via the fluvial-lacustrine sediments in the low relief areas (commonly wetlands) adjoining the lakes, mixes with groundwater from the saprolite. Incomplete mixing lowers the EC along the flow path, of the combined mineralised saprolite which then discharge into the lakes.

3.4.6 Variations in stable isotope ratios

Stable isotope ratios in groundwater and lake water can trace the source of water as well as identify the processes such as mixing and evaporation. Where direct recharge is significant, stable isotope ratios in the recharging waters (δ^2H and $\delta^{18}O$) approximate mean stable isotope ratios in precipitation, weighted by volume (Lloyd and Heathcote, 1985). Variations in the seasonal isotopic (δ^2H and $\delta^{18}O$) composition of the rainfall in the Upper Nile Basin reflect the “amount effect” (Fig. 3.19), which arises, in part, from

monsoonal rains derived from the movement of the ITCZ (Intertropical Convergence Zone). The amount effect describes conditions where the volume of precipitation is positively correlated to depletion in the heavy (^{2}H and ^{18}O) isotope contents of precipitation. These bimodal peaks in rainfall coincide with the most depleted isotopic signatures (Taylor and Howard, 1999b). Monsoonal rainfall in the Upper Nile Basin also originates from a more depleted source, the Indian Ocean ($\delta^{18}O = 0 \pm 1$ $^{o}/_{oo}$) than those derived from regional surface waters ($\delta^{18}O = +4 \pm 2$ $^{o}/_{oo}$) (Taylor and Howard, 1999b). The increased effect of evaporation on stable isotope signatures (section 3.2.3) of lighter rainfall outside of the monsoons is observable at Entebbe in records from 1961-1974 and 1998-2004 through a reduced slope of the local meteoric water line (LMWL) relative to the GMWL, i.e. $\delta^{2}H = 7.3*\delta^{18}O + 11.3$ ($R^2 = 0.88$, n = 155). Heavy monsoonal rains show a slope of 7.7 ($\delta^{2}H = 7.7*\delta^{18}O + 12.8$; n = 71; $R^2 = 0.88$) whereas lighter conventional rains (<138 mm mean monthly rainfall) regress along a slope of 7.0 ($\delta^{2}H = 7.0*\delta^{18}O + 10.6$; $R^2 = 0.86$; n = 84) (Fig. 3.20). Taylor and Howard (1999b) found that the heavy rains at Entebbe are parallel to the slope of GMWL ($\delta^{2}H/\delta^{18}O = 8.0 \pm 0.3$), whereas the lighter rains show a $\delta^{2}H/\delta^{18}O$ slope of 6.8 ± 0.4, for a cut-off mean monthly rainfall of 150 mm (1961-1974).

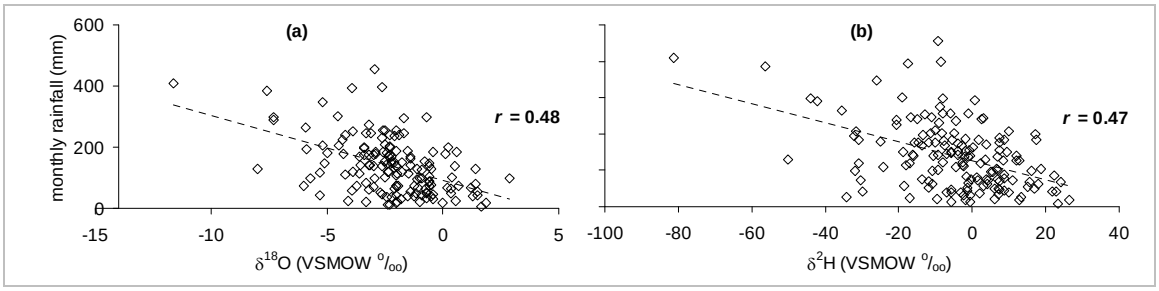

Figure 3.19 The amount effect on the (a) $\delta^{18}O$ and (b) $\delta^{2}H$ samples of the Entebbe rainfall from monthly rainfall averages of 1961-1974 and 1998-2004.

Stable isotope ratios in surface waters in East Africa are progressively enriched in the heavy isotopes through evaporation (e.g. Craig, 1961; Taylor and Howard, 1996).

Evaporation of surface waters produces stable isotope ratios ($\delta^2H = 5.7*\delta^{18}O + 6.9$) that deviate from both the GMWL and the Entebbe LMWL (Fig. 3.20). For the Entebbe groundwater piezometer (DWRM), isotopic ratios plot close to the both the GMWL and LMWL, which point to active recharge by the local rainfall. The DWRM isotopic ratio has a slight but analytically significant difference with the weighted mean average rainfall. This difference likely derives from the dominance of heavy rains with lighter isotopic ratios in generating effective groundwater recharge (Taylor and Howard, 1996; Mazor, 2004; section 5.3.7). Stable isotope ratios in groundwater sampled along the northern shore of Lake Victoria (Fig. 3.21), plot along the Entebbe LMWL. Significantly, regression of stable isotope ratios in groundwater and lake water samples produces a slope of 5.7 indicative of evaporation (Fig. 3.20). This stable isotope ratio relationship suggests that these groundwater samples are actively recharged by local rainfall which is unaffected by the lake waters. It is however, likely that groundwater mixes with lake waters.

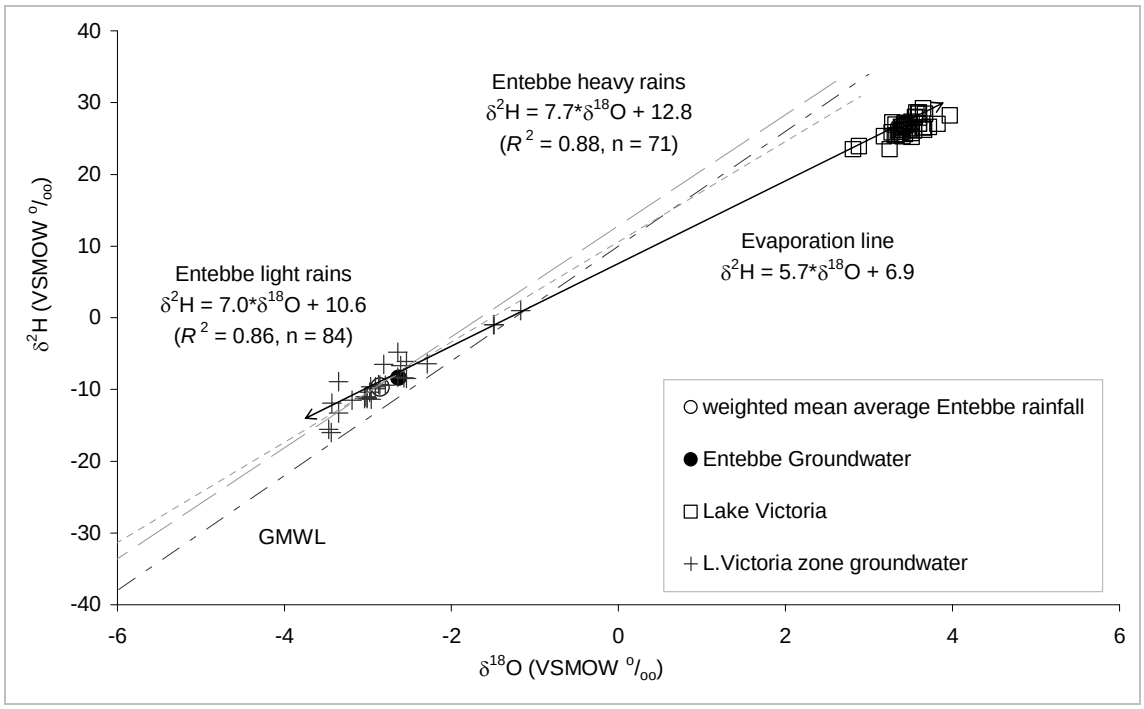

Figure 3.20 Entebbe LMWL from historical (1969-1974) and recent (1998-2004) precipitation isotopic (δ^2H and $\delta^{18}O$) data for light and heavy mean monthly rainfall

(mean rainfall of 138 mm), also showing a local evaporation line that links the Lake Victoria water with the groundwater fringing the lake.

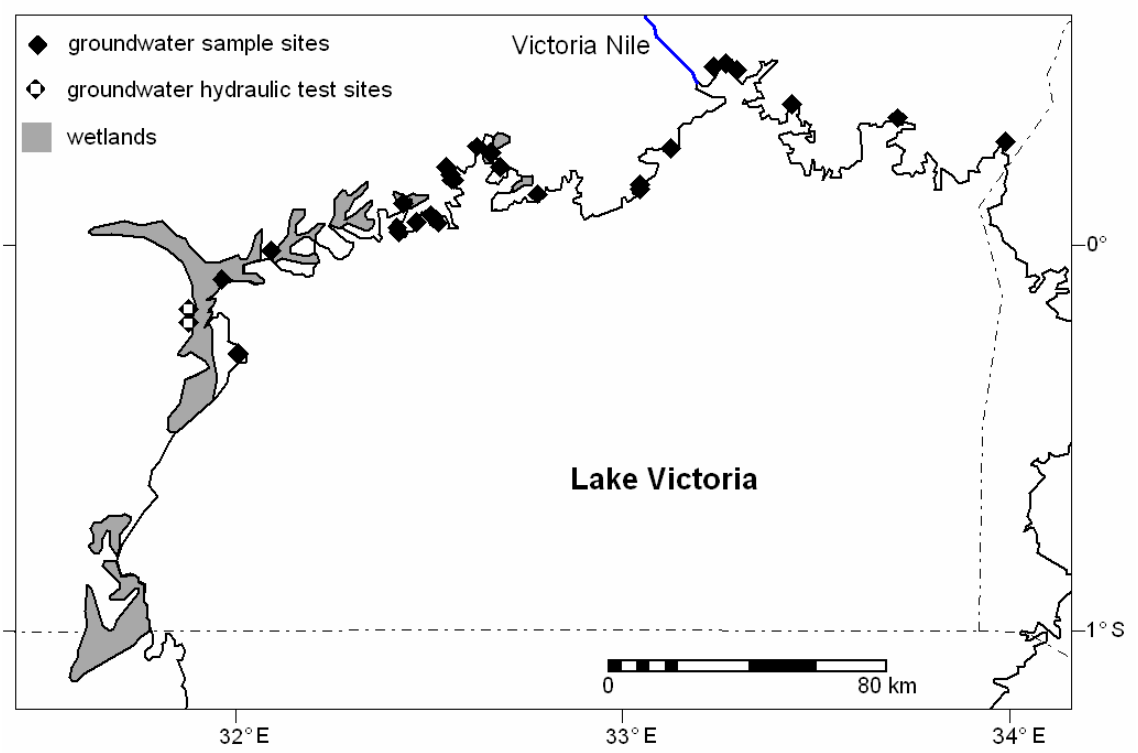

Figure 3.21 The groundwater (boreholes, shallow wells and springs) isotopic (δ^2H and $\delta^{18}O$) sample stations along the northern shore of Lake Victoria.

At Bugondo on the shore of Lake Kyoga, a comparison is made of the isotopic ratios in the local waters with both the GMWL and the Entebbe LMWL (Fig. 3.22). A cluster of groundwater and wetland samples have isotope ratios that regress along both the GMWL and LMWL. This cluster comprising groundwater and wetland samples with depleted isotope ratios together with a second cluster composed of lake and wetland samples having enriched isotope ratios regress along an evaporation line with a slope of 5.2 ($\delta^2H = 5.2*\delta^{18}O + 6.5$). The stable isotope ratios in groundwater indicate active recharge by rainfall. It is proposed that the wetlands receive waters from various sources that include groundwater.

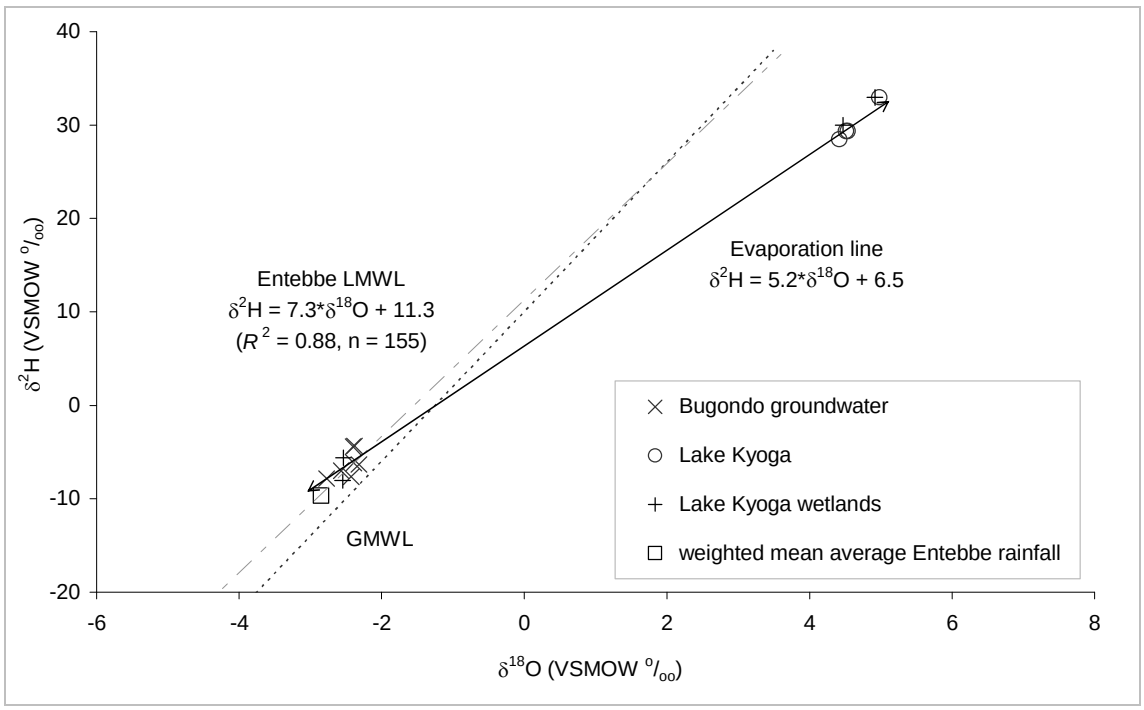

Figure 3.22 Lake Kyoga, wetlands, Bugondo stations isotopic (δ^2H and $\delta^{18}O$) plots also showing a local evaporation line that links the lake water with the groundwater fringing the lake.

Figure 3.23 shows lake and wetland samples enriched in $\delta^{18}O$ relative to groundwater and wetland samples at Bugondo on the shore of Lake Kyoga ($\delta^{18}O$ = 4 to 6 $^{o}/_{oo}$). Samples were collected during both the dry and wet seasons. All the groundwater samples are always depleted (-3 to -2 $^{o}/_{oo}$) in $\delta^{18}O$ and additionally, closely clustered together indicating similar sources and environments. Lake waters are always enriched (>4 $^{o}/_{oo}$) in $\delta^{18}O$ during all seasons. However, wetland waters are depleted (<-2 $^{o}/_{oo}$) in $\delta^{18}O$ with similar isotope ratios to groundwater during the wet season and conversely, enriched (>4 $^{o}/_{oo}$) with similar isotope ratios to lake waters during the dry season possibly due to evaporation.

In Jinja on the shore of Lake Victoria, there is a distinct and progressive enrichment (-0.02 to 2.8 $^{o}/_{oo}$) of $\delta^{18}O$ in groundwater from the furthest piezometer to the lake (JP03) right up to the lake for all the samples collected during the course of the monitoring period (Fig. 3.24). Similar to Lake Kyoga at Bugondo, Lake Victoria waters

are always enriched (3 to 4 $^{o}/_{oo}$) in $\delta^{18}O$. It is suggested that groundwater evolves along the flow path by mixing with lake waters at Jinja. Samples of JP01 in Jinja that was taken during hydraulic tests show a subtle enrichment in $\delta^{18}O$ after over 2 hours of groundwater abstraction. There is a distinct change in $\delta^{18}O$ signatures in the groundwater during pumping, from +2.71 to +2.78, a difference of 0.07 which slightly exceeds the measurement error of ±0.05, and may indicate contributions from lake water, a source enriched in the heavy isotopes.

A plot of $\delta^{18}O$ from the regional groundwater (599 samples) is compared with the surface water and groundwater samples analysed under this work (Fig. 3.25a). Summary statistics (Fig. 3.25b) show variations in the mean and standard error of the $\delta^{18}O$ in the regional groundwater (-2.3±0.02), Bugondo groundwater (-2.5±0.04), Jinja groundwater (1.4±0.3), Lake Kyoga wetlands (1.1±2.1), Lake Kyoga (4.8±0.2), and Lake Victoria (3.5±0.03). Stable isotopes of $\delta^{18}O$ in Bugondo groundwater strongly correlate to groundwater isotopic signatures observed through the Upper Nile Basin whereas groundwater at the Jinja station is clearly influenced by $\delta^{18}O$ isotopic signatures of surface waters enriched in $\delta^{18}O$.

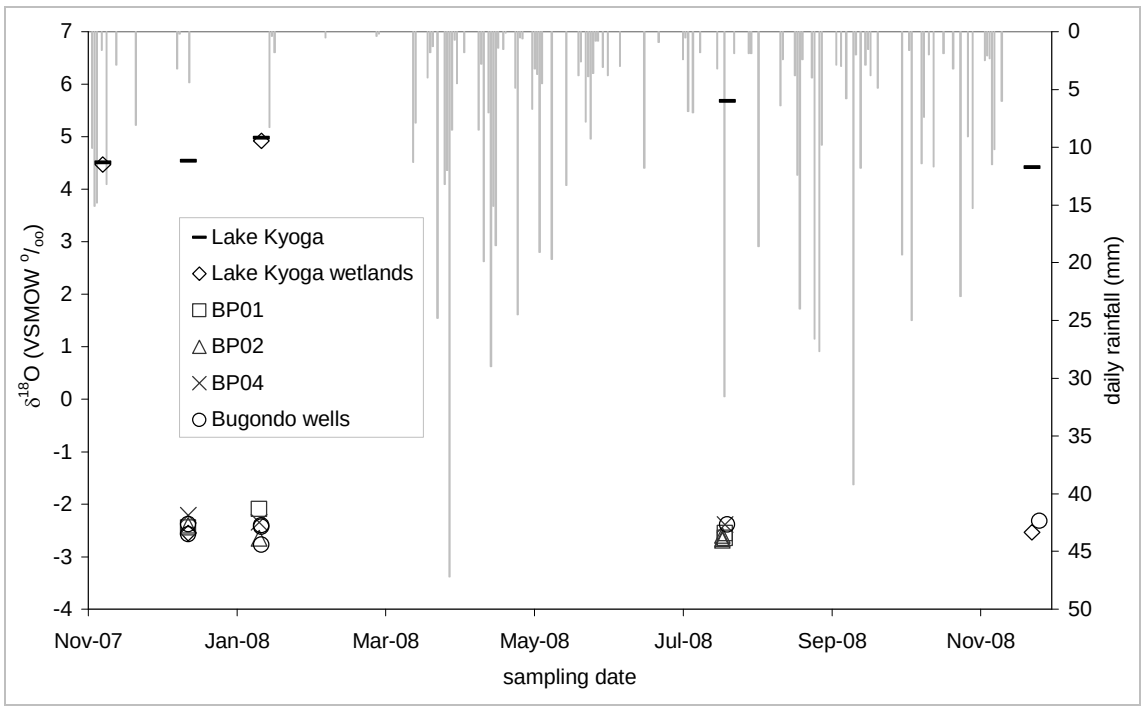

Figure 3.23 The $\delta^{18}O$ plots for the water samples from the Bugondo station on Lake Kyoga shore collected over different seasons from November 2007 to December 2008.

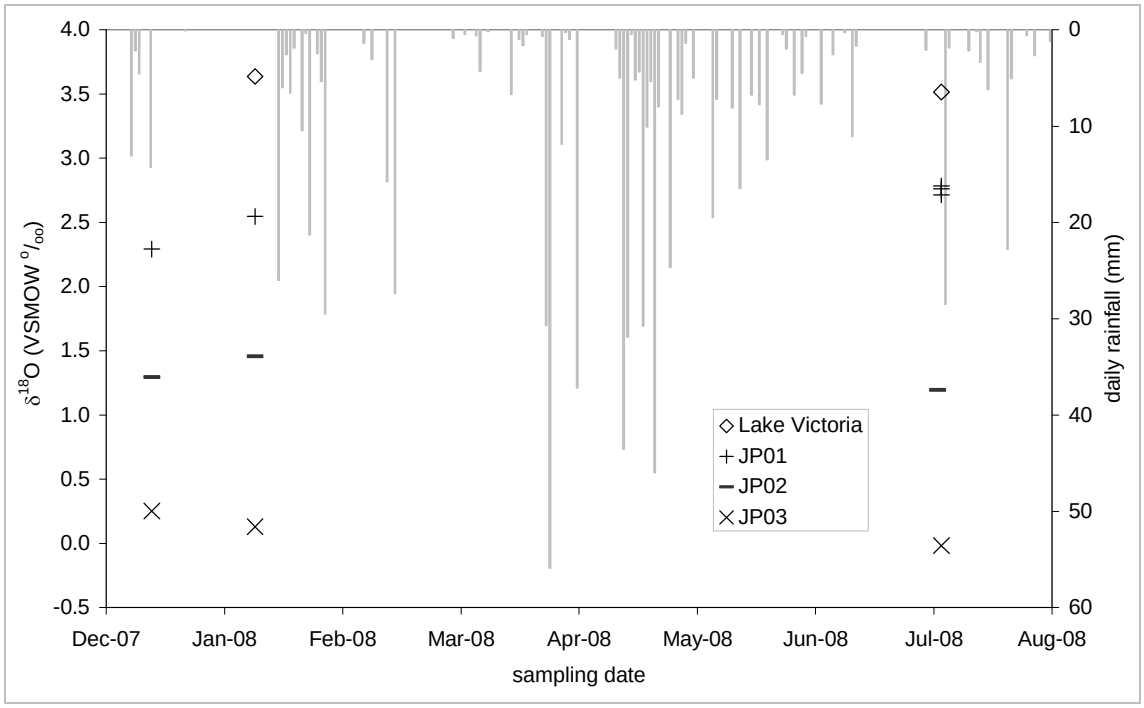

Figure 3.24 The $\delta^{18}O$ plots for the water samples from the Jinja station on Lake Victoria shore collected over different seasons from December 2007 to August 2008.

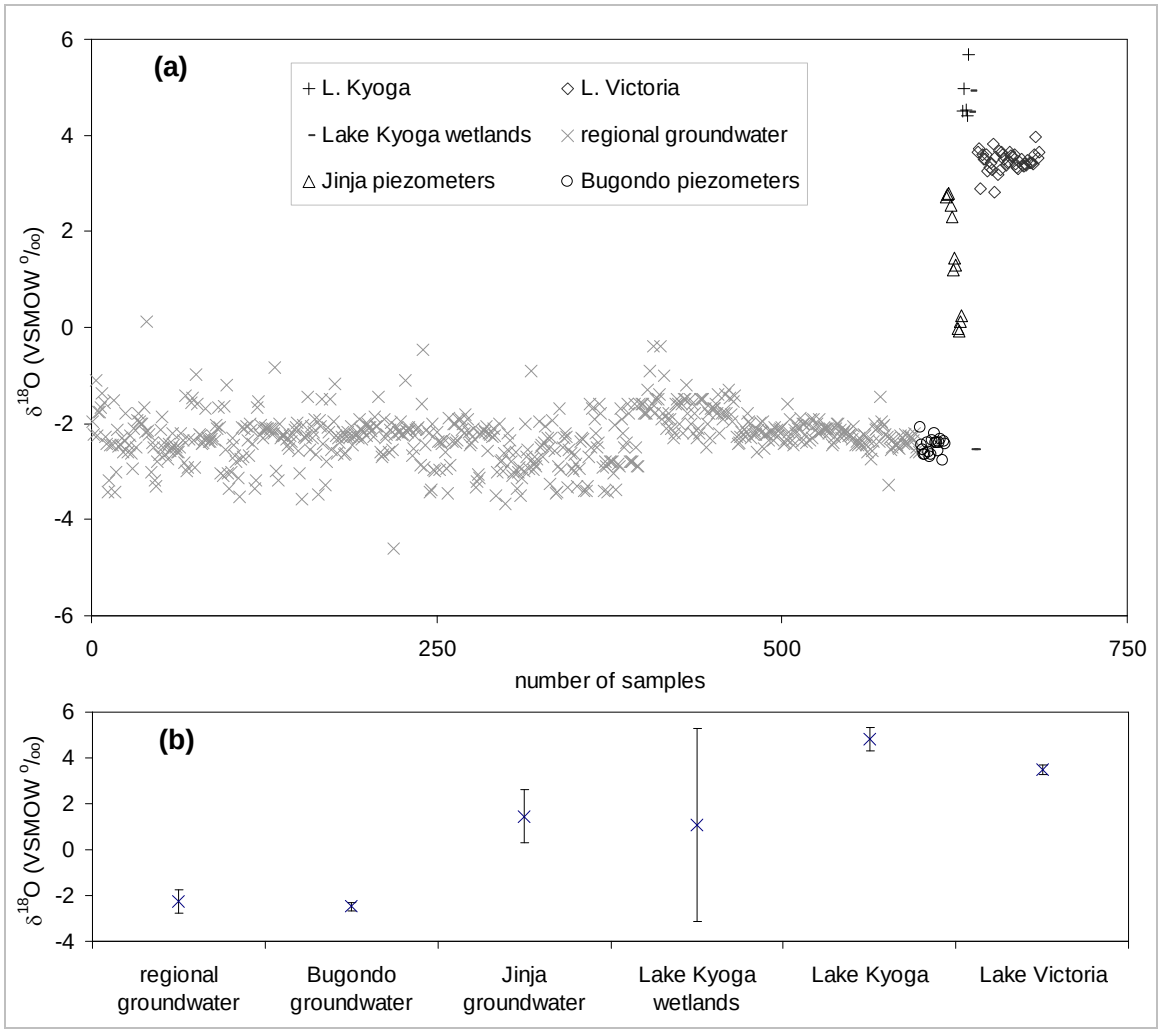

Figure 3.25 (a) The $\delta^{18}O$ plot of national groundwater samples compared with study surface water and groundwater samples, and (b) the $\delta^{18}O$ plots of mean and standard errors of all the analysed samples.

In general, isotopic ($\delta^{2}H$ and $\delta^{18}O$) chemistry suggest that groundwater is actively recharged by local rainfall at both Bugondo and Jinja. At Bugondo, groundwater is largely unaffected by the lake waters, however, it is likely that groundwater contributes to wetland waters during the wet seasons. In Jinja, it is proposed that groundwater evolves along the flow path by mixing with lake waters.

3.5 Relationship between the interface of groundwater and surface waters and drainage evolution

3.5.1 Groundwater interface with Lake Kyoga at Bugondo

The hydrostratigraphy of the fluvial-lacustrine sands and the underlying saprolite at Bugondo is shown in figure 3.26. At Bugondo, a variable layer (up to 5 m thick) of fluvial-lacustrine (quartz-rich) sands thins out towards the interfluves approximately 500 m from the lakeshore. Within ~100 m from the lakeshore, fringing wetlands form a zone of waterlogged, organic-rich matter (sapropel) which mixes with and obscures weathered sediments. On the interfluves, weathered clasts of medium sand to clay-rich lateritic residuum or colluvium occurs and includes a mottled zone whose base appears to mimic the relief of the terrain. This zone tapers out towards the lakeshore where the fluvial-lacustrine sands rest upon vesicular and pisolithic duricrust whose thickness (from a couple of metres) increases towards the interfluves. Underlying the duricrust, there are discrete zones of fine to medium sand-sized mottled material within which the proportion of sand-sized clasts increases with depth in saprolite. Below the saprolite, fractured bedrock (saprock) occurs at depths of >20 mbgl (Fig. 3.27). However, there is a wide spatial variability in the thickness of weathered profile above the fractured bedrock (regolith), depths range from 9 to 56 mbgl. Thick saprolite is prominent within the low-lying areas to the south of the Bugondo station. To the south and southwestern shores of Lake Kyoga, borehole logs show laterites at average depths from 0.5 to 43 mbgl overlying groundwater-bearing zones with average depth to saprock (regolith) of 33-80 mbgl.

Fluvial-lacustrine sands are likely to have been laid down during successive periods of progressive reduction in flow energies during stripping of the high surface of eastern Uganda (section 2.3.1), when rejuvenation through several drops in base level

occurred probably prior to the drainage reversal, and thus corresponds to a fluviatile environment (Fig. 2.6). Following drainage reversal, post-Neogene pluvial events promoted deep weathering that contributed to the formation of a thick weathering profile capped by a surficial vesicular and pisolithic duricrust (section 2.3.2). Whether this was through the isovolumetric or allovolumetric transformation from the leaching of upper parts of the interfluves by a perched, oscillating water table as proposed by McFarlane (1992) is debatable. However, it is inevitable that there was some degree of collapse of weathered lithology. A further drop in relative base level is likely to have followed with local stream incision and removal of the laterite cover from the valleys, followed by a rise of relative base level with consequent infilling of the intermediate valleys with alluvial material as proposed by Trendall (1965). The stratigraphy below the fluvial-lacustrine sands lends support to the differential leaching, saprolite collapse and landscape lowering represented by *in situ* hypothesis (McFarlane, 1992). This profile is also consistent with Taylor and Howard (1998)'s model of post-Palaeozoic evolution of weathered land surfaces in Uganda where since mid-Neogene, following the development of the western rift, prolonged deep weathering by meteoric water has been the dominant geomorphic process operating in eastern Uganda. Accordingly, the hydrostratigraphic profile of the Bugondo station inferred from the hydrochemistry and hydraulic gradient with surface waters suggests that the saprolite transmits the dominant proportion of the groundwater flux which then mixes with waters from the fluvial-lacustrine sands as it discharges into Lake Kyoga. Stable isotope ratios ($\delta^{2}H/\delta^{18}O$) relationship suggest that groundwater seasonally contributes to wetland waters.

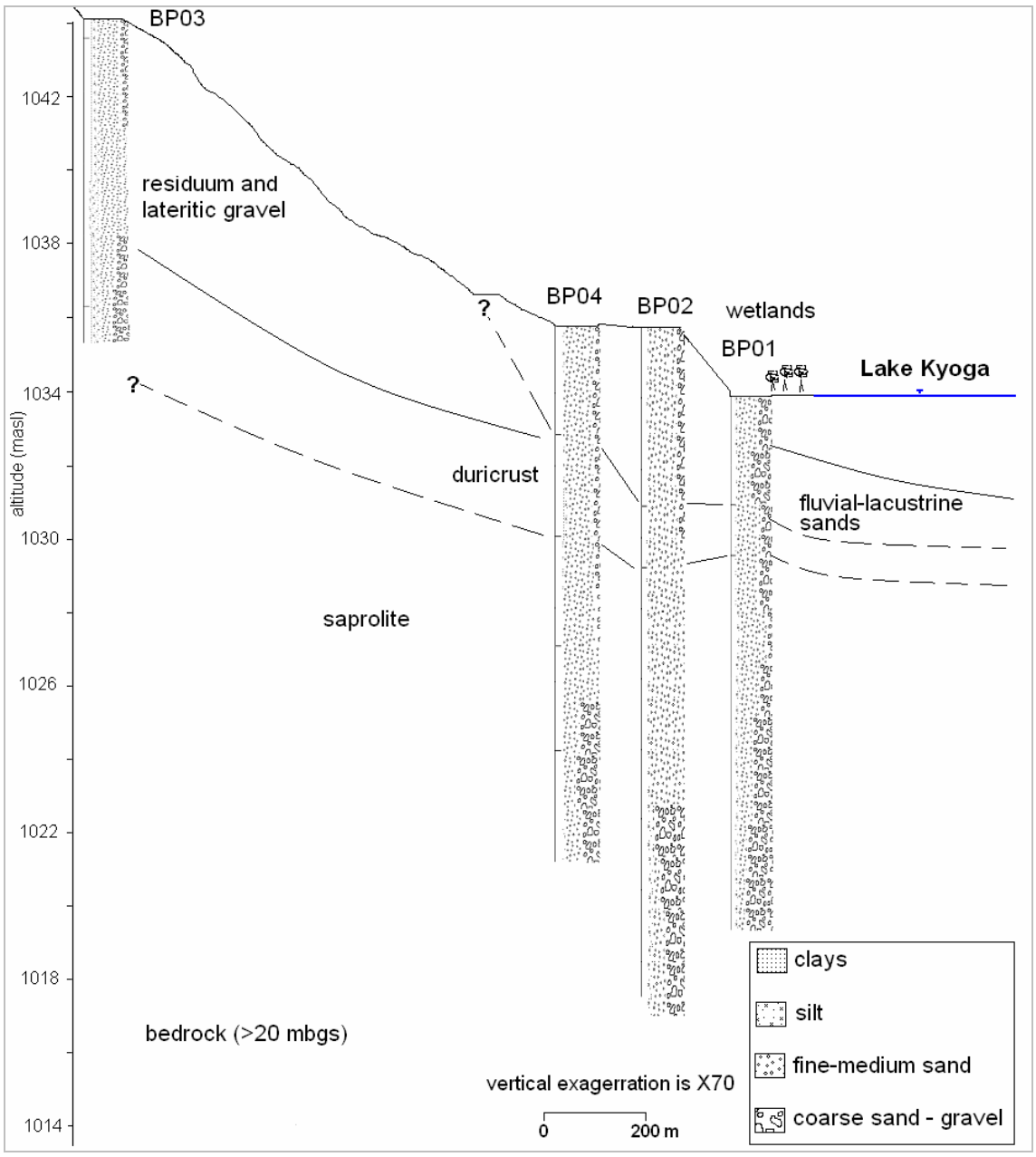

Figure 3.26 The general configuration of the interface between the fluvial-lacustrine sands and the underlying saprolite on the shore of Lake Kyoga at Bugondo.

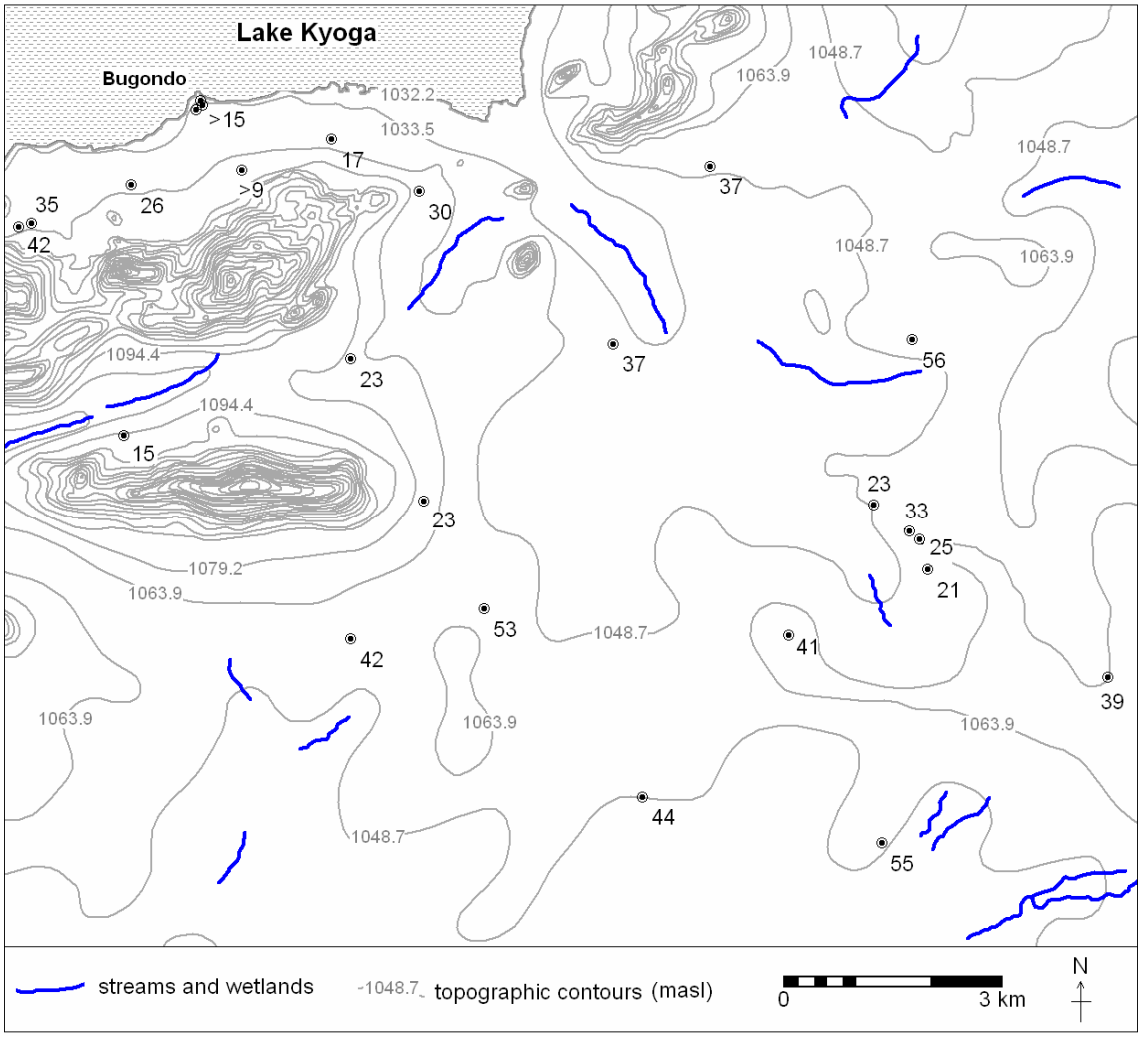

Figure 3.27 Spatial variability of depth (mbgl) to fractured bedrock (saprock) estimated from borehole records in the region south of the Bugondo station.

3.5.2 Groundwater interface with Lake Victoria at Jinja

At Jinja, the hydrostratigraphy of the interface between groundwater and surface water comprises a thin layer (up to 3 m thick) of swampy, waterlogged mixed sands and infill adjoining the lake which thins out towards the interfluves (Fig. 3.28). The interfluves have a residuum or colluvium of similar composition to that of Bugondo which also increases in thickness away from the lake. There is however, no duricrust beneath these layers. There is simply a thick saprolite that comprises weathered lithic fragments of the parent amphibolite bedrock. The depth to the fractured bedrock

(regolith) is relatively shallow in the vicinity of the lakeshore but increases and varies considerably (>40 mbgl) in the more elevated interfluves (Fig. 3.29). Generally, there is a thin layer of mixed sands whose original fluvial-lacustrine composition has been disrupted by the infill associated with the construction of a nearby pier. Except for the absence of the duricrust underlying the fluvial-lacustrine sands and the lateritic residuum or colluvium in Bugondo, the rest of the stratigraphy is similar. This environment has, however, been more active bearing the brunt of high energy fluctuating water levels than in Bugondo with less variability, and it is therefore likely that Fe-Al accumulation that was leached from the upper interfluve profiles were re-mobilised and eroded away during the down-cutting of the Victoria Nile outlet (Bishop, 1969; Kendall, 1969; Talbot *et al.*, 2000). The hydrostratigraphic profile of the Jinja station inferred from the hydrochemistry and hydraulic gradient with surface waters suggests that the saprolite transmits the regional groundwater flux but mixes with waters from the mixed fluvial-lacustrine sands before discharging into Lake Victoria. Stable isotopes ($\delta^{18}O$) indicate that groundwater evolves along the flow path by mixing with lake waters.

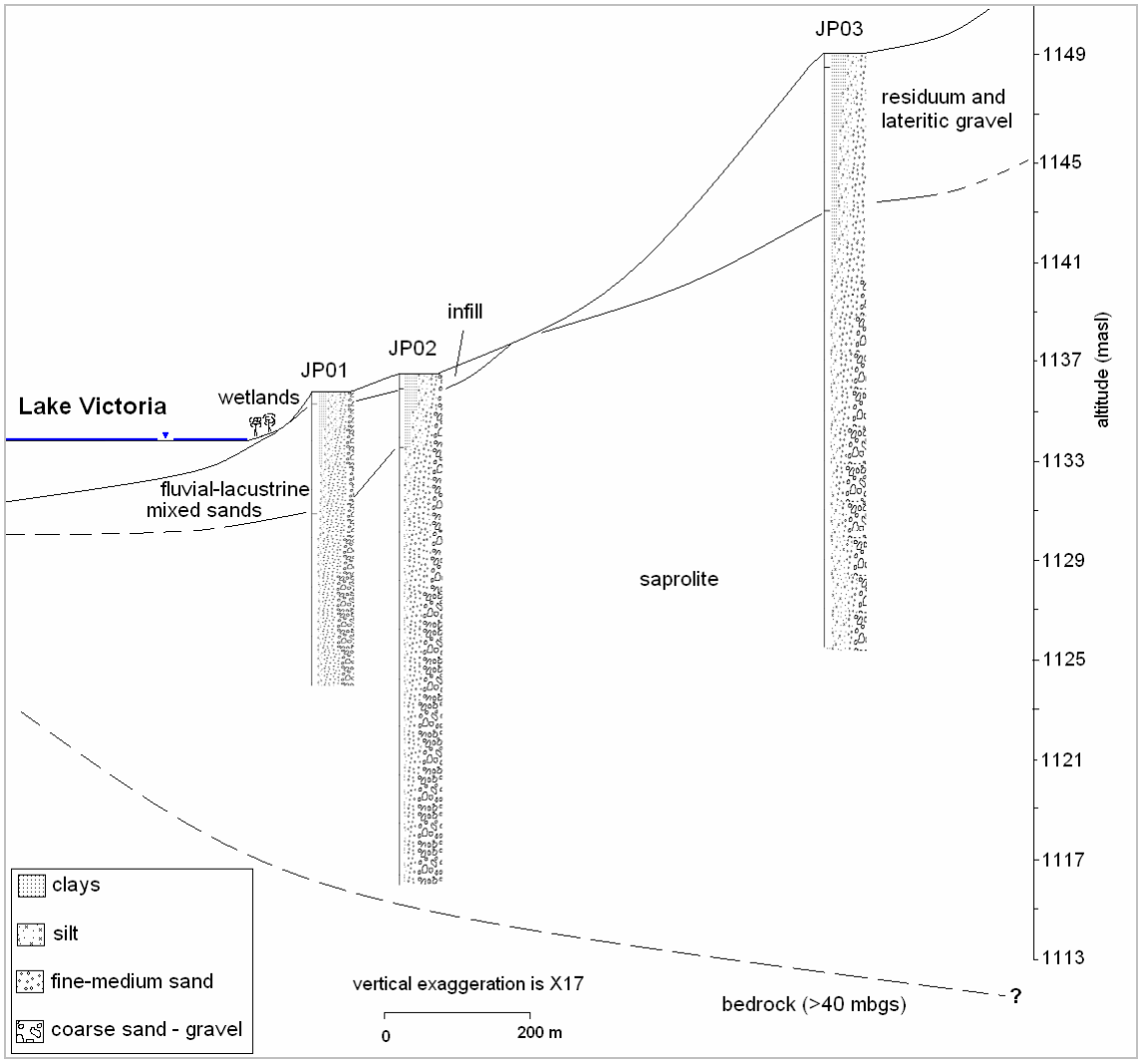

Figure 3.28 The general configuration of the interface between the fluvial-lacustrine sands and the underlying saprolite on the shore of Lake Victoria at Jinja.

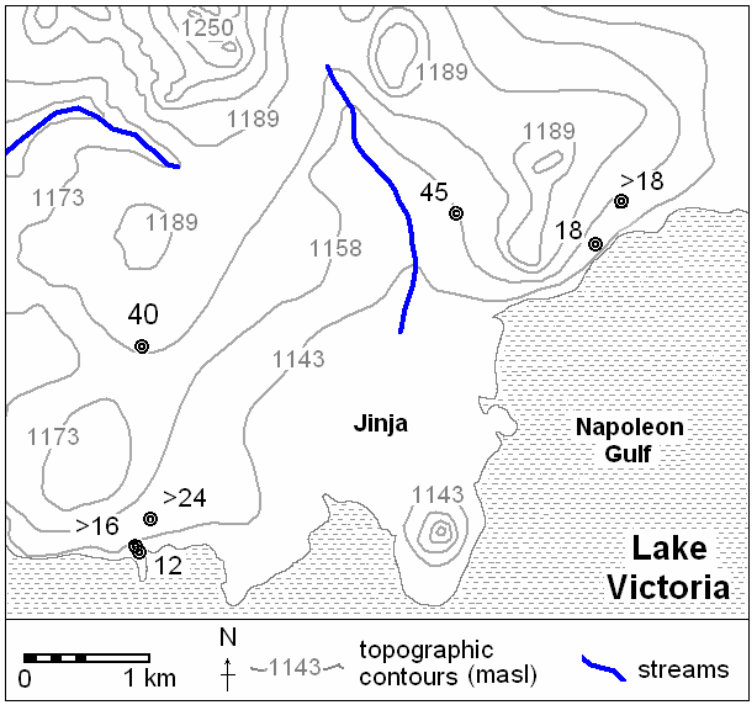

Figure 3.29 Spatial variability of depth (mbgl) to fractured bedrock (saprock) estimated from borehole records in the region north of the Jinja station.

3.5.3 Groundwater interface with Lake Victoria at Entebbe

At Entebbe, the hydrostratigraphy features fluvial-lacustrine sands (up to 5 m thick) that overlie a thick, fine to medium sandy lateritic residuum whose spatial extent is unclear (Fig. 3.30). Below this zone is coarse-grained saprolite. The fractured bedrock surface occurs at depths of >48 mbgl in DWRM and >67 mbgl noted around the well on the southwest of the peninsula (Fig. 3.6). The presence of lateritic nodules and of a massive laterite cap in the profiles of Bugondo and not in those of Jinja and Entebbe follows observations of Taylor and Howard (1999a) in northern Uganda, which contrasted with profiles from the western part of the country where it was also absent. Indurated laterites are found in the upper horizons of the mesa hills that cover much of the peninsula, e.g. the Nsamizi hill where McFarlane (1969) identified detrital pisolithic groundwater laterites to ~8 m depth. It is suggested that west of Lake Victoria, stripping of the landscape following mid-Pleistocene uplift (Taylor and Howard (1999a), formed

a low relief surface next to the lake which impeded further free flow of recharge, necessary, in part, for the formation of laterite caps.

Generally, Entebbe shares a similar stratigraphy with Jinja apart from the pronounced thicknesses of both the fluvial-lacustrine sands and the underlying lateritic gravel residuum. The hydrostratigraphy is considered to have a similar origin to that of Jinja. Marked thicknesses of the layers at Entebbe compared to Jinja can be attributed to enhanced deep weathering by meteoric waters following the tilting upward to the west of the old, indurated sequences which in Jinja was most likely affected by erosion of the Lake Victoria outlet. Accordingly, the hydrostratigraphic profile at Entebbe as well as stations along the northern shore of Lake Victoria inferred from lithologic logs and hydraulic gradient with surface waters indicate that groundwater flows into Lake Victoria. Stable isotopes ($\delta^{18}O$) suggest that in parts, groundwater mixes with lake waters through evaporation.

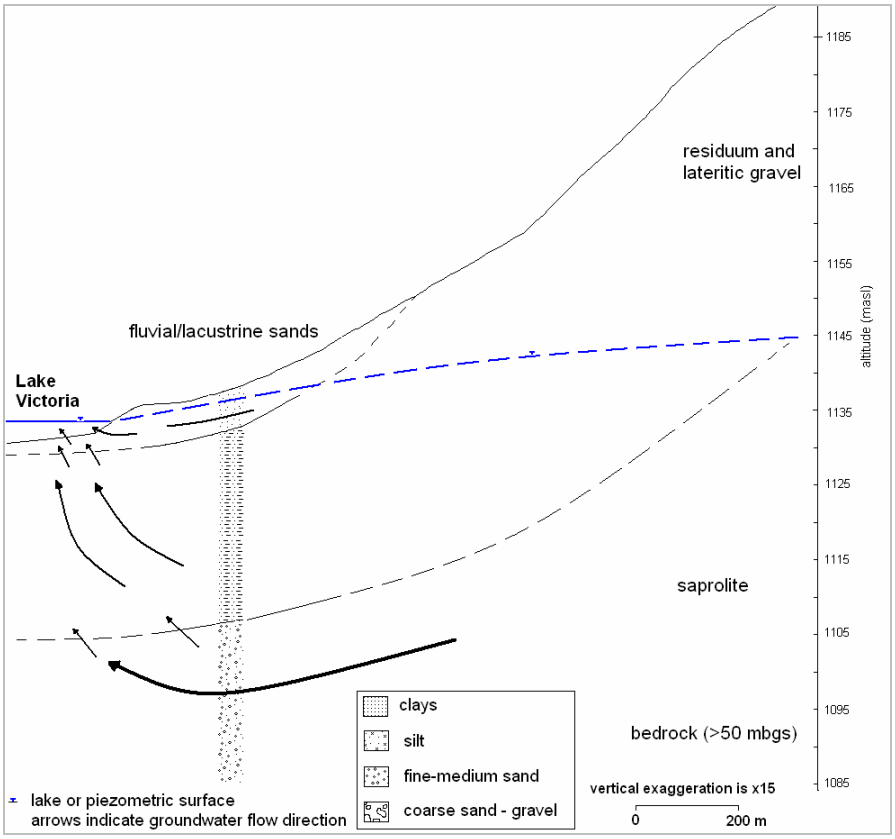

Figure 3.30 The general configuration of the interface between the fluvial-lacustrine sands and the underlying saprolite on the shore of Lake Victoria at Entebbe.

3.5.4 Implications of hydraulics for groundwater-surface water interactions

Observations at Bugondo, Jinja and Entebbe reveal distinct differences with key landscape evolution models proposed by McCartney and Neal (1999) and Bell *et al.* (cited in von der Heyden, 2004) reviewed in section 2.6. These two key models have lithological barriers that do not support fluxes between the dambo and the deeper regolith/saprolite layer which would allow upwelling of groundwater from the saprolite to the lakes. Of the fluviatile and *in situ* models proposed by McFarlane (1992), it is the latter that is consistent with the hydrostratigraphy observed at Bugondo, Jinja and Entebbe. The observations support the *in situ* hypothesis with regard to deep circulation of water within the saprolite being a key source of groundwater to the lakes via preferential pathways which are conduit zones or semi-confining layers that allow faster groundwater recharge and exfiltration to surface waters. These may include, for example, discontinuous clay horizons, quartz stringers and fractures in duricrust. However, key departures arise from the nature and extent of stratigraphic profiles as well as the modes of evolution where dominant deep weathering processes operate at the same time with lesser stripping, a view consistent with Taylor and Howard (1998)'s model of post-Palaeozoic evolution of weathered land surfaces in eastern Uganda. The hydrochemistry and positive hydraulic gradient from groundwater towards both Lakes Victoria and Kyoga at all the stations coupled with the depth profiles showing significant hydraulic conductivity within the saprolite suggest that groundwater interacts dynamically with lake waters.

3.6 Summary

Groundwater - surface water monitoring stations constructed on the shores of Lakes Victoria (Jinja) and Kyoga (Bugondo) combined with an existing groundwater monitoring station on the shore of Lake Victoria at Entebbe reveal a positive hydraulic gradient from groundwater towards the lakes coupled with the depth profiles showing K and S_y within the saprolite. All evidence suggests that groundwater interacts dynamically with lakes. Initial static water levels in all the stations occur above the main water strike zones and reflect leaky or confined aquifer conditions, with initial hydraulic gradients indicating groundwater flow into the lakes. Lithologic and geo-electrical resistivity surveys at Bugondo show relatively consistent hydrostratigraphy wherein fluvial-lacustrine sands are succeeded with depth by weathered rocks indicative of sub-aerial, *in situ* origin. At Jinja, laterite crust is absent and presumed to have been eroded when the lake's outlet at Jinja was curved out during the late Pleistocene (section 2.4.1).

The major ion chemistry suggests that mineralised groundwater upwell from saprolite, mix with local diffuse recharge via the fluvial-lacustrine sediments, which then discharge into the lakes. Additionally, isotopic chemistry indicates that groundwater contributes to wetland waters in Bugondo, groundwater evolves along the flow path by mixing with lake waters at Jinja, and groundwater mixes with lake waters in the fringing region on the northern shore of Lake Victoria. All the three sites support the *in situ* hypothesis where deep circulation of water within the saprolite is the primary source of groundwater upwelling into the lakes via preferential pathways, e.g. discontinuous clay horizons, quartz stringers and fractures in duricrust within the upper horizons of the saprolite.

Chapter 4
Hydrodynamic interactions between groundwater and surface water in Lakes Victoria and Kyoga basins

4.1 Introduction

This chapter reports new knowledge gained from observations of hydraulic interactions between groundwater and surface water in the Upper Nile Basin enabled by the construction of nested piezometer stations (chapter 3). A combination of historical data and new observations is used to assess water-level dynamics since 1998 using daily and hourly measurements derived from the new monitoring infrastructure. Hydraulic tests establish the hydrogeological controls on the dynamic gradient between groundwater and surface water at the three monitoring stations. Co-located borehole and lake-stage hydrographs for Lakes Victoria and Kyoga permit analysis of temporal variations in the hydraulic gradient between groundwater and surface water. Hydrodynamic conceptual models of the interaction between groundwater and surface waters at the stations are developed and integrated with the results from lithological analyses produced in chapter 3.

4.2 Groundwater – surface water interactions in the Great Lakes Region of Africa (GLRA)

In chapter 2 (section 2.6.2), the geomorphic evolution of dambos (wetlands) on low relief surfaces is discussed. Here, the hydrodynamic implications of these evolutionary models are reviewed as they provide the only conceptual models of groundwater-surface water interactions in the GLRA. Dambos feature extensively throughout the GLRA yet there is no consensus regarding the hydrology and hydrogeology of these surface waters.

von der Heyden and New (2003) use hydrological and geochemical data to describe the hydrological functions of a dambo in northwestern Zambia (Fig. 4.1). Their conceptual model suggests that a shallow aquifer perched on shale and dolomite together with saprolite contribute a large proportion of the baseflow during rainy and early dry seasons. A deeper dolomite aquifer provides baseflow to the dambo during middle to late dry season. This conceptual model is consistent with the McFarlane (1992) hypothesis discussed below.

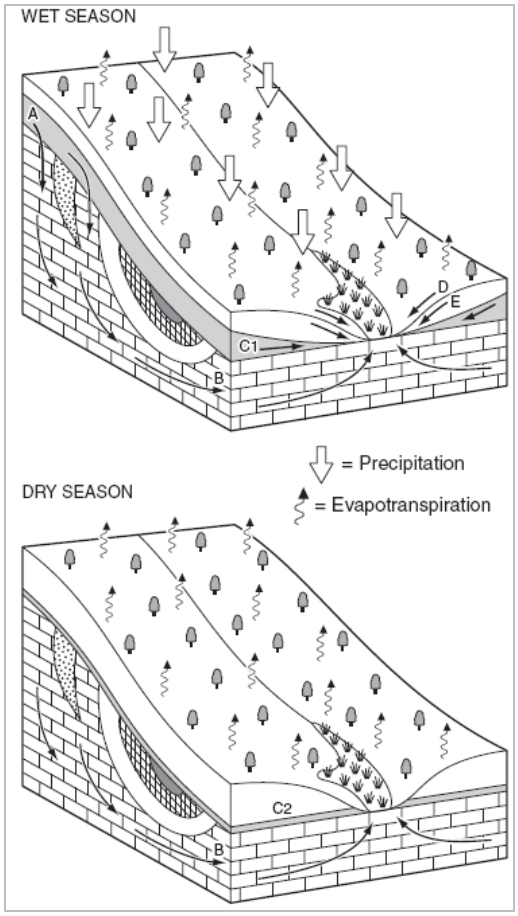

Figure 4.1 The seasonal hydrodynamic model showing (A) deep aquifer recharge, (B) deep aquifer discharge, (C1) soil aquifer discharge, (C2) perched water table, (D) overland stormflow, and (E) subsurface stormflow (von der Heyden and New, 2003).

In Malawi, McFarlane (1992) developed *fluviatile* and *in situ* landscape evolution models to describe the hydrology of dambos. During the wet season, she argued that precipitation infiltrates the interfluve profile to form a shallow and rapid

throughflow which discharges onto the dambo floor at the seepage zone (Fig. 4.2). This shallow subsurface flow combines with direct surface runoff from the dambo floor after the smectite clay wedge has absorbed sufficient water to seal the cracks. Recharge to the deep system occurs through the saprolite/residuum interface in the interfluves. Upwelling of deep water occurs at the dambo margin and as discrete springs on the dambo floor because the clay barrier laterally diverts deep groundwater. During the dry season, slow recharge to the deep groundwater continues through the interface of the interfluve profile. Shallow throughflow is reduced but continues to discharge at the dambo margins where it is largely lost by evaporation. Discharge at springs and lateral movement of deep water below the dambo clay continues but becomes progressively less dynamic as the hydraulic head within the interfluve is reduced.

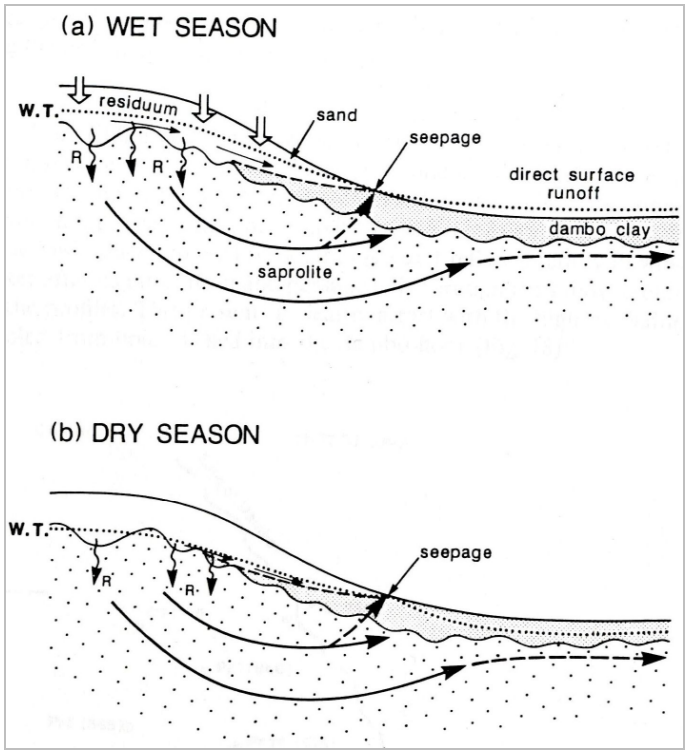

Figure 4.2 The seasonal hydrodynamic dambo model showing: (a) wet season shallow throughflow, deep groundwater recharge through the saprolite-residuum interface discharging at the dambo margin and as discrete springs on the dambo floor, and lateral flow beneath the dambo; and (b) dry season slow deep groundwater recharge and shallow throughflow, and less vigorous flow spring discharge and lateral movement of deep groundwater flow (McFarlane, 1992).

McCartney and Neal (1999) provide an alternative model (Fig. 4.3) that derives from hydrological and chemical markers (alkalinity and chloride) observed in a small catchment containing a dambo in Zimbabwe. This model features a low permeability clay lens which acts as a barrier to vertical water exchange with the dambo. Dry season recession flow is considered to be dominated by shallow water sources; differences in baseflow chemistry are attributed to alternative flow pathways and varying contributions from near-surface soil horizons. A water budget of the catchment estimates that only about 12 % of total water into the dambo comes from groundwater inflow from the interfluve with most (~80 %) of it occurring during the wet season (McCartney, 2000).

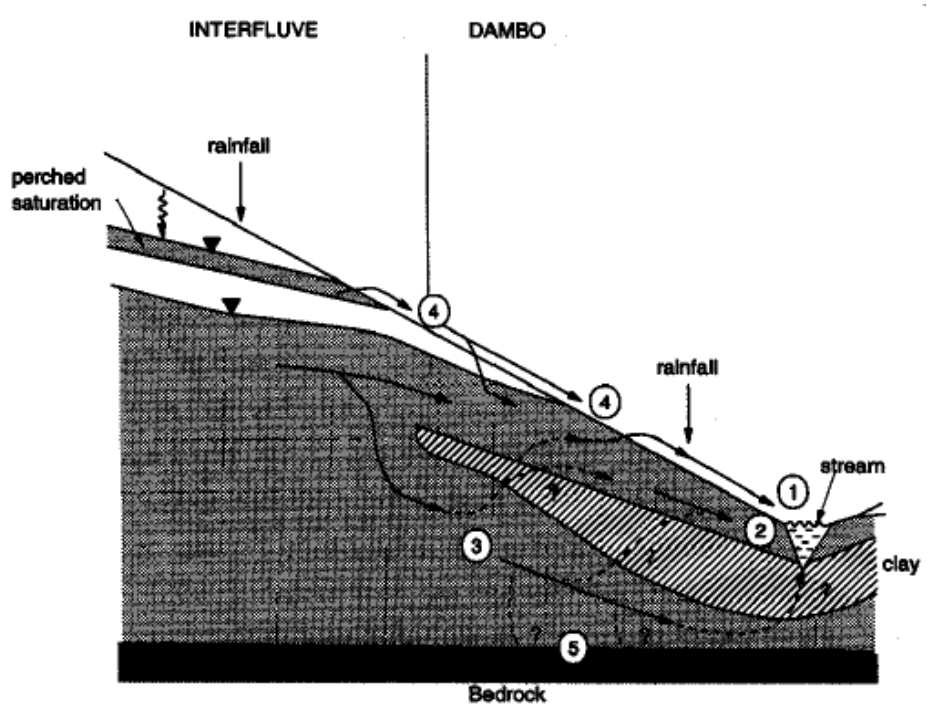

Figure 4.3 The seasonal hydrodynamic dambo model showing (1) surface runoff, a combination of return flow and saturation overland flow, (2) shallow throughflow and pipe flow moving above the clay lens, (3) groundwater moving blow the clay, (4) spring water discharge, and (5) deep groundwater drainage (McCartney and Neal, 1999).

Lithologic evidence, described in chapter 3, favours the *in situ* models but the hydrogeological context and pathways of the hydrodynamic interactions between

groundwater and surface water in the GLRA are still unclear. The most detailed research on the interactions between groundwater and surface waters within the GLRA has been carried out on Lake Naivasha within the eastern arm of the EARS. In contrast to Lakes Victoria and Kyoga which occupy large, shallow depressions formed by downwarping (section 2.4), Lake Naivasha is a comparatively small (surface area of 139 km^2) crater lake that rests on late Quaternary, highly differentiated alkaline volcanic and fluvial-lacustrine deposits derived from erosion and re-deposition of the volcanics (Ojiambo *et al.*, 2003). Regionally, groundwater flows from the flanks of the rift towards the floor where well yields and transmissivities are highest within the fluvial-lacustrine sediments adjacent to the lake. Groundwater flow also occurs, to a lesser extent within weathered contacts between lava flows and fractured volcanic rocks (Ojiambo *et al.*, 2001).

Becht and Harper (2002) suggest Lake Naivasha to be a through-flow lake with an estimated monthly groundwater outflow comprising approximately 18 % of the total outflow. Ojiambo *et al.* (2001) also use $^{3}H/^{3}He$ and $^{2}H/^{18}O$ ratios to indicate recent dynamic groundwater outflows to the south of the lake. This is supported further by strontium isotope compositions and mixing calculations using rare earth element concentrations that indicate that between 70 and 85 % of groundwater directly south of the lake is likely to be lake water with short residence times (Ojiambo *et al.*, 2003). Olago *et al.* (2009) additionally suggest that Lakes Nakuru, Elmenteita, Baringo and Bogoria which are found close to Lake Naivasha in the rift are also likely to have low but varying interconnectivity with groundwater. Similarly, major ion and stable isotope data analysed in sections 3.4.5 and 3.4.6 suggest that groundwater mixes and discharges into both Lakes Victoria and Kyoga. Fluxes between groundwater and surface water on low relief surfaces in the GLRA are, however, unknown.

4.3 Hydrogeological context of groundwater – surface water interactions in the Lakes Victoria and Kyoga basins

In chapter 3, spot hydraulic head measurements from newly constructed nested piezometers indicate that groundwater flows into Lakes Victoria and Kyoga. Groundwater-level measurements alone do not, however, reveal the hydrogeological conditions under which groundwater flow takes place. Hydraulic (pumping) tests are applied to establish the hydrogeological conditions controlling the hydrodynamic gradient between groundwater and surface water. Tests were conducted at Bugondo on Lake Kyoga and Jinja on Lake Victoria in July 2008. Step-drawdown tests were initially carried out and followed by constant-rate pumping tests. During all tests, water levels were monitored in nested piezometers as well as barometric pressure variations. At the end of each pumping period, the recovery of the water levels in all piezometers was monitored. The piezometers were then individually pumped for durations depending on their previous drawdown responses to the long duration constant-rate pumping of the middle piezometers. Physico-chemical water parameters and sampling for chemical and isotopic analyses were carried at intervals during the course of the pumping tests.

4.3.1 Hydraulic testing

Step-drawdown tests on each piezometer were conducted to determine optimal pumping rate (Kruseman and de Ridder, 2000). At Bugondo, BP02 piezometer (Fig. 3.3) was then steadily pumped at a rate of 1.3 $m^3 \cdot h^{-1}$ for over 10 hours. In Jinja, JP02 (Fig. 3.2) was pumped at a rate of 0.93 $m^3 \cdot h^{-1}$ for approximately 15 hours. Both piezometers were monitored close to full (>98 %) recovery (Table 4.1). Piezometers were pumped using a Grundfos medium-capacity pump with a voltage stabiliser. Drawdown in the pumped and observation wells was monitored using absolute (non-vented) pressure transducers. The direct-readout Solinst® Levelogger Gold determined

the water level equivalent of the total pressure reading, whereas the Solinst® Barologger Gold monitored barometric pressure to obtain the actual temperature-compensated water levels. Barometric pressure fluctuations were removed from the total pressure head measurements taken during the pumping tests in order to evaluate actual water-level responses (Davis and Rasmussen, 1993; Rasmussen and Crawford, 1997; Kruseman and de Ridder, 2000; Spane, 2002). Each piezometer at Bugondo and Jinja showed no marked response to actual pumping. Consequently, each piezometer was, in turn, pumped for a short period to investigate the hydrogeological conditions within its immediate vicinity (Kruseman and de Ridder, 2000). These short-duration tests, when the piezometers were also sampled, ranged from 0.2 to 3.0 hours at pumping rates of 0.1 to 1.7 $m^3 \cdot h^{-1}$ (Table 4.1).

Table 4.1 The hydraulic tests pumping conditions imposed on monitoring wells in Bugondo and Jinja during July 2008.

parameters	BP01	BP02	BP04	JP01	JP02	JP03
Step 1 pumping rate ($m^3 \cdot h^{-1}$)	1.3	0.4	1.1	0.4	0.1	0.9
Step 1 pumping duration (h)	0.5	0.3	0.2	0.8	0.7	1.3
Step 2 pumping rate ($m^3 \cdot h^{-1}$)		0.9	1.4	0.8	0.4	
Step 2 pumping duration (h)		0.5	3.0	2.7	0.7	
Step 3 pumping rate ($m^3 \cdot h^{-1}$)		1.3			0.8	
Step 3 pumping duration (h)		0.5			0.8	
Step 4 pumping rate ($m^3 \cdot h^{-1}$)		1.7			1.0	
Step 4 pumping duration (h)		0.4			0.9	
Constant pumping rate ($m^3 \cdot h^{-1}$)		1.3			0.9	
Constant pumping rate duration (h)		10.0			15.0	
Recovery duration (h)	3.2	8.1	14.7	0.9	7.7	16.6

4.3.2 Interpretation of hydraulic tests

Classical methods of pumping-tests analysis (e.g. Theis, 1935; Cooper and Jacob, 1946) involve type-curve data fitting of log-log plots or straight-line analysis of semi-logarithmic plots of drawdown with time. Such analyses commonly rely upon major assumptions and conditions that include (Kruseman and de Ridder, 2000):

- a seemingly infinite areal extent;
- homogeneous and uniform thickness;
- a horizontal piezometric surface or water table prior to pumping over area to be influenced by test;
- constant discharge rate;
- a well penetrates the entire thickness of the aquifer so that it receives water by horizontal flow.

These methods are, however, less informative than those based on the derivative of drawdown for quantitative analyses because part of the drawdown or recovery of these stressed wells includes well and formation inefficiencies or damage induced during the drilling process (Spane and Wurstner, 1993). More recently, analyses have been based on the derivative of drawdown with respect to the natural logarithm of time, (equation 4.1), where *s* is the drawdown; *t* is an appropriate time function (e.g. elapsed time); and the two weighted average of slopes are $\Delta s_{i-1} / \Delta \ln t_{i-1}$ and $\Delta s_{i+1} / \Delta \ln t_{i+1}$, known as the left and right derivative, respectively. Such analyses provide superior diagnostic and quantitative information due to the sensitivity of drawdown derivatives to test and formation conditions (Fig. 4.4) (Spane and Wurstner, 1993). Derivative analyses enable both the estimation of hydraulic properties as well as the identification of formational and non-formational conditions such as, wellbore storage, boundaries, and the establishment of radial flow conditions from the test data.

$$\left(\frac{\partial s}{\partial \ln t}\right)_i = \frac{(\Delta s_{i-1} / \Delta \ln t_{i-1})\Delta \ln t_{i+1} + (\Delta s_{i+1} / \Delta \ln t_{i+1})\Delta \ln t_{i-1}}{\Delta \ln t_{i-1} + \Delta \ln t_{i+1}} \qquad (4.1)$$

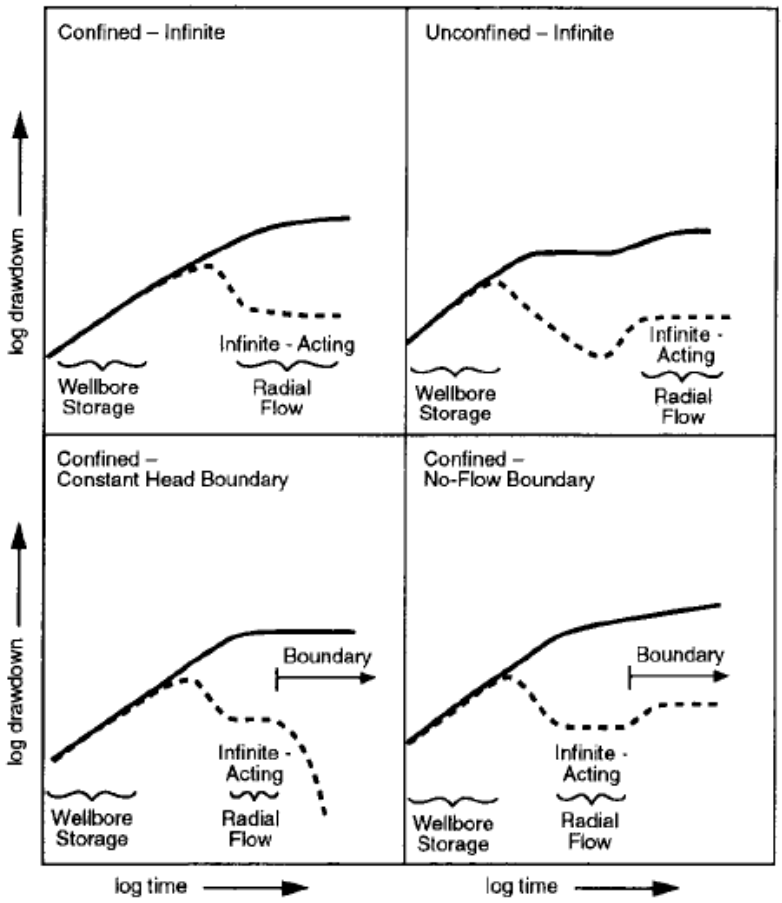

Figure 4.4 Characteristics of log-log drawdown (full line) and drawdown derivative (dashed line) plots for various hydrogeologic formations and boundary conditions (from Spane and Wurstner, 1993).

Commercial software, AQTESOLV for Windows (Duffield, 2008), was used to calculate drawdown derivatives for each constant-rate pumping test. AQTESOLV applies the principle of superposition in time to simulate variable-rate pumping tests including recovery, which treats the variable rate as a sequence of steps in which the discharge rate is constant in each step. The Bourdet method (Bourdet *et al.*, 1989) is commonly employed to compute the drawdown derivative (equation 4.1). It makes use of a simple 3-point formula that utilises a weighted average of slopes computed from data points on either side of a data point of interest. This typically results into broad fluctuations in the derivative signal due to pumping rate variations. In order to reduce the noise from the computations, the Bourdet method uses data points separated by a fixed distance measured in logarithmic time (L-spacing). Usually, the separation or

differentiation interval required to remove noise ranges between 0.1 and 0.5 of a log cycle.

At each of the two piezometers in Bugondo and Jinja, the existence of lakes within their vicinity would be expected to stabilise drawdown as lakes represent constant-head boundaries. Additionally, semi-confining conditions within these groundwater systems are indicated by continuous responses of the monitored water levels to changes in the barometric pressure (Rasmussen and Crawford, 1997; Kruseman and de Ridder, 2000) as well as hydraulic parameters from lithological data (chapter 3). Considering these two constraints, the Moench (1985) solution was considered an appropriate analytical model to assess hydrogeological conditions around 5 piezometers. The Moench solution assumes a homogeneous and isotropic aquifer, and unsteady flow in a fully or partially penetrating finite-diameter well with wellbore storage and wellbore skin. For the furthest piezometer from Lake Victoria within the elevated interfluve in Jinja (JP03), a second solution by Dougherty and Babu (1984) was adopted and assumes: a fully or partially penetrating finite-diameter well with wellbore storage and wellbore skin, and a homogeneous, isotropic confined aquifer.

Visual matching between each analytical solution and the recorded drawdown was used to estimate hydraulic properties. Results of the pumping tests carried out in all the 6 piezometers are shown in figure 4.5. The longest (15 hours) pumped piezometer in Jinja (JP02) exhausts wellbore storage from the derivative data, and then overcomes positive skin effects before it stabilises to reflect radial flow conditions (Fig. 4.5e). 'Skin effects' result from a zone of altered permeability near the wellbore which may be positive (i.e. inhibit flow - smearing of mud on well walls during drilling), or negative (i.e. enhance flow - a fracture zone) (Duffield, 2008). Figure 4.5e shows that the constant-head boundary is not reached during the course of this pumping period. A bulk T of 2 $m^2 \cdot d^{-1}$ is estimated (Table 4.2). The other two piezometers (JP01 and JP03) were

not pumped long enough to achieve fully radial flow conditions (Figs. 4.5d and f). From these shorter tests, bulk *T* estimates of 5 and 18 $m^2 \cdot d^{-1}$ are estimated, respectively.

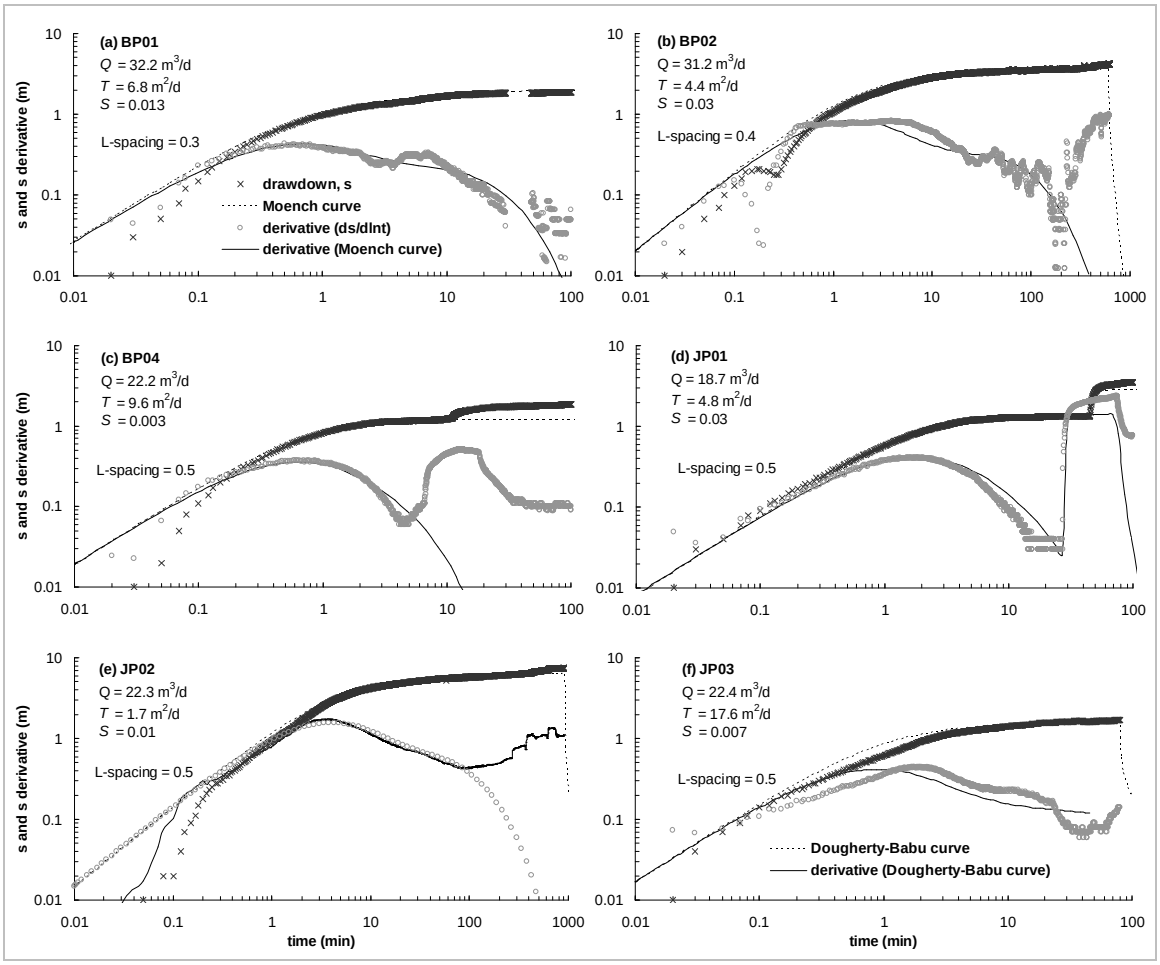

Figure 4.5 Drawdown and drawdown derivative plots for Moench (1985) leaky aquifer (a - BP01, b - BP02, c - BP04, d - JP01 and e - JP02) and Dougherty-Babu (1984) confined aquifer (f - JP03) analytical solutions for hydraulic tests during July 2008.

In Bugondo, BP02 was pumped for the longest (10 hours) duration and it likewise exhausted wellbore storage. The test overcomes positive skin effects before stabilising to reflect radial flow conditions (Fig. 4.5b). The radius of influence reaches the constant-head boundary (i.e. lake) from the late-time results, giving a bulk *T* of about 4 $m^2 \cdot d^{-1}$. BP01 was pumped for a short (0.5 hours) period but due to its proximity (<20 m) to the lake and fringing wetlands, realises a constant-head boundary. A bulk *T*

of 7 $m^2 \cdot d^{-1}$ is estimated (Fig. 4.5a). Piezometer BP04 on the other hand, does not appear to reach fully radial flow conditions and has an estimated bulk *T* of 10 $m^2 \cdot d^{-1}$ (Fig. 4.5c).

Previous pumping tests carried out by DWRM in two wells found within fluvial-lacustrine aquifers on the western shore of Lake Victoria (Fig. 3.21) give bulk *T* of 18-36 $m^2 \cdot d^{-1}$. There is thus variability in the groundwater fluxes around the lake region which is limited by the proportion of clay content within the unconsolidated and weathered sediments. These results are also consistent with the leaky fractured bedrock aquifers of Aroca, northern Uganda where similar ranges of bulk *T* values (0.06-12 $m^2 \cdot d^{-1}$) were found to fluctuate considerably over three orders of magnitude (Taylor and Howard, 2000). Results of the physico-chemical analyses of the water samples collected over the course of the constant-rate hydraulic tests on JP02 and BP02, show stable variations in both pH and EC at Jinja and Bugondo.

Table 4.2 The aquifer parameters derived from the hydraulic tests on the Bugondo and Jinja monitoring wells carried out during July 2008.

parameters	**BP01**	**BP02**	**BP04**	**JP01**	**JP02**	**JP03**
Bulk *T* ($m^2 \cdot d^{-1}$)	6.8	4.4	9.6	4.8	1.7	17.6
Indicative bulk *S* estimates	0.013	0.03	0.003	0.03	0.01	0.007

Generally, the semi-confining (leaky) hydrogeological conditions within the interface of groundwater and the lakes are supported by hydraulic parameters estimated from textural data (chapter 3) and pumping-test data. Bulk *T* estimates from the hydraulic tests range from 2 to 36 $m^2 \cdot d^{-1}$ within the lithologic interface between groundwater and Lakes Victoria and Kyoga which concur with fluctuating *K* (<0.02 – 15 $m \cdot d^{-1}$) estimates (chapter 3). Stratigraphic evidence suggests that there is substantial depth and spatial variability in *K* and S_y within saprolite and fluvial-lacustrine sands zones across the interface. A constant-head boundary defined by the lakes and fringing wetlands over time interacts with groundwater across the lithologic interface. These

tests suggest that the permeability of saprolite layers is variable and/or there is a high horizontal to vertical *K* anisotropy ratio (Banks *et al.*, 2009).

4.4 Historical variations in the levels of Lakes Victoria and Kyoga (1947-2009)

In chapter 2, the similar origin of Lakes Victoria and Kyoga by downwarping processes was reviewed. These lakes are hydraulically linked and thus co-dependent (Fig. 2.9). Natural (e.g. climate) and more recent human development (e.g. dams) have affected the levels of both lakes. Lake levels determine, in part, the hydraulic gradient between the lake and adjacent groundwater. Lake stage data from 1947 for Lakes Victoria at Jinja and Kyoga at Masindi Port and Bugondo are shown in figure 4.6. Seasonal variations in the level of Lake Victoria typically comprise maxima in May-June and minima in October. Annual variations are normally 20-40 cm but can reach 70 cm during the rest of the year (Crul, 1995).

An extreme rainfall event that extended over most of East Africa occurred from October to December 1960 (Krishnamurthy and Ibrahim, 1973). This caused Lake Victoria to rise by 105 cm followed by another sharp rise of 61 cm in June 1961 (Fig. 4.6). The lake rose more quickly on the western, northern and northeastern sides than the southern section from April to July; there is a greater rise of about 45 cm on northern shore relative to the south (Krishnamurthy and Ibrahim, 1973). From the late 1961, there was a similar dramatic rise which was also reflected in other lakes in the GLRA including Lakes Naivasha, Turkana, Tanganyika and Albert (Fig. 4.7). Crul (1995) reveals that during that period, water levels rose by more than 1 m in a few months. In 1964, the water level reached its maximum water level which was more than 2 m above the 1961 level and 1.4 m above the previous highest water level of 1906. From 1964 to 1983 the lake level stayed at least 1 m higher than the pre-1961 level.

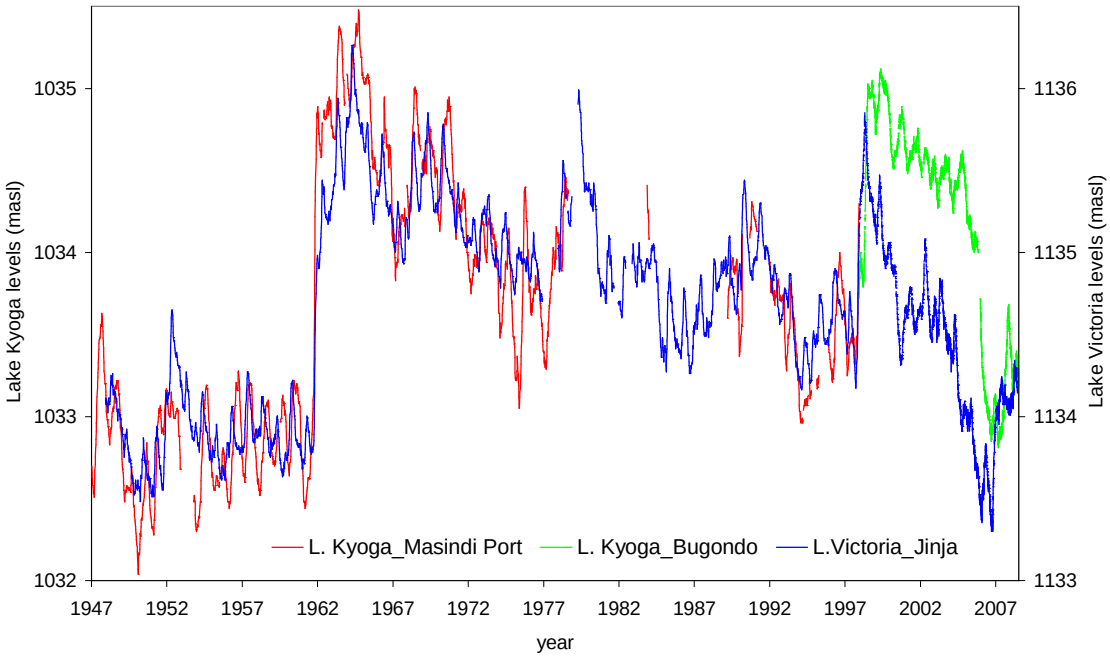

Figure 4.6 Historical average daily co-variations of Lake Kyoga at Masindi Port and Bugondo and Lake Victoria levels at Jinja from 1947 to 2008.

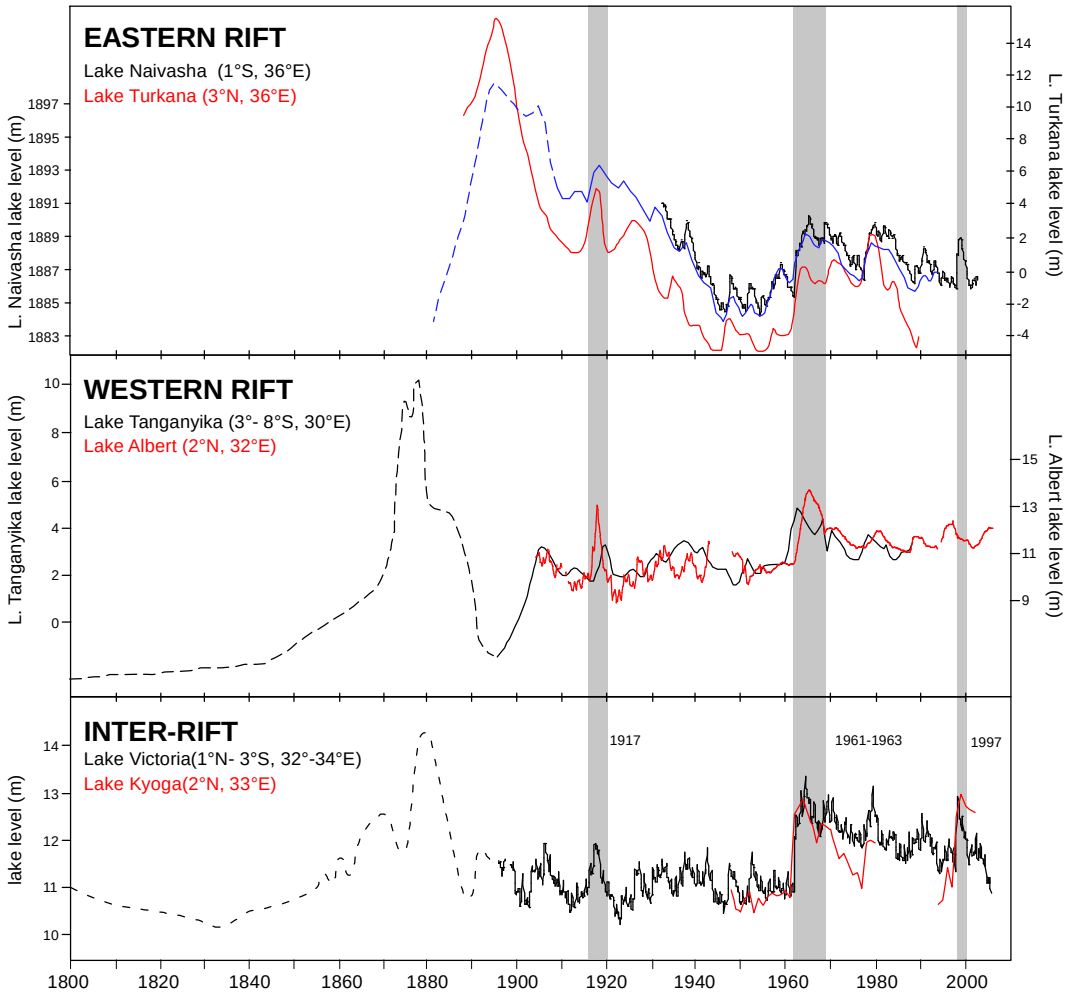

Figure 4.7 Water level variations of Lakes Naivasha, Turkana, Tanganyika, Albert, Victoria and Kyoga since 1800 (source: Taylor). Levels are above the zero datum of the local lake-stage gauge.

Historically, variations in Lake Kyoga levels are primarily determined by the flow of the Victoria Nile from Lake Victoria (Sutcliffe and Parks, 1999). Lake Kyoga levels are gauged on both the main lake at Bugondo and just downstream of the lake's outlet at Masindi Port. During 1997-1998, heavy rains led to an abnormal rise in Lakes Kyoga and Victoria which dislodged papyrus beds, floating suds, and water hyacinth mats (ILM, 2004). Dislodged weeds accumulated and blocked the outlet of Lake Kyoga in early 1998 and led to a rise in lake levels of over 2 m within one year (Fig. 4.8). There was a dramatic increase in lake levels from about 0.23 m before the blockage to nearly 1.5 m at Bugondo relative to Masindi Port which was beyond the blockage. In August 2000, a channel was dredged through the blockage which together with reduced inflow (dam releases) from Lake Victoria (section 4.7) lowered the trend of the Lake Kyoga levels from their peak level in June 1999 (ILM, 2004). By the end of 2003, the difference in water levels between Bugondo and Masindi Port had fallen to around 0.8 m. The Lake Kyoga levels at Bugondo once again respond to outflows from the Victoria Nile at Jinja without being unduly influenced by the obstruction. Recent co-changes in lake levels that are in part, due to dam releases at Jinja are discussed in section 4.7.

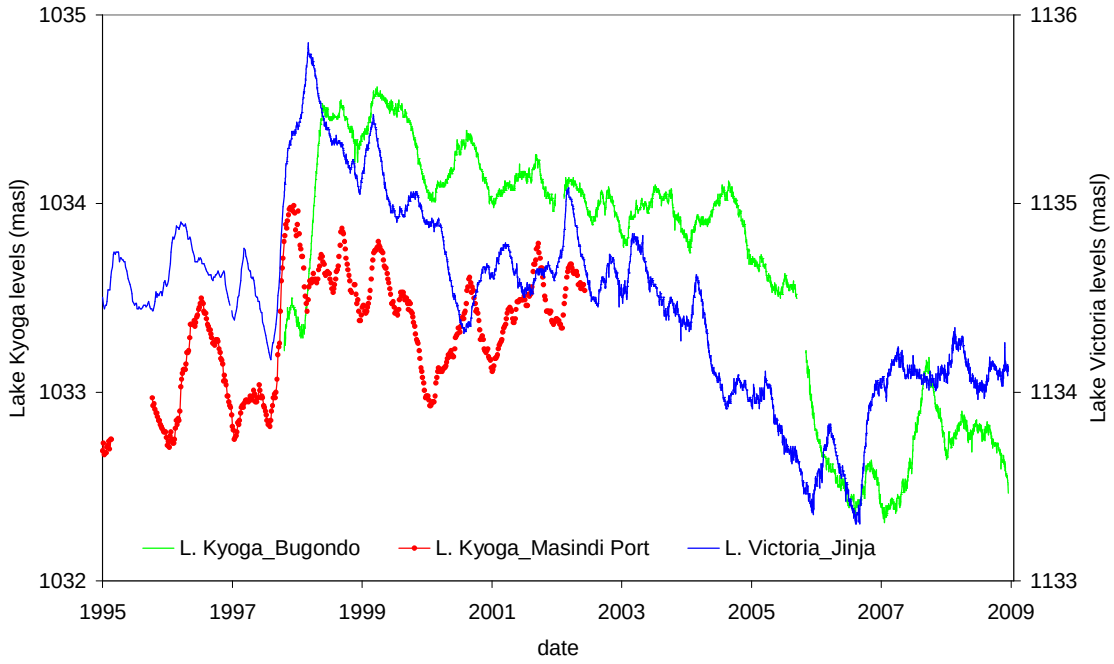

Figure 4.8 Recent average daily co-variations of Lake Kyoga at Masindi Port and Bugondo and Lake Victoria levels at Jinja from 1995 to 2009.

4.5 Long-term (1999-2009) hydrodynamics at Entebbe

4.5.1 Hydraulic gradient

The hydraulic gradient (*i*) between Lake Victoria and adjacent groundwater levels at Entebbe was determined using a piezometer that is 140 m upslope from the Lake Victoria gauge (Fig. 3.6). Both groundwater and lake levels were measured relative to mean sea level datum. Seasonal variability and a summary of statistics of lake stage and groundwater level monitoring data recorded at Entebbe from 1999 are shown in figure 4.9. There are several periods of up to 2 months when missing or faulty water level data had to be discarded. Mean groundwater and lake levels over this period are 1,135.4 masl and 1,134.5 masl, respectively (Fig. 4.9a). The observed *i* indicates groundwater flow towards the lake, except for the first half of 2005 when the groundwater levels fall below the lake level (Fig. 4.9c). Mean *i* is 0.007 $m \cdot m^{-1}$ (Fig. 4.9b); temporal variations reflect seasonal changes in the recharge and discharge

between groundwater and the lake. The *i* never exceeds 0.035 $m \cdot m^{-1}$ and, therefore, is on the low end of the relatively narrow range of hydraulic gradients of up to 0.2 $m \cdot m^{-1}$ that are usually found within lakebeds (Hayashi and van der Kamp, 2007).

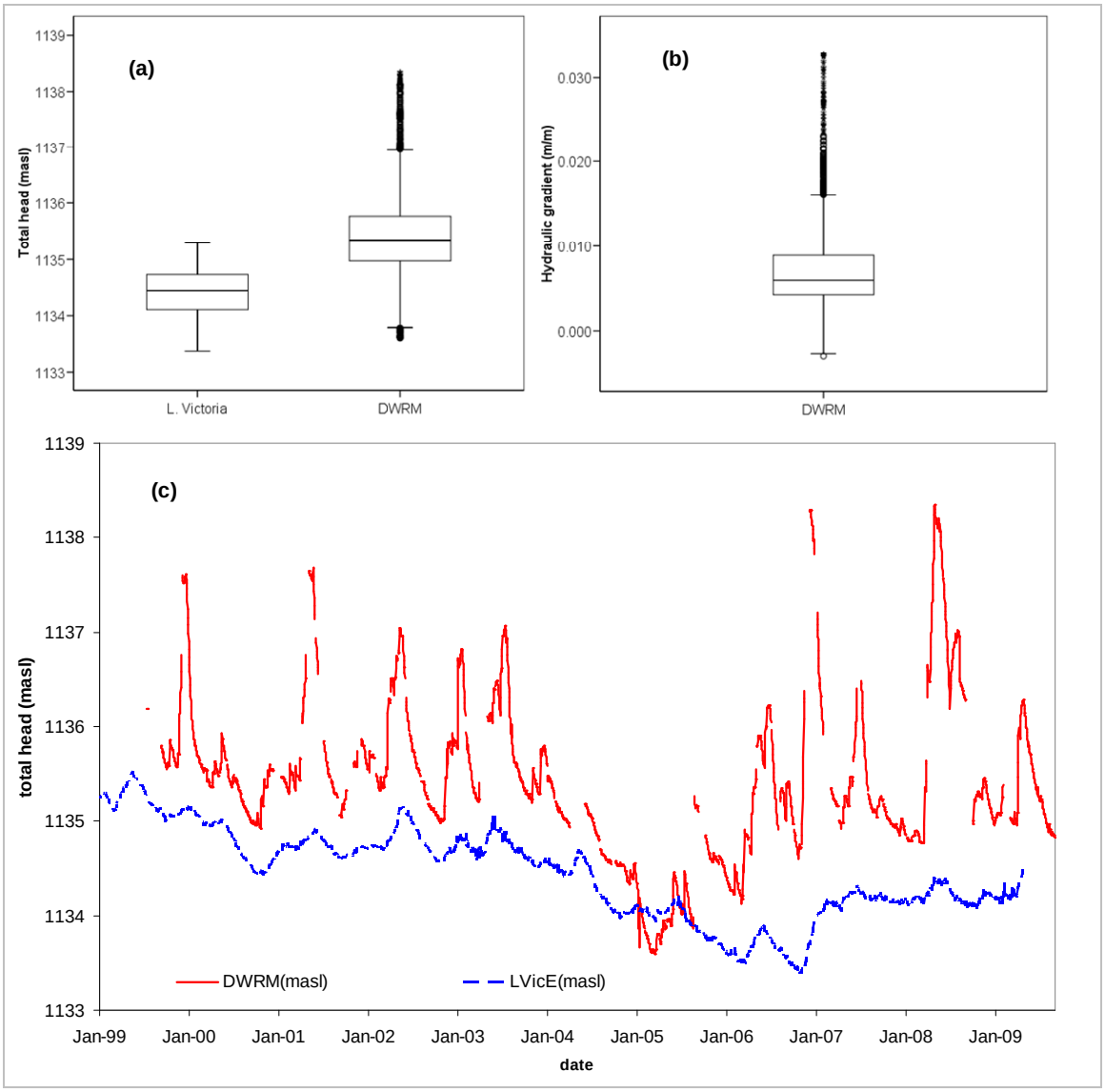

Figure 4.9 Box plots of the summary statistics of the average daily (a) seasonal variability of the levels and (b) hydraulic gradients between piezometer and the lake levels, and (c) seasonal variability of the levels of groundwater and Lake Victoria at Entebbe from January 1999 to July 2009. Bars in (a) and (b) represent upwards the minimum, lower quartile, median, upper quartile and maximum values with dots showing outliers.

A strong linear relationship (R^2 = 0.74) is evident between the *i* (groundwater and lake levels) and groundwater levels (Fig. 4.10a). In contrast, no clear relationship is

detected between the *i* and the lake levels (Fig. 4.10b). The local *i* is, therefore, largely controlled by the changes in the groundwater levels. This is considered primarily to result from the comparatively low storage of the localised saprolite/saprock aquifer on the north shore of Lake Victoria in relation to the large area and storage volume of the lake. In this location remote from abstraction, rainfall-fed groundwater recharge is expected to determine the magnitude of the hydraulic gradient and, hence, of groundwater discharge to the lake.

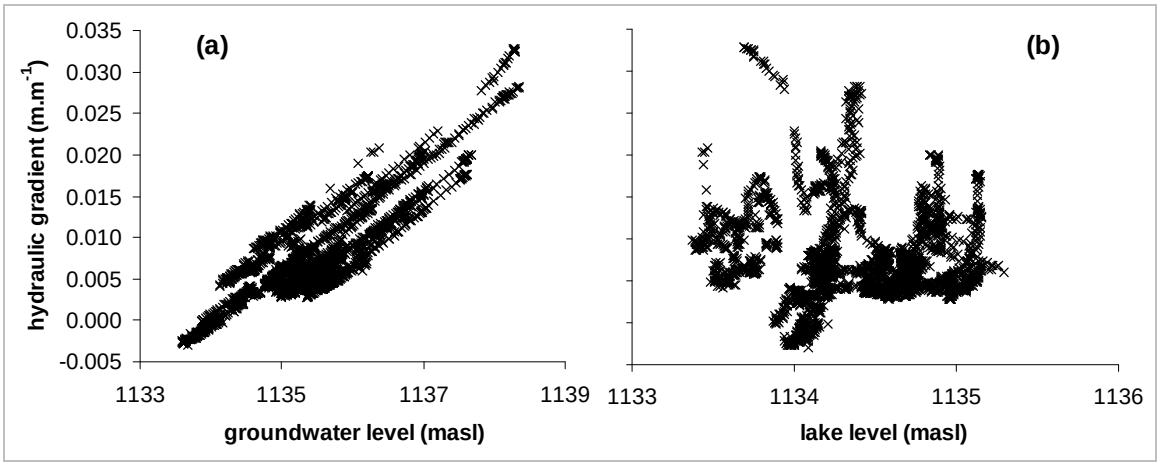

Figure 4.10 Observed hydraulic gradients as a function of (a) groundwater hydraulic head, and (b) Lake Victoria levels at Entebbe.

4.5.2 Lithological control on groundwater level recession at Entebbe

Over the period 1999-2009 groundwater levels varied by up to 4.8 m on the shore of Lake Victoria at Entebbe (Fig. 4.11). It is evident that the recession of the groundwater hydrograph follows two slopes. A more rapid response (>0.01 $m \cdot m^{-1}$) is apparent when the groundwater levels lie within the fluvial-lacustrine sands whereas slower response (<0.01 $m \cdot m^{-1}$) occurs when groundwater levels fall below the sand horizons into the underlying saprolite. The lower saprolite layer has a lower *K* composed of laterite with a high clay content mixed with quartz grains. The saprolite slows rates of recharge and discharge. Substantial groundwater flow via the fluvial-lacustrine sands into the lake is, therefore, expected to occur during wet seasons.

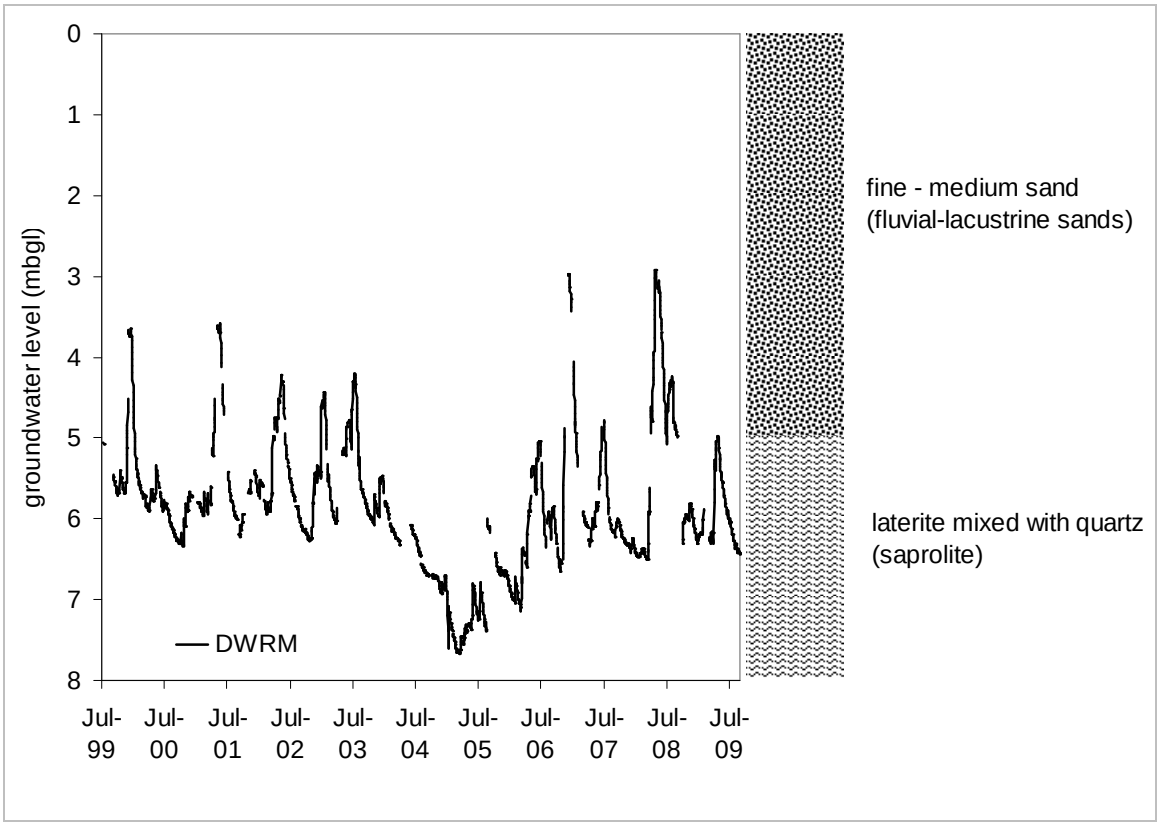

Figure 4.11 Lithologic controls on the average daily groundwater level recession at Entebbe from 1999 to 2009.

4.6 Groundwater - surface water monitoring at Bugondo and Jinja (2007-2009)

4.6.1 Influence of barometric pressure

In contrast to Entebbe, constructed groundwater – surface water monitoring stations at Bugondo and Jinja provide hourly observations. Changes in barometric pressure can induce high frequency but low amplitude groundwater level changes over time (Freeze and Cherry, 1979; Davis and Rasmussen, 1993; Rasmussen and Crawford, 1997; Kruseman and de Ridder, 2000; Spane, 2002; Todd and Mays, 2005; Gonthier, 2007). Groundwater was monitored at 1-hour intervals using absolute (non-vented) pressure transducers at both Bugondo and Jinja. This method records total hydraulic head changes which arise from changes in the water balance as well as barometric

pressure. As changes in water level depend on unsaturated and saturated zone properties and the hydraulic/storage characteristics (e.g. depth, diameter) of the well, it is necessary to remove barometric pressure changes in order to isolate water level responses due to changes in the water balance resulting from recharge, be it direct (rainfall) or indirect (seepage from surface water bodies), and abstraction. Hourly groundwater-level changes clearly reflect semi-diurnal harmonic changes in barometric pressure that influence total hydraulic heads observed at both Bugondo (Fig. 4.12) and Jinja (Fig. 4.13). Hastenrath (1991) explains that in the tropics atmospheric tides of interest include the solar diurnal (24-hourly) tide S_1, the solar semi-diurnal (12-hourly) tide S_2, and the solar ter-diurnal (8-hourly) tide S_3. Of the S_1, S_2 and S_3 tides, it is the 12-hourly travelling wave that dominates the daily march of pressure in the tropics, although the superimposition of the 24- and 8-hourly waves result in a generally larger morning than evening maximum, as well as some variation in the course of the year (Hastenrath, 1991). As for the larger inconsistent lower frequency pulses in total head at about 3-day intervals (Fig. 4.13) that can surge both up and down, these will be investigated in conjunction with the influence of the dam releases at Jinja (section 4.7).

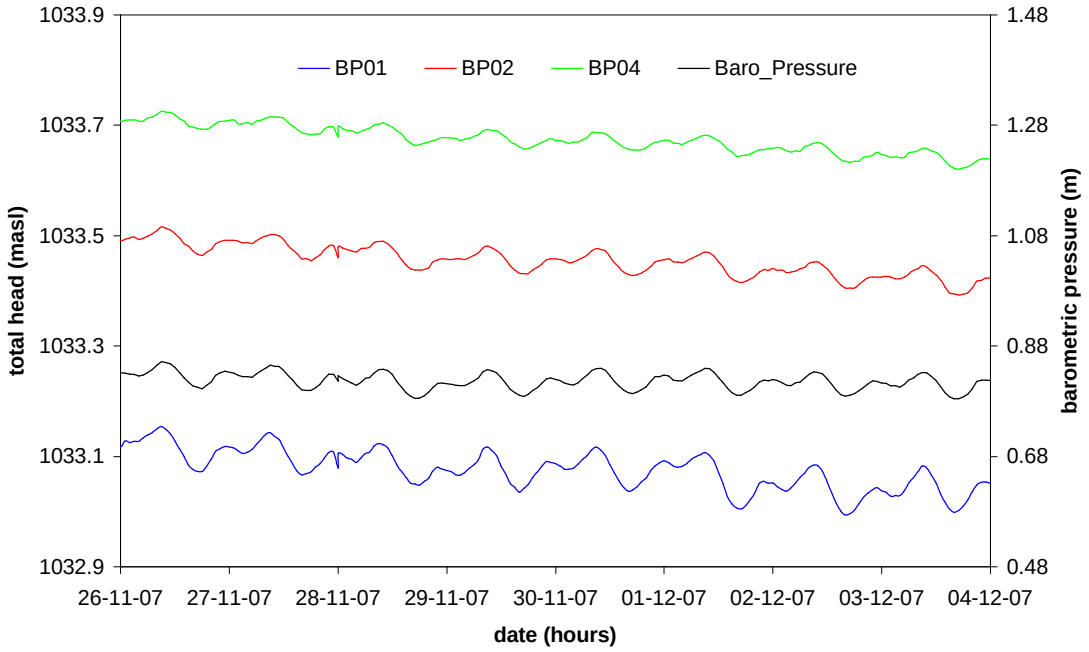

Figure 4.12 Hourly groundwater level fluctuations showing near instantaneous co-variations in total hydraulic head at piezometers BP01, BP02 and BP04 together with the barometric pressure at Bugondo from 26 November to 4 December, 2007.

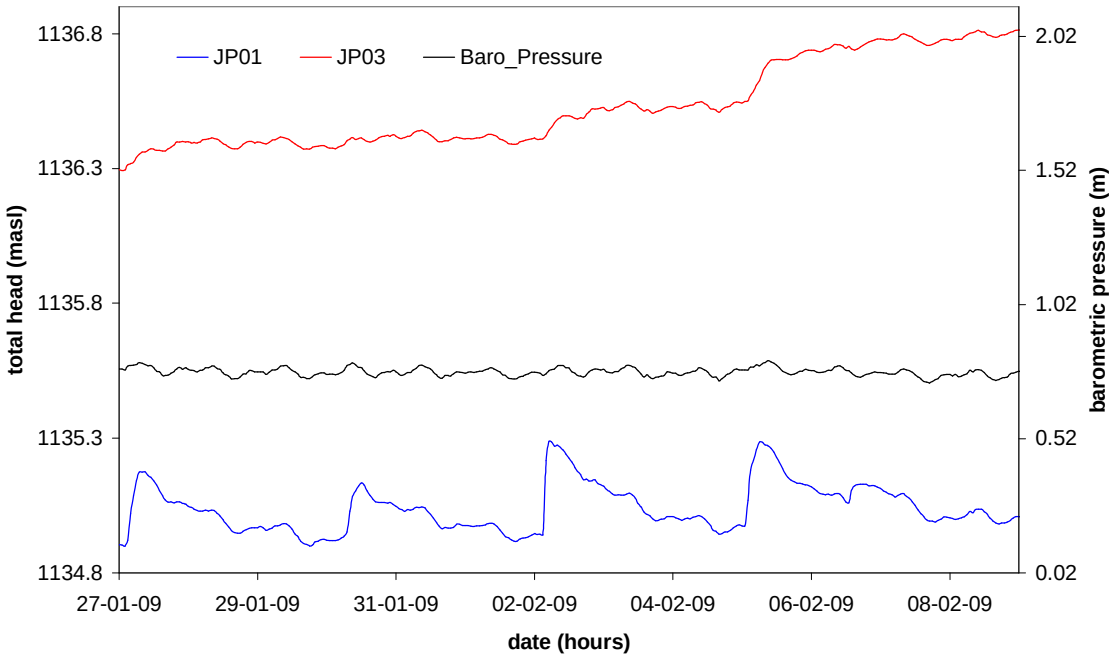

Figure 4.13 Hourly groundwater level fluctuations showing near instantaneous co-variations of the barometric pressure together with total hydraulic head at piezometers JP01 and JP03 onto which is superimposed on larger, lower frequency variations in total hydraulic heads at Jinja from 27 January to 10 February, 2009.

There are several methods to assess the influence of barometric pressure on groundwater-level observations including the barometric efficiency method (*BE*), multiple-regression deconvolution technique, vadose zone model and frequency-based method (Spane, 2002; Gonthier, 2007). Barometric efficiency, *BE* is the ratio of change in the hydraulic head to the change in barometric pressure where ΔH is the change in the total hydraulic head in the piezometer during an arbitrary time unit (e.g. hour); and ΔB is the change in the barometric pressure head at the water surface during the same time interval. (equation 4.2). The removal of water-level fluctuations caused by changes in barometric pressure is done by applying equation 4.3, where *WL* is corrected water level and *H* is the total hydraulic heat at time *t*.

$$BE = -\frac{\Delta H}{\Delta B} \qquad (4.2)$$

$$WL = H * (1 - BE) * \Delta B \qquad (4.3)$$

Apart from correcting hourly groundwater level observations for barometric influences, the calculation of *BE* also provides an indication of the degree to which the monitored aquifer is confined. Confined aquifers commonly exhibit instantaneous total hydraulic head response to barometric pressure whereas unconfined aquifers show a delayed total hydraulic head response due to the transmission of the barometric pressure perturbation through the unsaturated zone (Rasmussen and Crawford, 1997).

A range of methods to account for barometric corrections was considered including Clark's 1967 (BE_C) method (Davis and Rasmussen, 1993; Spane, 2002; Gonthier, 2007), modified Clark's method (BE_{RC}) (Davis and Rasmussen, 1993; Spane, 2002), linear regression using observed barometric pressures and total heads (BE_L), and using the first differences of the barometric pressures and the total hydraulic heads (BE_S) (Davis and Rasmussen, 1993; Rasmussen and Crawford, 1997). Details of BE_C and

BE_{RC} methods are summarised in Davis and Rasmussen (1993), and BE_L and BE_S methods are described in Rasmussen and Crawford (1997).

Clark's 1967 method (BE_C) is robust and particularly useful for calculating *BE* for confined aquifer wells that are influenced by other extraneous pressure trends, like distant groundwater abstractions (Spane, 2002). The modified Clark's method (BE_{RC}) is a recursive method that is useful when unequal numbers of positive and negative barometric changes and groundwater responses are present and the trend is linear (Davis and Rasmussen, 1993). Additionally, linear regression methods (BE_L and BE_S) complemented the previous methods where it was assumed that the water level changes were due to only changes in barometric pressure. In all the correction methods, the data were firstly detrended prior to removing the barometric pressure anomalies.

Calculated barometric efficiencies for piezometers at Jinja and Bugondo are presented in Table 4.3. Use of longer periods for the barometric corrections should, in effect, reduce the influence of non-barometric influences on the water levels changes (Gonthier, 2007), which however, resulted in much lower *BE* values. Rasmussen and Crawford (1997) stipulate that in confined aquifers with no borehole or storage effects, there is usually no difference between BE_L and BE_S responses to barometric pressure. Furthermore, for unconfined aquifers, the BE_S response should be higher than the BE_L response. If there is delayed yield response in a confined aquifer, the BE_S response should be smaller than the BE_L response.

Table 4.3 Groundwater hourly piezometers in Bugondo and Jinja showing barometric efficiency using observed barometric pressure and total head (BE_L), first differences of barometric pressure and total head (BE_S), Clark's Method (BE_C), and Modified Clark's Method (BE_{RC}) (expected value ± one standard error).

Piezometer	Dates	BE_L	BE_S	BE_C	BE_{RC}	n
BP01	25.11.07 - 12.12.07	0.836 ± 0.40	0.664 ± 0.002	0.672 ± 1.50	0.654 ± 0.85	403
BP01	12.12.07 - 09.01.08	0.850 ± 0.39	0.817 ± 0.003	0.841 ± 0.84	0.853 ± 0.92	658
BP01	10.01.08 - 07.02.08	0.675 ± 0.57	0.616 ± 0.001	0.602 ± 0.75	0.620 ± 0.86	666
BP01	18.02.09 - 30.06.09	0.452 ± 0.89	0.137 ± 0.002	0.149 ± 2.28	0.154 ± 0.35	3 161
BP01	All	0.606 ± 0.80	0.529 ± 0.002	0.311 ± 53.8	0.350 ± 0.48	4 935
BP02	25.11.07 - 12.12.07	0.926 ± 0.38	0.695 ± 0.002	0.699 ± 0.51	0.709 ± 0.88	403
BP02	13.12.07 - 09.01.08	0.969 ± 0.25	0.901 ± 0.002	0.919 ± 0.31	0.935 ± 0.97	663
BP02	10.01.08 - 07.02.08	0.865 ± 0.50	0.779 ± 0.001	0.777 ± 0.63	0.792 ± 0.98	667
BP02	20.07.08 - 18.02.09	0.114 ± 0.99	0.110 ± 0.000	0.102 ± 1.40	0.105 ± 0.41	5 118
BP02	18.02.09 - 30.06.09	0.417 ± 0.91	0.167 ± 0.001	0.172 ± 1.35	0.176 ± 0.69	3160
BP02	All	0.350 ± 0.94	0.446 ± 0.002	0.184 ± 65.2	0.258 ± 0.39	10 036
BP04	25.11.07 - 12.12.07	0.902 ± 0.43	0.705 ± 0.003	0.703 ± 0.57	0.709 ± 0.79	403
BP04	13.12.07 - 09.01.08	0.977 ± 0.21	0.853 ± 0.001	0.888 ± 0.80	0.905 ± 0.96	655
BP04	10.01.08 - 07.02.08	0.891 ± 0.45	0.817 ± 0.001	0.827 ± 0.66	0.842 ± 0.96	667
BP04	20.07.08 - 18.02.09	0.031 ± 1.00	0.074 ± 0.000	0.070 ± 1.01	0.069 ± 0.21	5 118
BP04	18.02.09 - 30.06.09	0.375 ± 0.93	0.135 ± 0.002	0.135 ± 1.96	0.139 ± 0.42	3 160
BP04	All	0.294 ± 0.96	0.424 ± 0.002	0.152 ± 67.4	0.224 ± 0.30	10 004
JP01	13.12.07 - 30.12.07	0.446 ± 0.90	0.401 ± 0.014	0.365 ± 0.57	0.381 ± 0.72	401
JP01	13.06.08 - 19.02.09	0.373 ± 0.93	0.140 ± 0.000	0.157 ± 7.41	0.153 ± 0.27	5 282
JP01	19.02.09 - 29.06.09	0.493 ± 0.87	0.201 ± 0.001	0.189 ± 2.90	0.187 ± 0.27	3 120
JP01	All	0.419 ± 0.91	0.196 ± 0.001	0.176 ± 10.8	0.174 ± 0.27	8 803
JP03	13.12.07 - 30.12.07	0.966 ± 0.26	0.862 ± 0.007	0.951 ± 0.46	0.925 ± 0.91	401
JP03	13.06.08 - 19.02.09	0.021 ± 1.00	0.046 ± 0.000	0.053 ± 1.14	0.047 ± 0.33	5 279
JP03	All	0.088 ± 1.00	0.260 ± 0.003	0.063 ± 13.6	0.097 ± 0.15	5 679

Using this guide, there is a general confined response during most periods for all the piezometers though there are also periods when some piezometers show unconfined/leaky tendencies (e.g. BP01). In addition, a general difference between the BE_L and BE_S readings can arise from wellbore storage or skin effects. To remove the barometric pressure effects, respective average *BE* estimates (BE_C, BE_{RC} and BE_S) during each course of the monitoring period were used to cater for temporal variations (Table 4.3). The results of the barometric pressure-corrected groundwater levels are shown for Bugondo (Fig. 4.14) and Jinja (Fig. 4.15). These barometric pressure-corrected groundwater levels are used to determine water level responses to changes in the water balance as a result of dam releases at Jinja (section 4.7) and rainfall-fed recharge (chapter 5).

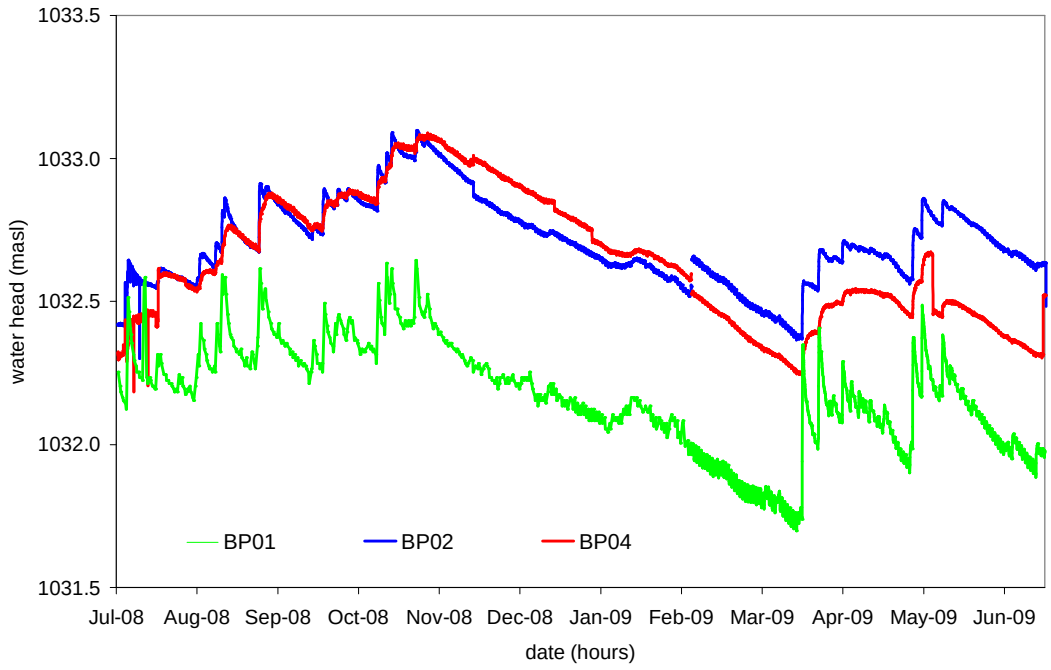

Figure 4.14 The hourly barometric pressure-corrected groundwater levels for piezometers BP01, BP02 and BP04 at Bugondo from July 2008 to July 2009.

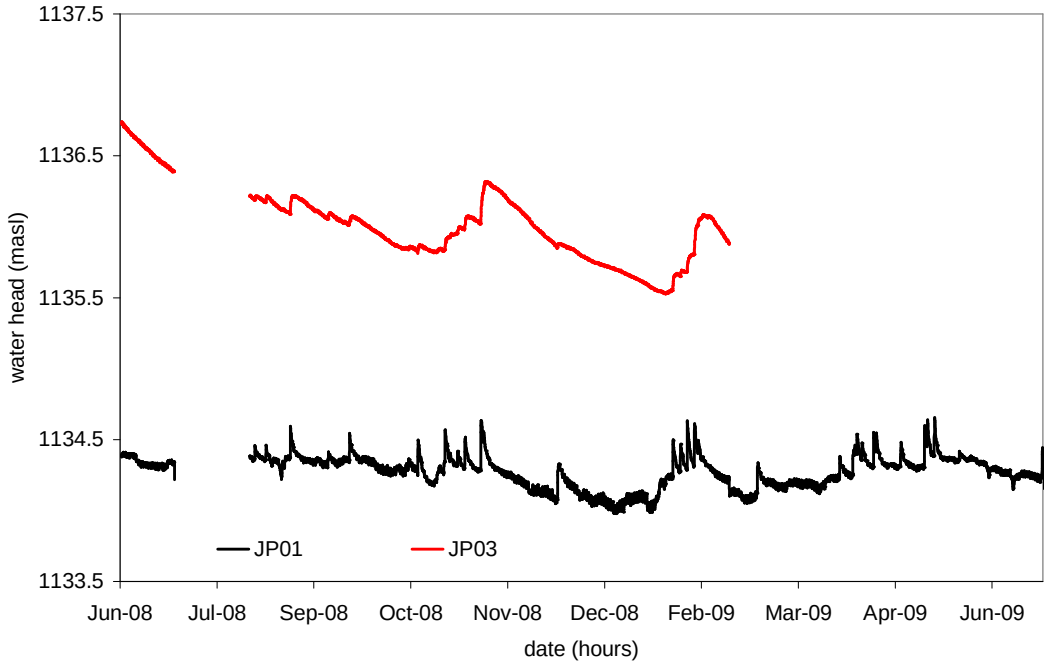

Figure 4.15 The hourly barometric pressure-corrected groundwater levels for piezometers JP01 and JP03 at Jinja from June 2008 to July 2009.

4.6.2 Hydraulic gradients at Bugondo

The total hydraulic head in each piezometer measured by an absolute (non-vented) pressure transducer is used to define the *i* with the lake levels. Both groundwater and lake levels are measured relative to mean sea level datum. Hydraulic gradient at Bugondo is determined for a horizontal distance between the water levels at the Lake Kyoga gauge and piezometers BP01, BP02 and BP04 at distances of 105, 172 and 218 m apart, respectively (Fig. 3.3). Seasonal variability and a summary of statistics of groundwater level and lake stage monitoring at Bugondo from December 2007 to June 2009 are shown in figure 4.16. Groundwater level data (BP01, BP02 and BP04) were lost between February and July 2008 as a result of the pressure transducer malfunctions. Mean total hydraulic heads for piezometers BP01, BP02, BP04 and Lake Kyoga are 1,032.8, 1,033.4, 1,033.4 and 1,032.7 masl, respectively (Fig. 4.16a). The mean *i* between each piezometer and the lake ranges from 0.002 to 0.004 $m \cdot m^{-1}$ (Fig. 4.16b). Additionally, the *i* towards the lake from all the three groundwater piezometers is highest during periods of groundwater recharge that predominantly occur from August to November and March to May (Fig. 4.16c). There are however brief periods such as in the late 2007 when groundwater levels at BP01, nearest to the lake, fall below the lake level. The groundwater levels in BP02 and BP04 closely follow each other, and form broad seasonal (up to 3 months) peaks superimposed on short-term (less than monthly) responses. At piezometer BP01, which has the shallowest water level and is closest to the lake, higher frequency responses of short duration indicate possible flooding during recharge events. The lake levels have short-term (less than monthly) variations within two large receding seasonal trends interspersed by two stable base levels.

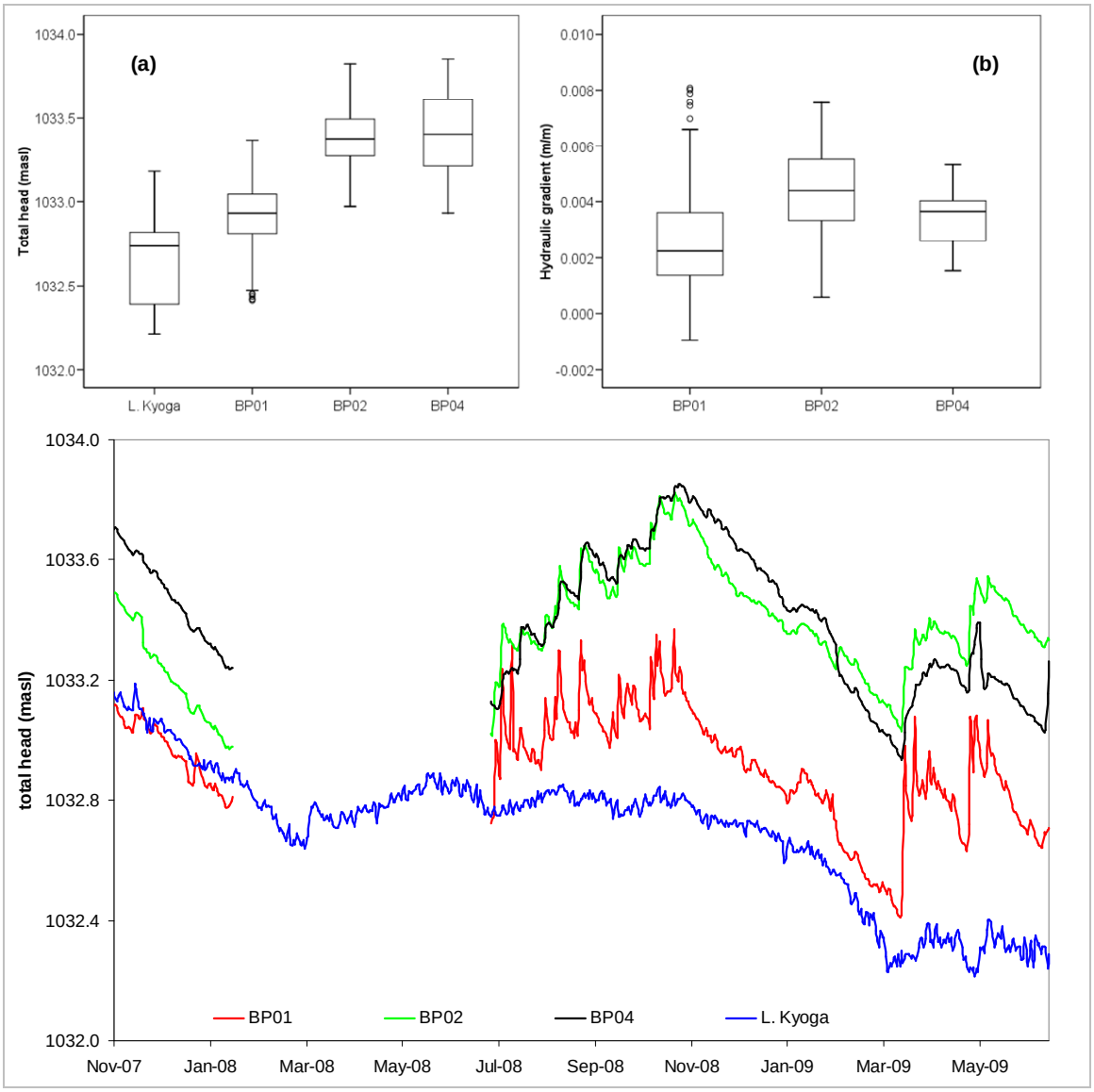

Figure 4.16 Box plots of the summary statistics of the average daily (a) seasonal variability of the levels and (b) hydraulic gradients between respective piezometer and the lake levels, and (c) seasonal variability of the levels of groundwater and Lake Kyoga at Bugondo from November 2007 to July 2009. Bars in (a) and (b) represent upwards the minimum, lower quartile, median, upper quartile and maximum values with dots showing outliers.

Figure 4.17 shows the *i* between the total hydraulic head of the respective piezometers (BP01, BP02 and BP04) plotted against the individual groundwater and Lake Kyoga levels at Bugondo. Linearity in the distribution of plotted observations that follow distinct slopes (Figs. 4.17a, c and e) reflect the dependence of the *i* on groundwater levels and recharge events which strongly determine the *i*. The *i* changes occur under comparably stable lake levels (Figs. 4.17b, d and f) and give rise to vertical linear distributions. All the correlations are significant (1 % level, 2-tailed; n = 424) despite the large spread and cluster of the data. The separate clusters correspond to data collected during three (November 2007 - February 2008, July 2008 - February 2009, and February - June 2009) main monitoring periods. Lake Kyoga levels over these three periods form distinct drainage base levels which group the *i* into distinct clusters (Fig. 4.16). Controlled inflows from the Victoria Nile into Lake Kyoga are responsible for these discrete level changes (section 4.7). The *i* is observed to increase seasonally associated with rainfall-fed recharge events and also episodically when the lake level declines (Figs. 4.17a, c and e). Declining lake levels are associated with both climate mechanisms and excessive dam releases (Figs. 4.17b, d and f). The influence of rising groundwater levels on the *i* is characterised by the two furthest piezometers (BP02 and BP04) from the lake (Figs. 4.17c and e) whereas the closest piezometer (BP01) is least affected (Figs. 4.17a). Figure 4.17 (b and d) show that the lake exerts the most influence on the two closest piezometers (BP01 and BP02) with the furthest (BP04) least affected (Fig. 4.17f).

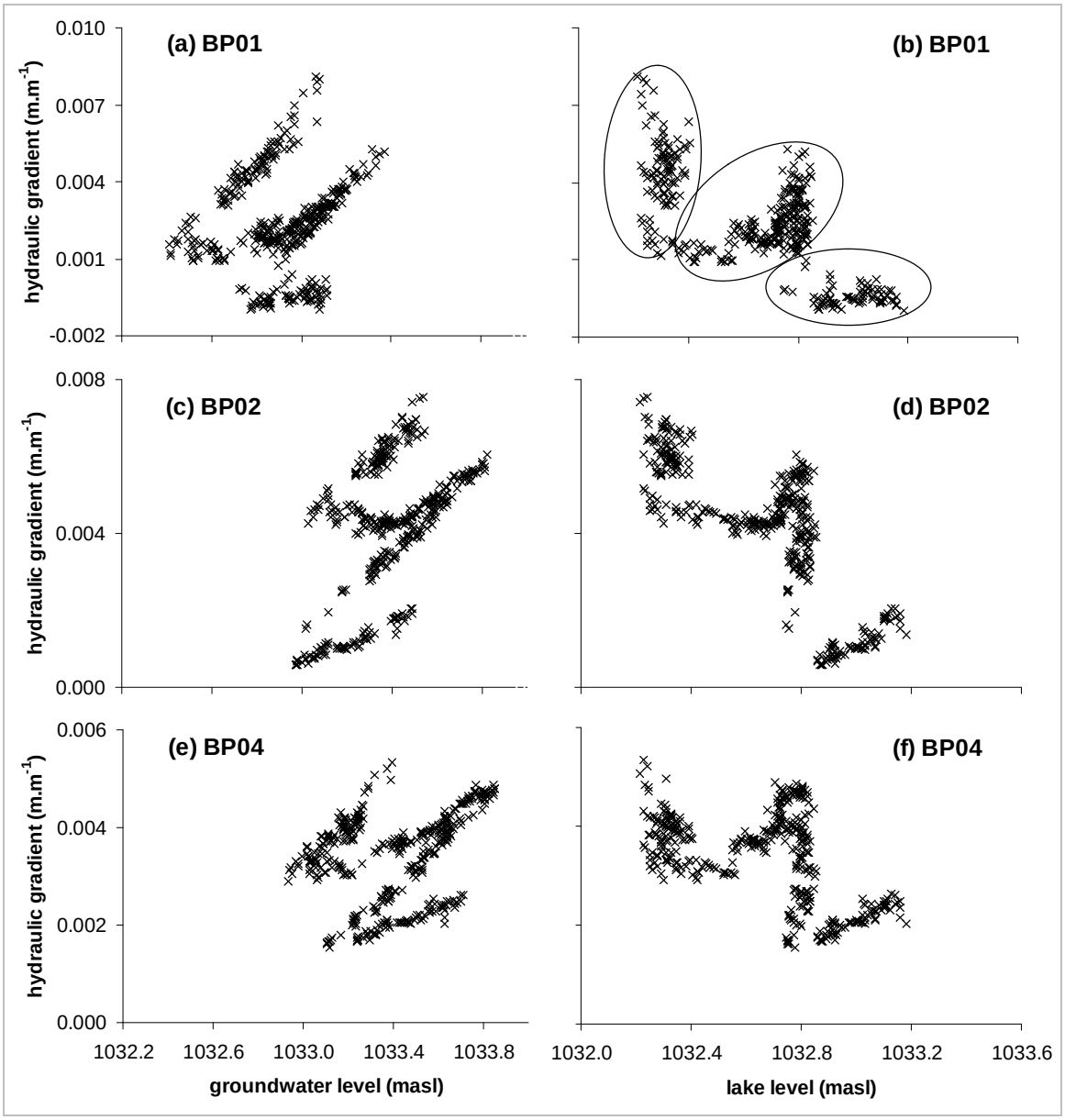

Figure 4.17 Observed hydraulic gradient as a function of total hydraulic head in (a) BP01, (c) BP02 and (e) BP04; total hydraulic head as a function of lake level in (b) BP01, (d) BP02, and (f) BP04.

4.6.3 Lithological control on groundwater level recession at Bugondo

At Bugondo, groundwater levels in all the 3 piezometers fluctuate within the topmost layer (3-m depth) comprising mixed fluvial-lacustrine sands (Fig. 4.18). Rapid, short-lived water level responses are apparent within the top 50 cm of the BP01 piezometer which is located in the wetlands next to the lake. When wetlands are flooded, it is suggested that groundwater is rapidly (up to 2 days) recharged (nearly 0.5 m rise) through macropores chiefly generated by the wetland vegetation roots which provide preferential flow paths to support the steep recharge and to later drain away excess water following recharge events. Wolski and Savenije (2006) argue that flood-induced replenishment of groundwater storage occurs at the flood front with inverse saturation, a process analogous to infiltration in disconnected ephemeral rivers. This is a type of bank storage water level rise where there is inundation of the wetland and, after the recession of the flood, return flow from the groundwater storage towards the wetland occurs. Root vegetation evapotranspiration is considered to also play some part in this fast groundwater level recession process after the flood event. The other two piezometers (BP02 and BP04) show slow water level responses in fluvial-lacustrine sediments and underlying less permeable (lateritic) upper saprolite horizons that is not directly influenced by wetland floods. Following the main (August - November) recharge event (Fig. 3.4), there is a long water level recession in all the three piezometers from November to March, which is expected to generate a large antecedent soil moisture deficit that has to be replenished before the subsequent (March - May) recharge event.

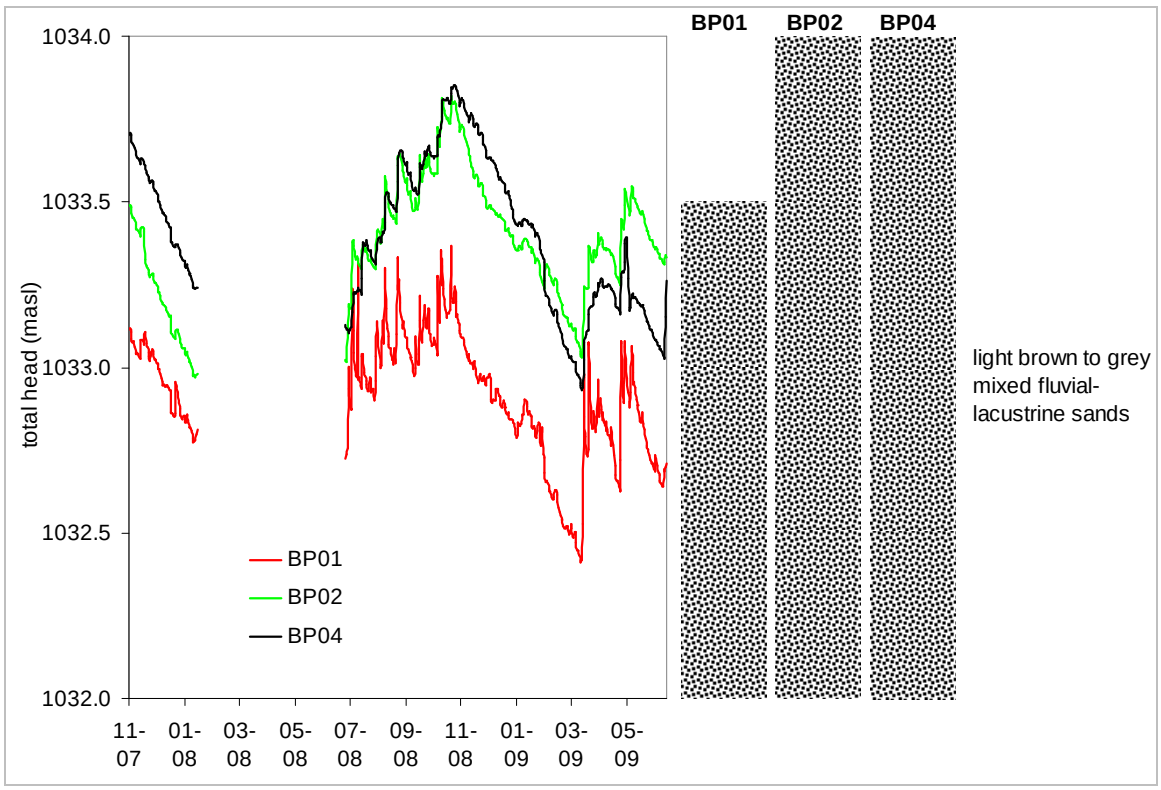

Figure 4.18 Lithologic controls on the average daily groundwater level recession at Bugondo from November 2007 to July 2009.

4.6.4 Hydraulic gradients at Jinja

The *i* is determined for horizontal distances between monitoring wells and the Lake Victoria gauge in Jinja of 69, 116 and 322 m (Fig. 3.2). Seasonal variability and a summary of statistics of groundwater level and lake stage monitoring at Jinja station from November 2007 are shown in figure 4.19. Daily water levels in piezometer JP02 were manually measured so the observations are less frequent and more prone to erroneous readings than the other two piezometers (JP01 and JP03) monitored using pressure transducers. Groundwater level data (JP01 and JP03) were however, entirely lost between February and July 2008 as a result of the pressure transducer malfunctions. Mean total heads for piezometers JP01, JP02, JP03 and Lake Victoria are 1,135.0, 1,136.1, 1,136.7 and 1,134.1 masl, respectively (Fig. 4.19a). Hydraulic gradient towards the lake from all the three groundwater piezometers is more pronounced during wet seasons. Piezometer JP01 has a mean *i* of 0.013 $m \cdot m^{-1}$, JP02 is 0.017 $m \cdot m^{-1}$, and JP03 averages 0.008 $m \cdot m^{-1}$ (Fig. 4.19b). Groundwater levels in JP03 vary most (by about 1.4 m), and form broad seasonal (up to 3 months) peaks superimposed on narrow short-term (less than monthly) peaks. Piezometer JP02 water levels have more subdued, seasonal peaks in addition to short-term variations. Similar to Bugondo, the piezometer (JP01) which is closest to the lake, reveals rapid, short-lived responses that suggest flooding has occurred during some recharge events. Lake levels are comparatively stable with short-term (less than monthly) variations in addition to two broad seasonal peaks.

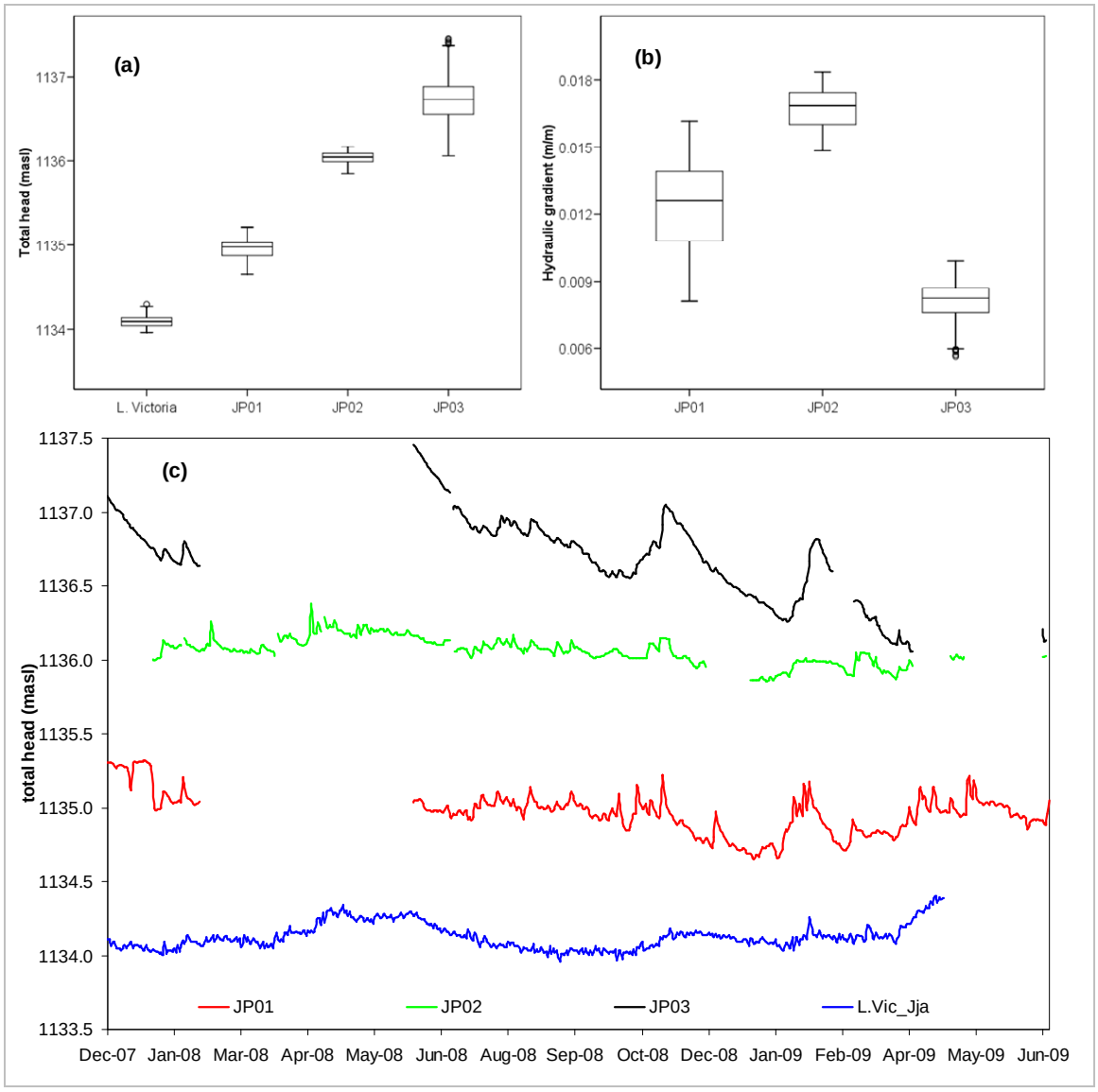

Figure 4.19 Box plots of the summary statistics of the average daily (a) seasonal variability of the levels and (b) hydraulic gradients between respective piezometer and the lake levels, and (c) seasonal variability of the levels of groundwater and Lake Victoria at Jinja from December 2007 to July 2009. Bars in (a) and (b) represent upwards the minimum, lower quartile, median, upper quartile and maximum values with dots showing outliers.

Figure 4.20 shows the *i* between the total hydraulic head of the respective piezometers (JP01, JP02 and JP03) plotted against the individual groundwater and Lake Victoria levels at Jinja. There is a significant linear distribution in the plotted observations that reveal the strong dependence of the *i* on groundwater level responses (Figs. 4.20a, c and e). Conversely, a scattered distribution reflects the lesser influence of relatively stable lake levels (Figs. 4.20b, d and f). All the correlations are significant (1 % level, 2-tailed; n = 401, 425 and 369 for JP01, JP02 and JP03, respectively) despite the large spread and cluster of the data. Controlled operations of the Kiira and Nalubale dams at Jinja provide stability in lake levels over the monitored period (section 4.7). The results suggest that rainfall-fed recharge augmenting groundwater (JP01, JP02 and JP03) levels (Figs. 4.20a, c and e) largely determines the *i* between groundwater and the lake. The 'controlled' drop in lake levels (Figs. 4.20b, d and f) from January to March 2009 (Fig. 4.19) also served to enhance the *i* most especially for the two piezometers (JP01 and JP02) closest to the lake. Figure 4.20e depicts the JP03 piezometer which is furthest and least influenced by the lake level variations (Fig. 4.20f) and is therefore most affected by groundwater recharge.

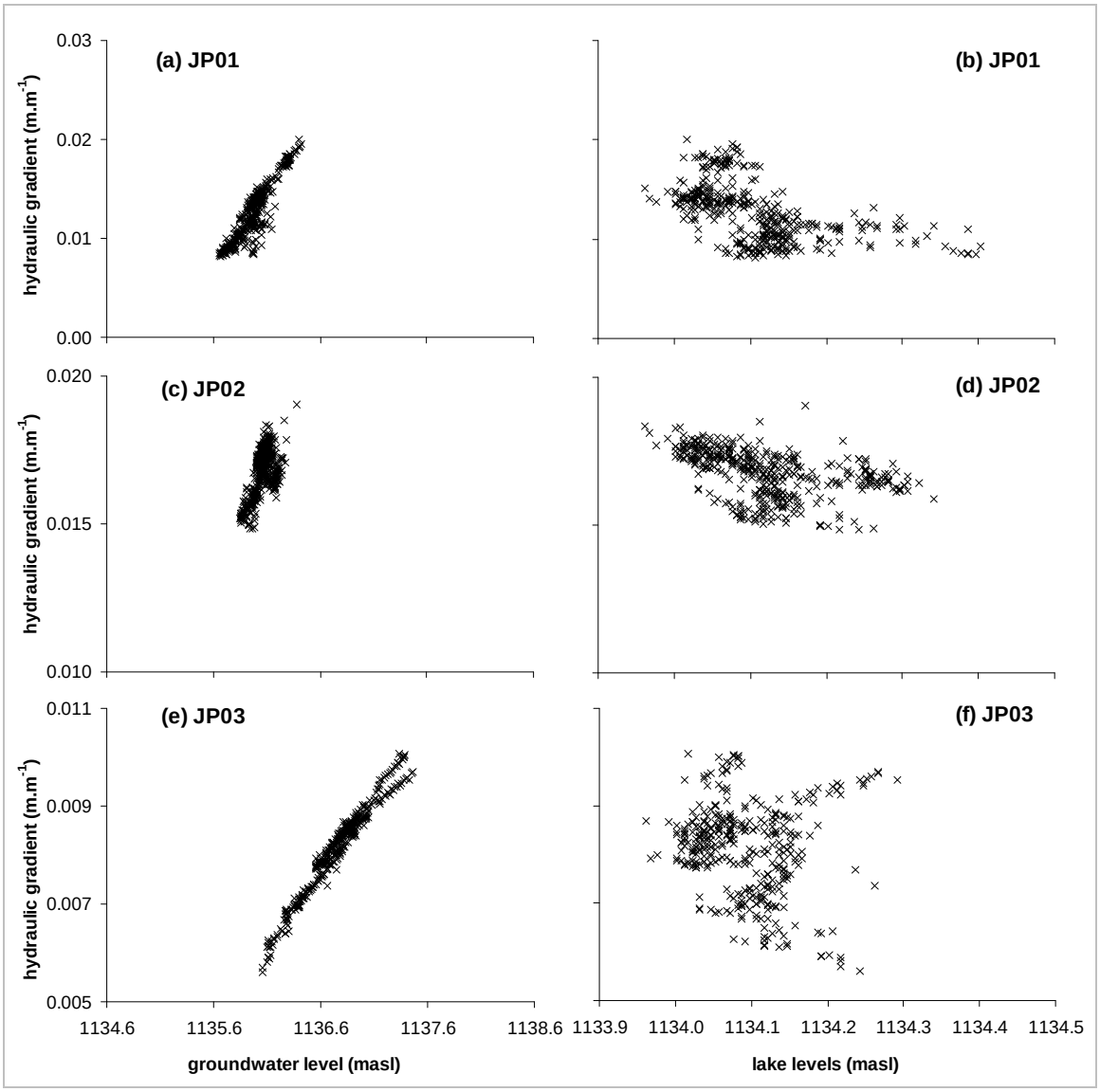

Figure 4.20 Observed hydraulic gradient as a function of total hydraulic head in (a) JP01, (c) JP02 and (e) JP03; total hydraulic head as a function of lake level in (b) JP01, (d) JP02, and (f) JP03.

4.6.5 Lithological control on groundwater level recession at Jinja

At Jinja, water levels in both piezometers JP01 and JP02 fluctuate within the top metre of the brown fluvial-lacustrine sands that are mixed with infill. As for piezometer JP03, all groundwater-level fluctuations occur within brown saprolite (Fig. 4.21). Both piezometers JP01 and JP02 are located within wetlands that are prone to flood during wet seasons. Water levels in piezometer JP01 have rapid, short-lived responses within the top 50 cm of the profile. Similarly, water levels in piezometer JP02 levels occur largely within the top 50 cm of the profile and are characterised by rapid, short-lived responses during wet seasons. Groundwater in this low-relief area is rapidly (up to 2 days) recharged (nearly 0.5 m rise) and drained. Flow is considered to be enhanced by wetland root macropores when flooding occurs. Water levels in piezometer JP03 however, form slow and broad, rise and recession profiles that reflect relatively permeable saprolite with low clay content and the fact that this location is not susceptible to flooding. Compared to Bugondo, the Jinja piezometers not prone to flooding exhibit less asymmetric water level responses during March-May and September-November wet seasons which is attributed to a lower antecedent soil moisture deficit between these recharge events.

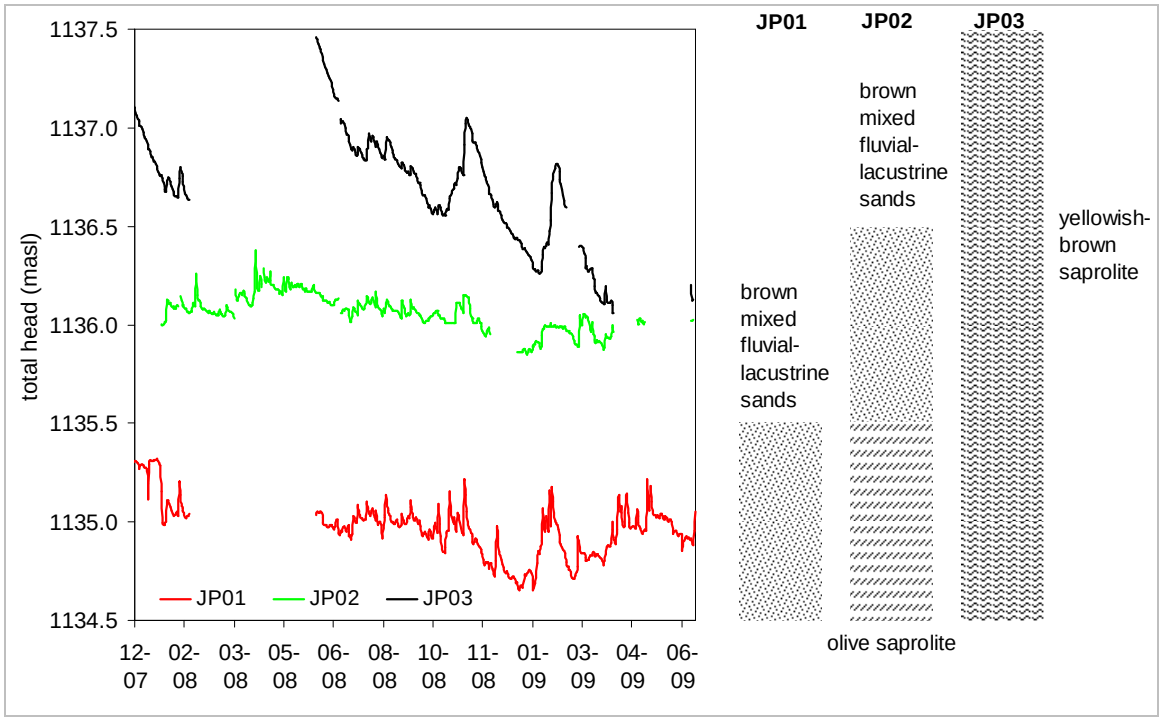

Figure 4.21 Lithologic controls on the average daily groundwater level recession at Jinja from December 2007 to July 2009.

4.7 Influence of dam releases on groundwater-surface water interactions: The Entebbe, Jinja and Bugondo experiment

4.7.1 Jinja dam releases and Lakes Victoria and Kyoga levels

Recent dam operations have affected the hydraulically linked levels of Lakes Victoria and Kyoga, which in turn, influence the *i* between groundwater and lakes. Regulation of the outflow from Lake Victoria began in 1954 with the construction of Nalubale hydroelectric dam. To enable pre-dam outflow to catchments downstream the lake, a relation ("Agreed Curve") was established between the lake level at the Jinja outlet and the total outflow. Sene and Plintson (1994) show that dam releases have largely adhered to the Agreed Curve with compensatory discharges made in order to minimise the effects of departures from expected outflow. In 2002, a second

hydroelectric dam (Kiira) was commissioned parallel to the Nalubale dam. These two hydroelectric dams together currently regulate the outflow of Lake Victoria at Jinja. The combined outflows facilitate exceedance of the dam release policy (Agreed Curve) which plays a large part in modifying expected lake level variations (Kite, 1982, 1984; Sutcliffe and Peterson, 2007; Awange *et al.*, 2007; Swenson and Wahr, 2009).

In order to simulate likely influences of dam releases on the groundwater – surface water interactions at Entebbe, Jinja and Bugondo, daily dam outflow data were obtained from January 1999 to September 2009 (Fig. 4.22). Individual dam releases from Nalubale and Kiira dams and Agreed Curve data are available from January 2004 to September 2009. Total dam releases rise steadily from about August 1999 to December 2004 (nearly twice the Agreed Curve), when it was reduced through 2005 to the present stable rates. From 2004 to the beginning of 2007 total dam releases greatly exceed (> 20 %) the Agreed Curve. Since 2007, the total releases have more closely followed the Agreed Curve. The level of Lake Victoria steadily fell (~1.2 m) from July 2004 to February 2006 when dam releases substantially exceeded the Agreed Curve (Fig. 4.23). Since 2007, the lake levels have been more stable largely as a result of sustained reduction in dam releases.

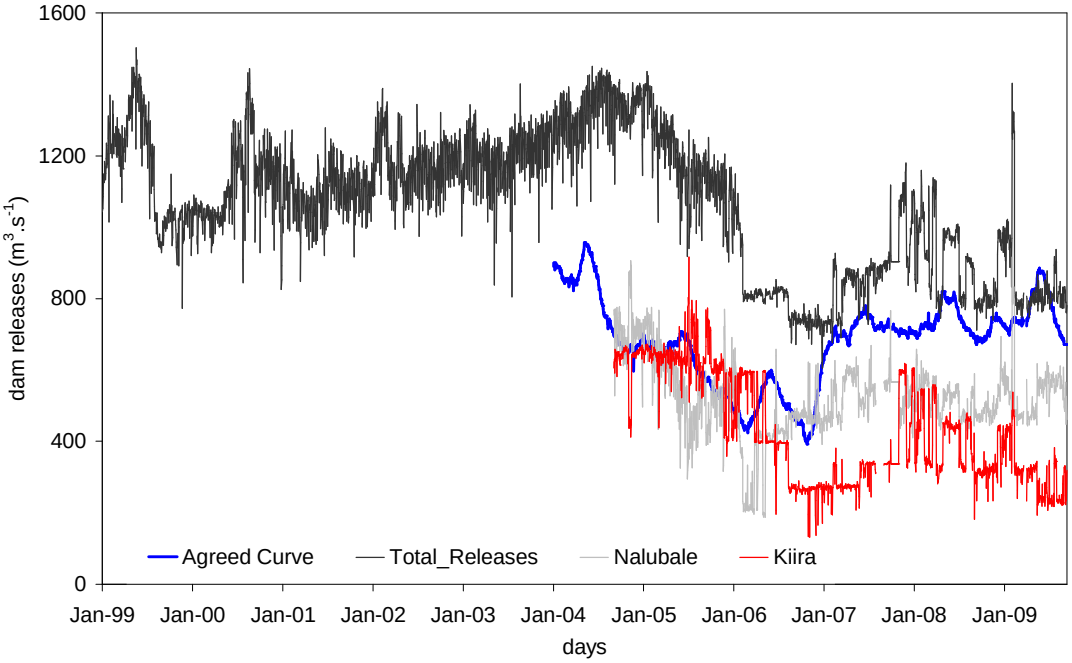

Figure 4.22 A comparison of daily total dam releases from Nalubale and Kiira dams with the Agreed Curve at Jinja from January 1999 to September 2009.

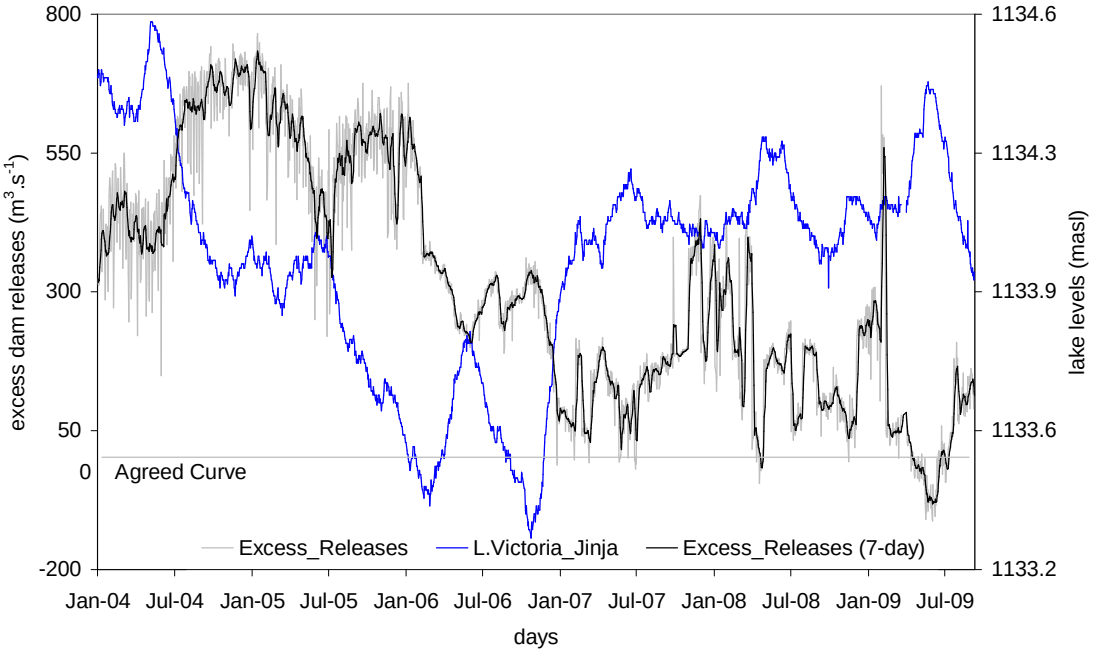

Figure 4.23 The relationship between excess daily and 7-day moving average dam releases and the average daily Lake Victoria levels at Jinja from January 2004 to September 2009.

The relationship between the dam outflow and Lake Victoria level monitored from January 1999 to September 2009 at both Entebbe and Jinja is shown in figure 4.24. Lake level variations at Entebbe and Jinja closely follow each other; levels at Jinja are slightly lower than Entebbe due to the gentle gradient to the lake's outlet. Dam outflow ranges from about 605 to 1,503 $m^3 \cdot s^{-1}$ with a mean of 1,069 $m^3 \cdot s^{-1}$. The lake stage at Jinja is more susceptible than Entebbe to the episodic daily variations in regulated outflow. From August 1999 to December 2004, there is a steady rise in outflow. These dam releases are followed by an initial fall and then stable but variable change in lake levels. Finally, there is a steady fall (~2 m) in lake levels from the late 2003. A sharp decline in dam releases occur over 2005 then stabilise out at two (850 and 750 $m^3 \cdot s^{-1}$, respectively) distinct discharge levels in 2006 during which period the falling lake levels ultimately stabilise. These two reductions in dam releases decreased the outflow to closely follow the Agreed Curve (Fig. 4.22). Since January 2007, there is a gradual but steady rise in discharge which stabilises during the later half of the year to the current levels (similar to the late 1999). The point of stability is followed by a sharp rise in lake levels before balancing out from mid-2007. Dam releases influence the lake levels (Fig. 4.22), although compensatory releases do not always induce immediate or concomitant responses in lake levels even at Jinja. This affirms the hypothesis that other influences such as climate (Sutcliffe and Petersen, 2007) also influence lake levels.

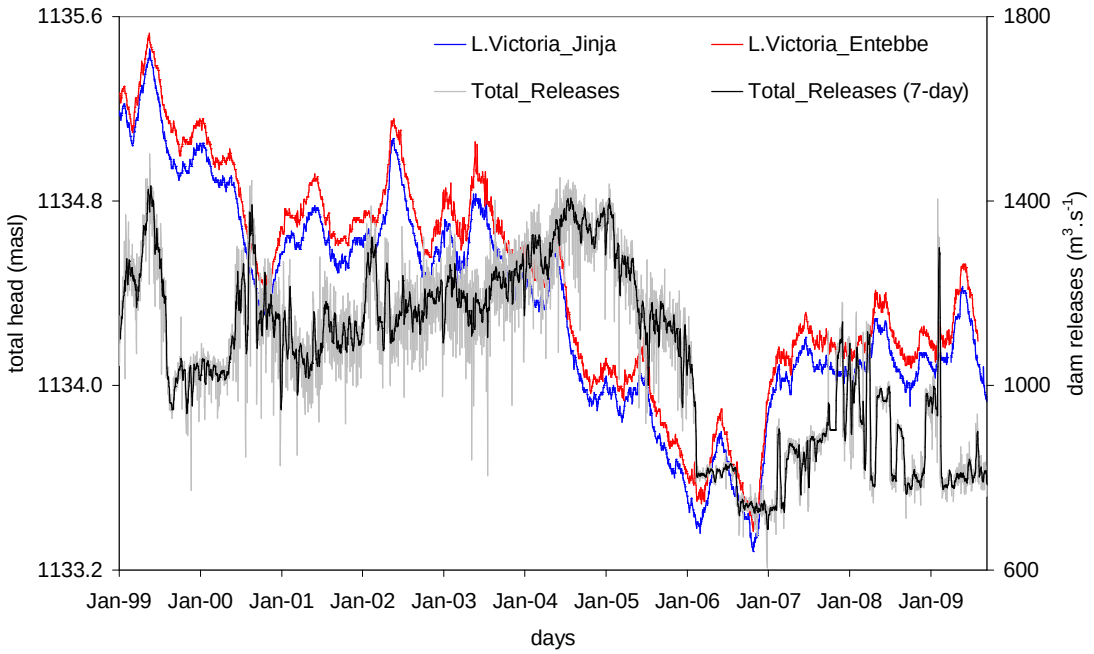

Figure 4.24 The average daily Lake Victoria levels at Entebbe and Jinja compared with daily and 7-day moving average dam releases at Jinja from January 1999 to September 2009.

Regulated outflow of Lake Victoria influences Lake Kyoga levels at Bugondo, R^2 = 0.58 (Fig. 4.25a). The difference in lake levels shows a reduction in covariation from early 1999 until late 2005 in response to increasing dam releases (Fig. 4.25b). From 2006, there is a divergence in lake levels as the dam releases are reduced. From the high dam release outputs of 1999, a reduction is made later in the year to decrease outflow to the blocked Lake Kyoga (Fig. 4.8). The dredging of the blocked outlet that had created excessively high lake levels results in a steady fall in stage levels despite the steady increase in dam releases from late 1999 to 2005. When the dam releases are reduced from January 2005 to 2006, this accelerates the lake stage fall until early 2007 when it starts to recover again. Since 2007, the lake levels have been positively responding to the daily variable but stable dam releases at Jinja.

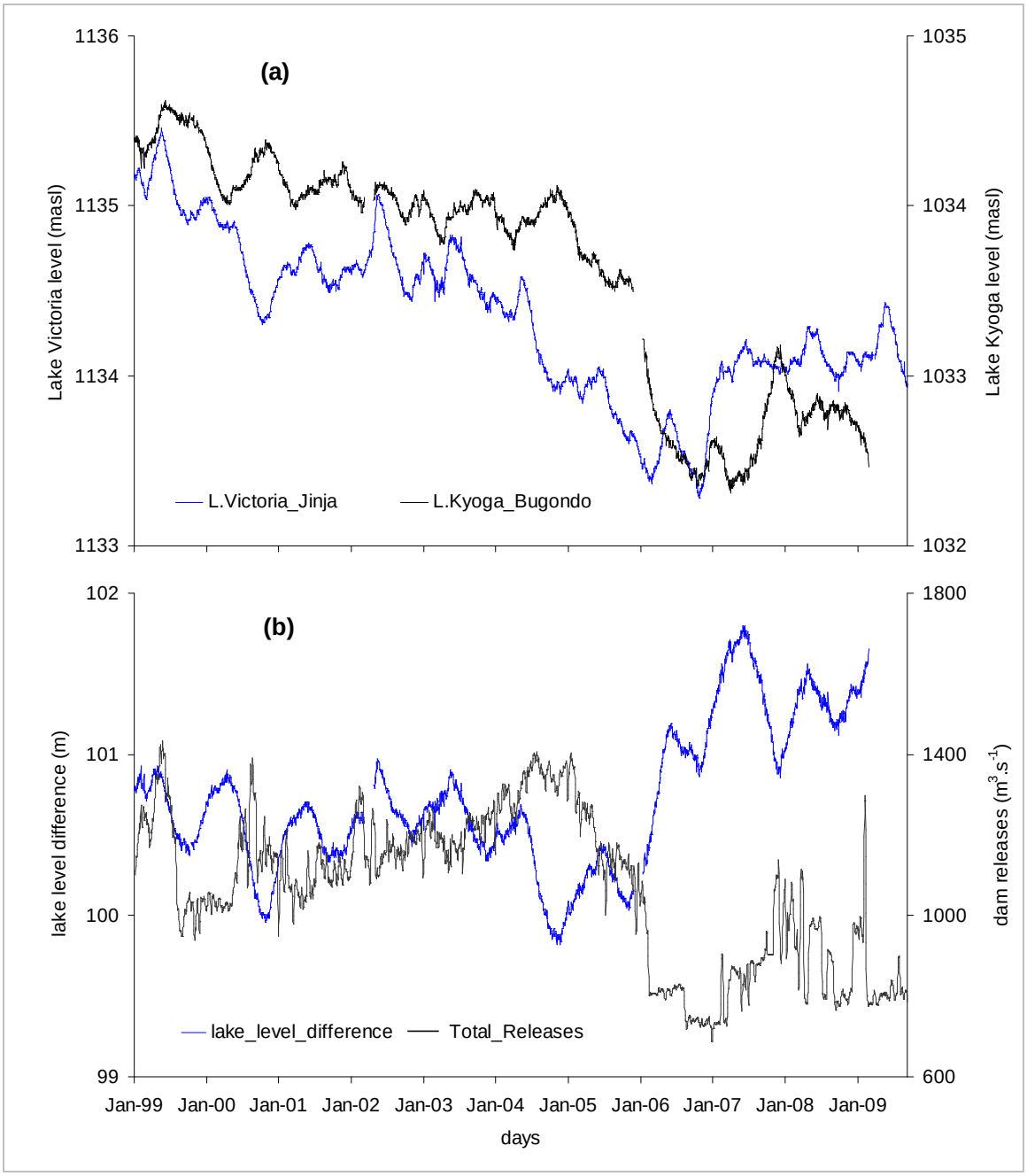

Figure 4.25 Lakes Victoria and Kyoga (a) average daily levels and (b) difference in levels showing their covariation and divergence, associated with 7-day moving average dam releases at Jinja from January 1999 to September 2009.

4.7.2 Jinja dam releases and the hydraulic gradient

At Entebbe, dam releases at Jinja influence Lake Victoria levels which in turn, affect the *i* between groundwater and the lake from January 1999 to July 2009 (Fig. 4.26). From mid-1999 to December 2003, the *i* shows a stable trend with high seasonal variability. During 2004, there is minimal seasonal variability and the trend remains stable. In early 2005, there is a sharp decline in the *i* which quickly recovers by the end of the year to once again stabilise with high seasonal variability. This anomaly reflects limited groundwater storage that requires significant lake-level changes to induce sufficient dynamic changes in the *i*. During the first half of 2005, the drainage base (lake) level is at its lowest and the *i* drops and even reverses. It is also during this period (from late 2004 to 2005) when there is a reduction in rainfall in the region (Sutcliffe and Peterson, 2007). Thus, the peaks in *i* is in part, driven by the changes in drainage (lake) base levels caused by consistent daily surges in the dam releases.

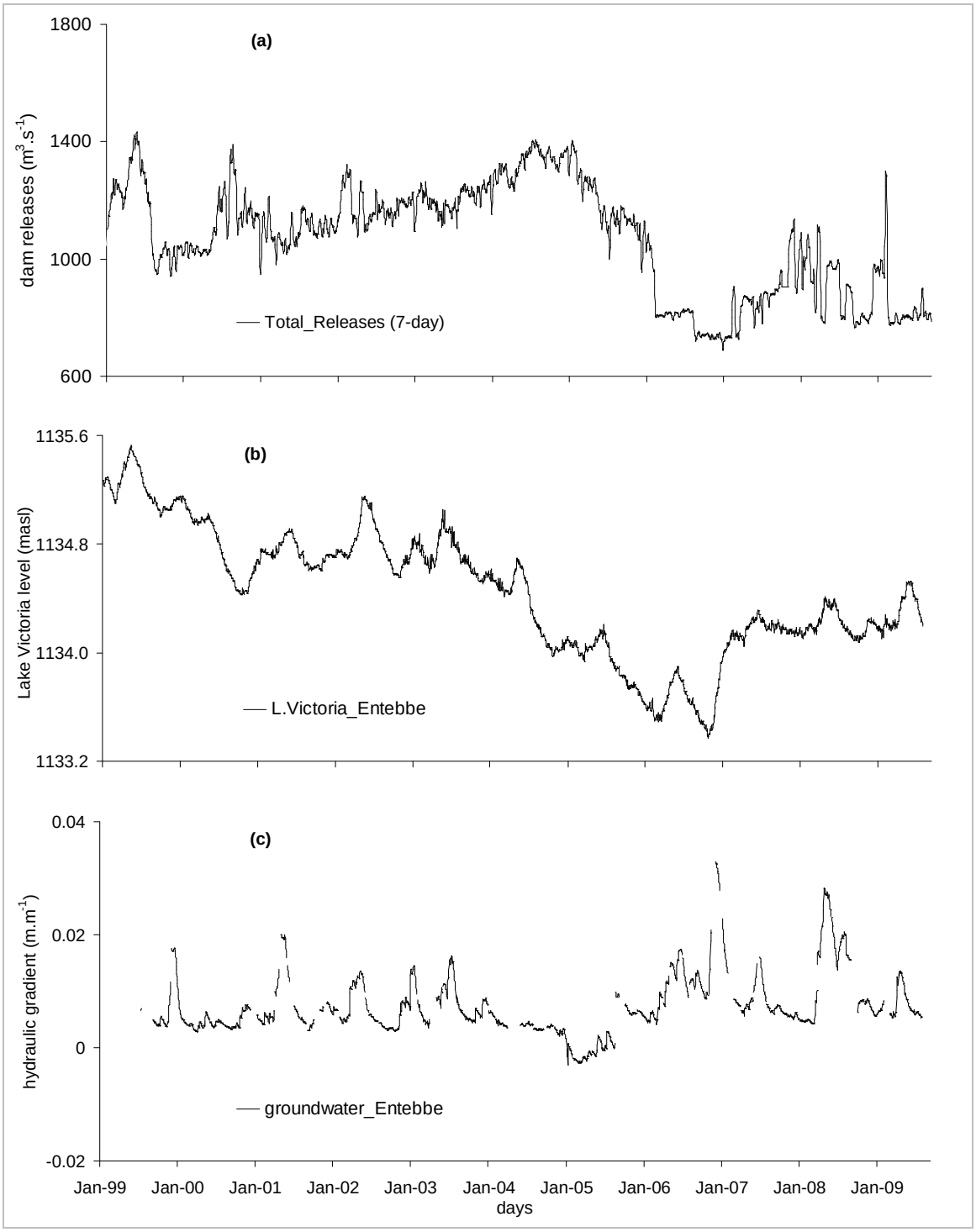

Figure 4.26 Daily measurements of the hydraulic gradient between mean groundwater and Lake Victoria levels at Entebbe and 7-day moving average dam releases at Jinja from January 1999 to July 2009.

Changes in the *i* at JP01 are further compared with Lake Victoria levels and dam releases at Jinja from November 2007 to July 2009 (Figs. 4.27a, b and d). This is the period when dam releases have been systematically reduced to enable recovery in the level of Lake Victoria (Figs. 4.26a and b). There is a *i* from groundwater to the lake over the whole period. Periods (e.g. November 2007 to February 2008 or March to May 2009) with consistent changes in dam releases induce large variations in the level of Lake Victoria, which in turn modify *i*. High dam release periods generally create a large net *i* from the groundwater due to lower lake levels whereas low releases reduce the *i* as the lake levels are boosted. However, this relationship is most evident for the dry season when other external influences (e.g. recharge) are minimal. It is possible that reduced dam releases are due to low natural (e.g. drought) lake levels in which case the net *i* from the groundwater towards the lake remains high.

At Bugondo, changes in the *i* at BP01 are also compared with Lake Kyoga levels and dam releases at Jinja from November 2007 to July 2009 (Figs. 4.27a, c and e). Apart from November 2007 to February 2008 when the *i* reverses, there is a net *i* from groundwater towards the lake. Similar to Jinja, periods (e.g. November 2007 to February 2008 or December 2008 to February 2009) with consistent changes in dam releases induce large variations in the lake level, which in turn modify *i*. Reduced outflow from Jinja tends to keep the drainage base (lake) level low which boosts the *i*, whereas extra outflow raises the lake level, that in turn reduces the *i*.

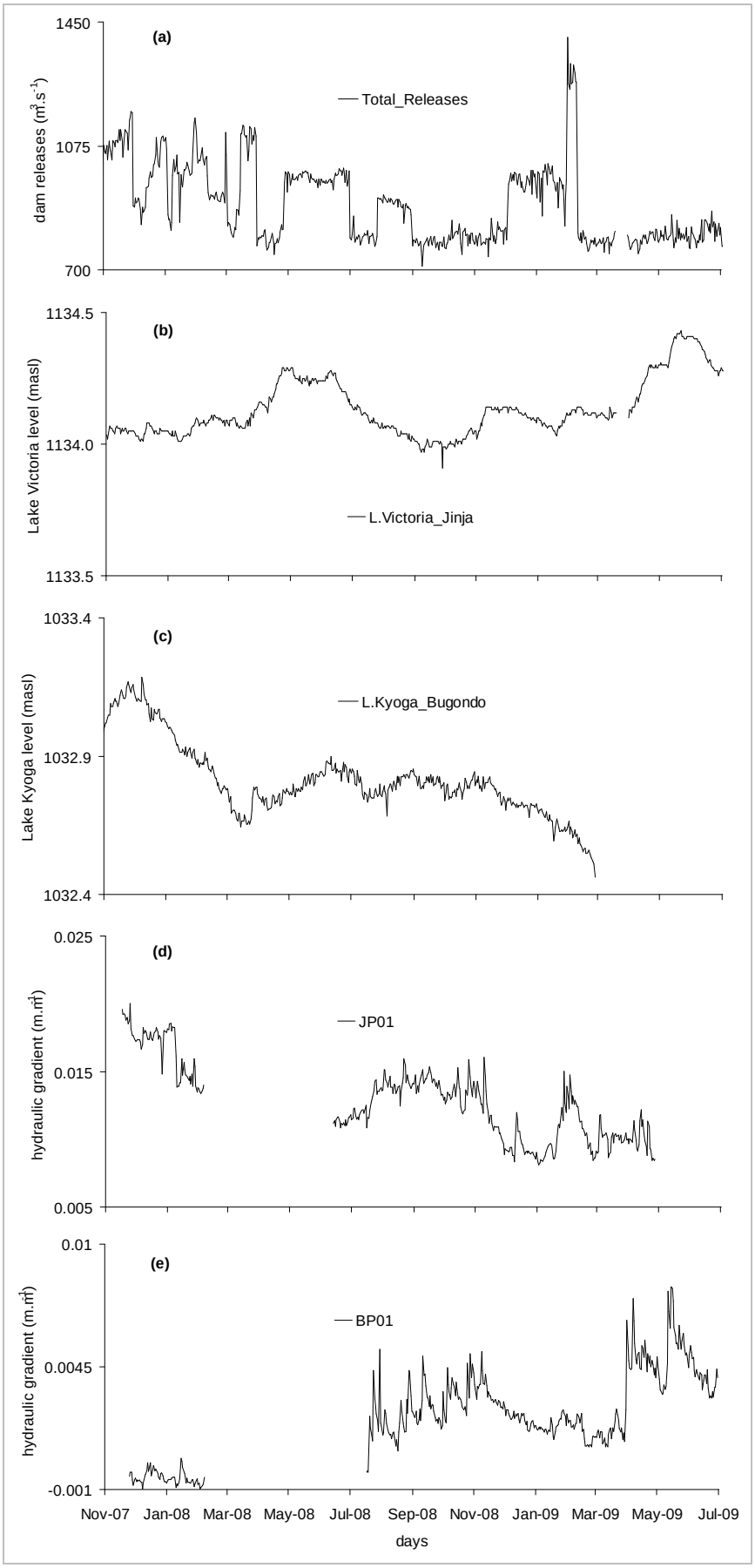

Figure 4.27 Daily measurements of the hydraulic gradient between mean groundwater (JP01 and BP02) and Lakes Victoria at Jinja and Kyoga at Bugondo and total dam releases at Jinja from November 2007 to July 2009.

4.7.3 Jinja dam releases and anomalous water level response at Jinja

Hourly observations of total hydraulic head in the piezometers at Jinja show fluctuations of ~0.4 m that occur over 3-day intervals over some of the monitoring period (Fig. 4.13). The origin of these pulses that are higher in amplitude but lower in frequency than those induced by barometric pressure changes, is unclear. A possible relationship between these fluctuations and dam releases ~3 km downstream is discussed here. Total hydraulic head in piezometer JP01 shows sharp rises following 3 to 4 days after reductions in total dam releases at Jinja (Fig. 4.28), which indicates a relationship between the surges in daily dam releases and the pulse responses in JP01. It is suggested that when dam releases are reduced, the back surge creates return flow to groundwater which quickly augments the water level. When the dam releases are raised and outflow increases, thus lowering the drainage base (lake) level, this groundwater slowly discharges back to the surface water.

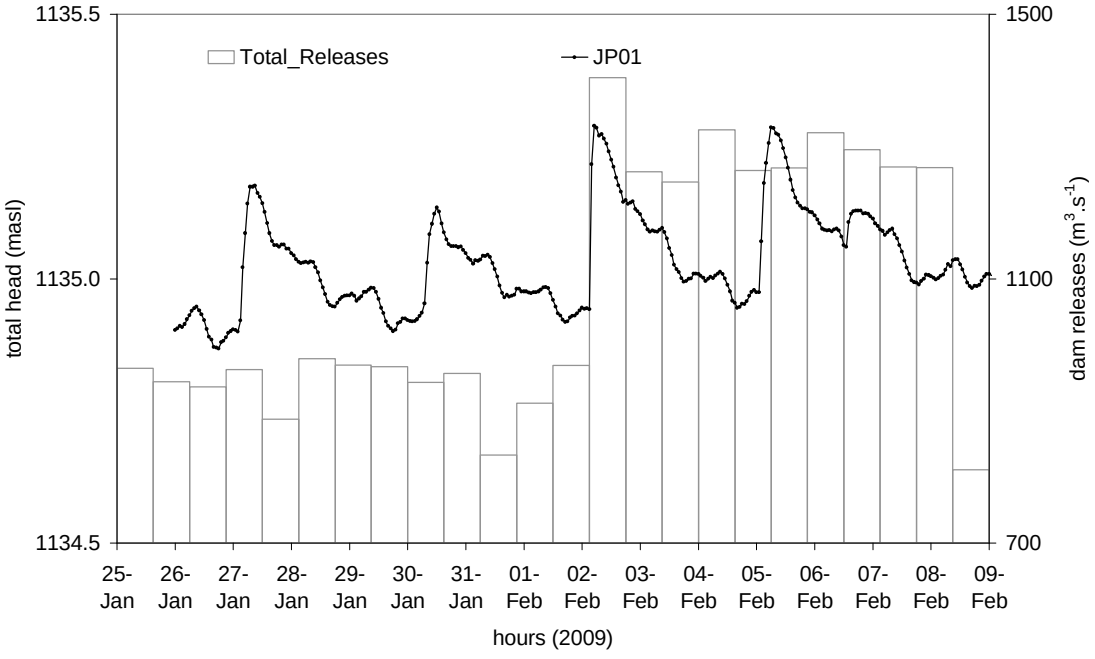

Figure 4.28 Daily dam releases at Jinja and the hourly total heads at JP01 in Jinja from 25 January to 9 February, 2009.

4.8 Conceptual models of the hydrodynamic interactions between groundwater and lakes

4.8.1 Lake Kyoga at Bugondo

From chapter 3, the hydrostratigraphy of the interface between Lake Kyoga and adjacent groundwater at Bugondo is as follows: fluvial-lacustrine sands (~1-5 m thick) overlie discontinuous or perforated duricrust (~2-4 m thick) which intersperse the upper horizons of a thick saprolite layer. Indicative K and S_y estimates vary with depth from fluvial-lacustrine sands (K of 1-15 $m \cdot d^{-1}$ and S_y 0.15-0.25) to saprolite (K of 0.04-3 $m \cdot d^{-1}$ and S_y of <0.01-0.02). The major ion water chemistry indicates mixing within groundwater that discharge into Lake Kyoga whereas isotopic ($\delta^{18}O$ and $\delta^{2}H$) data suggests that groundwater contributes to wetlands during wet periods.

A conceptual model of the temporal hydrodynamic interaction between groundwater and Lake Kyoga at Bugondo is presented in (Fig. 4.29). It is proposed that during the wet season, precipitation infiltrates the interfluve where within the fluvial-lacustrine sands, it forms shallow groundwater throughflow which seeps into the lake, and within the wetlands. Groundwater levels quickly rise and recede. Deep percolation within the interfluve recharges the saprolite aquifer. It is also possible that saprolite recharge takes place through peripheral fractures and seepage zones at the interface with the southern-lying amphibolite ridge (Fig. 3.3). Upwelling of saprolite groundwater occurs via preferential pathways (e.g. discontinuous clay horizons, quartz stringers and fractures in duricrust) into the wetlands and lake. In the dry season, there is minimal shallow fluvial-lacustrine aquifer subsurface runoff and deep saprolite groundwater recharge through the interfluve. Discharge into the lake is mainly derived from upwelling of the saprolite groundwater. The wetlands dry up due to a large soil moisture

deficit from evapotranspiration. Fluvial-lacustrine sediments within the wetlands can receive recharge from the lake when the hydraulic head falls below the lake level.

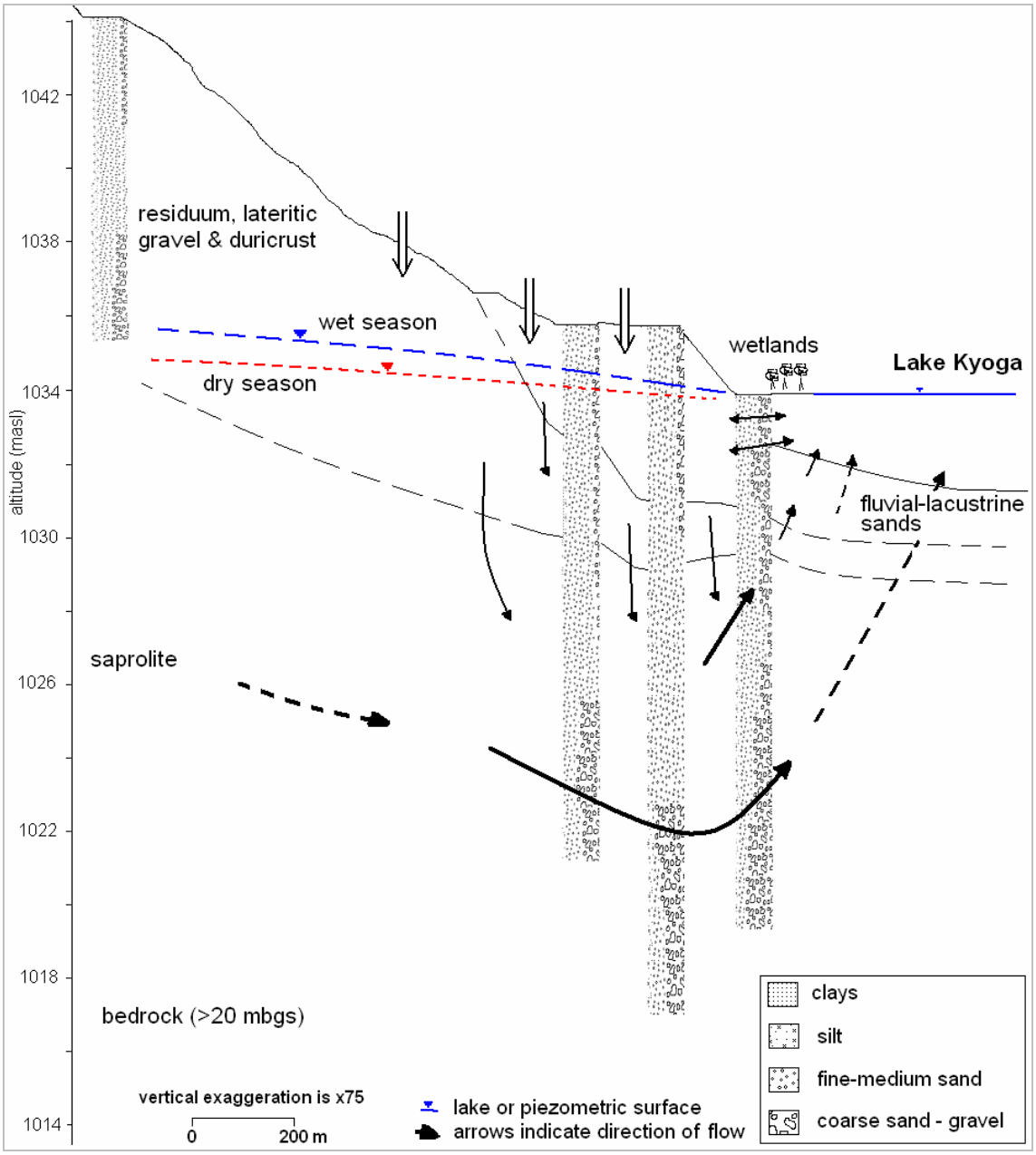

Figure 4.29 A hydrodynamic conceptual model showing the direction of fluxes within the lithologic interface with Lake Kyoga at Bugondo.

4.8.2 Lake Victoria at Jinja

From chapter 3, the hydrostratigraphy of the interface between Lake Victoria and adjacent groundwater at Jinja is as follows: fluvial-lacustrine sands with infill (~2-7

m thick) overlie a thick saprolite layer (from ~10 m depth). Indicative K and S_y estimates vary with depth from fluvial-lacustrine sands with infill (K of <0.02 $m \cdot d^{-1}$ and S_y of <0.01) to saprolite (K of <0.02-3 $m \cdot d^{-1}$ and S_y of <0.01-0.18). Both major ion and isotopic ($\delta^{18}O$ and $\delta^{2}H$) water chemistry suggest mixing relations between groundwater and lake at Jinja.

The conceptual model of the temporal hydrodynamic interaction between groundwater and Lake Victoria at Jinja is presented in (Fig. 4.30). It is proposed that in the wet season, precipitation infiltrates through the interfluves and generates shallow groundwater flow that rapidly discharges into the wetlands. As water rises in the wetlands, it provides indirect recharge to fluvial-lacustrine groundwater; groundwater levels swiftly rise and recede giving rise to rapid, short-lived hydrograph peaks. There is also deep recharge of the saprolite aquifer through the residuum and lateritic gravel on the interfluve. Upwelling of saprolite groundwater occurs through preferential pathways (e.g. discontinuous clay horizons and quartz stringers) into the wetlands and lake. During the dry season, there is low shallow fluvial-lacustrine aquifer subsurface runoff and deep saprolite groundwater recharge in the interfluve. Discharge into the lake is mainly derived from upwelling of the saprolite groundwater. Despite the high evapotranspiration, wetlands continue to receive discharge from upwelling saprolite groundwater which maintains a higher hydraulic head.

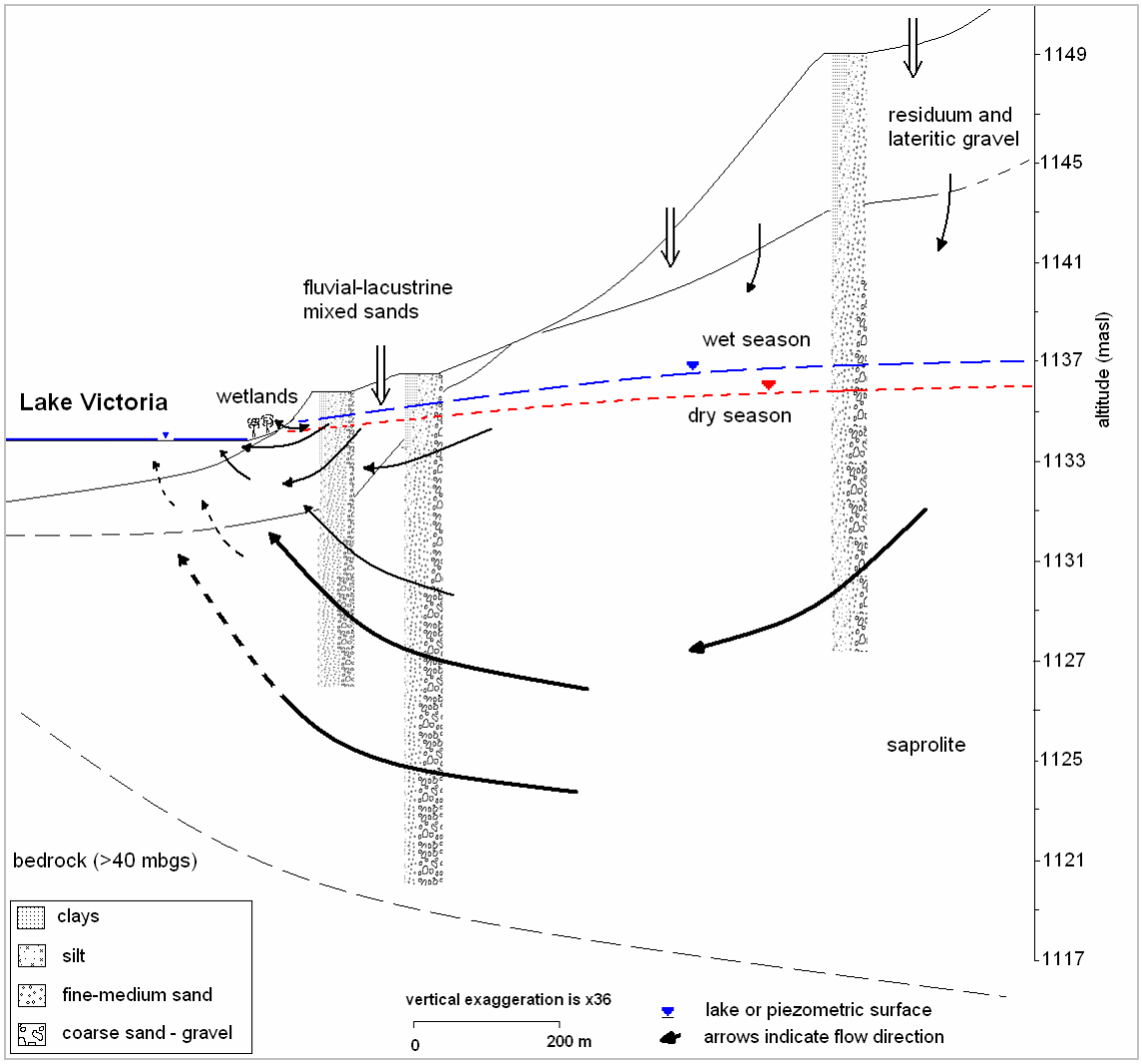

Figure 4.30 A hydrodynamic conceptual model showing the direction of fluxes within the lithologic interface with Lake Victoria at Jinja.

4.8.3 Lake Victoria at Entebbe

From chapter 3, the hydrostratigraphy of the interface between Lake Victoria and adjacent groundwater at Entebbe shares a similar stratigraphy with Jinja where pronounced thicknesses of both the fluvial-lacustrine sands (~5 m thick) and the underlying lateritic gravel residuum (15 m thick), overlie a thick (>17 m thick) saprolite (Fig. 3.30). The *T* bulk estimates from fluvial-lacustrine aquifers on the western shore of Lake Victoria give values of 18-36 $m^2 \cdot d^{-1}$ which for aquifer thickness of 50 m, provides bulk *K* estimates of 0.4-0.7 $m \cdot d^{-1}$. Isotopic ($\delta^{18}O$ and $\delta^{2}H$) water chemistry suggests that groundwater mixes with lake waters in parts of the fringing region on the northern shore of Lake Victoria.

A conceptual model of the temporal hydrodynamic interaction between groundwater and Lake Victoria at Jinja is presented in (Fig. 4.31). It is argued that during the wet season, precipitation infiltrates in the interfluve and generates shallow groundwater flow which discharges through the fluvial-lacustrine sands into the lake. This flux is evident from the observed rise in water levels above the interface between the fluvial-lacustrine sands with a higher *K*, overlying saprolite of laterite mixed with clayey-sands. Deep percolation within the interfluve recharges the saprolite aquifer through the residuum and lateritic gravel. Upwelling of saprolite groundwater occurs through preferential pathways (e.g. discontinuous clay horizons and quartz stringers) into the lake. In the dry season, shallow groundwater flow to the lake via the fluvial-lacustrine aquifer and recharge of saprolite on the interfluve is low. Seepage into the lake is mainly derived from upwelling of saprolite groundwater. Occasionally, fluvial-lacustrine sediments may receive infiltration from the lake as the hydraulic head falls below the lake level.

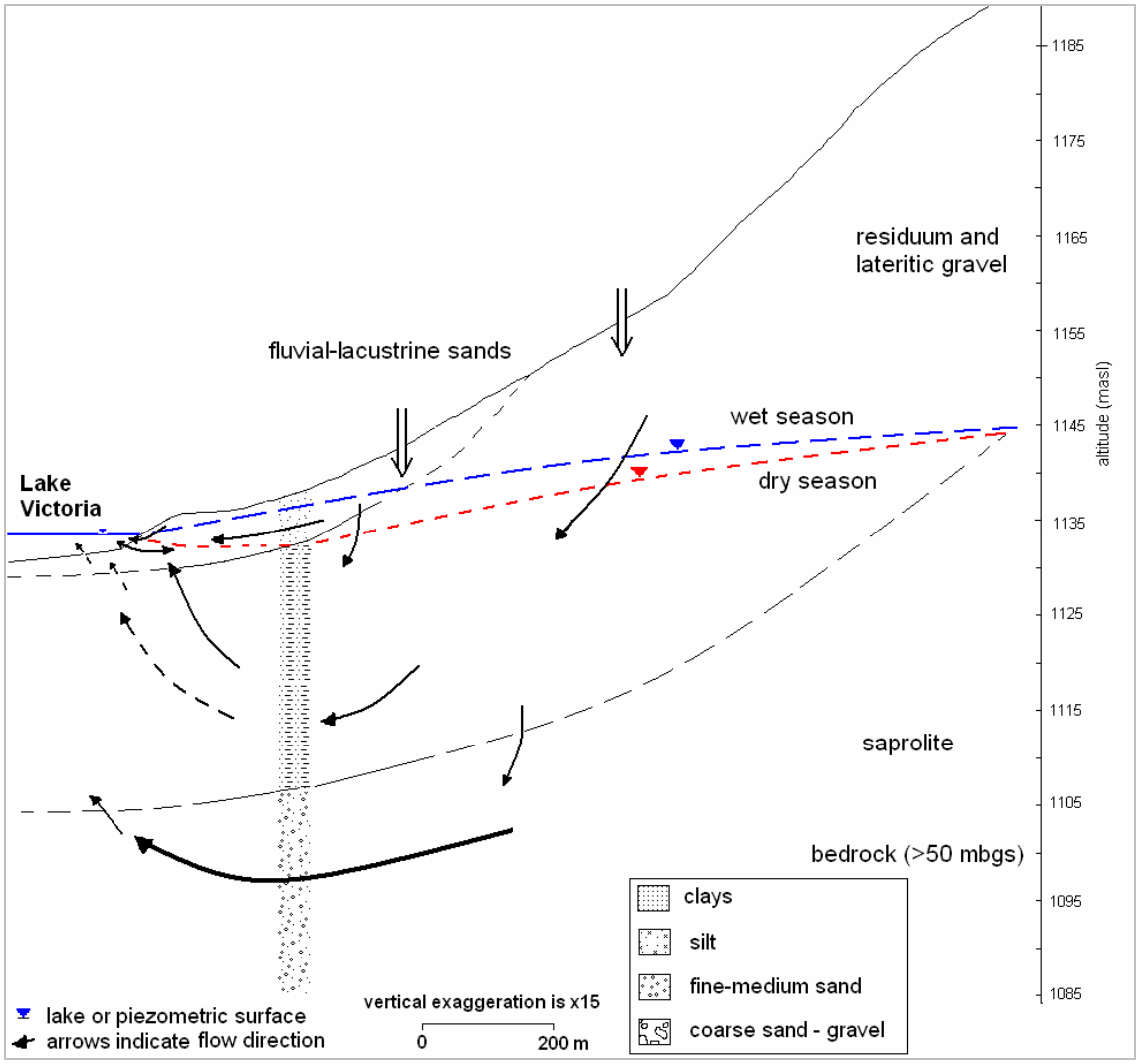

Figure 4.31 The hydrodynamic conceptual model showing the direction of fluxes within the lithologic interface with Lake Victoria at Entebbe.

4.8.4 General hydrodynamic models

According to Banks *et al.* (2009) conceptual models of hydrogeologic controls on groundwater-surface water interactions in a saprolite-fractured bedrock geological setting, commonly assume 3 model types: a single homogenous geological system, dominance by the saprolite system, or explicit fluxes by both the saprolite layer and fractured bedrock aquifer system. Apart from Bugondo, where there is a discontinuous duricrust layer, the three piezometers (Bugondo, Jinja and Entebbe) have otherwise similar hydrostratigraphic profiles. There is a shared similarity with the von der Heyden and New (2003) model from Zambia where discharge into surface water is provided by a shallow aquifer during the wet period and from a deep groundwater system in the dry season via preferential pathways (Fig. 4.1). It differs from the McCartney and Neal (1999) model derived from a dambo in Zimbabwe where a clay barrier prevents vertical deep groundwater discharge and the bulk of the dry season flow comes from shallow water sources (Fig. 4.3). Likewise, there is a difference from the Bell *et al.* model (cited in von der Heyden, 2004) which has an impermeable bedrock/laterite layer underlying shallow interfluve and dambo soils that are hydraulically connected and dry season flow is derived from the interfluves (section 2.6.3). All the three Upper Nile models provide further support for aspects of the McFarlane (1992) *in situ* hypothesis from Malawi (Fig. 4.2). This profile is consistent with the Taylor and Howard (1998) model of post-Palaeozoic evolution of weathered land surfaces in eastern Uganda.

Similar to the McFarlane (1992) *in situ* model, it is suggested that during the wet season, precipitation infiltrates the interfluve profile and partly recharges saprolite groundwater through the residuum-saprolite interface, with preferential flow into the lakes taking place within fluvial-lacustrine sands overlying saprolite. Groundwater in saprolite aquifers also upwells into the lakes through preferential pathways, probably

via discontinuous clay horizons, quartz stringers and fractures in duricrust, through the diatomaceous sapropel (mud) layer on the lakebed. The evidence from chapter 5 and previous studies (Taylor and Howard, 1996; 1999b) showing seasonal groundwater-level fluctuations in response to rainfall, suggests infiltrating rainfall is able to recharge coarser horizons in the saprolite though the precise pathways through shallow, clay-rich horizons in the saprolite remain unclear. In the dry season, recharge of the saprolite groundwater continues through the interface of the interfluve profile, whereas shallow subsurface runoff is low and most of it is lost to evapotranspiration. Discharge and upwelling of saprolite groundwater through the preferential flow paths continue to take place, albeit less dynamically with time as the interfluve hydraulic head is reduced. It is thus inferred that deep circulation of water within the saprolite is likely to be the primary source of groundwater seeping into the lakes during the dry period.

4.9 Summary

Historical variations in the levels of Lakes Victoria and Kyoga (1947-2009) demonstrate that variations in Lake Kyoga levels are primarily determined by the flow of the Victoria Nile with natural (e.g. vegetation) and more recent human development (e.g. dams) influencing the variations of both lake levels. The two lakes are therefore hydraulically linked and co-dependent.

Saturated K (0.01-15 $m \cdot d^{-1}$) estimates from well logs together with estimates of bulk T (2-36 $m^2 \cdot d^{-1}$) from hydraulic tests demonstrate vertical and horizontal variability in groundwater flow paths across the interface of groundwater and surface water. Hydraulic tests show semi-confining, constant-head boundary (lake and fringing wetland waters) hydrogeological conditions within the groundwater-bearing interface, signifying groundwater fluxes over time reaching surface water.

The local *i* between groundwater and lake at Entebbe (since 1999) shows that it is largely controlled by the changes in the groundwater levels as a result of the comparatively low storage of the localised saprolite/saprock aquifer in relation to the large area and storage volume of Lake Victoria. Semi-diurnal harmonic changes in barometric pressure influence groundwater total hydraulic heads at both Bugondo and Jinja (since 2007). Hydraulic gradients are generally towards the lake from all the piezometers and are highest during the recharge periods. Groundwater flows primarily into lakes, which dynamically varies seasonally and with proximity to lake. The closest piezometers to the lake, form rapid, short-lived groundwater level responses that indicate possible flooding during recharge events.

Layered heterogeneity in the saprolite aquifer suggests a two-component recession in groundwater levels (fluvial–lacustrine sands and saprolite system). Temporal variations in the fluxes between the groundwater and the lakes reflect that groundwater hydrographs form rapid, short-lived responses when the levels rise above the fluvial-lacustrine sands which overlie the saprolite system, indicative of the vertical variability in storage.

Along the Lake Victoria shore, consistently high dam releases at Jinja decrease the levels of the lake which, in turn, raise the *i* between groundwater and lake; low releases decrease the *i* as the lake level rises. However, on the shore of Lake Kyoga, the reverse is true. Consistently high dam releases enhance lake levels which, in turn, lower the *i* between groundwater and lake; low releases increase the *i* as the lake level declines.

General hydrodynamic conceptual models illustrate temporal dynamic interactions between groundwater and surface water, which support prolonged, deep weathering under the *in situ* (*etchplanation*) model proposed by McFarlane (1992). During the wet season preferential flow into surface water is derived from shallow and

rapid groundwater flow within fluvial-lacustrine sands overlying saprolite. In the dry season the dominant discharge into surface water is transmitted from deeper saprolite fluxes that are upwelled into the lakes via preferential pathways.

Chapter 5
Influence of climate on groundwater – surface water interactions in the Upper Nile Basin

5.1 Introduction

Chapter 4 established that observed interactions between groundwater and Lakes Victoria and Kyoga are largely controlled by the variations in groundwater levels. Groundwater levels are, in turn, determined by recharge as each monitoring station is remote from groundwater abstraction. Evidence from the application of stable isotope tracers and soil-moisture balance models across tropical Africa (Vogel and Van Urk, 1975; Taylor and Howard, 1996; Taylor and Howard, 1999b; Eilers *et al.*, 2007; Mileham *et al.*, 2008) highlights the importance of heavy rainfall events (>10 $mm \cdot d^{-1}$) during the monsoons (wet seasons) in determining the magnitude and timing of rainfall-fed recharge. This chapter investigates the influence of climate, primarily rainfall, on groundwater recharge in the Upper Nile Basin and, in turn, groundwater – surface water interactions at the three study stations (Entebbe, Bugondo and Jinja) on Lakes Victoria and Kyoga.

Factors that influence diffuse recharge include weather patterns, properties of surface soils, vegetation, local topography, depth to the water table, and the temporal and spatial scales over which estimations are made (Alley *et al.*, 2002). Several methods have been previously applied to estimate recharge across Equatorial Africa (Table 5.1); their diversity complicates comparisons due to assumptions inherent to each method (Tayor *et al.*, 2004). Recharge estimates in tropical Africa broadly range from 12 to 281 $mm \cdot a^{-1}$. Across Uganda, recharge is highly variable (12-200 $mm \cdot a^{-1}$) within the crystalline basement aquifers which feature a highly variable composition and thickness of saprolite overlying fractured bedrock (saprock). More rainfall is estimated to

replenish deeply weathered aquifers in the low relief region of central Uganda compared to the zone of stripping within the western arm of the EARS (Taylor and Howard, 1996; 1999b). The saprolite is considered to transmit the vast majority (over 99 %) of recharge in comparison to the underlying bedrock fractures which have traditionally been developed for rural water supplies.

[1]**Table 5.1** Estimates of annual groundwater recharge in sub-Saharan Africa (adapted from Tayor *et al.*, 2004 and regional references cited therein).

Recharge ($mm \cdot a^{-1}$)	**Method**	**Aquifer**	**Region**	**Source**
80 - 281	SMB[1]		Zambia	Houston in 1982
50 - 60	Soil infiltration		Kenya	Singh *et al.* in 1984
12	Chloride tracers		Zimbabwe	Houston in 1990
172	BS[2]		Ghana	Asomaning in 1992
84-133	SMB		Tanzania	Sandström in 1995
10 - 16	Chloride tracers		Tanzania	Nkotagu in 1996
17	SMB	Saprock	Uganda	Howard and Karundu (1992)
200	SMB/flow modelling	Saprolite-saprock	Uganda	Taylor and Howard (1996)
120	BS/SMB/borehole hydrographs	Saprolite-saprock	Uganda	Taylor and Howard (1999b)
113 - 161	flow modelling/SMB	Saprolite-saprock	Uganda	Tindimugaya (2000)
104	SMB	Saprolite	Uganda	Mileham *et al.* (2009)

[1]SMB: soil moisture balance; [2]BS: Baseflow separation

5.1.1 Controls on rainfall variability in the Upper Nile Basin

The spatial and temporal distribution of rainfall in the Upper Nile Basin is strongly controlled by the movement of the ITCZ. Low-level north-easterlies (northern hemisphere) and upper-level south-easterlies (southern hemisphere) converge at the ITCZ that shifts north and south of the equator annually. Within the Upper Nile Basin, seasonal movements of the ITCZ produce two distinct rainfall seasons from March-April-May (MAM) and September-October-November (SON) (Fig. 5.1). During the MAM rainy season, the ITCZ convergence is broad and moves more slowly northward,

[1] SMB estimates recharge when excess water drains through the soil after it reaches the field capacity.

[2] BS techniques use stream flow hydrographs to derive the component of river discharge originating from groundwater discharges; under steady-state conditions, groundwater discharge is equal to groundwater recharge.

producing heavy rainfall. SON rains in contrast, are less than MAM rains and are more pronounced in southern Uganda (Fig. 5.1a). In north and northwestern Uganda, the MAM rains start later and the SON rains begin earlier resulting in a near uni-modal rainfall pattern centred around August (Fig. 5.1b). Regionally, the MAM rains are less variable; interannual rainfall variability is primarily associated with SON rains, which feature a complex seasonal trend and high spatial variability (Ogallo; 1989; Basalirwa, 1995; Nicholson, 1996; Phillips and McIntyre, 2000; Olago *et al.*, 2009).

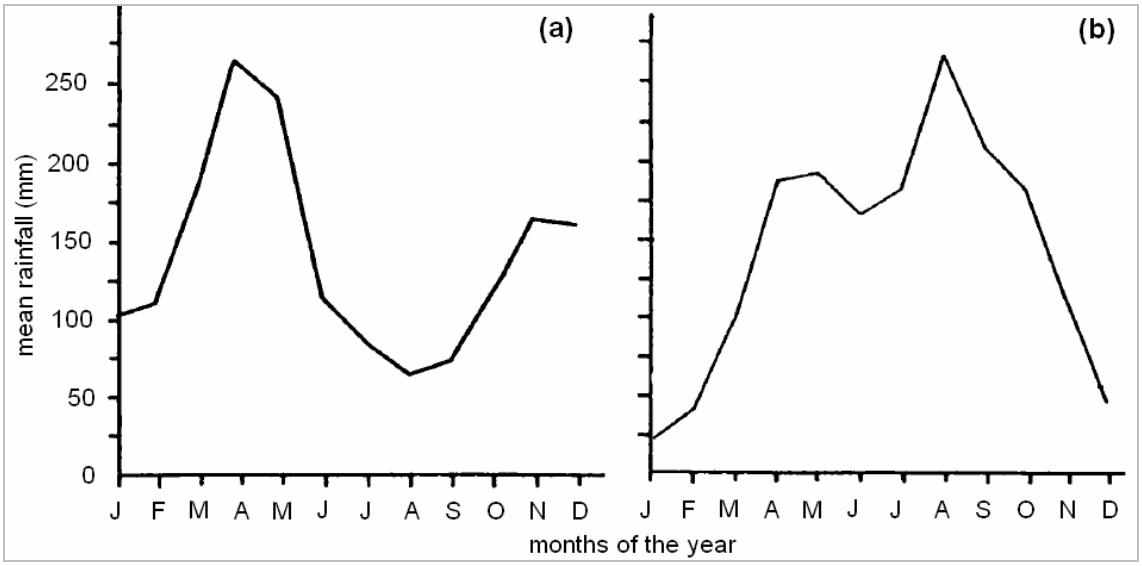

Figure 5.1 Seasonal rainfall distribution in climatological rainfall zones of stations in (a) Lake Victoria region of southern Uganda, and (b) central northern Uganda (adapted from Basalirwa, 1995).

Main synoptic controls on inter-annual climate variability in the Upper Nile Basin include: (i) El Niño - Southern Oscillation (ENSO) phenomenon; (ii) sea surface temperatures (SST) – primarily Indian but also Atlantic Oceans; (iii) the Indian Ocean Dipole (IOD); and (iv) the Quasi-biennial oscillation (QBO) (Ogallo, 1988; Nicholson, 1996; Nicholson and Kim, 1997; Saji *et al.*, 1999; Indeje *et al.*, 2000; Nicholson and Selato, 2000; Philips and McIntyre, 2000; Camberlin *et al.*, 2001; Mistry and Conway, 2003; Black, 2005; Mileham, 2007; Olago *et al.*, 2009). Olago *et al.* (2009) further

suggest that observed decadal-scale rainfall variability, both spatially and in terms of amount, relates to variations in the strength and phase of interactions between ENSO, IOD, deep westerly airstreams from the Atlantic, and the Congo air mass. Spatial and temporal variability is also locally induced and modulated by (a) land cover/use, (b) topography, (c) large inland lakes (e.g. Lake Victoria), and (d) the seasonal migration of the ITCZ (Nicholson, 1996; FAO, 2001; Bounoua *et al.*, 2002; Olago *et al.*, 2009). The north-east monsoons carry relatively dry continental air masses from December-March, whereas the shallow south-easterlies mostly from the warm Indian Ocean prevail from June to September.

5.1.2 Projected impacts of climate change on rainfall in the Upper Nile Basin

Global warming is expected to intensify the global hydrological system through a net transfer of freshwater from long-term stores in ice and increased precipitation and evapotranspiration associated with a warmer atmosphere. Considerable uncertainty remains, however, in how a net rise in global freshwater fluxes will be distributed in time and space. Increased rainfall intensities are expected to be especially pronounced in the tropics where warmer air temperatures will lead to larger absolute rises in the moisture content of the atmosphere (Allen *et al.*, 2002; Trenberth *et al.*, 2003; Pall *et al.*, 2007). This change in the distribution of rainfall will give rise to more variable river discharges and soil moisture. The IPCC AR4 projects wetter conditions in East Africa (Kundzewicz *et al.*, 2007). In the long term (by 2080), Lake Victoria level is projected to rise as increased precipitation surpasses increased evaporation as a result of rising temperatures (Tate *et al.*, 2004). In the short term (by 2030) however, greater evaporation is expected to offset rises in precipitation. There is, however, considerable uncertainty in the estimation of potential evaporation and evapotranspiration as a result of climate change so that current projections are highly uncertain (Kingston *et al.*,

2009). Although rainfall is projected to be more intense, it remains uncertain whether the Upper Nile Basin will get wetter or drier as a result of climate change.

The impact of changing rainfall intensities on groundwater recharge in the tropics is unclear. Substantial (70%) declines in groundwater recharge, recently cited in IPCC AR4 (Kundzewicz *et al.*, 2007), have been projected in northeast Brazil and southwest Africa in association with higher air temperatures and lower rainfall (Döll and Florke, 2005). These projections fail, however, to consider changes in the distribution of daily precipitation. Recent research in the Upper Nile Basin (Mileham *et al.*, 2009) shows that failure to consider projected changes in rainfall intensities can influence both the direction and magnitude of the climate change signal for groundwater recharge. In the River Mitano Basin of Uganda, Mileham *et al.* (2009) show that projections of groundwater recharge that employ an historical (baseline) distribution of daily rainfall are 55 % lower than the baseline period (1961–1990); transformation of the rainfall distribution to account for projected changes in rainfall intensity results in a 53 % increase in recharge relative to the same baseline period.

5.1.3 Analysis of recharge events response to rainfall intensity and rainfall intensity thresholds

Saprolite and saprock exhibit considerable heterogeneity laterally and with depth due to the *in situ* weathered origin of each aquifer. Despite recent research (Taylor and Howard, 2000; Taylor *et al.*, 2009b), substantial uncertainty remains in storage properties of saprolite and saprock in Uganda and elsewhere in the tropics. In light of substantial uncertainty in the storage coefficients for saprolite and saprock, observed recharge was quantified from borehole hydrographs in terms of the magnitude of the water-level rise (Healy and Cook, 2002; Lee *et al.*, 2006). Cross correlations of observed rainfall and recharge at each piezometer provide estimates of the lag time

between observed rainfall and recharge events (Healy and Cook, 2002). The period of rainfall contributing to a recharge event was estimated from the mean lag time between rainfall and recharge events and the duration of the recharge event indicated by the period of water-level rise.

The magnitude of each recharge event was related to both the sum of daily rainfall (ΣP_i) and the annual sum of daily rainfall exceeding a threshold of 10 $mm \cdot d^{-1}$ ($\Sigma(P_i\text{-}10)$). The first correlation assumes that all rainfall events contribute to recharge whereas the second assumes that only heavy rainfall events (> 10 $mm \cdot d^{-1}$) contribute to recharge. This latter criterion is consistent with recent modelling of recharge in the tropics (Döll and Florke, 2005). Correlations additionally assume that daily rainfall events contribute proportionally to recharge. In reality, the magnitude of the recharge flux derived from rainfall is influenced by not only antecedent soil moisture conditions but also intra-annual variability in soil-infiltration capacities and evapotranspiration. Additionally, the influence of the proximity to the drainage base (lake) level for the stations closest to the lakes is scrutinised. In the absence of observations of soil moisture, rainfall is directly correlated to recharge observations in order to avoid the possibility of introducing model bias in relating rainfall intensity to recharge.

5.2 Methods

5.2.1 Monitoring stations

Daily rainfall records were obtained from Entebbe and Jinja stations on the northern shore of Lake Victoria, in addition to Bugondo on the northeastern shore of Lake Kyoga (Fig. 5.2). As outlined in section 5.1.1, rainfall follows a bimodal pattern in the Upper Nile Basin (Fig. 5.3). Rains fall commonly during heavy thunderstorms, typically not exceeding an hour or two with high local variability over distances of a

few kilometres (Carter, 1956). Standard rain gauge measurements are manually carried out usually up to three times a day; at 9 a.m. in the morning, as well as 12 p.m. and 3 p.m. in the afternoon. Mean annual rainfall is 1,195 mm in Jinja (1903-2007), 1,541 mm in Entebbe (1954-2007) and is 1,228 mm (1916-1956) in Bugondo. Recent (2001-2008) observations indicate a substantial decline in mean annual rainfall at Bugondo (781 mm). 'Nocturnal lake breeze effect' is suggested to enhance rainfall over Lake Victoria by about 30 % compared to that over the surrounding land area of the catchment (Yin and Nicholson, 1998; Nicholson *et al.*, 2000). Most of the rainfall that falls on the surrounding land area of the lake is derived from the south-easterly winds which pick up moisture from the central and western part of the lake that condenses to form heavy rainfall on the northern and western shores of the lake.

Across the Upper Nile basin, annual potential evapotranspiration (PET) increases from about 1,500 mm on the shore of Lake Victoria to over 2,200 mm in northern Uganda (Hanna, 1971). A recent estimate from mean monthly pan evaporation at Entebbe (1987-2008, Fig. 3.5), is 1,520 mm based on a mean monthly pan coefficient of 0.9 (Hanna, 1971; Dagg, 1972; START, 2006). At Entebbe it is apparent that most of the open water evaporation takes place during the start or end (February, June and November) of the relatively dry seasons as well as during the midst (April and September) of the rainy seasons (Fig. 3.5).

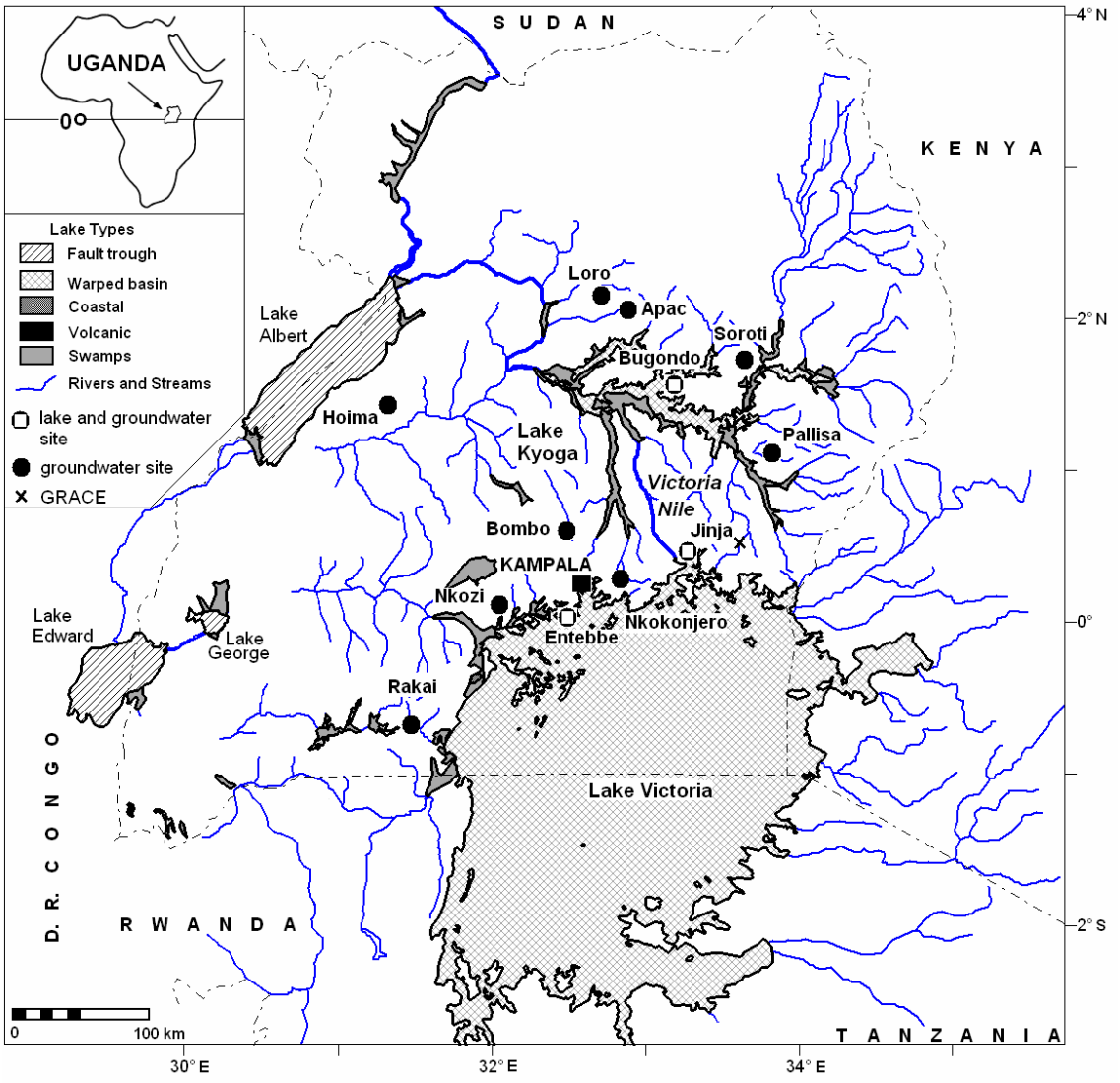

Figure 5.2 Map of drainage basins in Upper Nile Basin showing the location of combined groundwater-surface water, regional groundwater and rainfall monitoring stations.

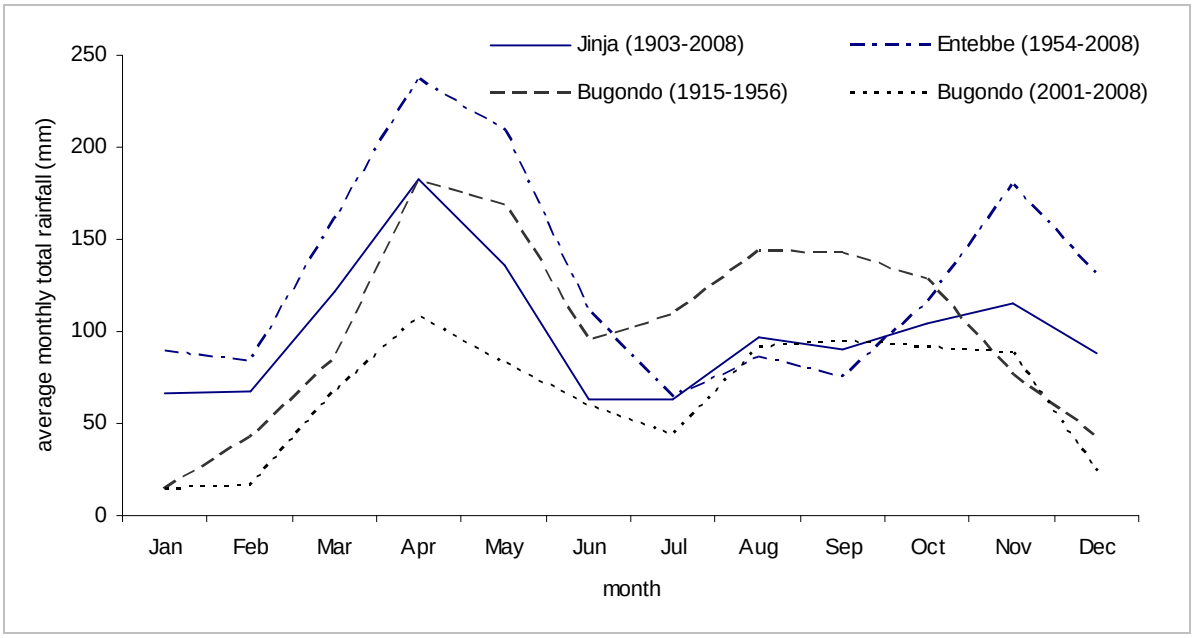

Figure 5.3 Mean monthly rainfall for Jinja (1903-2008) and Entebbe (1954-2008) on the shores of Lake Victoria and Bugondo (1925-1956 and 2001-2008) on the shore of Lake Kyoga.

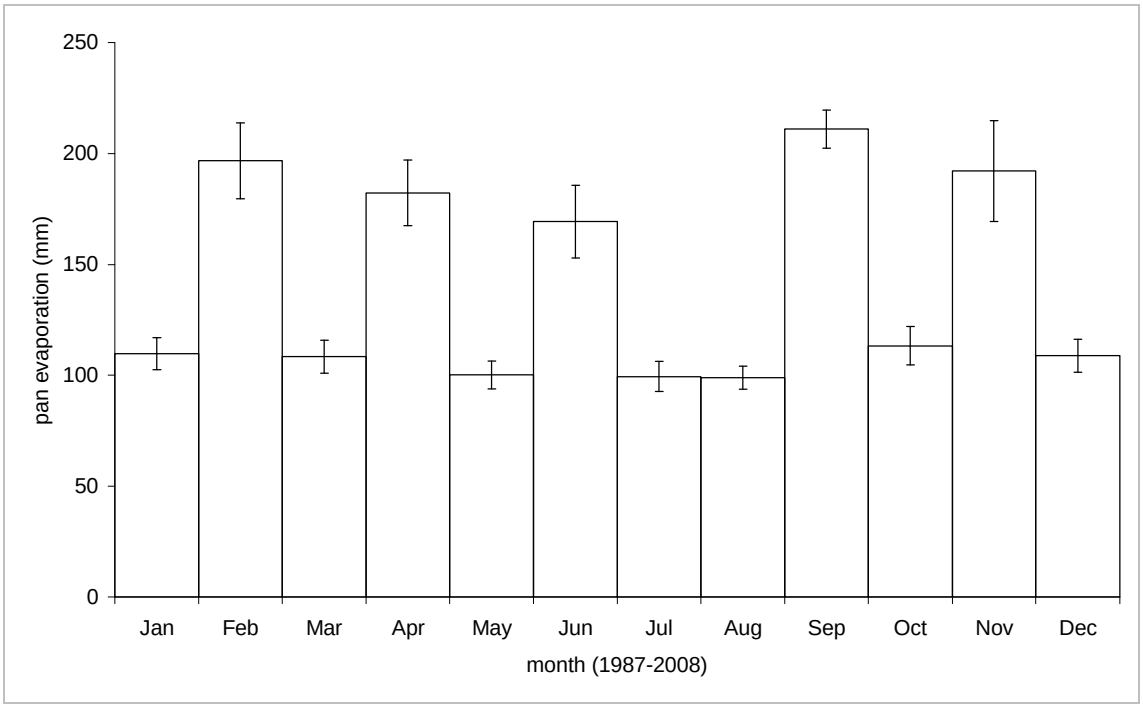

Figure 5.4 Mean monthly (1987-2008) pan evaporation with standard error bars on the shore of Lake Victoria at Entebbe.

Combined rainfall–groundwater monitoring stations were established in the Upper Nile Basin of Uganda by the Ministry of Water and Environment (Uganda) in 1998 (Fig. 5.2). Monitoring stations were installed into discrete aquifers that occur

within an unconsolidated weathered overburden (saprolite) and underlying fissured bedrock (saprock). Daily rainfall and groundwater levels are monitored and combined with lake-level monitoring of Lake Victoria at both Entebbe and Jinja and Lake Kyoga at Bugondo. The analysis of rainfall and groundwater-level records was considered for 10 piezometers (Apac, Bombo, Entebbe, Hoima, Loro, Pallisa, Nkokonjero, Nkozi, Rakai and Soroti) but 6 of these were excluded from further analysis due to excessive gaps in their records. Three rainfall-groundwater (Nkokonjero, Apac, Pallisa) and 1 rainfall-groundwater-surface water station (Entebbe) with complete records were compared with recently constructed stations at Bugondo and Jinja. Comparisons between hydrological observations are aided by the fact that all piezometers occur within a surface of low relief (Taylor and Howard, 1998) and feature similar soil conditions (i.e. ferallitic sandy loam) (Uganda Government, 1967) and land cover (i.e. bushland and grassland) (Drichi, 2003). Details of each monitoring well are summarised in Table 5.2. The surface slope for each piezometer and 8 surrounding (90-m) grid cells were determined from the Shuttle Radar Topography Mission (SRTM) digital terrain model data downloaded in April 2009 (SRTM, 2009). Daily groundwater and surface water level measurements were recorded using a float and chart recorder except for recently constructed groundwater - lake stage monitoring stations (Bugondo and Jinja) which employ absolute (non-vented) groundwater pressure transducers. Daily rainfall was recorded using a British standard 5-inch diameter rain gauge at each combined rainfall-groundwater monitoring station and meteorological stations.

Table 5.2 Local drainage, aquifer conditions, slope (mean and standard deviation in parentheses) and depth of analysed groundwater-surface water level monitoring stations as well as regional groundwater monitoring stations in the Upper Nile Basin.

piezometer	catchment	aquifer	local slope (°)	depth (mbgl)
Bugondo (BP01)	L. Kyoga	saprolite	1.7 (1.2)	13.6
Bugondo (BP02)	L. Kyoga	saprolite	1.9 (1.2)	17.0
Bugondo (BP04)	L. Kyoga	saprolite	2.0 (0.9)	13.2
Jinja (JP01)	L. Victoria	saprolite	0.4 (0.7)	12.0
Jinja (JP02)	L. Victoria	saprolite	0.7 (1.0)	21.0
Jinja (JP03)	L. Victoria	saprolite	2.2 (1.2)	24.0
Entebbe	L. Victoria	saprolite	3.6 (0.8)	48.0
Nkokonjero	L. Victoria	saprock	4.6 (1.3)	48.0
Apac	R. Victoria Nile	saprolite	1.4 (0.7)	15.0
Pallisa	L. Kyoga	saprock	1.0 (0.4)	61.0

5.3 Results

5.3.1 Rainfall intensity thresholds

The threshold to define "heavy rainfall" is supported by sensitivity analyses in which this threshold is varied from 5 to 25 mm·d^{-1} in increments of 1 mm·d^{-1} (Table 5.3). Each rainfall threshold was regressed with the corresponding water level rise for all the recharge events to obtain a co-efficient of determination (Figs. 5.5 - 5.8). Highest co-efficients of determination relating total precipitation to recharge which reduce with the heavy rainfall events at recent piezometers, are evident at JP01 (R^2 = 0.65), BP02 (R^2 = 0.95) and BP04 (R^2 = 0.99). For JP02, there is generally a low relationship (maximum of R^2 = 0.02 for a threshold of 12 mm·d^{-1}) between the rainfall and recharge, which is attributed to the manual groundwater-level measurements which were less reliable and frequent than those derived from the pressure transducers in the rest of the piezometers. It is only for BP01 where the highest co-efficient of determination improves with the heavy rainfall events (R^2 = 0.92) at a threshold of 13 mm·d^{-1}. There are only two significant recharge events for JP03 which has no logical statistical relationship. The number (2-6) of events considered for these recent (BP01, BP02,

BP04, JP01, JP02 and JP03) piezometers is limited and influences the analysis of rainfall-recharge relationships.

The long-term monitoring stations show that highest co-efficients of determination relating heavy rainfall to recharge are realised with a threshold of 10 $mm \cdot d^{-1}$ for Apac and Entebbe. Marginal improvements in the correlation for Pallisa (R^2 = 0.72) are achieved by employing thresholds of 15 $mm \cdot d^{-1}$ (R^2 = 0.74) to 20 $mm \cdot d^{-1}$ (R^2 = 0.75). At Nkokonjero the co-efficients of determination is not computed because no consistent, significant rainfall lag time precedes recharge responses. Mean lag times indicate average linear (response) velocities through unsaturated saprolite at each piezometer of between 0.1 and 1.2 $m \cdot d^{-1}$.

Table 5.3 Sensitivity analyses using the coefficients of determination (R^2) to define the threshold of the sum of the heavy rainfall events.

R^2	BP01	BP02	BP04	JP01	DWRM	Apac	Pallisa
ΣP	0.48	**0.95**	*0.99*	0.65	**0.74**	**0.73**	0.54
$\Sigma(P\text{-}5)$	0.65	*0.90*	0.99	0.58	**0.85**	**0.79**	*0.67*
$\Sigma(P\text{-}6)$	**0.70**	*0.90*	0.97	0.57	**0.86**	**0.79**	*0.68*
$\Sigma(P\text{-}7)$	**0.75**	*0.89*	0.96	0.56	**0.86**	**0.79**	*0.69*
$\Sigma(P\text{-}8)$	**0.79**	*0.88*	0.95	0.56	**0.87**	**0.80**	*0.70*
$\Sigma(P\text{-}9)$	**0.83**	*0.87*	0.92	0.57	**0.87**	**0.80**	*0.71*
$\Sigma(P\text{-}10)$	**0.87**	*0.85*	0.90	0.57	**0.87**	**0.80**	*0.72*
$\Sigma(P\text{-}11)$	**0.90**	*0.84*	0.86	0.57	**0.87**	**0.72**	*0.73*
$\Sigma(P\text{-}12)$	**0.92**	*0.84*	0.82	0.57	**0.87**	**0.73**	*0.74*
$\Sigma(P\text{-}13)$	**0.92**	*0.83*	0.79	0.57	**0.86**	**0.73**	*0.74*
$\Sigma(P\text{-}14)$	**0.91**	*0.82*	0.76	0.57	**0.86**	**0.73**	*0.74*
$\Sigma(P\text{-}15)$	**0.91**	*0.80*	0.72	0.56	**0.86**	**0.80**	*0.74*
$\Sigma(P\text{-}16)$	**0.91**	*0.79*	0.68	0.56	**0.85**	**0.73**	*0.74*
$\Sigma(P\text{-}17)$	**0.90**	*0.78*		0.56	**0.84**	**0.73**	*0.75*
$\Sigma(P\text{-}18)$	**0.89**	*0.77*		0.56	**0.83**	**0.74**	*0.75*
$\Sigma(P\text{-}19)$	**0.87**	0.75		0.57	**0.82**	**0.74**	*0.75*
$\Sigma(P\text{-}20)$	**0.84**	0.73		0.58	**0.81**	**0.80**	*0.75*
$\Sigma(P\text{-}21)$	**0.80**	0.70		0.58	**0.80**	**0.73**	*0.75*
$\Sigma(P\text{-}25)$	0.58	0.55		0.52	**0.75**	**0.72**	*0.74*

Bold: Correlation significant at the 0.01 level (2-tailed); Italics: Correlation is significant at the 0.05 level (2-tailed); Normal: Correlation significant at the 0.1 level (2-tailed).

5.3.2 Groundwater - surface water variations and recharge at Entebbe

Average daily groundwater and surface-water level observations from January 1999 to June 2009 in response to daily rainfall for Lake Victoria at Entebbe are presented in figure 5.5. Bimodal distributions of annual groundwater-level fluctuations followed closely but less dynamically by the Lake Victoria levels in many years and arise from MAM and SON rains (Basalirwa, 1995). There is a gap in observations of rainfall at Entebbe in 2002. During this period, regional station rainfall data indicate that annual rainfall exceeded the long-term mean. The bimodal annual distribution in rainfall produces seasonal recharge with the first rains commonly generating greater recharge. Significant (95 % level) cross correlations are observed between rainfall and groundwater levels at Entebbe.

The annual recharge pattern is severely disrupted in 2004 - 2005. A sharp decline in the groundwater level coincides with a steady drop in the level of Lake Victoria that began in late 2003. From July 2003 to July 2004, the level of the lake and groundwater at Entebbe fall by an average of 0.5 m and 1.9 m respectively due, in part, to anomalously low rainfall in early 2004, but also due to excessive dam releases (Figs. 4.22 and 4.23). A slight stabilisation in the lake level in early 2005 is accompanied by sudden drop in the adjacent groundwater level reversing the *i* between the lake and groundwater for a period of 5 months. Despite a continued decline in the level of Lake Victoria until late 2006, the groundwater level recovers in late 2005 in response to the hitherto seasonal pattern of recharge which resumes from 2006, and the stabilisation of dam releases (Figs. 4.22 and 4.23). Since early 2007, the lake levels have also stabilised in response to a steadier regulated outflow regime which, however, resulted in a decline in the levels of Lake Kyoga (Fig. 5.6). These observational data highlight not only the strong influence exerted by rainfall on the seasonality of the groundwater levels but also

dam releases on groundwater - surface water interactions. Substantial lag times (up to several days) in the influence of lake-level changes on groundwater levels may arise from the low lakebed conductance between groundwater and Lake Victoria at Entebbe (Fig. 3.30).

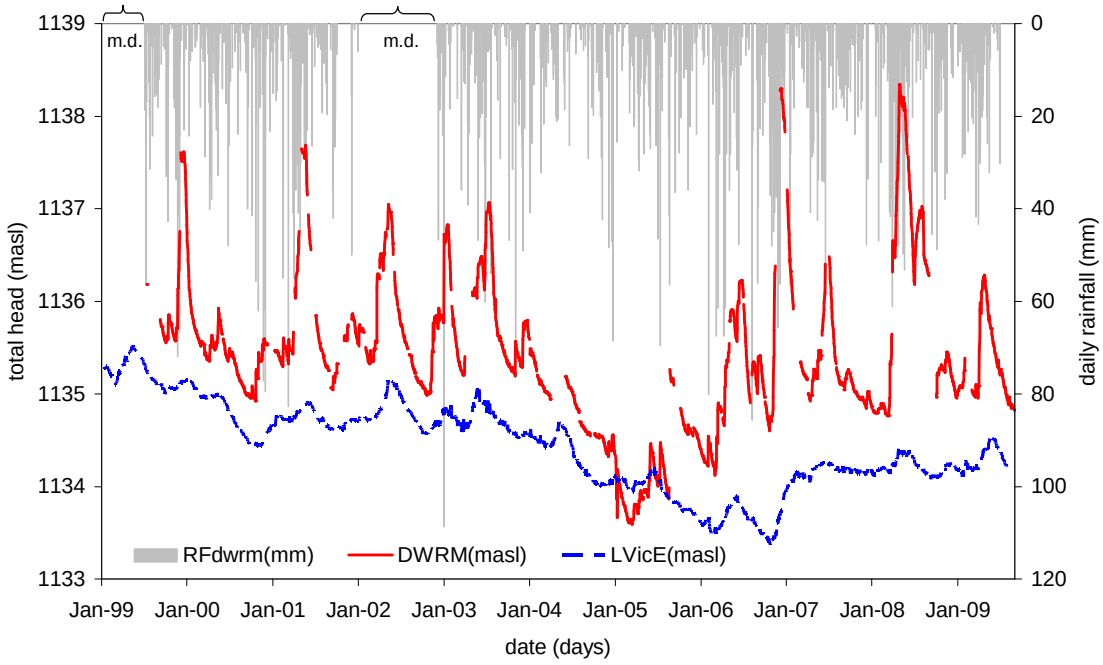

Figure 5.5 Daily rainfall and average daily groundwater and Lake Victoria level variations at Entebbe station from January 1999 to July 2009. m.d. is missing rainfall data.

5.3.3 Groundwater - surface water variations and recharge at Bugondo

Average daily groundwater and surface water level observations from December 2007 to June 2009 in response to daily rainfall in the Lake Kyoga catchment at Bugondo are depicted in figure 5.6. Groundwater-level observations (BP01, BP02 and BP04) were lost between February and July 2008 as a result of the pressure transducer malfunctions. This period coincided with the first rainy period when lake levels stabilise from the short steady decline of the late 2007 (Fig. 4.25). Asymmetry in the response of water tables to bimodal precipitation in the Upper Nile Basin stations has previously

been observed and attributed to lower soil-moisture deficits that develop during the shorter dry season from June to July and greater intensity of the short (SON) rains in the Lake Kyoga catchment (Taylor and Howard, 1996; Taylor and Howard, 1999b). On an annual basis, the second rains induce the largest response in both groundwater and lake levels. Rapid (order of a few days) and short-lived responses to specific heavy rainfall events are evident for the piezometer (BP01) closest to the lake which controls drainage base level to cause flooding. Groundwater levels follow sharp declines in lake levels in early 2008 and 2009. The drop in lake levels stems from variable dam releases (Fig. 4.25). During the dry season (November-February) of 2007-2008, the *i* between piezometer BP01 and Lake Kyoga reverses due to large variable dam releases which raised the drainage (lake) base level as groundwater levels receded. The drainage base (lake) level is 30-50 cm lower in 2009 than in 2008, which is largely a response to the stabilisation of the regulated Lake Victoria outflow (Fig. 4.25). Variable Victoria Nile outflow, also mostly explains why the *i* forms several clusters corresponding to different data collection periods when correlated with the lake or groundwater levels (Fig. 4.17).

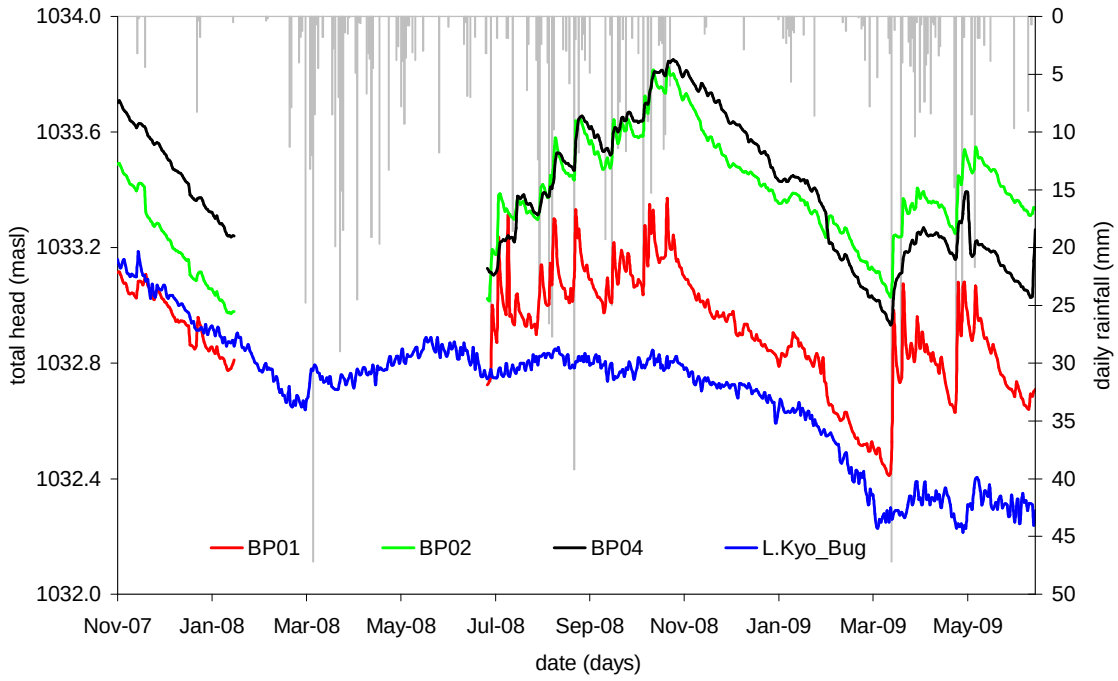

Figure 5.6 Daily rainfall and average daily groundwater and Lake Kyoga level variations at Bugondo station from November 2007 to July 2009.

5.3.4 Groundwater - surface water variations and recharge at Jinja

Average daily groundwater and surface water level observations from November 2007 to June 2009 are plotted alongside daily rainfall in the Lake Victoria catchment at Jinja is illustrated in figure 5.7. Two main groundwater recharge regimes which are closely followed by the lake levels occur in response to the bimodal rainfall distribution, although the larger differences in total hydraulic head result in less pronounced variations. Similar to Entebbe, greater recharge is again realised from the long (MAM) rains which, on this northern shore of Lake Victoria, are typically greater in magnitude than the short (SON) rains. Observed correspondence in the magnitude of groundwater-level fluctuations arises from not only comparable recharge fluxes but also suggest similar aquifer storage properties. The drainage base (lake) level is stable without any discernable trend between November 2007 and June 2009. The record of piezometer JP01, adjacent to the lake, is influenced the most by the lake-level variations and,

similar to Bugondo, shows rapid (order of a few days) and short-lived responses to specific heavy rainfall events. Both piezometers JP01 and JP02 respond fastest (1-2 days) to the rainfall inputs. On the other hand, piezometer JP03 whose static water level rests much deeper (about 12 mbgl) within the saprolite takes several days for the recharge pulse to be realised. Whereas the recharge responses in piezometers JP01 and JP02 appear to be influenced by the base level of lake, the furthest piezometer (JP03) shows gentle hydrograph rise and recession characteristic of a fairly thick, extensive saprolite system unaffected by a constant-head boundary. Lake level variations are up to 0.5 m, whereas the groundwater levels range by about 1 m since December 2007.

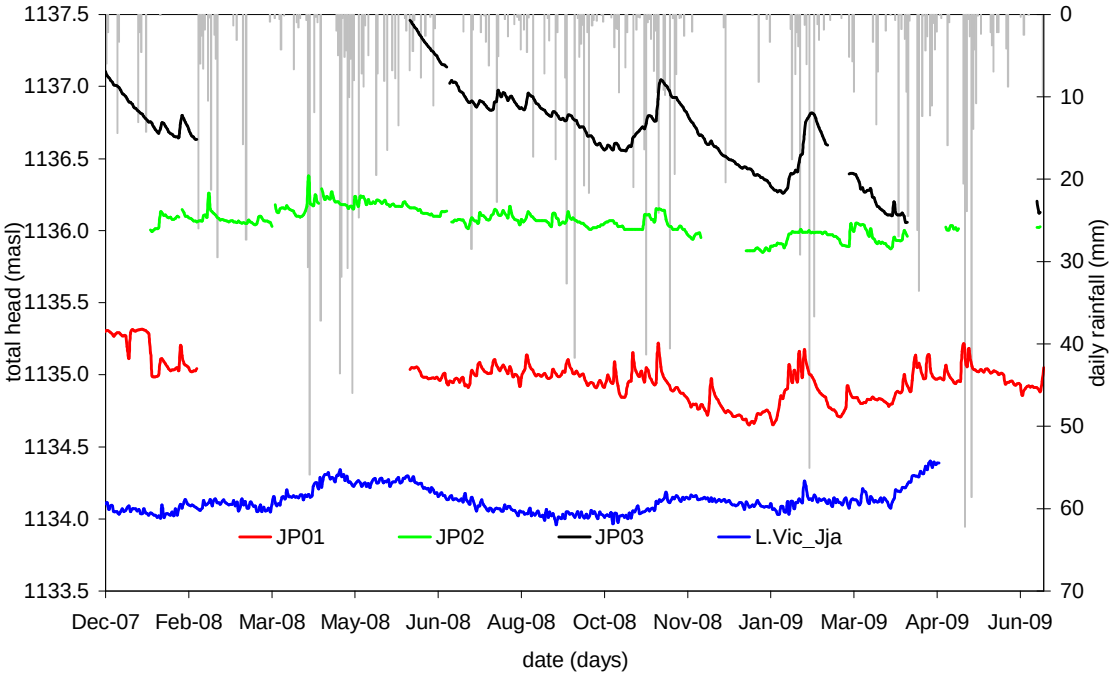

Figure 5.7 Daily rainfall and average daily groundwater and Lake Victoria level variations at Jinja station from December 2007 to July 2009.

5.3.5 Groundwater - surface water variations and recharge remote from surface waters

Average groundwater level observations from January 1999 to December 2008 at Nkokonjero on the northern shore of Lake Victoria are compared with Apac and Pallisa piezometers that are situated in the northern catchments of the Upper Nile Basin in figure 5.8 (Fig. 5.2). Bimodal recharge pulses are asymmetric with larger responses during the second (SON) rainfall inputs. Similar to Bugondo (section 5.3.3), asymmetry is attributed to lower soil moisture deficits that develop during the second dry season. In northern Uganda, the main recharge season lag the SON rains, which is characterised by piezometers of Apac and Pallisa. Nkokonjero piezometer alternatively, has consistent bimodal distributions of annual groundwater-level fluctuations with larger responses commonly during the first rainy season (MAM). At Nkokonjero, the trends in Lake Victoria variations (about 2 m) since 1998 including the decline starting from late 2003, are closely followed by the groundwater levels which exhibit larger (nearly 4 m) responses. Groundwater levels in Nkokonjero, similar to Entebbe, rise in advance of the partial rebound in lake levels from late 2006. Over a similar period, groundwater levels remote from surface waters are either stable (nearly 2 m range) at Apac or even show a rising trend (>4 m range) at Pallisa. Pallisa additionally, responds very strongly to the heavy (MAM) rains of 2003. Observed differences in the magnitude of groundwater-level fluctuations arise from not only different recharge fluxes but also spatial variations in aquifer storage properties. Apac piezometer is installed within saprolite with higher matrix storage properties than both Nkokonjero and Pallisa piezometers which monitor the saprock aquifer with low storage properties associated with fractured media. The temporal association between changes in lake levels and groundwater levels at

Nkokonjero reflects the interaction between groundwater and the lakes which is also manifest at Entebbe, Jinja and Bugondo.

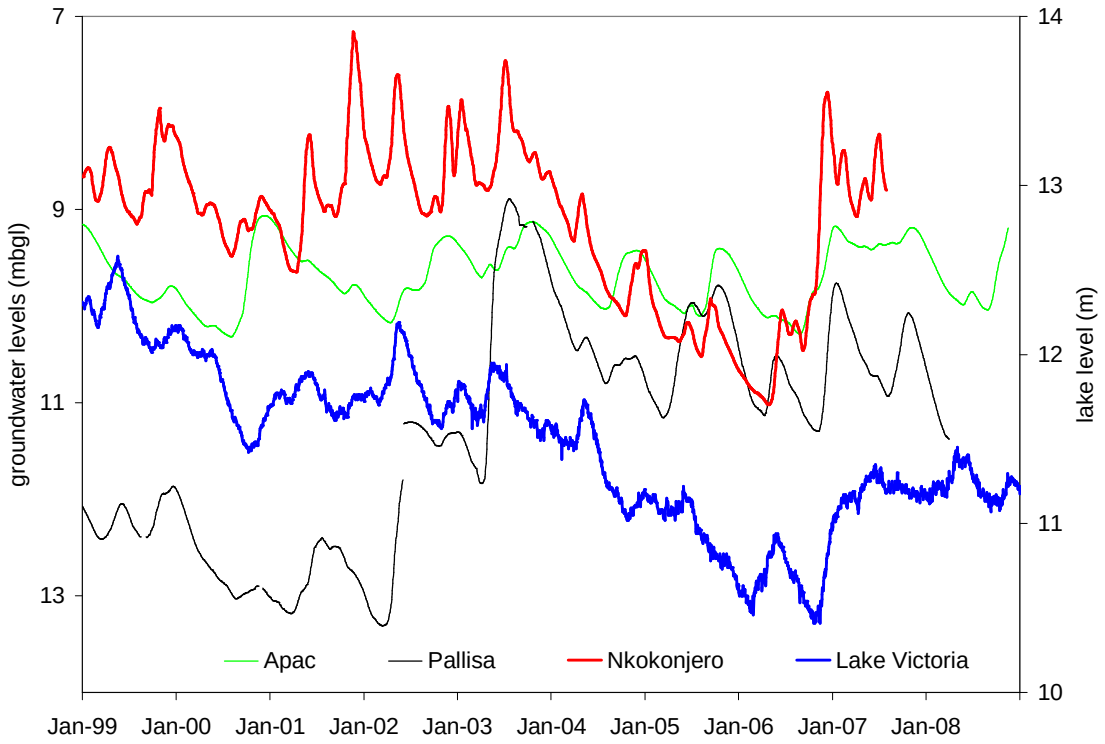

Figure 5.8 Average daily groundwater level variations on the shore of Lake Victoria at Nkokonjero compared with the regional groundwater levels at Apac and Pallisa piezometers from 1999 to 2009.

5.3.6 Regional water storage variations

Lake and groundwater observations together with modelled soil moisture data are compared to assess how well they compare with regional water storage variations indicated by satellite data. Changes in the Earth's gravitational field reflect changes in mass at the Earth's surface. Monthly gravity anomalies observed by satellites under GRACE (Gravity Recovery and Climate Experiment) can be transformed into estimates of vertically integrated water storage with a spatial resolution of at least a few hundred km (Tapley *et al.*, 2004; Wahr *et al.*, 2004; Rodell *et al.*, 2006; Winsemius *et al.*, 2006; Yeh *et al.*, 2006). GRACE datasets reflect variations in terrestrial water storage which

include groundwater, soil moisture, snow and ice, vegetative water and surface water. It therefore produces an estimate of the net change in total terrestrial water storage. For example, Rodell *et al.* (2009) use GRACE data from 2002-2008 to estimate groundwater depletion due to withdrawal in India. Processed GRACE data by Chambers (2006) based on Wahr *et al.* (1998), were downloaded (16 April 2009) from the NASA Jet Propulsion Laboratories of California Institute of Technology website [3]. The mean half-width of the equivalent Gaussian smoothened over 300 km for the three centres (GRACE_300) is processed as equivalent water thickness normalised with respect to monthly means from January 2003 to December 2007. A central grid node in the Upper Nile Basin of Uganda (33.5^{o}E, 0.5^{o}N) is around which the regional water storage estimates are derived. Monthly datasets range from August 2002 through December 2008 with a few missing monthly gaps.

The soil horizon plays a vital role in regional water storage variations by partly storing infiltrating meteoric water that recharges groundwater. Monthly gridded (1^{o}) data were obtained from the average of 4 regional soil moisture models based on observational and satellite data from January 2002 to December 2008 (Rodell *et al.*, 2004). Soil moisture (kg·m^{2}) is summed up for soil layers of up to 3.4 m depth over the region (longitude 30.5-35.5^{o}E and latitude 3.5^{o}S-2.5^{o}N). Data is converted to depth (m) assuming a water density of 1,000 kg·m^{3}, and normalised with respect to monthly means from January 2003 to December 2007.

A direct comparison is made with the average of 10 regional long-term piezometers (Fig. 5.2) of groundwater level variations due to uncertainty in storage co-efficients for saprolite and saprock (Fig. 5.9). Groundwater level anomaly is determined as a difference of the water level from the mean of the monthly measurements from January 2003 to December 2007. Strong relationships are observed between the total

[3] http://grace.jpl.nasa.gov/data/mass/

water storage anomalies and hydrographs for soil moisture (R^2 = 0.69), groundwater (R^2 = 0.57) and Lake Victoria (R^2 = 0.52) levels which suggests that the level of Lake Victoria influences groundwater storage in small catchments along its northern boundary. A general decline in regional water storage is observed from Aug 2002 to about Dec 2006, a feature that has been largely attributed to anomalously low rainfall in the region. Regional water storage falls by about 0.3 m whereas the groundwater levels drop by nearly 1.5 m before rebounding from late 2006. Swenson and Wahr (2009) use GRACE data to estimate a decline in regional water storage of ~60 $mm \cdot a^{-1}$ in East Africa between 2003 and 2008. Seasonality is also apparent where the observations follow regional rainfall patterns (March-May and September-November). A steady decline (2002-2006) in water storage in both lake levels and lakeshore groundwater is attributed to both excessive dam releases at Jinja exceeding the Agreed Curve (Figs. 4.24 and 4.26), and anomalously low rainfall (Fig. 5.3). These data support the analyses of Kull (2006), Sutcliffe and Peterson (2007), and Swenson and Wahr (2009) who indicate that drought and dam releases played nearly equal roles in Lake Victoria's decline.

It is apparent from the strong seasonal trends and similar interannual variability that lake water, soil moisture and groundwater storage all play significant integral roles in regional water storage variations. Interacting waters between groundwater and the lakes are therefore likely to be directly influenced by variations in antecedent soil moisture conditions.

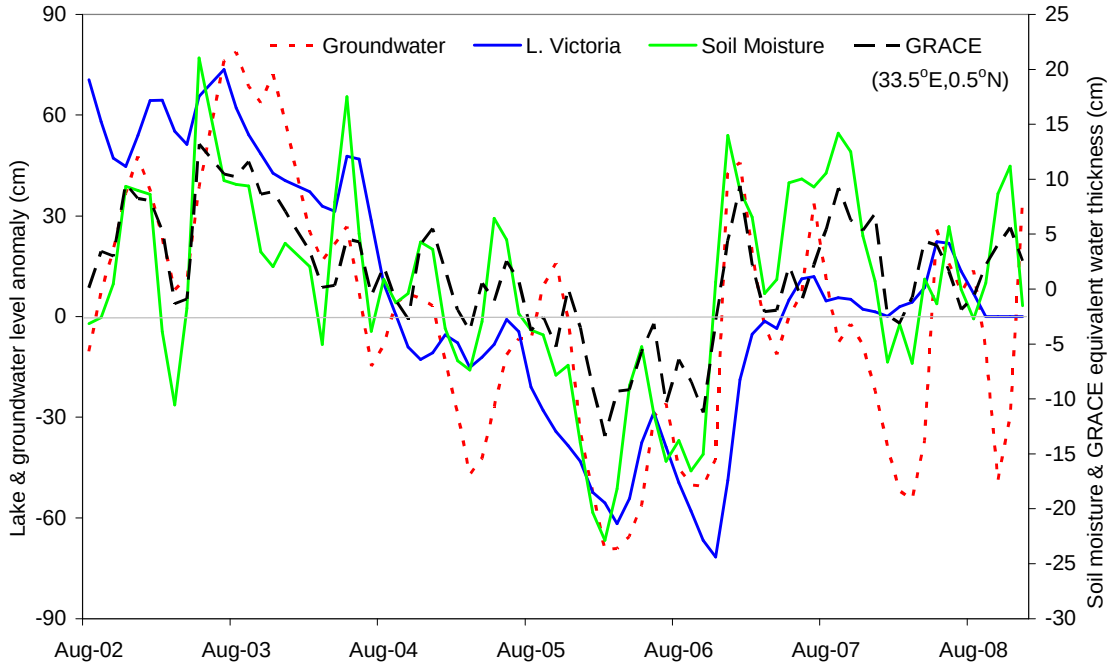

Figure 5.9 Average daily groundwater-level observations over the period 1999 to 2008 from 10 stations in the Upper Nile Basin together with changes in the level of Lake Victoria at Entebbe, soil moisture (from Rodell *et al.*, 2004) and regional water storage, as an 'equivalent water thickness' indicated by gravity anomalies (GRACE), normalised with respect to monthly means from 2003 to 2007 with Gaussian filter destripped over 300 km (from Chambers, 2006).

5.3.7 Influence of rainfall intensity on the groundwater – surface water hydraulic gradient

Recently constructed groundwater - surface water monitoring stations show mean lag times in days of 1 at BP01, 3 at BP02, 2 at BP04, 1 at JP01, 1 at JP02, and 3 at JP03 that are determined from significant (95 % level) cross correlations between rainfall and groundwater levels (Table 5.4). Of the long-term monitoring stations adjacent to the lakes, mean lag times of 5 and 26 days were derived from significant (95 % level) cross correlations for the long-term stations at Entebbe and Nkokonjero, respectively. Whereas the significant lag times at the rest of the piezometers are well constrained, Nkokonjero piezometer has anomalously variable significant lag times from 0 to 57 days which is suggested to be related to variations in intensity of rains, evaporation, antecedent soil moisture conditions and soil-infiltration capacities.

Temporal variations in groundwater levels at the Nkokonjero piezometer follow the level of Lake Victoria (Fig. 5.8) indicating that the groundwater level is largely controlled by drainage base (lake) level changes. Thus, except for Nkokonjero piezometer with inconsistent significant (95 % level) lag times, the rest of the long-term stations are considered to have consistent mean significant lag times. Since Nkokonjero piezometer does not have a consistent range of lag times (Table 5.4), it has been excluded from the regression with the rainfall. Mean significant (95 % level) lag times of 13 and 11 days derived from cross correlations for the regional long-term stations were detected at Apac and Pallisa, respectively. Furthermore, the long-term monitoring stations have several (5-9), extended (over several months) events compared to recent stations with less (2-6) and brief (over several days) recharge events. Generally, groundwater - surface water monitoring stations show near-instantaneous lag times compared to interfluve monitoring stations derived from significant (95 % level) cross correlations between rainfall and groundwater levels. These short-lived groundwater level responses to rainfall reflect a dynamic transmissive interface with lakes.

Table 5.4 Summary statistics of the results of the significant lag times of station daily rainfall inducing specific groundwater recharge events.

Region	**piezometer**	**range lag** (days)	**mean lag** (days)	**number** (events)
Bugondo	BP01	1	1	6
Bugondo	BP02	1 - 9	3	5
Bugondo	BP04	2	2	3
Jinja	JP01	0 - 2	1	6
Jinja	JP02	0 - 3	1	6
Jinja	JP03	1 - 4	3	2
Entebbe	DWRM	0 - 12	5	8
Nkokonjero	Nkokonjero	0 - 57	26	5
Apac	Apac	0 - 19	13	9
Pallisa	Pallisa	4 - 16	11	7

Figures 5.10 and 5.11 and Table 5.5 summarise the results of a linear regression of observed recharge against both ΣP_i and $\Sigma(P_i\text{-}10)$ for all monitoring stations. Gaps of up to a month or more in daily rainfall records limit the number of recharge events considered in the analyses and thereby constrain the robustness of statistical relationships. For piezometers BP01 and BP04 in Bugondo, the magnitude of recharge is more strongly correlated to $\Sigma(P_i\text{-}10)$ than ΣP_i (Figs. 5.10a and c); BP02 has a strong relationship with both $\Sigma(P_i\text{-}10)$ and ΣP_i (Fig. 5.10b). Groundwater levels in Bugondo respond strongly to both the local heavy rainfall events as well as regional drainage base (lake) level variations. Conversely, there is no clear relationship with both ΣP_i and $\Sigma(P_i\text{-}10)$ and recharge at the Jinja piezometers. Apart from JP01 which is statistically significant with both $\Sigma(P_i\text{-}10)$ and ΣP_i (Fig. 5.7d), JP02 is not statistically significant (Fig. 5.7e), just as JP03 does not have enough data points for a statistical correlation (Fig. 5.7f). This is attributed, in part, to the noted influence on groundwater levels of the lake level which is controlled by a regional, rather than local climatology and the operation of the dams at Jinja.

Linear regression results of the long-term monitoring stations are shown in figure 5.11 and Table 5.5. At Entebbe, the magnitude of recharge is more strongly correlated to $\Sigma(P_i\text{-}10)$ than ΣP_i (Fig. 5.11a). These data demonstrate the strong dependence upon rainfall of the groundwater levels (Fig. 5.2), despite the proximity of observations to Lake Victoria, that respond more strongly to the heavy rainfall events than to the drainage base (lake) levels (Fig. 4.8). The stronger correlation to $\Sigma(P_i\text{-}10)$ than ΣP_i relationship is also observed at Apac and Pallisa where piezometers are remote from surface waters (Figs. 5.11b and c). Improved coefficients of determination (R^2) for the correlation of recharge and $\Sigma(P_i\text{-}10)$, relative to ΣP_i, are also associated with a lower root mean square error (rmse) between the regression model and observations. The relationship between heavy rainfall and recharge events has also been observed from

high-frequency monitoring of shallow groundwater quality in Kampala (Fig. 5.2) where episodic deterioration in bacteriological water quality is associated with recharge from heavy rainfall events (Taylor *et al.*, 2009a).

Quantitative inferences can also be drawn from observed long-term correlations between rainfall and recharge (Fig. 5.11). Differences in slope, evident from differences in axis scales in figure 5.11, primarily reflect variations in the storage properties of the monitored aquifer as recharge environments (e.g. land cover, relief, soil type) at each station are similar. The lower slope of the correlation between water-level rise (observed recharge) and $\Sigma(P_i\text{-}10)$ at Apac reflects a higher storage coefficient for the saprolite aquifer (Taylor *et al.*, 2009b) compared to the saprock and saprolite/saprock aquifers (Howard and Karundu, 1992) monitored in Pallisa and Entebbe, respectively. The regression of observed recharge and sum of total rainfall (dashed lines) to positive intercepts (158 to 189 mm) on the x (rainfall) axis (Figs. 5.11a, b and c) supports previous assertions (Eilers *et al.*, 2007) that rainfall exceeding 200 mm in a given year is required for recharge to occur in tropical Africa.

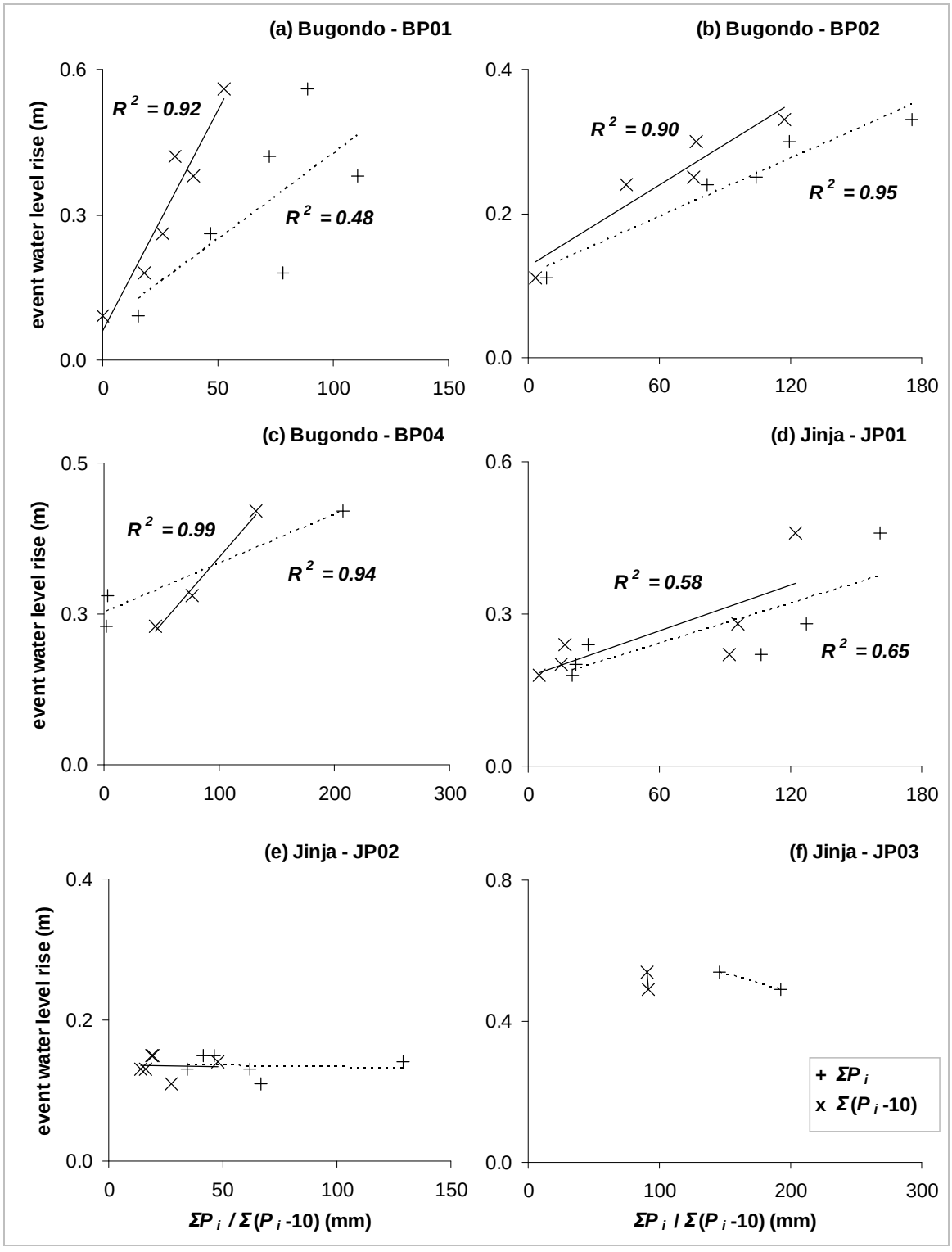

Figure 5.10 Scatter plots of the relationship between observed recharge events and both daily rainfall (ΣP_i), and daily rainfall exceeding 10 mm·d^{-1} ($\Sigma(P_i$-10)) at (a) BP01, (b) BP02, (c) BP04, (d) JP01, (e) JP02, and (f) JP03 recent piezometers in the Upper Nile Basin. Dashed and solid lines represent the linear regression between observed recharge events and both ΣP_i and $\Sigma(P_i$-10), respectively.

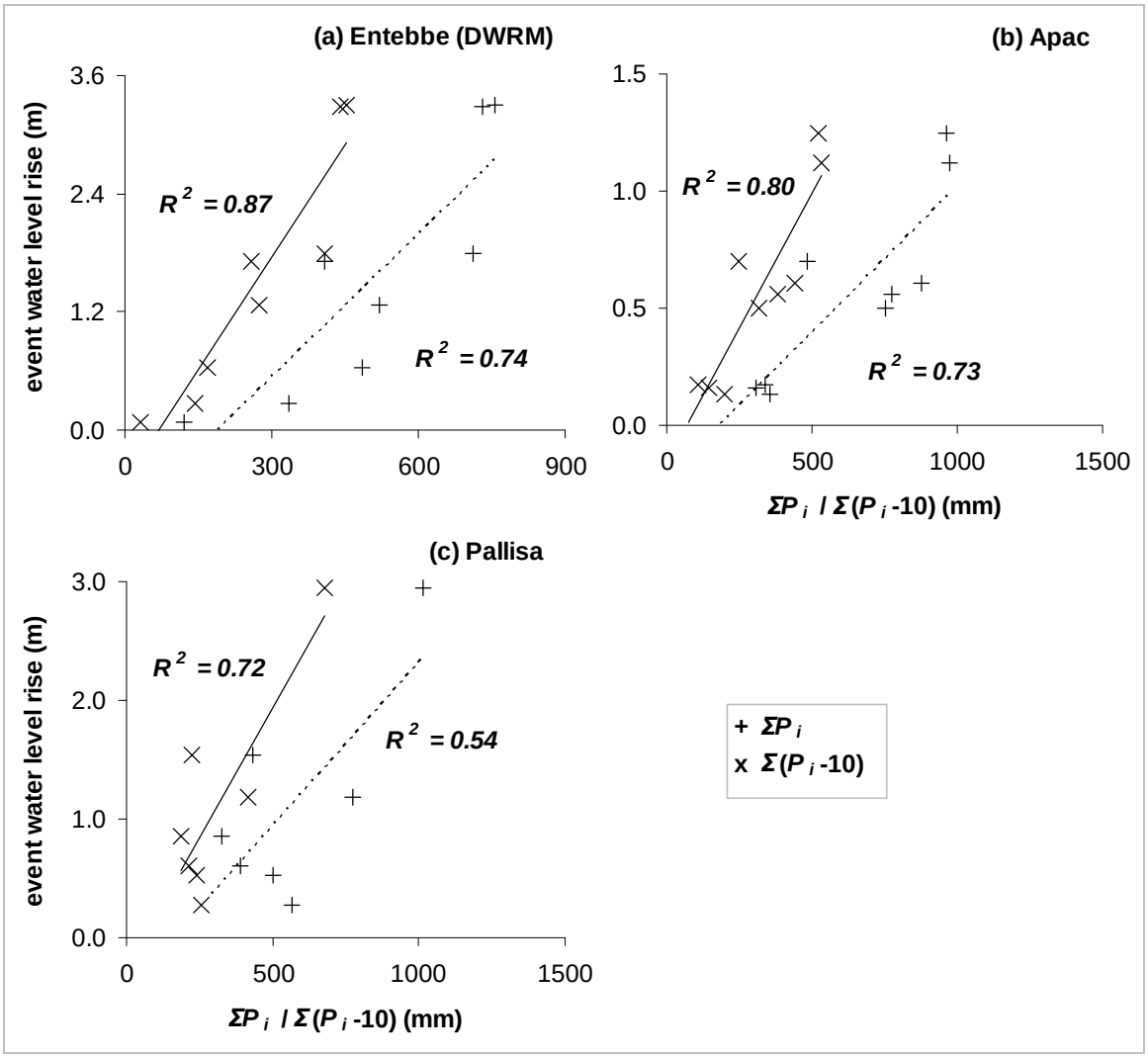

Figure 5.11 Scatter plots of the relationship between observed recharge events and both daily rainfall (ΣP_i), and daily rainfall exceeding 10 mm·d^{-1} ($\Sigma(P_i$-10)) at (a) Entebbe, (b) Apac, and (c) Pallisa long-term monitoring stations in the Upper Nile Basin. Dashed and solid lines represent the linear regression between observed recharge events and both ΣP_i and $\Sigma(P_i$-10), respectively.

Table 5.5 Summary of results of the linear regression of the observed station recharge and both total rainfall depth (ΣP_i) and rainfall depth of events exceeding 10 mm·d^{-1} ($\Sigma(P_i$-10)). rmse represents the root mean square error.

Region	piezometer	number	ΣP_i		$\Sigma(P_i$-10)	
		(events)	R^2	rmse (m)	R^2	rmse (m)
Bugondo	BP01	6	0.48	0.08	0.92	0.66
Bugondo	BP02	5	0.95	0.00	0.90	0.33
Bugondo	BP04	3	0.94	0.00	0.99	0.30
Jinja	JP01	6	0.65	0.02	0.58	0.43
Jinja	JP02	6	0.01	0.00	0.001	0.11
Entebbe	Entebbe	8	0.74	0.60	0.87	0.42
Apac	Apac	9	0.73	0.20	0.80	0.17
Pallisa	Pallisa	7	0.54	0.54	0.72	0.44

5.3.8 Influence of rainfall intensity on recharge

The limited duration of observations constrains the robustness of observed relationships between rainfall and recharge but the results from the analysis of these observational datasets are consistent with recent modelling work (Mileham *et al.*, 2009) highlighting the importance of explicitly considering changing rainfall intensities in the assessment of climate change impacts on groundwater recharge. Results suggest, contrary to previous assertions (Döll and Florke, 2005), that a shift to more intensive rainfall may promote rather than restrict groundwater recharge. Substantial uncertainty remains, however, as to whether potential rises in recharge will be offset by increased evapotranspiration associated with warmer atmospheres. Further research that includes enhanced field monitoring is clearly required to refine the understanding of the terrestrial hydrological response to changing rainfall intensities and to inform the simulation of groundwater recharge in the tropics where increases in rainfall intensities are expected to be especially pronounced.

5.4 Summary

Groundwater levels in monitoring stations proximate to the lakes rise and fall rapidly in response to rainfall. These short-lived responses reflect a dynamic transmissive interface. Rainfall has strong influence on the seasonality of the groundwater levels and the *i* between groundwater and the lakes are largely determined by local recharge events. Groundwater fluxes into Lakes Victoria and Kyoga are further modified by the *i* in response to changing drainage base (lake) levels. The latter control on the interaction between groundwater and the lakes is, heavily determined by a regional, rather than local, climatology and the operation of the dams at Jinja. It is also

apparent from similar seasonality and interannual variability in lake-water, soil moisture and groundwater storage that each of the components contribute to regional water storage variations.

Bimodal rainfall patterns induce seasonality in groundwater levels with the first (MAM) rains commonly generating greater recharge on the northern shore of Lake Victoria. Conversely, the second (SON) rains induce the largest response in groundwater levels on the shore of Lake Kyoga. Heavy (monsoonal) rainfall events (>10 $mm \cdot d^{-1}$) determine the magnitude and timing of recharge in areas remote from surface water. Analyses further indicate that rainfall exceeding 200 mm in a given year is required for recharge to occur in the Upper Nile Basin. Saprolite aquifers not directly influenced by lakes show that rainfall-fed recharge occurs with mean average linear vertical velocities ranging in the unsaturated zone from about 0.1 to 1.2 $m \cdot d^{-1}$. Results suggest, contrary to previous assertions (Döll and Florke, 2005), that a shift to more intensive rainfall may promote rather than restrict groundwater recharge. Substantial uncertainty remains, however, as to whether potential rises in recharge will be offset by increased evapotranspiration associated with warmer atmospheres.

Chapter 6
Estimating groundwater discharges to Lake Victoria: A thought experiment

6.1 Introduction

In this chapter, the results from site investigations of groundwater fluxes into Lake Victoria are extrapolated around the lake's entire circumference to derive a very rough, first approximation of the contribution of groundwater to the lake-water balance. This is expected to provide regional-scale estimate of groundwater contributions from the onshore catchments to Lake Victoria. As pointed out in chapter 1, the role of groundwater in maintaining lake and wetland water levels during periods of low or absent rainfall on the African plateau is unknown. Most water balance studies of Lake Victoria and Lake Kyoga have, to date, either ignored the contribution of groundwater or assumed it was negligible. Shahin (1985) for example, presumes that groundwater contribution to lakes in the Nile Basin is less than 0.2 % of the total mean annual runoff to them. Determination of groundwater inflow to lakes by direct hydrogeological methods permits a more precise indication of other water balance elements in addition to providing a quantitative assessment of groundwater discharge (Zekster, 1996).

6.2 Water balance studies in the Upper Nile Basin

The long-held view is that Lake Victoria receives more than 90 % of the water input from rainfall and generates 70-80 % of its own rainfall from evaporation and re-precipitation (Sene and Plinston, 1994). Sutcliffe and Peterson (2007) more explicitly indicate that the fractions of total lake inflows that derive from rainfall and river flow are 84 % and 16 %, respectively. Inter-annual variability of rainfall and river flow is 30

% and 10 %, respectively. There have been more than 20 studies of the water balance of Lake Victoria (Table 6.1). Mean fluxes from these studies carried out from 1900-2007 are for a mean lake area of 69,000 km^2 (67,000 – 69,000 km^2). Mean fluxes from all studies are 111 $km^3 \cdot a^{-1}$ (rainfall), 100 $km^3 \cdot a^{-1}$ (evaporation), 20 $km^3 \cdot a^{-1}$ (river inflow), and 30 $km^3 \cdot a^{-1}$ (river outflow) assuming no changes in lake storage over this period. River inflow includes both gauged tributaries and estimated ungauged inflows whereas river outflow constitutes the gauged discharge at the lake outlet in Jinja. Lake levels are considered to vary over similar ranges to the net basin supply which is defined as the net inflow arising from direct rainfall on the lake surface, the losses owing to lake evaporation and the tributary inflows into the lake (Sene, 1998). The net basin supply is 30 $km^3 \cdot a^{-1}$. The net basin supply is important because over the long term, it defines the limits of the amount of water that can be stored in or released from a lake.

Comparatively fewer water balance studies have been conducted for Lake Kyoga and are summarised in Table 6.2. Mean fluxes from 1948 to 2007 for a mean lake and wetland area of 4,540 km^2 (1,760 – 4,700 km^2) are 5 $km^3 \cdot a^{-1}$ (rainfall), 7 $km^3 \cdot a^{-1}$ (evaporation), 32 $km^3 \cdot a^{-1}$ (Victoria Nile inflow), 2 $km^3 \cdot a^{-1}$ (local river inflow), and 33 $km^3 \cdot a^{-1}$ (Victoria Nile outflow). The net basin supply is 32 $km^3 \cdot a^{-1}$ assuming no changes in lake storage over this period (Table 6.2). Lake Victoria is considered to have an excess of rainfall over evaporation; the surplus is offset by the greater river outflow of the Victoria Nile relative to river inflow. This surplus supplies Lake Kyoga downstream where it mostly flows through the lake. The lake deficit of rainfall over evaporation is largely made up by local river inflow. These mean fluxes explain, in part, why there is a comparable net basin supply for both Lakes Victoria and Kyoga. However, some of the water balance components (e.g. lake evaporation estimates for Lake Kyoga) are derived simply from estimates for Lake Victoria or estimated from the water balance assuming no changes in lake storage.

Table 6.1 Previous results of the Lake Victoria annual water balance estimates ($km^3 \cdot a^{-1}$) from 1900 to 2007.

Period	Lake Rainfall	Lake Evaporation	Inflows	Outflows	Net Basin Supply	Storage change	Source
1973	98	98	18	24	18	-6	Krishnamurty and Ibrahim (1973)
1970-1974	114	109	29	39	34	-5	Kite (1982)
1906-1932	79	77	19	21	21	0	Hurst and Phillips, 1938 (cited in Shahin, 1985)
1969	122	110	19	47	30	-17	WMO, 1974 (cited in Shahin, 1985)
1970	126	96	24	45	54	9	WMO, 1974 (Cited in Shahin, 1985)
1946-1970	117	101	19	29	34	5	WMO, 1974 (In Shahin, 1985)
1900-1970	108	101	19	24	26	2	Shahin (1985)
1956-1978	124	107	23	34	40	7	Piper *et al.* (1986)
1925-1990	115	107	20	31	28	-3	Sene and Plinston (1994)
-	98	93	16	21	21	0	Hurst, 1952 (cited in Yin and Nicholson, 1998)
-	79	78	16	21	17	-4	Merelieu, 1961 (cited in Yin and Nicholson, 1998)
1925-1959	112	105	18	21	25	4	de Baulny and Baker, 1970 (cited in Yin and Nicholson, 1998)
-	113	101	16	29	29	-1	WMO, 1974, 1981 (cited in Yin and Nicholson, 1998)
1945-1984	117	101	19	31	35	3	Flohn, 1983 (cited in Yin and Nicholson, 1998)
-	114	104	17	28	28	0	Hastenrath and Kutzbach, 1983 (cited in Yin and Nicholson, 1998)
1950-1979	114	101	-	35	-	-	Flohn and Burkhardt, 1985 (cited in Yin and Nicholson, 1998)
1956-1978	125	110	24	36	39	2	Howell et al., 1988 (cited in Yin and Nicholson, 1998)
-	100	95	18	23	23	0	Spigel and Colter, 1996 (cited in Yin and Nicholson, 1998)
-	102	97	17	22	22	0	Balek, 1997 (cited in Yin and Nicholson, 1998)
1956-1978	123	105	23	36	41	5	Yin and Nicholson (1998)
1956-1978	122	106	23	36	40	4	Nicholson *et al.* (2000)
1950-2004	114	105	25	33	34	1	LVBC (2006)
2003-2007	80	122	55	38	13	-26	Swenson and Wahr (2009)
average	**111**	**100**	**20**	**30**	**30**	**0**	

Generation of water balance estimates for Lake Victoria are based on a variable number of rain gauges (average of 8) and satellite data. Inflows from 17 rivers include both gauged rivers (Rivers Kagera, Nzoia, Yala, Sondu, Awach Kaboun, Mara, Nyando, Migori, Simiyu, Gurumeti and Sio) and ungauged catchment (Fig. 3.1). Evaporation is estimated from several methods, e.g. Penman method, evaporation pans, temperature-based methods, water balance, remote sensing and energy balance (Kite, 1982; Shahin, 1985; Piper *et al.* 1986; Sene and Plinston, 1994; Yin and Nicholson, 1998; Nicholson *et al.*, 2000; LVBC, 2006, Swenson and Wahr, 2009). The different methods and periods of analysis increase uncertainty in estimates for each water balance component (Yin and Nicholson, 1998). For example, earlier negative water balances (Table 6.1) have been attributed to inadequate lake rainfall (ranging from 79 to 126 $km^3 \cdot a^{-1}$) and evaporation (ranging from 78 to 122 $km^3 \cdot a^{-1}$) (Yin and Nicholson, 1998; Swenson and Wahr, 2009). Similarly, estimates for the water balance of Lake Kyoga depend upon a variable number of rain gauges (up to 15 stations). Victoria Nile inflows are added to varying numbers of several local inflows (e.g. Rivers Sezibwa, Sironko, Sipi, Simu, Namata, Namalu, Mpologoma, Muyemba, Manafwa, Malaba, Kerim, Enget, Akokorio, Agu, Abuket, Kafu, Awoja, Omunyal, Abalang and Olweny). The flow of the River Victoria Nile is well constrained because it is gauged at two downstream stations, Masindi Port and Kamdini. Lake evaporation, on the contrary, is complicated by a small open water area in a large lake swamp system which is estimated using a range of methods including evaporation pans, temperature-based methods and satellite data. All water balance studies of both Lakes Victoria and Kyoga have, to date, with the exception of Swenson and Wahr (2009), either considered the contribution from groundwater to be negligible or failed to assess its role.

Table 6.2 Previous results of the Lake Kyoga annual water balance estimates ($km^3 \cdot a^{-1}$) from 1917 to 2003.

Period	Lake Rainfall	Lake Evaporation	Nile Inflows	Nile Outflows	Local Inflows	Net Basin Supply	Storage change	Source
1917-1932	4	6	14	13	1	13	0	Hurst *et al.*, 1966 (cited in Shahin, 1985)
1969	5	8	42	45	3	42	-1	WMO, 1974 (cited in Shahin, 1985)
1970	6	8	41	44	4	43	1	WMO, 1974 (cited in Shahin, 1985)
1948-1970	6	9	29	30	3	29	0	Shahin (1985)
1951-1960	6	7	19	19	2	20	0	Sutcliffe and Parks (1999)
1966-1975	6	7	40	42	3	42	0	Sutcliffe and Parks (1999)
1962-2003	5	6	38	39	2	39	0	ILM (2004)
average	**5**	**7**	**32**	**33**	**2**	**32**	**0**	

6.3 Methods

6.3.1 Darcy flux method

The contribution of groundwater to Lake Victoria is estimated from the application of Darcy's Law for fluid movement in a porous medium (equation 6.1) where Q is the discharge of groundwater and K_h is the saturated average horizontal hydraulic conductivity. A is estimated from an aquifer thickness, b and width, p, the circumference of the lake. The i is estimated from the hydraulic gradient between groundwater level and the lake stage. There is a linear distance of 140 m between the Entebbe piezometer and the lakeshore.

$$Q = K_h \cdot A \cdot i \qquad (6.1)$$

The underlying assumptions to the application of Darcy's Law are: (1) the interface is isotropic, homogeneous, and extends horizontally; (2) the interface is of a constant thickness, b with simple groundwater flow conditions around the lake perimeter; (3) the direction of flow is perpendicular to the shoreline as water enters and leaves the lake body; and (4) the i between the piezometer and lake levels is uniform. Under these conditions, all water exchanges between groundwater and lake pass horizontally through a vertical plane positioned at the shoreline that extends to a finite depth, b, beneath the surface of the lake (Fig. 6.1). Any fluxes that exist deeper than b, are not considered to exchange with the lake body. Groundwater flow lines bend sharply upward as they approach the lake from the groundwater bearing zone, ultimately discharging through the face of a near-shore discharge zone (Figs. 4.29, 4.30 and 4.31). The principal direction of groundwater flow at the point of discharge is then commonly perpendicular to the lake side, with seepage rates usually greatest near the shore and

decrease nonlinearly with distance from the shoreline (Fig. 6.1). In reality, it is expected that the groundwater flow is likely to be significantly more complex (Woessner, 2000) especially across the varied geology around the lake (section 2.2.1).

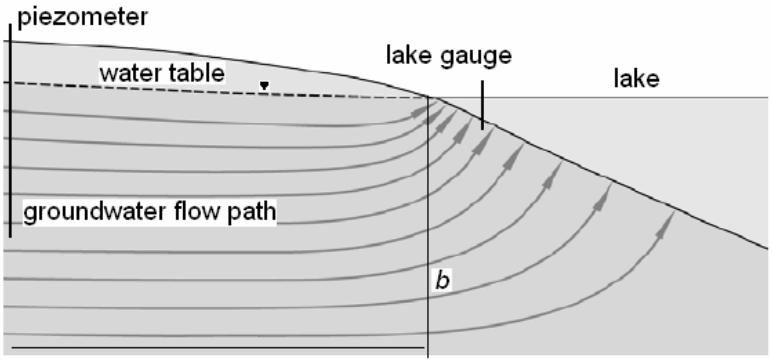

Figure 6.1 Conceptual section of a homogeneous aquifer medium with seepage rates into the lake decreasing nonlinearly with distance from the lake shoreline.

6.3.2 Saturated hydraulic conductivity

Estimates of saturated horizontal hydraulic conductivity, K_h derived from the application of empirical relationships based on lithologic texture (section 3.4.4) to the lithological interface between groundwater and lakes in Jinja and Bugondo, vary from 15 $m \cdot d^{-1}$ in the fluvial-lacustrine lake sands to <0.02 $m \cdot d^{-1}$ with depth in the saprolite. Bulk transmissivity (2-36 $m^2 \cdot d^{-1}$) estimates derived from hydraulic tests in Jinja, Bugondo (section 4.3.2) and on the western shore of Lake Victoria (Fig. 3.21) for average groundwater-bearing lithologic interface thicknesses of 20 m result in *K* values of 0.1 - 1.8 $m \cdot d^{-1}$. Coarse materials such as sand and gravel generally have *K* ranging from 0.01 - 14 $m \cdot d^{-1}$ (Freeze and Cherry, 1979) whereas weathered granite yield 0.005 - 0.07 $m \cdot d^{-1}$ (Domenico and Schwartz, 1998). Taylor and Howard (2000) based on slug tests report a *K* value of 0.04 - 0.7 $m \cdot d^{-1}$ for weathered-mantle aquifers in the Upper Nile Basin. Chilton and Smith-Carington (1984) similarly estimate *K* values of 0.2 - 1.8 $m \cdot d^{-1}$ from hydraulic tests of high yielding stations in the weathered basement aquifers

of Malawi. Ojiambo *et al.* (2001) estimate the average horizontal *K* using $^{3}H/^{3}He$ age-dating of groundwater outflow from Lake Naivasha at 6 $m \cdot d^{-1}$. Kishel and Gerla (2002) slug test analysis indicate that hydraulic conductivity *K* estimates range from 0.39 to 21 $m \cdot d^{-1}$ for the sands and 0.005 to 4 $m \cdot d^{-1}$ for organic sediments along the shore of Shingobee Lake, Minnesota, USA with most of the flow preferentially focused and discharged within 1 m of the shoreline, and appears strongly influenced by the larger hydraulic conductivity of the shoreline sediments. It is acknowledged that the heterogeneity in lakebed sediments causes *K* of the groundwater flux to substantially vary widely even within small areas (Kishel and Gerla, 2002). Despite the varied geology, the upper saprolite through which groundwater interacts with the lake is likely to bear fairly similar hydraulic properties around the lake perimeter that should reduce the errors involved in the extrapolation of the single point measurement to a much larger lake area. A range of conservative K_h values of between 0.1 and 1.0 $m \cdot d^{-1}$ are used to depict low to high permeability interfaces, respectively around the lake perimeter.

6.3.3 Area of lithologic interface

The area of the lithologic interface perpendicular to groundwater flow is estimated from three sources (Fig. 6.2). Firstly, a bathymetric map by Whitehouse and Hunter (1955) derived from depth soundings of Lake Victoria from 1900 to 1906 with corrections and additions to 1955 (Fig. 6.2a). Secondly, a modified bathymetric map by Anyah *et al.* (2009) is also used (Fig. 6.2c) as well as that of Crul (1995) (Fig. 6.2b). Using ArcGIS 9.1, the perimeter of the lake area for an average level of about 1,134 masl is calculated for each of the three defined bathymetries. It is argued that there could be a decrease in flux rates with the distance from the lakeshore which is likely to concentrate the discharge close to the shores (Lee, 1977; Shaw and Prepas, 1990; Yong and Wang, 2007). However, it is recognised that differences in underlying geology can

increase groundwater discharge with distance from shores (Woessner and Sullivan, 1984) or even provide variable discharge to lakes (Krabbenhoft and Anderson, 1986).

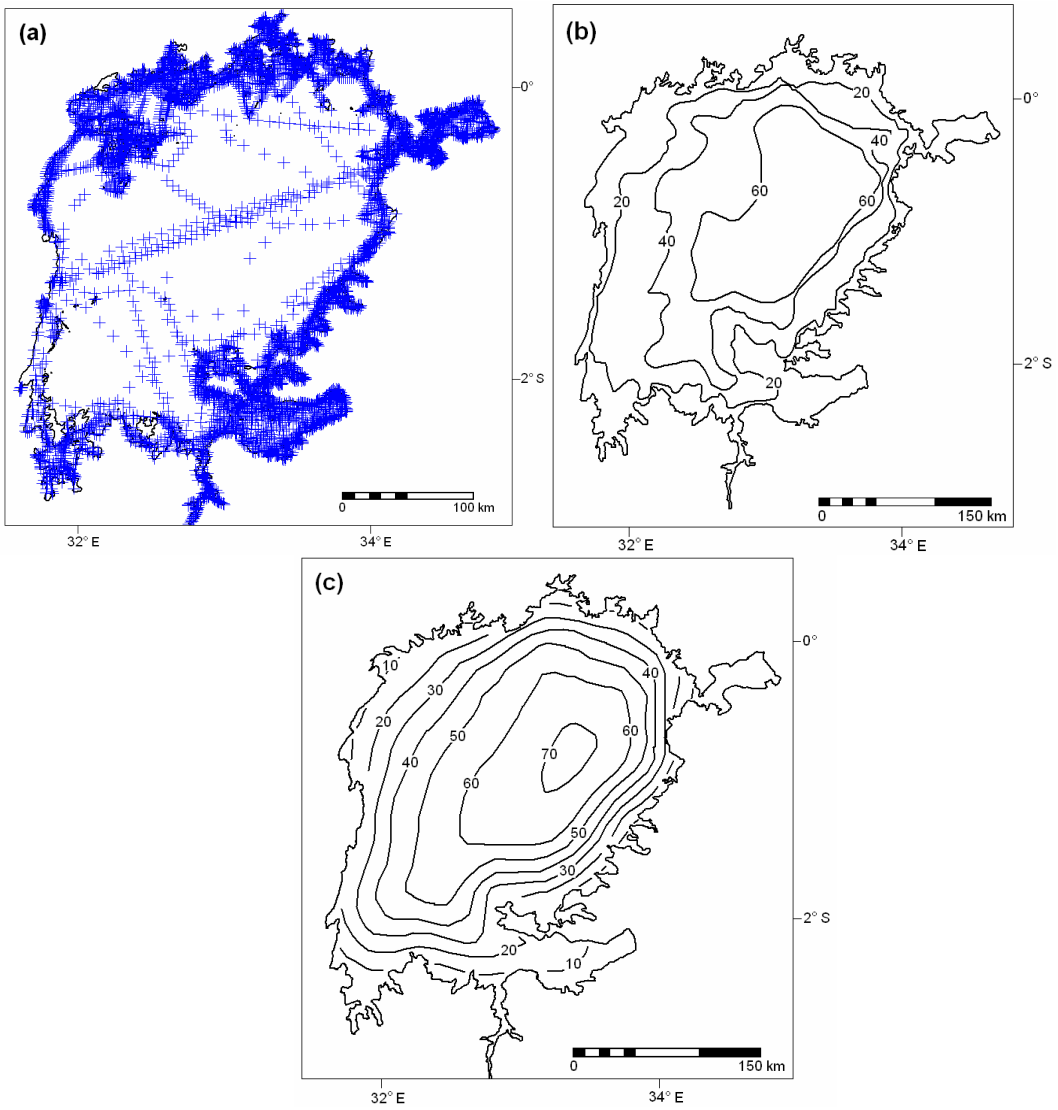

Figure 6.2 Lake Victoria perimeter estimates derived from bathymetric maps of (a) Whitehouse and Hunter (1955) where crosses indicate depth of the lakebed in metres below lake level, (b) Crul (1995) with contours in metres below lake level and (c) Anyah *et al.* (2009) with contours in metres below lake level.

Depth to saprock which defines the thickness of the saprolite is variable but considerable around the northern shore of Lake Victoria. For example, at Entebbe it ranges from 48 to 67 mbgl (Fig. 3.6) whereas at Jinja evidence from drilling logs suggests it ranges from 12 to 45 mbgl (Fig. 3.29). Wells fringing Lake Victoria are also all within saprolite with depths of over 20 mbgl (Fig. 3.21). Johnson *et al.* (1996)

describes up to 60 m thick fluvial-lacustrine sediments of variable texture underlying Lake Victoria (section 2.4.2). From figure 6.3, it is apparent that despite the shallow lake depth, there is a large weathered lithologic interface with the lake, in the western and eastern (Fig. 6.3b) as well as the southern and northern (Fig. 6.3c) shores. The vertical bathymetric gradient at <1,100 masl on the eastern shore of the lake (Fig. 6.3b) is attributed to old fault zones, strike of resistant rocks or upwarp (section 2.4.1). Therefore an average effective thickness (*b*) of 10 m is applied around the lake perimeter. The length of the lake perimeter together with the constant effective thickness is used to represent the interface area through which the groundwater discharges to the lake. Applying the bathymetry of Whitehouse and Hunter (1955), the lake perimeter and area are 3,650 km and 69,400 km^2 for a lake level of 1,136.5 masl. For an interface thickness of 10 m, the lithological interface area is 36.5 km^2. The bathymetry of Crul (1995) alternatively, has a perimeter and area of 3,120 km and 70,900 km^2. For an interface thickness of 10 m, the lithological interface area is 31.2 km^2. Similarly, for the bathymetry of Anyah *et al.* (2009), the lake perimeter and area are 3,180 km and 68,300 km^2 for a lake level of 1,134 masl. For an interface thickness of 10 m, a lithological interface area is 31.8 km^2.

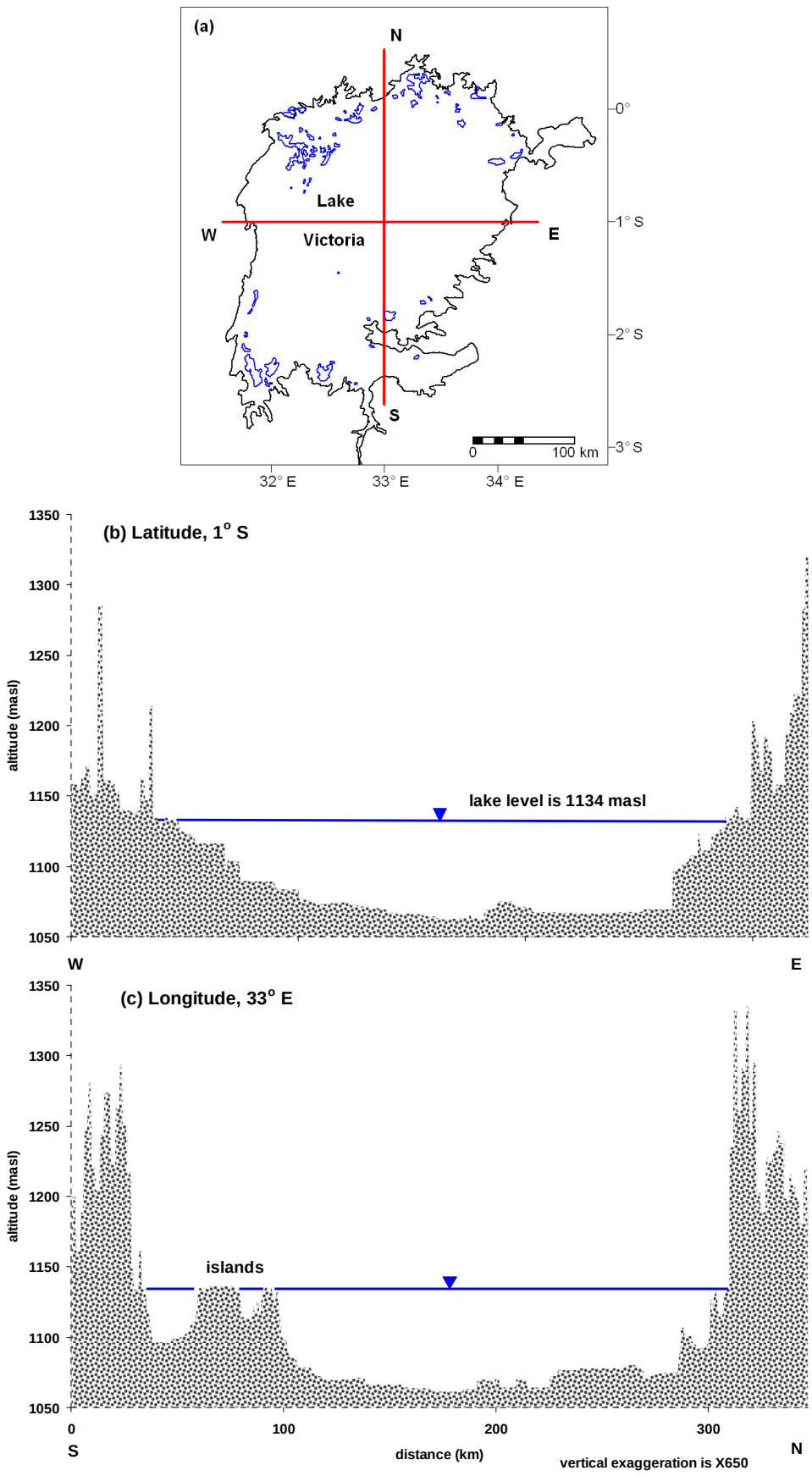

Figure 6.3 (a) Current average Lake Victoria shoreline derived from depth sounding maps of Whitehouse and Hunter (1955) and also showing cross sections of the bathymetry (from 90-m SRTM, 2009 digital terrain model) across its surface area from (b) west to east (along latitude, 1^{o} S) and, (c) south to north (along longitude, 33^{o} E).

6.3.4 Hydraulic gradient between groundwater and Lake Victoria

An estimate of the *i* between groundwater and Lake Victoria is taken from monitoring data since July 1999 at Entebbe (Fig. 6.4). Observed *i* varies substantially as a result of seasonal rainfall driving recharge events (chapters 4 and 5). The mean *i* over the observed period (~10 years) is ~0.008 $m \cdot m^{-1}$. During the monsoons, the *i* commonly reaches 0.015 $m \cdot m^{-1}$ but recedes to 0.003 $m \cdot m^{-1}$. The cut-off value between high *i* and low *i* is 0.009 $m \cdot m^{-1}$. Summary statistics of the mean of low (0.006 $m \cdot m^{-1}$) and high (0.012 $m \cdot m^{-1}$) *i* are shown in Table 6.3. The periods of high *i* occur for about 20 % of the duration of the monsoonal events.

The direction of the *i* is primarily towards the lake, over the observed period except for a short period in 2005 when the flow was influent. The seasonality of the *i* reflects the bimodal water level responses to annual recharge events where the second peak is less pronounced than the earlier one which is expected to occur around much of the lakeshore. Isotopic (δ^2H and $\delta^{18}O$) data also indicate groundwater mixing with lake waters along parts of the northern shore of the lake (Figs. 3.20 and 3.21). As discussed in section 4.4, the lake rises more quickly on the western, northern and northeastern sides than the southern section from April to July when there is a rise of about 45 cm on the northern relative to the southern parts (Krishnamurthy and Ibrahim, 1973). This is however, likely to provide a lower *i* in the southern areas.

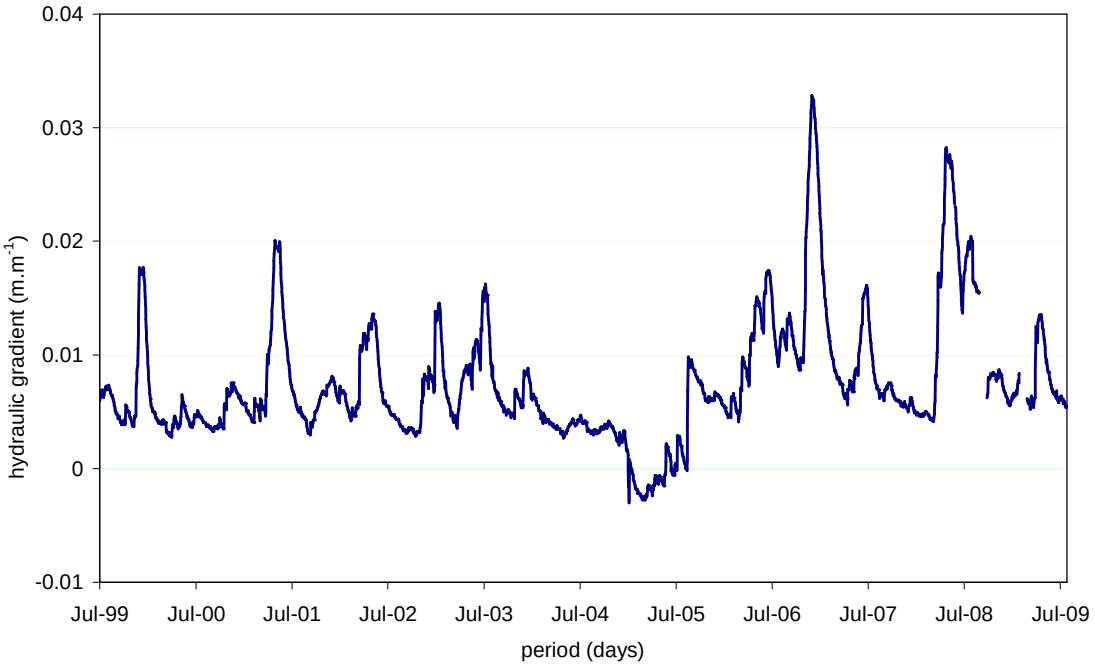

Figure 6.4 Hydraulic gradients between average daily groundwater and Lake Victoria levels (1999-2009) at Entebbe monitoring station.

Table 6.3 Summary statistics and thresholds used to define low and high hydraulic gradient between groundwater and Lake Victoria from temporal (1999-2009) variations at Entebbe.

parameter	**low *i***	**high *i***
Mean ($m \cdot m^{-1}$)	0.006	0.012
Standard deviation ($m \cdot m^{-1}$)	0.002	0.002
Minimum ($m \cdot m^{-1}$)	0.003	0.009
Maximum ($m \cdot m^{-1}$)	0.009	0.015
number of days	2419	553

6.4 Groundwater discharges to Lake Victoria based on monitoring at Entebbe

From the average long-term Lake Victoria water balance derived from several previous studies carried out from 1900-2007, the total river outflow of which groundwater is part, is estimated at 20 $km^3 \cdot a^{-1}$ (Table 6.1)**.** A range of scenarios for estimating groundwater discharge to Lake Victoria are presented in Table 6.4. The first scenario employs the lowest mean *i* (0.006 $m \cdot m^{-1}$) and *K* (0.1 $m \cdot d^{-1}$) and yields an estimate of ~0.04 % of the total river inflow to Lake Victoria. Whereas the second

scenario of using only a high mean *i* (0.012 $m \cdot m^{-1}$) but low *K* (0.1 $m \cdot d^{-1}$), doubles the percentage of groundwater to total river inflow to ~0.08 %. A third scenario of employing a high *K* (1.0 $m \cdot d^{-1}$) and keeping the mean *i* low (0.006 $m \cdot m^{-1}$), gives ~0.38 % of total river inflow. The last scenario where both high *K* (1.0 $m \cdot d^{-1}$) and mean *i* (0.012 $m \cdot m^{-1}$) are applied yields the highest fraction of ~0.76 % for groundwater of the total river inflow.

Irrespective of whether high or low estimates of *K* ad *i* are applied, estimates of the contribution of groundwater, as a fraction of total river inflow to Lake Victoria, are less than 1 %. This first analysis based on hydrogeological data and employing gross simplifications, supports the untested assumptions of previous water-balance studies that the contribution of groundwater is negligible and within the error of the other components of the lake water balance (Neff and Nicholas, 2005). It is possible that groundwater fluxes are greater in deeper parts of the lake (Grannemann *et al.*, 2000), but this remains speculative. Swenson and Wahr (2009) using remote sensing data, contend that baseflow may contribute as much as a few hundred mm of water to the lake each year. They estimate that groundwater flows into the lake at an average of about 420 $mm \cdot a^{-1}$ (~29 $km \cdot a^{-1}$). These generous estimates are however, not supported by the hydraulic properties of the lithostratigraphic interface in the Upper Nile Basin. The value of 0.05 to 1 % is therefore, a first estimate of the groundwater discharge to Lake Victoria and needs to be better constrained by a more detailed monitoring network around the lake. As a single point measurement which has been extrapolated it may not necessarily be representative of the hydrodynamics in other parts of the lakeshore.

Table 6.4 Results of the estimates of the annual groundwater discharges to Lake Victoria derived from bathymetric maps of Whitehouse and Hunter (1955), Crul (1995) and Anyah *et al.* (2009).

Scenario	*K*	Area for 10-m depth		mean *dh/dx*	Q	Contribution to inflows
	($m \cdot d^{-1}$)	Source	(km^2)	($m \cdot m^{-1}$)	($km^3 \cdot a^{-1}$)	(%)
1) low *K*, low *i*	0.1	Crul (1995)	31.2	0.006	0.01	0.04
2) low *K*, low *i*	0.1	Ayah (2008)	31.8	0.006	0.01	0.04
3) low *K*, low *i*	0.1	Whitehouse and Hunter (1955)	36.5	0.006	0.01	0.04
4) low *K*, high *i*	0.1	Crul (1995)	31.2	0.012	0.01	0.07
5) low *K*, high *i*	0.1	Ayah (2008)	31.8	0.012	0.01	0.07
6) low *K*, high *i*	0.1	Whitehouse and Hunter (1955)	36.5	0.012	0.02	0.08
7) high *K*, low *i*	1.0	Crul (1995)	31.2	0.006	0.07	0.36
8) high *K*, low *i*	1.0	Ayah (2008)	31.8	0.006	0.07	0.37
9) high *K*, low *i*	1.0	Whitehouse and Hunter (1955)	36.5	0.006	0.08	0.42
10) high *K*, high *i*	1.0	Crul (1995)	31.2	0.012	0.14	0.72
11) high *K*, high *i*	1.0	Ayah (2008)	31.8	0.012	0.14	0.73
12) high *K*, high *i*	1.0	Whitehouse and Hunter (1955)	36.5	0.012	0.16	0.84

6.5 Summary

Previous water balance studies for Lake Victoria from 1900-2007 indicate the following mean fluxes: rainfall of 111 $km^3 \cdot a^{-1}$, evaporation of 100 $km^3 \cdot a^{-1}$, total inflows of 20 $km^3 \cdot a^{-1}$, total outflows of 30 $km^3 \cdot a^{-1}$, assuming no changes in lake storage over this period. For Lake Kyoga on the other hand, water balance studies carried out from 1948 to 2003 indicate the following mean fluxes: rainfall of 5 $km^3 \cdot a^{-1}$, evaporation of 7 $km^3 \cdot a^{-1}$, Victoria Nile inflows of 32 $km^3 \cdot a^{-1}$, local inflows of 2 $km^3 \cdot a^{-1}$, Victoria Nile outflows of 33 $km^3 \cdot a^{-1}$ assuming no changes in lake storage over this period. A first estimate of the contribution of groundwater is in the order of ~1 % of river inflow. For these findings to be better constrained, it requires a more detailed monitoring network

around the lake and to be complimented by other methods (e.g. stable isotope mass balance).

The implications of these estimates of groundwater inflows to Lakes Victoria and Kyoga are: (i) despite dynamic groundwater interactions with the lakes, during periods of low or absent rainfall, baseflow is not sufficient to sustain the lake levels, (ii) limited subsurface transport of hydrochemical (e.g. Ca^{2+}, Na^{+}, HCO_3^{-}, Fe) fluxes from mineralised saprolite aquifer to the lakes is not expected to influence surface water quality, and (iii) low permeability of saprolite indicate that heavy rainfall events could mobilise and transport the bulk of contaminants (e.g. microorganisms, non-aqueous phase liquids) from onshore anthropogenic activities (e.g. domestic and municipal wastes) as surface runoff and shallow throughflow into the lakes.

Chapter 7
Conclusions and Recommendations

7.1 Introduction

As the first study to investigate the interaction between groundwater and surface waters in the Upper Nile Basin of Uganda, the overall aim of this doctoral research is to improve understanding of the interactions on the highly weathered surfaces of low relief ("African surface") within the Great Lakes Region of Africa. The specific objectives of the study include: (i) to characterise the lithological interface between groundwater and surface waters of Lakes Victoria and Kyoga, (ii) to relate the observed interface to models of the evolution of landscape and drainage in the GLRA, (iii) to assess how rainfall and dam operations influence the observed interaction between groundwater and surface waters in time and space, and (iv) to quantify the hydrological fluxes between groundwater and surface water.

7.2 Key findings in relation to specific, scientific objectives

7.2.1 Characteristics of the lithologic interface between groundwater and surface waters

Lithologic analyses and geo-electrical resistivity surveys at Bugondo and Jinja reveal a relatively consistent hydrostratigraphy in which fluvial-lacustrine sands are succeeded with depth by weathered rocks indicative of a sub-aerial, *in situ* origin. At Bugondo, the mixed fluvial-lacustrine sands (~1-5 m thick) rest on a duricrust of lateritic gravel (~2-4 m thick) which, in turn, overlies a thick groundwater-bearing saprolite. At Jinja, a mixed fluvial-lacustrine sands and infill (~2-7 m thick) overlie a thick groundwater-bearing saprolite of variable thickness (from ~10 m depth). At Jinja,

laterite crust is absent and presumed to have been eroded when the lake's outlet at Jinja was carved out during the late Pleistocene. At Entebbe, fluvial-lacustrine sands (~5 m thick), overlie lateritic gravel and sands (15 m thick) beneath which is the main groundwater-bearing saprolite layer (>17 m thick). Saturated K estimates (0.01-15 $m \cdot d^{-1}$) from well logs together with estimates of bulk T (2-36 $m^2 \cdot d^{-1}$) from hydraulic tests at each site attest to the variability vertically and horizontally in groundwater pathways that constitute the interface of groundwater and surface water in the Upper Nile Basin.

The groundwater - surface water monitoring stations constructed on the shores of Lakes Victoria (Jinja) and Kyoga (Bugondo) combined with an existing groundwater monitoring station on the shore of Lake Victoria at Entebbe reveal a positive hydraulic gradient from groundwater towards both lakes. The hydrogeological conditions of the interface between groundwater and surface water, deduced from (i) borehole logs showing static water levels above the main water strike zones; (ii) aquifer responses to barometric pressures; and (iii) hydraulic tests, indicate a semi-confined aquifer linked to the constant-head boundary. The layered heterogeneity in the saprolite aquifer suggests a two-part recession in groundwater levels (fluvial–lacustrine sands and saprolite system). Temporal variations in the fluxes between the groundwater and the lake show that groundwater hydrographs form rapid, short-lived responses when groundwater levels are within the more permeable fluvial-lacustrine sands that overlie the saprolite system. These observations coupled with the depth profiles showing significant K and S_y within the saprolite indicate that groundwater interacts dynamically with lakes.

It is suggested that deep circulation of water within the saprolite is the primary source of groundwater that is upwelled into the lakes via preferential pathways (e.g. discontinuous clay horizons, quartz stringers and fractures in duricrust) within the upper horizons of saprolite layer from (i) lithological layered heterogeneity in K and storage;

(ii) rainfall and temporal groundwater - surface water interactions; and (iii) well hydraulics (semi-confined system).

7.2.2 The relationship of the observed interface to the evolution of the landscape and drainage on low relief surfaces

A sequence of rift-related, tectonic processes since early Miocene (~15 Ma) is considered to have primarily shaped the present landscape of the GLRA and its surface hydrology. Reversal of flow direction by these processes eventually led to the formation of Lakes Victoria and Kyoga which dominate the low relief surface of the Upper Nile Basin. Fluvial-lacustrine sediments underlying Lake Victoria show 4 to 5 main sequences separated by erosional unconformities up to 60 m thick (Johnson *et al.*, 1996). A diatomaceous sapropel (mud) layer of variable thickness is underlain by stiff silty clay (~8 m thick), followed by a highly stratified layer of suspected similar texture that is tilted upward to the west (~23-35 m thick) which, overlies an old, indurated sequence (related to regional bedrocks). Deeply weathered surfaces (saprolite) within the Upper Nile Basin are usually capped by a variety of iron-rich to alumina-enriched residua horizons (laterite). Weathered crystalline basement rocks capped by lateritic profiles often have substantial water bearing horizons within the leached lateritized zone under the cuirass or in the decomposed zone (saprolite/saprock interface) just above the solid rock. Evidence from all three stations, Bugondo, Jinja and Entebbe, support prolonged, deep weathering under an *in situ* etchplanation model previously described by McFarlane (1992) for the evaluation of the landscape and interface rather than the *fluviatile* (pediplanation) hypothesis.

7.2.3 Rainfall and dam operations influence on the observed interaction between groundwater and surface waters in time and space

Historical variations in the levels of Lakes Victoria and Kyoga (1947-2009) demonstrate that variations in Lake Kyoga levels are primarily determined by the flow of the Victoria Nile with natural (e.g. vegetation) and more recent human development (e.g. dams) influencing the variations of both lake levels. The two lakes are therefore hydraulically linked and co-dependent. Groundwater levels in monitoring stations proximate to the lakes rise and fall rapidly (1-9 days) in response to rainfall. These short-lived responses reflect a dynamic transmissive interface. The closest stations to the lakes also form dynamic, high frequency, short-lived reversible interactions with lake water which indicate possible flooding during recharge events. Rainfall has strong influence on the seasonality of the groundwater levels and the *i* between groundwater and the lakes are largely determined by local recharge events. This is a result of the comparatively low storage of the localised saprolite/saprock aquifer in relation to the large area and storage volume of the lakes. Hydraulic gradients are generally towards the lake from all the piezometers and are highest during the recharge periods. Groundwater flows primarily into lakes, which dynamically varies seasonally and with proximity to lake. Groundwater fluxes into the lakes are further modified by the *i* in response to changing drainage base (lake) levels. The latter control on the interaction between groundwater and the lakes is, heavily determined by a regional, rather than local, climatology and the operation of the dams at Jinja. On the Lake Victoria shore, consistently high dam releases at Jinja decrease the levels of the lake which, in turn, raise the *i* between groundwater and lake; low releases decrease the *i* as the lake level rises. However, on the shore of Lake Kyoga, the reverse is true. Consistently high dam releases enhance lake levels which, in turn, lower the *i* between groundwater and lake; low releases increase the *i* as the lake level declines. It is also apparent from similar

seasonality and interannual variability in lake-water, soil moisture and groundwater storage that each of the components contribute to regional water storage variations. During the wet season preferential flow into surface water is derived from shallow and rapid groundwater flow within fluvial-lacustrine sands overlying saprolite. In the dry season the dominant discharge into surface water is transmitted from deeper saprolite fluxes that are upwelled into the lakes via preferential pathways.

Bimodal rainfall patterns induce seasonality in groundwater levels with the first (MAM) rains commonly generating greater recharge on the northern shore of Lake Victoria. Conversely, the second (SON) rains induce the largest response in groundwater levels on the shore of Lake Kyoga. Cross correlations between rainfall and borehole hydrographs (groundwater levels) show that heavy (monsoonal) rainfall events (>10 $mm \cdot d^{-1}$) determine the magnitude and timing of recharge in areas remote from surface water. Analyses further indicate that rainfall exceeding 200 mm in a given year is required for recharge to occur in the Upper Nile Basin. Saprolite aquifers not directly influenced by lakes show that rainfall-fed recharge occurs with mean average linear vertical velocities ranging in the unsaturated zone from about 0.1 to 1.2 $m \cdot d^{-1}$. Results suggest, contrary to previous assertions (Döll and Florke, 2005), that a shift to more intensive rainfall may promote rather than restrict groundwater recharge. Substantial uncertainty remains, however, as to whether potential rises in recharge will be offset by increased evapotranspiration associated with warmer atmospheres.

7.2.4 Estimates of hydrological fluxes between groundwater and surface water

The major ion chemistry suggests that mineralised groundwater upwell from saprolite, mix with local diffuse recharge via the fluvial-lacustrine sediments, which then discharge into the lakes. Additionally, isotopic chemistry indicates that in the wet season groundwater discharges into wetlands at Bugondo, groundwater evolves along the flow path by mixing with lake waters at Jinja, and groundwater mixes with lake waters in parts of the fringing region on the northern shore of Lake Victoria.

A first estimate of the contribution of groundwater to the lake's water balance is in the order of ~1 % of river inflow. A more comprehensive monitoring network around the lake is required to better constrain this first approximation and to verify the estimates of Swenson and Wahr (2009) based on remote sensing. Stable isotope tracers may also prove useful in constraining the relative proportions of inflow to Lake Victoria. The implications of these estimates of groundwater inflows to Lakes Victoria and Kyoga are: (i) despite dynamic groundwater interactions with the lakes, during periods of low or absent rainfall, baseflow is not sufficient to sustain the lake levels, (ii) limited subsurface transport of hydrochemical (e.g. Ca^{2+}, Na^{+}, HCO_3^{-}, Fe) fluxes from mineralised saprolite aquifer to the lakes is not expected to influence surface water quality, and (iii) low permeability of saprolite indicate that heavy rainfall events could mobilise and transport the bulk of contaminants (e.g. microorganisms, non-aqueous phase liquids) from onshore anthropogenic activities (e.g. domestic and municipal wastes) as surface runoff and shallow groundwater flow into the lakes.

7.3 Recommendations and further work

Observations of the interactions between groundwater and lakes in the Upper Nile Basin show that a temporally and spatially dynamic interaction exists between groundwater and surface waters. Groundwater contributes, albeit to a very limited extent, to the maintenance of surface water levels during dry periods. Monitoring of groundwater-surface water interactions is an ongoing process and if sustained, may help to transform current conceptual models into predictive models. This is an iterative process which identifies information gaps and requires further data gathering and evaluation. Indeed, the present infrastructure and coverage is inadequate concerning the connectivity of groundwater and surface water in the region. Expansion of the present network would enable better representation of the spatial heterogeneity of the groundwater-surface water interface around each lake. Piezometers should be carefully located to define the complex temporal and spatial dynamic configuration of *i*; nested piezometers should be placed in the drainage area, nearshore of surface water bodies and interfluves so that the nearshore, distant configuration as well as vertical *i* can be monitored (Winter, 1983). To better constrain fluxes, meteorological (e.g. rainfall, evapotranspiration, temperature) monitoring should be carried out proximate to the groundwater – surface water stations. Furthermore, a greater range of the methods should be used to assess the connectivity between surface water and groundwater (e.g. artificial and isotopic tracers, geophysics and remote sensing, hydrochemistry and environmental tracers, seepage measurement) in order to develop a better understanding of the interactions between groundwater and lakes in the GLRA.

References

Acres, B.D., Rains, A.B., King, R.B., Lawton, R.M., Mitchell, A.J.B. and Rackman, L.J. (1985). *African dambos: their distribution, characteristics and use*. Zeitschrift für Geomorphologie Supplementbande, 52, 62-83.

Alagbe, S.A. (2002). *Groundwater resources of river Kan Gimi Basin, north-central, Nigeria*. Environmental Geology, 42, 404-413.

Aleva, G.J.J. (1994). *Laterites. Concepts, geology, morphology, and chemistry*. ISRIC, Wageningen, The Netherlands, 169p.

Allen, M.R. and Ingram, W.J. (2002). *Constraints on future changes in climate and the hydrologic cycle*. Nature, 419, 224-232.

Aller, L., Bennett, T.W., Hackett, G., Petty, R.J., Lehr, J.H., Sedoris, H., Nielsen, D.M. and Denne, J.E. (1989). *Handbook of Suggested Practices for the Design and Installation of Ground-Water Monitoring Wells*. EPA/EMSL-Las Vegas, U.S. EPA Cooperative Agreement CR-812350-01, EPA/600/4-89/034, NTIS #PB90-159807.

Alley, M.W., Healy, W.R., LaBaugh, W.J. and Reilly, E.T. (2002). *Flow and storage in groundwater systems*. Science, 296, 1985-1990.

Anyah, R.O. (2009). Impact of groundwater reservoir on simulated extreme hydroclimatic conditions: case study from the United States. In: Taylor, R., Tindimugaya, C., Owor, M. and Shamsudduha, M. (eds.), Groundwater and Climate in Africa, Proceedings of the Kampala Conference, June 2008, International Association of Hydrological Sciences (IAHS) Publication, 334, 94-100.

Awange, J.J., Sharifi, M.A., Ogonda, G., Wickert, J., Grafarend, E.W. and Omulo, M.A. (2007). *The falling Lake Victoria water level: GRACE, TRIMM and Champ satellite analysis of the basin*. Water Resource Management, 22, 775-796.

Balirwa, J.S. (1995). *The Lake Victoria environment: Its fisheries and wetlands - a review*. Wetlands Ecology and Management, 3(4), 209-224.

Banks, E.W., Simmons, C.T., Love, A.J., Cranswick, R., Werner, A.D., Bestland, E.A., Wood, M. and Wilson, T. (2009). *Fractured bedrock and saprolite hydrogeologic controls on groundwater/surface-water interaction: a conceptual model (Australia)*. Hydrogeology Journal, 17, 1969-1989.

Basalirwa, C.P.K. (1995). *Delineation of Uganda into climatological rainfall zones using the method of principal component analysis*. International Journal of Climatology, 15, 1161-1177.

Bates, R.L. and Jackson, J.A. (eds.). 1987. *Glossary of Geology* (*3rd edn.*) American Geological Institute, Alexandria.

Batte, A., Muwanga, A., Sigrist, P.W. and Owor, M. (2008). *Vertical electrical sounding as an exploration technique to improve on the certainty of groundwater yield in the fractured crystalline basement aquifers of eastern Uganda*. Hydrogeology Journal, 16, 1683-1693.

Becht, R. and Harper, D.M. (2002). *Towards an understanding of human impact upon the hydrology of Lake Naivasha, Kenya*. Hydrobiologia, 488, 1-11.

Beuning, K.R.M., Kelts, K., Russell, J. and Wolfe, B.B. (2002). *Reassessment of Lake Victoria–Upper Nile River paleohydrology from oxygen isotope records of lake-sediment cellulose*. Geology, 30(6), 559-562.

Binley, A. andf Kemna, A. (2005). Electrical Methods. In: Rubin and Hubbard (eds.), Hydrogeophysics, Springer, Dordrecht, 129-156.

Biryabarema, M. (2001). *Groundwater contamination and the role of geologic strata in retaining pollutants around waste disposal sites in greater Kampala*. Unpublished PhD thesis, Makerere University, Kampala, Uganda.

Bishop, W.W. (1959). *Raised swamps of Lake Victoria*. Records of Geological Surveys, Uganda, 1955-6, 1-10.

Bishop, W.W. (1969). *Pleistocene Stratigraphy in Uganda*. Geological Survey of Uganda, memoir no. X.

Bishop, W.W. and Trendall, A.F. (1967). *Erosion-surfaces, tectonics and volcanic activity*. Quarterly Journal of Geologic Society, London, 122, 385-420.

Bisset, C.B. (1949). *Geological report on the hydroelectric project at Jinja*. Geological Survey of Uganda report.

Black, E. (2005). *The relationship between Indian Ocean sea-surface temperature and East African rainfall*. Philosophical Transactions of the Royal Society, 363, 43-47.

Boast, R. (1990). *Dambos: a review*. Progress in Physical Geography, 14, 153-177.

Bounoua, L., Defries, R., Collatz, G.J., Sellers, P.J. and Khan, H. (2002). *Effects of Land Cover Conversion on Surface Climate*. Climatic Change, 52, 29-64.

Bourdet, D., Ayoub, J.A. and Pirard, Y.M. (1989). *Use of pressure derivative in well-test interpretation*. SPE Formation Evaluation, 293-302.

Brassington, R. (1998). *Field Hydrogeology* (*2nd edn.*). John Wiley and Sons, 248p.

Brodie, R., Sundaram, B., Tottenham, R., Hostetler, S., and Ransley, T. (2007) *An overview of tools for assessing groundwater-surface water connectivity*. Bureau of Rural Sciences, Canberra, 133p.

Brown, J.M. (1950). Records of the Geological Survey of Uganda, Entebbe, 1950.

Brown, J.M. and Gittins, R.T. (1959). *A geological and geophysical investigation of a proposed dam site on the Victoria Nile near Jinja*. Records of the Geological Survey of Uganda, Entebbe, 1955-56, 45-50.

Bugenyi, F.W.B. (2001). *Tropical freshwater ecotones: their formation, functions and use*. Hydrobiologia, 458, 33-43.

Bullock, A. (1992). *Dambo hydrology in southern Africa: review and reassessment*. Journal of Hydrology, 134, 373-396.

Butterworth, J.A., Macdonald, D.M.J., Bromley, J., Simmonds, L.P., Lovell, C.J. and Mugabe, F. (1999). *Hydrological processes and water resources management in a dryland environment III: Groundwater recharge and recession in a shallow weathered aquifer*. Hydrology and Earth System Sciences, 3(3), 345-352.

Cahen, L., Snelling, N.J., Delhal, J., Vail, J.R., Bonhomme, M. and Ledent, D. (1984). *The Geochronology and evolution of Africa*. Clarendon Press, Oxford, 512p.

Camberlin, P., Janicot, S. and Poccardi, I. (2001). *Seasonality and atmospheric dynamics of the teleconnection between African rainfall and tropical ocean surface temperature: Atlantic vs. ENSO*. International Journal of Climatology, 21(8), 973-1005.

Carter, G. S. (1956). *The papyrus swamps of Uganda*. W. Heffer and Sons Ltd. Cambridge, England, 25p.

Cassiani, G., Binley, A.M. and Ferré, T.P.A. (2006). Unsaturated zone processes. In: Vereecken, H., Binley, A.M., Cassiani, G., Revil, A. and Titov, K. (eds.), Applied Hydrogeophysics, Springer, 75-116.

Chambers, D.P. (2006). *Evaluation of new GRACE time-variable gravity data over the ocean*. Geophysical Research Letters, 33, L17603.

Chatterjee, B., Howitt, R.E. and Sexton, R.J. (1998). *The optimal joint provision of water for irrigation and hydropower*. Journal of Environmental-Economics and Management, 36(3), 295-313.

Cheney, E.M. (1960). *An introduction to the soils of the Uganda protectorate*. Memoirs of the Research Division; Series I – Soils No. 1, Department of Agriculture, Uganda Protectorate.

Chilton, P.J. and Foster, S.S.D. (1995). *Hydrogeological characterisation and water-supply potential of Basement aquifers in tropical Africa*. Hydrogeology Journal, 3(1), 36-49.

Chilton, P.J. and Smith-Carington, A.K. (1984). *Characteristics of the weathered basement aquifer in Malawi in relation to rural water supplies. Challenges in African Hydrology and Water Resources*. Proceedings of the Harare Symposium, July 1984, International Association of Hydrological Sciences (IAHS) Publication, 144.

Combe, A.D. (1932). *The geology of south-west Ankole and adjacent territories with special references to the tin deposits*. Geological Surveys Uganda, memoir no. 2.

Cooper, H.H. and Jacob, C.E. (1946). *A Generalized Graphical Method for Evaluating Formation Constants and Summarizing Well Field History*. Transactions of American Geophysical Union, 27, 526-534.

Coplen, T.B. (1993). Uses of Environmental Isotopes. In: Alley, W.M. (ed.), Regional Ground-Water Quality, Van Nostrand Reinhold, New York, 227-254.

Coplen, T.B., Herczeg, A.L. and Barnes, C. (2000). Isotope engineering – using stable isotopes of the water molecule to solve practical problems. In: Cook, P.G. and Herczeg, A.L. (eds.), Environmental tracers in subsurface hydrology, Kluwer Academic, Boston, 529p.

Craig, H. (1961). *Isotopic Variations in Meteoric Waters*. Science, 133(3465), 1702-1703.

Cronican, A.E. and Gribb, M.M. (2004). *Hydraulic conductivity prediction for sandy soils*. Ground Water, 42(3), 459-464.

Crul, R.C.M. (1995). *Limnology and hydrology of Lake Victoria*. Studies and reports in hydrology, 53, UNESCO Publishing.

Dagg, M. (1972). East Africa its peoples and resources. In: Morgan, W.T.W (ed.), Chapter 10: water requirements of crops, Oxford University Press, London, 119-125.

Daily Monitor (2007). *Factories, farms polluting Lake Victoria*. Headline news story of Saturday, 28 April 2007. The Monitor Publications Ltd., Kampala, Uganda.

Davis, D.R. and Rasmussen, T.C. (1993). *A Comparison of Linear Regression With Clark's Method for Estimating Barometric Efficiency of Confined Aquifers*. Water Resources Research, 29(6), 1849-1854.

de Swardt, A.M.J. and Trendall, A.F. (1969). *The physiographic development of Uganda*. Overseas Geology and Mineral Resources, 10, 241-288.

Döll, P. and Florke, M. (2005). *Global-scale estimation of diffuse groundwater recharge*. Frankfurt Hydrology Paper 03, Institute of Physical Geography, Frankfurt University, Frankfurt AM Main, Germany.

Domenico, P.A. and Schwartz, F.W. (1998). *Physical and chemical hydrogeology* (*2nd edn.*). Wiley, New York, 506p.

Doornkamp, J.C. (1968). *The Role of Inselbergs in the Geomorphology of Southern Uganda*. Transactions of the Institute of British Geographers, 44, 151-162.

Doornkamp, J.C. and Temple, P.H. (1966). *Surface, drainage and tectonic instability in part of southern Uganda*. Geographical Journal, 132, 238-252.

Dougherty, D.E. and Babu, D.K. (1984). *Flow to a partially penetrating well in a double-porosity reservoir*. Water Resources Research, 20(8), 1116-1122.

Drichi, P. (2003). *National Biomass Study*. Tech. Rep. 1996–2002. Forest Department, Kampala, Uganda.

Du Bois, O.G.B. and Jeffery, P.G. (1955). *The composition and origin of the laterites of the Entebbe peninsula, Uganda Protectorate*. Colonial geology and mineral resources: The Quarterly Bulletin of the Colonial Geological Society, 387-408.

Duffield, G.M. (2008). *AQTESOLV for Windows, Aquifer Test Analysis Software, Ver. 4.50 - Professional*. ARCADIS Geraghty and Miller Inc., Virginia, U.S.A.

Eaton, A.D., Greenberg, A.E., Clesceri, L.S. and Franson, M.A.H. (eds.) (1995). *Standard methods for examination of water and wastewater* (*19th edn.*). American Public Health Association (APHA), the American Water Works Association (AWWA), and the Water Environment Federation (WEF).

Edwards, L.S. (1977). *A modified pseudosection for resistivity and induced-polarization*. Geophysics, 42, 1020-1036.

Eilers, V.H.M., Carter, R.C. and Rushton, K.R. (2007). *A single layer soil water balance model for estimating deep drainage (potential recharge): An application to cropped land in semi-arid North-east Nigeria*. Geoderma, 140, 119-131.

FAO (2001). *Global Forest Resources Assessment 2000*. Food and Agriculture Organization of the United Nations, Rome, 2001. http://www.fao.org/forestry/fo/fra/index.jsp. Accessed on January 24 2007.

Freeze, R.A. and Cherry, J.A. (1979). *Groundwater*. Prentice-Hall, Inc. Englewood Cliffs, New Jersey, 604p.

Gambrell, R.P. (1994). *Trace and toxic metals in wetlands - A Review*. Journal of Environmental Quality, 23, 883-891.

Gonthier, G.J. (2007). *A Graphical Method for Estimation of Barometric Efficiency from Continuous Data - Concepts and Application to a Site in the Piedmont, Air Force Plant 6, Marietta, Georgia*. U.S. Geological Survey Scientific Investigations Report 2007-5111, 29p.

Goodwin, A.M. (1991). *Precambrian Geology*. Academic Press, New York, 666p.

Grannemann, N.G., Hunt, R.J., Nicholas, J.R., Reilly, T.E. and Winter, T.C. (2000). *The Importance of Ground Water in the Great Lakes Region*. U.S. Geological Survey Water-Resources Investigations Report 00-4008, 19p.

Groves, A.W. (1934). *The Physiography of Uganda: The Evolution of the Great Lakes and the Victoria Nile Drainage System*. Journal of the Royal African Society, 33(130), 59-69.

GSEGWP (1977). *The description of rock masses for engineering purposes. Report by the Geological Society Group Working Party*. Quaternary Journal of Engineering Geology, 10, 355-388.

Hanna, L.W. (1971). *The effects of water variability on tea yields in Uganda*. Journal of Applied Ecology, 111, 791-813.

Hastenrath, S. (1991). *Climate dynamics of the tropics*. Kluwer Academic, 488p.

Hayashi, M. and Rosenberry. D.O. (2002). *Effects of Ground Water Exchange on the Hydrology and Ecology of Surface Water*. Ground Water, 40(3), 309-316.

Hayashi, M. and van der Kamp, G. (2007). Water level changes in ponds and lakes: The hydrological processes. In: Edward A. Johnson, E.A. and Miyanishi, K. (eds.). Chapter 10: Plant Disturbance Ecology: The Process and the Response, Elsevier Academic Press, 311-339.

Healy, R.W. and Cook, P.G. (2002). *Using groundwater levels to estimate recharge*. Hydrogeology Journal, 10, 91-109.

Hoefs, J. (1997). *Stable isotope geochemistry (4th, completely revised, updated, and enlarged edn)*. Springer, Berlin, 201p.

Howard, G., Pedley, S., Barrett, M., Nalubega, M. and Johal, K. (2003). *Risk factors contributing to microbiological contamination of shallow groundwater in Kampala, Uganda*. Water Research, 37(14), 3421–3429.

Howard, K.W.F. and Karundu, J. (1992). *Constraints of the development of basement aquifers in East Africa - water balance implications and the role of the regolith*. Journal of Hydrology, 139, 183-196.

Hurst, H.E. (1925). *The Lake Plateau Basin of the Nile. Physical Department Paper no. 21*, Physical Department. Government Press, Cairo, Egypt.

IAEA (2004). International Atomic Energy Agency (IAEA). Water and Environment News, Isotope Hydrology Section, Issue 18, August 2004.

ILM (2004). *Support to the Management of Sudd Blockage on Lake Kyoga*. Produced for the Integrated Lake Management (ILM) Project by Environmental Impact Assessment Centre of Finland, EIA Ltd., 81p.

Indeje, M., Semazzi, F.H.M. and Ogallo, L.J. (2000). *ENSO signals in East African rainfall seasons*. International Journal of Climatology, 20, 19-46.

Isiorho, S.A., and Matisoff, G. (1990). *Groundwater recharge from Lake Chad*. Limnology and Oceanography, 35(4), 93l-938.

ISO 284 (2003). *Conveyor belts - Electrical conductivity - Specification and test method*. International Organization for Standardization (ISO). http://www.iso.org/iso/home.htm.

ISO 5814 (1990). *Water quality - Determination of dissolved oxygen - Electrochemical probe method*. International Organization for Standardization (ISO). http://www.iso.org/iso/home.htm.

ISO 10523 (2008). *Water quality - Determination of pH*. International Organization for Standardization (ISO). http://www.iso.org/iso/home.htm.

Jarsjö, J. and Destouni, G. (2004). *Groundwater discharge into the Aral Sea after 1960*. Journal of Marine Systems, 47, 109-120.

Johnson, R.J. (1960). *Explanation of the geology of sheet 69 (Lake Wamala)*. Geological Survey of Uganda report.

Johnson, T.C., Scholz, C.A., Talbot, M.R., Kelts, K., Ricketts, R.D., Ngobi, G., Beuning, K., Ssemmanda, I. and McGill, J.W. (1996). *Late Pleistocene desiccation of Lake Victoria and rapid evolution of cichlid fishes*. Science, 273, 1091-1093.

Jones, M.J. (1985). *The weathered zone aquifers of the basement complex areas of Africa*. Quarterly Journal of Engineering Geology, London, 18, 35-46.

Kalbus, E., Reinstorf, F. and Schirmer, M. (2006). *Measuring methods for groundwater, surface water and their interactions: a review*. Hydrology and Earth System Sciences Discussions, 3, 1809-1850.

Kansiime, F., Nalubega, M., van Bruggen J.J.A. and Denny, P. (2003). *The effect of wastewater discharge on biomas production and nutrient content of Cyperus papyrus and Miscanthidium violaceum in the Nakivubo wetland, Kampala, Uganda*. Water Science and Technology, 48(5), 233-240.

Kasenow, M. (2008). *Determination of hydraulic conductivity from grain size analysis*. Water Resources Publications, LLC, 110p.

Kattan, Z. (2006). *Characterization of surface water and groundwater in the Damascus Ghotta basin: hydrochemical and environmental isotopes approaches*. Environmental Geology, 51, 173-201.

Kendall, R.L. (1969). *An ecological history of the Lake Victoria basin*. Ecological Monographs, 39(2), 121-176.

King, L.C. (1962). *Morphology of the Earth*. Oliver and Boyd, London, 699p.

Kingston, D. G., Todd, M. C., Taylor, R. G., Thompson, J. R. and Arnell, N. W. (2009). *Uncertainty in the estimation of potential evapotranspiration under climate change*. Geophysical Research Letters, 36, L20403, doi:10.1029/2009GL040267.

Kishel, H.F. and Gerla, P.J. (2002). *Characteristics of preferential flow and groundwater discharge to Shingobee Lake, Minnesota, USA*. Hydrological Processes, 16, 1921-1934.

Kite, G.W. (1982). *Analysis of Lake Victoria levels*. Hydrological Sciences Journal, 27(2,6), 99-110.

Kite, G.W. (1984). *Regulation of the White Nile*. Hydrological Sciences Journal, 29(2,6), 191-201.

Krabbenhoft, D.P. and Anderson, M.P. (1986). *Use of a Numerical Ground-Water Flow Model for Hypothesis Testing*. Ground Water, 24(1), 49-55.

Krishnamurthy, K.V. and Ibrahim, A.M. (1973). Hydrometeorological studies of Lakes Victoria, Kyoga and Albert. In: Ackermann, W.C., White, G.F. and Worthington, E.B. (eds.), Man-Made Lakes: Their Problems and Environmental Effects. Geophysical monograph 17, American Geophysical Union, Washington, D.C.

Kruseman, G.P. and de Ridder, N.A. (2000). *Analysis and Evaluation of Pumping Test Data (2nd edn - completely revised)*. IIRI Publication 47, 377p.

Kull, D. (2006). *Connections Between Recent Water Level Drops in Lake Victoria, Dam Operations and Drought. Working paper*. http://www.irn.org/programs/nile/pdf/060208vic.pdf. Accessed on 2 February 2007.

Kundzewicz, Z.W., Mata, L.J., Arnell, N.W., Döll, P., Kabat, P., Jiménez, B., Miller, K.A., Oki, T., Zekai, S. and Shiklomanov, I. (2007). Freshwater resources and their management. In: Parry, M.L., Canziani, O.F., Palutikof, J.P., van der Linden, P.J. and Hanson, C.E. (eds.) Climate Change 2007: Impacts, Adaptation and Vulnerability. Contributions of Working Group II to the Fourth Assessment report of the Inter-governmental Panel on Climate Change. Cambridge University Press Cambridge, 173-210.

Lee, L.J.E., Lawrence, D.S.L. and Price, M. (2006). *Analysis of water-level response to rainfall and implications for recharge pathways in the Chalk aquifer, SE England*. Journal of Hydrology, 330, 604-620.

Lee, R.L. (1977). *A device for measuring seepage flux in lakes and estuaries*. Limnology and Oceanography, 22(1), 140-147.

Leggo, P.J. (1974). *A geochronological study of the basement complex of Uganda*. Journal of Geological Society, London, 130, 263-277.

Livingstone, D.A. (1980). Environmental changes in the Nile head-waters. In: Williams, M.A.J. and Faure, H. (eds.), The Sahara and the Nile. Balkema, Rotterdam, 339-359.

Lloyd, J.W. and Heathcote, J.A. (1985). *Natural inorganic hydrochemistry in relation to groundwater*: An introduction: for hydrogeologists, civil engineers, and chemists involved in the application of groundwater chemistry to water resource studies. Clarendon Press, Oxford, 296p.

Loke, M.H. (2004). *Tutorial: 2-D and 3-D electrical imaging surveys*, www.geoelectrical.com.

LVBC (2006). *Special Report on the declining of water levels of Lake Victoria*. Lake Victoria Basin Commission, East African Community Secretariat, Arusha, April 2006, 15p.

MacDonald, A., Davies, J., Calow, R. and Chilton, J. (2005). *Developing Groundwater: A Guide for Rural Water Supply*. IDTG Publishing, 358p.

Mackel, R. (1974). Dambos. *A study of morphodynamic activity on the plateau regions of Zambia*. Catena, 1, 327-365.

Maignien, R. (1966). *Review of research on laterites*. Natural Resources Research IV, UNESCO Publishing.

Maslin, M.A. and Christensen, B. (2007). *Tectonics, orbital forcing, global climate change, and human evolution in Africa: introduction to the African paleoclimate special volume*. Journal of Human Evolution, 53, 443-464.

Mazor, E. (2004). *Chemical and isotopic groundwater hydrology (3rd edn.)*. Dekker, New York, 453p.

McBride, M.S. and Pfannkuch, H.O. (1975). *The distribution of seepage within lakebeds*. Journal of Research, US Geological Survey, 3(5), 505-512.

McCartney, M.P. (2000). *The Water Budget of a Headwater Catchment Containing a Dambo*. Physics and Chemistry of the Earth (B), 25(7-8), 611-616.

McCartney, M.P. and Neal, C. (1999). *Water flow pathways and the water budget within a headwater catchment containing a dambo: inferences drawn from hydrochemical investigations*. Hydrology and Earth System Sciences, 3(4), 581-591.

McFarlane, M.J. (1969). *Lateritisation and landscape development in parts of Uganda*. Unpublished PhD thesis, University College London, U.K.

McFarlane, M.J. (1976). *Laterization and landscape development in Kyagwe, Uganda*. Quarterly Journal of Geologic Society, London, 126, 501-539.

McFarlane, M.J. (1991). *Some sedimentary aspects of lateritic weathering profile development in the major bioclimatic zones of tropical Africa*. Journal of African Earth Sciences, 12(1/2), 267-28.

McFarlane, M.J. (1992). Groundwater movement and water chemistry associated with weathering profiles of the African surface in parts of Malawi. In: Wright, E.P. and Burgess, W.G. (eds.), Hydrogeology of crystalline basement aquifers in Africa. London Geological Society Special Publication, 66, 101-129.

Micklin, P.P. (1988). *Desiccation of the Aral Sea: A water management disaster in the Soviet Union*. Science, 241, 1170-1176.

Mileham, L. (2007). *Nature and mechanisms of climate variability and change in East and Central Africa and their impact on terrestrial hydrology in Uganda*. Unpublished PhD thesis, University College London, UK.

Mileham, L., Taylor, R.G., Thompson, J., Todd, M. and Tindimugaya, C., (2008). *Impact of rainfall distribution on the parameterisation of a soil-moisture balance model of groundwater recharge in equatorial Africa*. Journal of Hydrology, 359, 46-58.

Mileham, L. Taylor, R.G., Thompson, J., Todd, M. and Tindimugaya, C. (2009). *Climate change impacts on the terrestrial hydrology of a humid, equatorial catchment: sensitivity of projections to rainfall intensity*. Hydrological Sciences Journal, 54, 727-738.

Mistry, V.V. and Conway, D.C. (2003). *Remote forcing of East African rainfall and relationships with fluctuations in levels of Lake Victoria*. International Journal of Climatology, 23, 67-89.

Moench, A.F. (1985). *Transient flow to a large-diameter well in an aquifer with storative semiconfining layers*. Water Resources Research, 21(8), 1121-1131.

Mwanja, W.W. (2004). *The role of satellite water bodies in the evolution and conservation of Lake Victoria Region fishes*. African Journal of Ecology Supplement, 42(1), 14-20.

Mwanuzi, F, Aalderink, H. and Mdamo, L. (2003). *Simulation of pollution buffering capacity of wetlands fringing the Lake Victoria*. Environment International, 29, 95-103.

Neff, B.P. and Nicholas, J.R. (2005). *Uncertainty in the Great Lakes Water Balance*. U.S. Geological Survey Scientific Investigations Report 2004-5100, 42p.

Ngatcha, B.N., Mudry, J. and Leduc, C. (2008). Water resources management of the Lake Chad basin: Diagnosis and action plan. In: Adelana, S. and MacDonald, A. (eds.), Applied Groundwater Studies in Africa, CRC Press/Balkema, London, 65-84.

Nicholson, S.E. (1996). A Review of Climate Dynamics and Climate Variability in Eastern Africa. In: Johnson, T.C. and Odada, E. (eds.), The Limnology, Climatology and Paleoclimatology of the East African Lakes, Amsterdam: Gordon and Breach, 25-56.

Nicholson, S.E. and Kim, J. (1997). *The Relationship of the El-Niño Southern Oscillation to African Rainfall*. International Journal of Climatology, 17, 117-135.

Nicholson, S.E. and Selato, J.C. (2000). *The influence of La Niña on African rainfall*. International Journal of Climatology, 20, 1761-1776.

Nicholson, S.E. and Yin, X. (2001). *Rainfall conditions in equatorial East Africa during the nineteenth century as inferred from the record of Lake Victoria*. Climatic Change, 48(2-3), 387-398.

Nicholson, S.E., Yin, X. and Ba, M.B. (2000). *On the feasibility of using a lake water balance model to infer rainfall: an example from Lake Victoria*. Hydrological Sciences Journal, 45(1), 75-95.

NWP (2008). *National Wetlands Programme, Uganda*. http://www.wetlands.go.ug/downloads.htm. Accessed on 23 January 2009.

Odada, E.O., Olago, D.O., Kulindwa, K., Ntiba, M. and Wandiga, S. (2004). *Mitigation of environmental problems in Lake Victoria, East Africa: causal chains and policy options analyses*. Ambio, 33, 19-23.

Ogallo, L.J. (1988). *Relationships between seasonal rainfall in East Africa and the Southern Oscillation*. Journal of Climatology, 8, 31–43.

Ogallo, L.J. (1989). *The spatial and temporal patterns of the East African seasonal rainfall derived from principal component analysis*. Journal of Climatology, 9, 145-167.

Ojany, F.F. (1970). Drainage Evolution in Kenya. In: Ominde, S.H. (ed.). Studies in East African Geography and Development, Heinemann, London, 137-145.

Ojiambo, B.S., Lyons, W.B., Welch, K.A., Poreda, R.J. and Johannesson, K.H. (2003). *Strontium isotopes and rare earth elements as tracers of groundwater - lake water interactions, Lake Naivasha, Kenya*. Applied Geochemistry, 18, 1789-1805.

Ojiambo, B.S., Poreda, R.J. and Lyons, W.B. (2001). *Groundwater/Surface water interactions in Lake Naivasha Kenya using $\delta^{18}O$, δD, and $^{3}H/^{3}He$ Age-Dating*. Ground Water, 39(4), 526-533.

Okonga, J.R. (2000). *Hydrologic Budget and Decision Support System for Lake Kyoga*. Unpublished MSc Thesis, University of Dar es Salaam, Tanzania.

Olago, D., Opere, A. and Barongo, J. (2009). *Holocene palaeohydrology, groundwater and climate change in the lake basins of the Central Kenya Rift*. Hydrological Sciences Journal, 54(4), 765-780.

Ollier, C.D. and Galloway, R.W. (1990). *The laterite profile, ferricrete and unconformity*. Catena 17, 97-109.

Ouma, J.B. (1970). Evolution of Meander Traits in the Basin of Lake Victoria. In: Ominde, S.H. (ed.). Studies in East African Geography and Development. Heinemann, London, 137-145.

Owor, M., Hartwig, T, Muwanga, A., Zachmann, D. and Pohl, W. (2007). *Impact of tailings from the Kilembe copper mining district on Lake George, Uganda*. Journal of Environmental Geology, 51(6), 1065-1075.

Pall, P., Allen, M.R. and Stone, D.A. (2007). *Testing the Clausius-Clapeyron constraint on changes in extreme precipitation under CO2 warming*. Climate Dynamics, 28, 351-363.

Pallister, J.W. (1959) The *Geology of Southern Mengo: Explanation for of sheet North A-36/U and part of sheet North A-36/V*. Geological Survey of Uganda, report no. 1.

Parasnis, D.S. (1997). *Principles of Applied geophysics* (*5th edn.*). Chapman and Hall, London, 429p.

Phillips, J.G. and McIntyre, B. (2000). *ENSO and interannual rainfall variability in Uganda: Implications for agricultural management*. International Journal of Climatology, 20, 171-182.

Pickford, M. (1995). *Fossil land snails of East Africa and their palaeoecological significance*. Journal of African Earth Sciences, 20(3-4), 167-226.

Piper, B.S., Plinston, D.T. and Sutcliffe, J.V. (1986). *The water balance of Lake Victoria*. Hydrological Sciences Journal, 31(1,3), 25-37.

Rasmussen, T.C. and Crawford, L.A. (1997). *Identifying and removing barometric pressure effects in confined and unconfined aquifers*. Ground Water, 35 (3), 502-511.

Revil, A. and Leroy, P. (2001). *Hydroelectric coupling in a clayey material*. Geophysical Research Letters, 28, 1643-1646.

Rodell, M., Chen, J., Kato, H., Famiglietti, J.S., Nigro, J. and Wilson, C.R. (2006). *Estimating groundwater storage changes in the Mississippi River basin (USA) using GRACE*. Hydrogeology Journal, 15, 159-166.

Rodell, M., Houser, P. R., Jambor, U., Gottschalck, J., Mitchell, K., Meng, C.-J., Arsenault, K., Cosgrove, B., Radakovich, J., Bosilovich, M., Entin, J. K., Walker, J. P., Lohmann, D. and Toll, D. (2004). *The Global Land Data Assimilation System*. Bulletin of American Meteorological Society, 85(3), 381-394.

Rodell, M., Velicogna, I. and Famiglietti, J.S. (2009). *Satellite-based estimates of groundwater depletion in India*. Nature. doi: 10.1038.

Saji, N.H., Goswami, B.N., Vinayachandran, P.N. and Yamagata, T. (1999). *A dipole mode in the tropical Indian Ocean*. Nature, 401, 360-363.

Schlüter, T. (1997). *Geology of East Africa. With contributions by Craig Hampton*. Gebrueder Borntraeger, Berlin-Stuttgart, 484p.

Schlüter, T. (2006). *Geological atlas of Africa: with notes on stratigraphy, tectonics, economic geology, geohazards and geosites of each country*. Springer, Berlin. 272p.

Sene, K.J. (1998). *Effect of variations in net basin supply on lake levels and outflows*. Hydrological Processes, 12, 559-573.

Sene, K.J. (2000). *Theoretical estimates for the influence of Lake Victoria on flows in the upper White Nile*. Hydrological Sciences Journal, 45(1), 125-145.

Sene, K.J. and Plintson, D.T. (1994). *A review and update of the hydrology of Lake Victoria in East Africa*. Hydrological Sciences Journal, 50(1-2), 177-208.

Sene, K.J., Tate, E.L. and Farquharson, F.A.K. (2001). *Sensitivity studies of the impacts of climate change on White Nile flows*. Climatic Change, 50(1-2), 177-208.

Sepulchre, P., Ramstein, G., Fluteau, F., Schuster, M., Tiercelin, J.J. and Brunet, M. (2006). *Tectonic Uplift and Eastern Africa Aridification*. Science, 313, 1419-1423.

Shahin, M. (1985). *Hydrology of the Nile Basin*. Amsterdam, Elsevier, 575p.

Shaw, R.D. and Prepas, E.E., (1990). *Groundwater–lake interactions, II. Nearshore seepage patterns and the contribution of ground water to lakes in central Alberta*. Journal of Hydrology, 119, 121-136.

Sobieraj, J.J. Elsenbeer, H. and Vertessy, R.A. (2001). *Pedotransfer functions for estimating saturated hydraulic conductivity: implications for modeling storm flow generation*. Journal of Hydrology, 251, 202-220.

Sophocleous, M. (2002). *Interactions between groundwater and surface water: the state of the science*. Hydrogeology Journal, 10, 52-67.

Spane, F.A. (2002). *Considering barometric pressure in groundwater flow investigations*. Water Resources Research, 38(6), 1078.

Spane, F.A. and Wurstner, S.K. (1993). DERIV: *A computer Program for Calculating Pressure Derivatives for Use in Hydraulic Test Analysis*. Ground Water, 31(5), 814-822.

SRTM (2009). *Shuttle Radar Topography Mission, 90m Digital Elevation Data*. http://srtm.csi.cgiar.org/. Accessed on 01 April 2009.

Stager, J.C., Cumming, B. and Meeker, L. (1997). *A High-Resolution 11,400-Yr Diatom Record from Lake Victoria, East Africa*. Quaternary Research, 47, 81-89.

START (2006). *Assessing the impacts of climate change and variability on water resources in Uganda: developing an integrated approach at the sub-regional scale*. System for Analysis, Research and Training (START) final report, Project no: 202 457 5859.

Sutcliffe, J.V. and Parks, Y.P. (1999). *The Hydrology of the Nile*. International Association of Hydrological Sciences (IAHS) Publication, 5.

Sutcliffe, J.V. and Peterson, G. (2007). *Lake Victoria: derivation of a corrected natural water level series*. Hydrological Sciences Journal, 52(6), 1316-1321.

Swenson, S. and Wahr, J. (2009). *Monitoring the water balance of Lake Victoria, East Africa, from space*. Journal of Hydrology, 370, 163–176.

Talbot, M.R., Williams, M.A.J. and Adamson, D.A. (2000). *Strontium isotope evidence for late Pleistocene reestablishment of an integrated Nile drainage network*. Geology, 28(4), 343–346.

Tapley, B.D., Bettadpur, S., Ries, J.C., Thompson, P.F. and Watkins, M.M. (2004). *GRACE Measurements of Mass Variability in the Earth System*. Science, 305, 503-505.

Tate, E., Sutcliffe, J., Conway, D. and Farquharson, F. (2004). *Water balance of Lake Victoria: Update to 2000 and climatic change modelling to 2100*. Hydrological Sciences Journal, 49(4), 563-574.

Taylor, D.M. (1990). *Late Quaternary pollen records from two Ugandan mires: evidence for environmental change in the Rukiga Highlands of southwest Uganda*. Palaeogeography, Palaeoclimatology, Palaeoecology, 80, 283-300.

Taylor, R.G. Source of Figure 4.7. Water level variations of Lakes Naivasha, Turkana, Tanganyika, Albert, Victoria and Kyoga since 1800.

Taylor, R.G., Barrett, M.H. and Tindimugaya, C. (2004). Urban areas of sub-Saharan Africa: weathered crystalline aquifer systems. In: Lerner, D.N. (ed.), Urban Groundwater Pollution. International Association of Hydrogeologists contribution to the 5th phase of the UNESCO International Hydrological Programme Project 3.4 "Groundwater contamination due to urban development", 155-179.

Taylor, R.G. and Howard, K.W.F. (1996). *Groundwater recharge in the Victoria Nile basin of East Africa: support for the moisture balance approach using stable isotope tracers and flow modelling*. Journal of Hydrology, 180, 31-53.

Taylor, R.G. and Howard, K.W.F. (1998). *Post-Palaeozoic evolution of weathered landsurfaces in Uganda by tectonically controlled deep weathering and stripping*. Geomorphology, 25, 173-192.

Taylor, R.G. and Howard, K.W.F. (1999a). *Lithological evidence for the evolution of weathered mantles in Uganda by tectonically controlled cycles of deep weathering and stripping*. Catena, 35, 65-94.

Taylor, R.G. and Howard, K.W.F. (1999b). *The influence of tectonic setting on the hydrological characteristics of deeply weathered terrains: evidence from Uganda*. Journal of Hydrology, 218, 44-71.

Taylor, R.G. and Howard, K.W.F. (2000). *A tectono-geomorphic model of the hydrogeology of deeply weathered crystalline rock: evidence from Uganda*. Hydrogeology Journal, 8, 279-294.

Taylor, R.G., Miret-Gaspa, M., Tumwine, J., Mileham, L., Flynn, R., Howard, G. and Kulabako, R. (2009a). Increased risk of diarrhoeal diseases from climate change: evidence from communities supplied by groundwater in Uganda. In: Taylor, R., Tindimugaya, C., Owor M. and Shamsudduha, M. (eds.), Groundwater and Climate in Africa, Proceedings of the Kampala Conference, June 2008, International Association of Hydrological Sciences (IAHS) Publication, 334, 15-19.

Taylor, R.G. and Tindimugaya, C. (1996). The role of groundwater in the Victoria Nile Basin of Uganda: implications of a catchment water balance. In: Comprehensive Water Resources Development of the Nile Basin: Action Plan, Proceedings of the IVth Nile 2002 Conference, Kampala (Uganda), A-87 - A-94.

Taylor, R.G., Tindimugaya, C., Barker, J.A., Barrett, M.H., Macdonald, D., Kulabako, R., Nalubega, M. and Rwarinda, E. (2009b). *Convergent radial tracing of ground water flow and storage in gneiss saprolite of Uganda*. Ground Water (Africa special issue), doi:10.1111/j.1745-6584.2008.00547.x.

Telford, W.M., Geldart, L.P. and Sheriff, R.E. (1990). *Applied Geophysics* (*2nd edn*). Cambridge University Press, Cambridge, 770p.

Temple, P.H. (1966). *Evidence of changes in the level of Lake Victoria and their significance*. Unpublished PhD thesis, University of London, U.K.

Temple, P.H. (1970). The lakes of Uganda. In: Ominde, S.H. (ed.). Studies in East African Geography and Development. Heinemann, London, 86-98.

Theis, C.V. (1935). *The relation between the lowering of the piezometric surface and the rate and duration of discharge of a well using groundwater storage*. Transactions of American Geophysical Union, 16, 519-524.

Tindimugaya, C. (2000). *Assessment of groundwater development potential for Wobulenzi town, Uganda*. Unpublished MSc. dissertation, International Institute for Infrastructural, Hydraulic and Environmental Engineering, (IHE), Delft, The Netherlands.

Todd, D.K. and Mays, L.W. (2005). *Groundwater hydrology* (*3rd edn*). John Wiley and Sons, Inc., Hoboken, NJ, 636p.

Tóth, J. (1963). *A theoretical analysis of groundwater flow in small drainage basins*. Journal of Geophysical Research, 68, 4795-4812.

Trauth, M.H., Maslin, M.A., Deino, A.L. and Strecker, M.R. (2005). *Late Cenozoic Moisture History of East Africa*. Science, 309, 2051-2053.

Trauth, M.H., Maslin, M.A., Deino, A.L., Strecker, M.R., Bergner, A.G.N. and Dühnforth, M. (2007). *High- and low-latitude forcing of Plio-Pleistocene East African climate and human evolution*. Journal of Human Evolution, 53, 475-486.

Trenberth, K.E., Dai, A., Rasmussen, R.M. and Parsons, D.B. (2003). *The changing character of precipitation*. Bulletin of American Meteorological Society, 84, 1205-1217.

Trendall, A.F. (1965). *Explanation of the geology of sheet 44 (Lake Magoro)*. Geological Survey of Uganda report no. 11.

Uganda Government (1967). *Uganda Soils* map, 1:1 500 000.

UGS (1921). Uganda Geological Survey (UGS) annual report 1919-20. Uganda Government.

Uluocha, N.O. and Okeke, I.C. (2004). *Implications of wetlands degradation for water resources management: Lessons from Nigeria*. GeoJournal, 61(2), 151-154.

Verschuren, D., Laird, K.R. and Cumming, B.F. (2000). *Rainfall and drought in equatorial east Africa during the past 1,100 years*. Nature, 403, 410-414.

Vogel, J.C. and Van Urk, H. (1975). *Isotopic composition of groundwater in semi-arid regions of southern Africa*. Journal of Hydrology, 25, 23-26.
von der Heyden, C.J. (2004). *The hydrology and hydrogeology of dambos: a review*. Progress in Physical Geography, 28(4), 544-564.
von der Heyden, C.J. and New, M.G. (2003). *The role of a dambo in the hydrology of a catchment and the river network downstream*. Hydrology and Earth System Sciences, 7(3), 339-357.
Wahr, J., Molenaar, M. and Bryan, F. (1998). *Time-variability of the Earth's gravity field: Hydrological and oceanic effects and their possible detection using GRACE*. Journal of Geophysical Resources, 103, 32205-30229.
Wahr, J., Swenson, S., Zlotnicki, V. and Velicogna, I. (2004). *Time-variable gravity from GRACE: First results*. Geophysical Research Letters, 31, L11501-L11505.
Way, H.J.R. (1939). *Some petrographic notes on the Jinja area*. Bulletin of the Geological Survey of Uganda, 140-144.
Wayland, E.J. (1929). *Rift valleys and Lake Victoria*. Compte Rendu, XVth Session of the International Geological Congress, Pretoria, II, Section IV, 323-353.
Wayland, E.J. (1934). Peneplains and some other erosional platforms. In: Annual Report, Geology Survey of Uganda, 1933, 77-78.
Wentworth, C.K. (1922). *A scale of grade and class terms for clastic sediments*. Journal of Geology, 30, 377-392.
Whitehouse, R.N. and Hunter, C.S. (1955). *Victoria Nyanza (Northern Portion) and Victoria Nyanza (Southern Portion)* maps. 1:294 000 at lat. 1 degree 15 minutes south. Admiralty, London.
Whitlow, J.R. (1985). *Dambos in Zimbabwe: a review*. Zeitschrift für Geomorphologie Supplementbande, 52, 115-46.
Winsemius, H.C., Savenije, H.H.G., van de Giesen, N.C., van den Hurk, B.J.J.M., Zapreeva, E.A. and Klees, R. (2006). *Assessment of Gravity Recovery and Climate Experiment (GRACE) temporal signature over the upper Zambezi*. Water Resources Research, 42, W12201-W12209.
Winter, T.C. (1983). *The Interaction of Lakes With Variably Saturated Porous Media*. Water Resources Research, 19(5), 1203-1218.
Winter, T.C. (1999). *Relation of streams, lakes, and wetlands to groundwater flow systems*. Hydrogeology Journal, 7, 28-45.
Winter, T.C., Harvey, J.W., Franke, O.L. and Alley, W.M. (1998). *Ground Water and Surface Water A Single Resource*. U.S. Geological Survey Circular, 1139, 79p.
Woessner, W.W. (2000). *Stream and fluvial plain ground-water interactions: re-scaling hydrogeologic thought*. Ground Water, 38(3), 423-429.
Woessner, W.W. and Sullivan, K.E. (1984). *Results of Seepage Meter and Mini-Piezometer Study, Lake Mead, Nevada*. Ground Water, 22(5), 561-568.
Wolski, P. and Savenije, H.H.G. (2006). *Dynamics of floodplain-island groundwater flow in the Okavango Delta, Botswana*. Journal of Hydrology, 320, 283-301.
Yates, D.N. (1998). *Modelling the Nile Basin under climatic change*. Journal of Hydrologic Engineering, 3(2), 98-108.
Yeh, P.J.-F., Swenson, S.C., Famiglietti, J.S., and Rodell, M. (2006). *Remote sensing of groundwater storage changes in Illinois using the Gravity Recovery and Climate Experiment (GRACE)*. Water Resources Research, 42, W12203.
Yin, X. and Nicholson, S.E. (1998). *The water balance of Lake Victoria*. Hydrological Sciences Journal, 43(5), 789-812.
Yong, L. and Chao Wang, C. (2007). *Theoretical estimation of groundwater discharge and associated nutrient loading to a lake with gentle slope bottom*. Journal of Hydrodynamics, 19(1), 30-35.
Zekster, I.S. (1996). Groundwater *discharge into lakes: a review of recent studies with*

particular regard to large saline lakes in central Asia. International Journal of Salt Lake Research, 4, 233-249.

Appendices

Appendix 1 Well construction parameters

parameters	BP01	BP02	BP04	JP01	JP02	JP03	BP03
Site	Bugondo	Bugondo	Bugondo	Jinja	Jinja	Jinja	Bugondo
UTM Coordinates X	530949	530968	530888	522979	522954	523066	
UTM Coordinates Y	179534	179465	179397	246172	246211	246430	
casing radius (m)	0.0508	0.0508	0.0508	0.0508	0.0508	0.0508	
well depth (m)	13.6	17	13.2	12	21	24	
depth to well bottom (m)	13.1	16.5	12.7	11.5	20.5	23.5	
screen radius (m)	0.0508	0.0508	0.0508	0.0508	0.0508	0.0508	
screen length (m)	5.68	8.52	8.52	5.68	8.52	8.52	
borehole radius (m)	0.1016	0.1016	0.1016	0.1016	0.1016	0.1016	
depth to top of screen (m)	7.92	8.48	4.68	6.32	12.48	15.48	
depth to water level (m)	0	2.1	1.67	0	0	11.9	
saturated thickness (m)	13.1	14.4	11.03	11.5	20.5	11.6	
saturated depth to screen top (m)	7.42	5.88	2.51	5.82	11.98	3.08	
Well altitude (masl)	1033.9	1035.9	1035.9	1136.0	1136.6	1149.3	1079*
Airlift discharge ($m3 \cdot h^{-1}$)	2.4	2.2	2.0	0.7	0.8	1.7	
height of casing (m)	0.7	0.4	0.6	0.5	0.52	0.5	
SWL(masl) at construction	1033.20	1033.42	1033.60	1135.46	1136.03	1136.90	
drilling depth (m)	15	19.5	15	12	21	24	9
ground altitude (masl)	1033.204	1035.5	1035.3	1135.5	1136.0	1148.8	
lake altitude (masl)	1033.172	1033.172	1033.172	1134.072	1134.072	1134.072	
date	25.11.07	25.11.07	25.11.07	14.11.07	14.11.07	14.11.07	
distance from lake (m)	10	60	80	10	50	260	

*Handheld GPS reading

Appendix 2 Geodetic station surveys

All stations were surveyed using a Kern dumpy level theodolite and a measuring staff. Altitudes of the zero gauges at the Bugondo, Entebbe and Jinja lake level gauging stations.

Station	Altitude (masl)
Bugondo (Lake Kyoga)	1021.479
Entebbe (Lake Victoria)	1123.437
Jinja (Lake Victoria)	1122.892

i) Entebbe

Survey of difference in elevation between Lake Victoria and groundwater level on 5 July 2007.

BS (m)	HI (m)	IS(m)	FS(m)	RL(m)	Remarks
0.599	100.599			100	BM – assumed
0.187	98.02		2.766	97.833	
0.714	95.993		2.741	95.279	
0.597	95.668		0.922	95.071	top well (depth WL) = 4.87
				90.201	Water Level in well
0.597	95.668			95.071	top well (depth WL) = 4.87
0.077	93.501		2.244	93.424	
0.675	92.05		2.126	91.375	
0.191	90.169		2.072	89.978	
			2.105	88.064	Water Level in lake
				2.137	Difference in Level

NB: Groundwater level is higher than lake level as of 5/07/07.

ii) Jinja

Survey of difference in elevation between Lake Victoria and groundwater level on 13 December 2007.

BS (m)	IS (m)	FS (m)	HI (m)	RL Local Datum (m)	RL MSL (m)	Remarks
0.1			13.76	13.66	1136.552	Well 2-Top
	0.69		13.76	13.07	1135.962	Well 1-Top
1.71		0.94	13.76	12.82	1135.712	Shade floor
2.28		2.53	14.28	12	1134.892	Top Gauge 12
0.43		0.1	14.61	14.18	1137.072	Change point
1.45		1.91	14.15	12.7	1135.592	Corner House
3.555		0.06	17.645	14.09	1136.982	
3.03		0.035	20.64	17.61	1140.502	
2.3		0.115	22.825	20.525	1143.417	
3.895		1.05	25.67	21.775	1144.667	
2.53		0.545	27.655	25.125	1148.017	
		1.248		26.407	1149.299	Well 3 -Top

iii) Bugondo

Survey of difference in elevation between Lake Victoria and groundwater level on 12 December 2007.

BS (m)	IS (m)	FS (m)	HI (m)	RL Local Datum (m)	RL MSL (m)	Remarks
0.8			15.195	14.395	1035.874	Well 3 -Top
	0.75		15.195	14.445	1035.924	Well 2 -Top
2.415		2.77	15.195	12.425	1033.904	Well 1-Top
0.665		1.065	14.84	13.775	1035.254	
		2.44		12	1033.479	Top Gauge 12

Appendix 3 Well log lithological texture

Laboratory weight (g) wet sieving for grain size analyses of the well lithological samples using nylon sieves at UCL.

Well	Munsell colour codes	Depth (m)	<63µm	<125µm	<250µm	<500µm	>500µm
BP01	10YR 7/1 Light gray	0-1.5	20.25	18.03	10.51	50.01	63.4
BP01	2.5Y 7/2 Light gray	1.5-3	18.79	9.33	7.51	47.39	119.3
BP01	7.5YR 6/3 Light brown	3-4.5	10.88	9.08	12.55	54.71	39.36
BP01	7.5YR 6/4 Light brown	4.5-6	12.94	7.39	10.39	66.72	56.5
BP01	10YR 6/4 Light yellowish brown	6-7.5	25.09	12.34	16.31	71.28	22.11
BP01	10YR 6/4 Light yellowish brown	7.5-9	30.03	14.74	19.61	45.55	57.32
BP01	10YR 7/4 Very pale brown	9-10.5	19.01	5.42	11.67	19.8	60.47
BP01	10YR 7/4 Very pale brown	10.5-12	26.13	8.38	15.4	23.74	75.26
BP01	10YR 7/4 Very pale brown	12-13.5	22.65	6.85	12.36	15.44	106.21
BP01	10YR 7/4 Very pale brown	13.5-15	21.1	4.57	8.55	16.41	119.95
BP02	10YR 6/2 Light brownish gray	0-1.5	10.36	5.94	8.8	87.34	39.98
BP02	10YR 7/2 Light gray	1.5-3	9.83	6.77	9.57	90.37	36.26
BP02	10YR 7/1 Light gray	3-4.5	5.73	7.22	8.64	75.06	33.57
BP02	10YR 7/4 Very pale brown	4.5-6	7.89	7.35	11.76	71.78	26.41
BP02	7.5YR 6/3 Light brown	6-7.5	8.3	9.3	27.06	96.87	0.99
BP02	10YR 6/4 Light yellowish brown	7.5-9	16.41	15.65	58.51	62.47	0.96
BP02	10YR 6/4 Light yellowish brown	9-10.5	13.39	11.54	70.95	17.56	0.15
BP02	10YR 6/4 Light yellowish brown	10.5-12	15.09	6.93	17.46	108.07	0.21
BP02	10YR 6/4 Light yellowish brown	12-13.5	12.9	4.43	7.03	88.56	0.25
BP02	10YR 7/4 Very pale brown	13.5-15	14.11	2.69	2.11	2.11	73.94
BP02	10YR 7/4 Very pale brown	15-16.5	31.79	6.94	7.01	13.3	108.37
BP02	10YR 7/4 Very pale brown	16.5-18	30.1	7.57	19.75	26.6	92.76
BP02	10YR 7/4 Very pale brown	18-19.5	22.04	6.88	16.23	21.46	68.16

Well	Munsell colour codes	Depth (m)	<63µm	<125µm	<250µm	<500µm	>500µm
BP03	10YR 7/4 Very pale brown	0-1.5	40.99	13.39	21.74	77.09	49.36
BP03	10YR 7/4 Very pale brown	1.5-3	35.33	9.12	13.25	69.35	32.82
BP03	10YR 7/4 Very pale brown	3-4.5	47.77	12.69	19.49	74.87	12.68
BP03	10YR 6/6 Brownish yellow	4.5-6	38.21	18.12	25.22	45.33	1.92
BP03	7.5YR 6/4 Light brown	6-7.5	44.97	19.63	18.77	23.38	56.89
BP03	7.5YR 5/4 Brown	7.5-9	52.75	14.37	10.26	20	73.53
BP04	10YR 7/1 Light gray	0-1.5	29.08	16.25	20.38	86.92	25.41
BP04	10YR 7/1 Light gray	1.5-3	18.98	6.68	12.27	95.52	36.23
BP04	2.5Y 7/2 Light gray	3-4.5	25.62	12.21	16.15	78.38	23.4
BP04	2.5Y 6/3 Light yellowish brown	4.5-6	32.42	14.21	19.39	42.26	24.04
BP04	10YR 7/4 Very pale brown	6-7.5	23.31	10.73	32.84	84.63	26.08
BP04	10YR 6/4 Light yellowish brown	7.5-9	15.62	8.75	21.03	88.57	13.95
BP04	10YR 6/4 Light yellowish brown	9-10.5	12.87	11.49	22.77	52	1.22
BP04	10YR 6/4 Light yellowish brown	10.5-12	15.61	5.56	6.2	43.44	68.55
BP04	10YR 7/3 Very pale brown	12-13.5	19.37	14.6	14.15	19.25	92.96
BP04	10YR 7/4 Very pale brown	13.5-15	29.89	11.28	14.78	39.22	71.89
JP01	7.5YR 4/6 Strong brown	0-1.5	109	8.62	12.98	17.44	36.92
JP01	10YR 4/4 dark yellowish brown	1.5-3	64.81	9.18	13.96	18.55	33.93
JP01	2.5Y 5/4 Light olive brown	3-4.5	38.02	10.37	16.29	48.87	22.1
JP01	2.5Y 5/4 Light olive brown	4.5-6	38.67	15.79	32.86	36.41	31.75
JP01	2.5Y 6/4 Light yellowish brown	6-7.5	23.36	9.98	11.87	59.08	46.99
JP01	2.5Y 6/4 Light yellowish brown	7.5-9	23.62	10.83	18.23	37.39	85.3
JP01	2.5Y 6/4 Light yellowish brown	9-10.5	20.21	8.84	16.44	30.45	69.31
JP01	5Y 5/3 Olive	10.5-12	26.14	13.99	26.64	28.95	55.22

Well	Munsell colour codes	Depth (m)	<63µm	<125µm	<250µm	<500µm	>500µm
JP02	7.5Y 4/4 Brown-dark brown	0-1.5	81.48	4.99	8.27	9.23	15.45
JP02	2.5Y 5/3 Light olive brown	1.5-3	55.32	5.88	8.38	6.73	24.43
JP02	5Y 6/2 Light olive gray	3-4.5	28.88	3.26	14.19	35.63	28.44
JP02	5Y 6/3 Pale olive	4.5-6	30.41	8.95	21.25	30.76	34.79
JP02	5Y 6/3 Pale olive	6-7.5	18.77	8.34	25.34	51.8	39.3
JP02	5Y 6/3 Pale olive	7.5-9	14.65	11.76	17.24	30	33.64
JP02	5Y 6/3 Pale olive	9-10.5	13.33	6.09	9.6	11.39	41.4
JP02	5Y 6/3 Pale olive	10.5-12	24.15	10.89	13.63	30.03	81.43
JP02	5Y 6/3 Pale olive	12-13.5	21.19	9.1	12.86	29.46	72.79
JP02	5Y 6/3 Pale olive	13.5-15	16.7	7.81	11.66	19.39	94.54
JP02	5Y 6/3 Pale olive	15-16.5	16.5	7.22	12.58	29.26	71.56
JP02	5Y 6/3 Pale olive	16.5-18	16.56	5.44	9.02	21.17	94.18
JP02	5Y 6/3 Pale olive	18.19.5	20.38	6.49	11.88	24.97	113.8
JP02	5Y 6/3 Pale olive	19.5-21	15.55	4.89	8.97	21.77	92.33
JP03	2.5YR 3/6 Dark red	0-1.5	93.08	4.24	10.76	8.75	1.47
JP03	2.5YR 4/6 Red	1.5-3	86.26	4.39	9.7	23.1	2.35
JP03	2.5YR 4/6 Red	3-4.5	82.39	7.97	16.6	26.13	4.5
JP03	2.5YR 4/4 Reddish brown	4.5-6	85.06	11.35	18.42	24.95	3.91
JP03	2.5YR 4/6 Red	6-7.5	85.98	8.8	15.42	24.63	9.01
JP03	2.5YR 4/6 Red	7.5-9	62.26	12.34	17.12	37	8.42
JP03	7.5YR 5/6 Strong brown	9-10.5	37.7	8.55	15.81	28.25	24.61
JP03	7.5YR 5/6 Strong brown	10.5-12	35.35	4.79	15.47	29.41	39.16
JP03	7.5YR 5/6 Strong brown	12-13.5	39.98	6.49	13.35	24.25	47.28
JP03	7.5YR 5/6 Strong brown	13.5-15	38.36	5.44	9.12	16.32	46.29
JP03	7.5YR 5/6 Strong brown	15-16.5	37.98	4.16	8.22	15.37	67.69
JP03	10YR 6/4 Light yellowish brown	16.5-18	26.06	6.23	9.43	14.78	71.48
JP03	10YR 6/4 Light yellowish brown	18.19.5	60.38	6.28	8.34	12.99	87.98
JP03	10YR 6/4 Light yellowish brown	19.5-21	47.71	4.54	5.51	8.91	38.21
JP03	10YR 6/4 Light yellowish brown	21-22.5	68.39	6.74	6.16	7.63	29.08
JP03	10YR 6/4 Light yellowish brown	22.5-24	56.87	5.95	5.32	6.57	40.56

Appendix 4 Geophysical resistivity surveys

Geophysical resistivity surveys at Jinja and Bugondo using an Abem terrameter SAS 300C.

i) Geophysical apparent resistivity (ohm·m) surveys carried out in August 2007.

L/2 (m)	a/2 (m)	Bugondo VES1 (ohm·m)	Bugondo VES2 (ohm·m)	Jinja VES1 (ohm·m)	Jinja VES2 (ohm·m)
1.5	0.5	1.34	3.64	1.66	1.74
2.1	0.5	0.64	0.991	0.824	0.872
3	0.5	0.3	0.473	0.467	0.671
4.4	0.5	0.17	0.231	0.191	0.197
6.3	0.5	0.11	0.124	0.089	0.091
9.1	0.5	0.06	0.073	0.055	0.034
13.2	0.5	0.041	0.042	0.039	0.044
13.2	5	0.423	0.38		
19	0.5	0.024	0.021	0.024	0.014
19	5	0.201	0.178		
27.5	0.5	0.009	0.021		0.004
27.5	5		0.054		

ii) Bugondo geophysical resistivity surveys on 17 July 2008.

VES 1 Site close to BP02 (530972/179460)				VES 2 station (531570/ 178027)			
	L/2 (m)	a/2 (m)	R(ohm·m)		L/2 (m)	a/2 (m)	R(ohm·m)
1	1.5	0.5	3.25	1	1.5	0.5	29.5
2	2.1	0.5	0.691	2	2.1	0.5	10.66
3	3	0.5	0.275	3	3	0.5	4.37
4	4.4	0.5	0.1561	4	4.4	0.5	1.801
5	6.3	0.5	0.0858	5	6.3	0.5	0.729
6	9.1	0.5	0.0525	6	9.1	0.5	0.293
7	13.2	0.5	0.0294	7	13.2	0.5	0.137
	13.2	5	0.358		13.2	5	1.781
8	19	0.5	0.0142	8	19	0.5	0.082
	19	5	0.176		19	5	0.929
9	27.5	0.5	0.0064	9	27.5	0.5	0.047
	27.5	5	0.0689		27.5	5	0.519
10	40	5	0.034	10	40	5	0.253
11	50	5	0.014				

VES 3 station (9531650/178134)

	L/2 (m)	a/2 (m)	R(ohm·m)
1	1.5	0.5	44.4
2	2.1	0.5	22.4
3	3	0.5	12.22
4	4.4	0.5	6.69
5	6.3	0.5	3.65
6	9.1	0.5	2.17
7	13.2	0.5	1.22
	13.2	5	
8	19	0.5	0.59
	19	5	
9	27.5	0.5	0.28
	27.5	5	2.73
10	40	5	1.557

Profiling between BP02 and BP04, trending 50-230 degrees.

	stage 4 (L/2=4.4 m, a/2=0.5 m) R (ohm·m)	stage 9 (L/2=27.5 m, a/2=0.5 m) R (ohm·m)	X	Y	Remark
1	1.331	0.111	530878	179379	
2	0.0997	0.127	530884	179386	
3	0.168	0.113	530891	179393	
4	0.137	0.112	530898	179401	
5	0.081	0.097	530905	179408	
6	0.185	0.092	530912	179415	
7	0.222	0.103	530919	179422	
8	0.085	0.065	530926	179430	
9	0.194	0.1	530932	179437	
10	0.141	0.072	530939	179444	
11	0.171	0.83	530945	179449	
12	0.209	0.092	530951	179458	
13	0.183	0.071	530959	179465	
14	0.128	0.059	530966	179472	
15	0.302	0.118	530972	179481	murram road
16	0.257	0.091	530979	179488	

iii) Jinja geophysical resistivity surveys on 23 July 2008.

VES Site 1 in pier between JP01 and JP02 (522970/ 46180) trending 60-240 degrees (E-W).

	L/2 (m)	a/2 (m)	R(ohm·m)	Remark
1	1.5	0.5	1.685	
2	2.1	0.5	0.824	
3	3	0.5	0.39	
4	4.4	0.5	0.18	
5	6.3	0.5	0.081	
6	9.1	0.5	0.04	
7	13.2	0.5	0.021	
	13.2	5	0.223	next to stream
8	19	0.5	0.012	
	19	5	0.115	
9	27.5	0.5	0.008	
	27.5	5		external influence; no result
10	40	5		external influence; no result
11	50	5		external influence; no result

VES Site 2 close to tarmac (along roadside - about 3 m away) (522930/ 46315) trending 60-240 degrees (NE-SW).

	L/2 (m)	a/2 (m)	R (ohm·m)
1	1.5	0.5	3.34
2	2.1	0.5	1.387
3	3	0.5	0.581
4	4.4	0.5	0.234
5	6.3	0.5	0.094
6	9.1	0.5	0.039
7	13.2	0.5	0.017
	13.2	5	0.184
8	19	0.5	0.008
	19	5	0.073
9	27.5	0.5	0.004
	27.5	5	0.037
10	40	5	0.02
11	50	5	0.014

Profiling between BP02 and BP04 trending 30-210 degrees along road side (murram).

		stage 4 (L/2=4.4 m, a/2=0.5 m)	stage 8 (L/2=19 m, a/2=5 m)
X	Y	R (ohm·m)	R (ohm·m)
522930	46192	0.132	0.079
522932	46204	0.094	0.079
522939	46210	0.115	0.073
522943	46215	0.117	0.076
522953	46220	0.115	0.076
522963	46229	0.122	0.064
522973	46237	0.136	0.076
522981	46242	0.139	0.072
522992	46248	0.152	0.076
523000	46255	0.153	0.084

Profiling along tarmac road about 3 m from road; altitude estimated at 1148 m.

X	Y	stage 4 (L/2=4.4 m, a/2=0.5 m)	stage 8 (L/2=19 m, a/2=5 m)
522906	46305	0.257	0.071
522914	46304	0.224	0.073
522923	46309	0.214	0.065
522927	46313	0.238	0.071
522946	46320	0.226	0.075
522962	46320	0.265	0.063
522963	46320	0.284	0.078
522973	46324	0.221	0.07
522975	46331	0.23	0.073
522994	46329	0.246	0.079
523001	46332	0.09	0.083

Appendix 5 Hydraulic test data

Pumping tests parameters in piezometers at Bugondo and Jinja.

parameters	BP01	BP02	BP04	JP01	JP02	JP03
Date	19.07.08	17.07.08	19.07.08	07.07.08	05.07.08	07.07.08
Coordinates X	530949	530968	530888	522979	522954	523066
Coordinates Y	179534	179465	179397	246172	246211	246430
Casing radius (m)	0.0508	0.0508	0.0508	0.0508	0.0508	0.0508
Well depth (m)	13.6	17	13.2	12	21	24
Depth to well bottom (m)	13.1	16.5	12.7	11.5	20.5	23.5
Screen radius (m)	0.0508	0.0508	0.0508	0.0508	0.0508	0.0508
Screen length (m)	5.68	8.52	8.52	5.68	8.52	8.52
Borehole radius (m)	0.1016	0.1016	0.1016	0.1016	0.1016	0.1016
Pumping rate ($m^3 \cdot min^{-1}$)	0.0223	0.0216	0.0154	0.0065 0.0130	0.0155	0.0156
Pumping duration (min)	29.82	603.73	191	204.97	900.43	78.95
Recovery duration (min)	190.73	484	1009.85	54	463	997.22
Monitoring duration (min)	220.55	1087.73	2041.1	258.97	1363.43	1076.17
Distance of well from lake (m)	20	90	130	40	70	220
Depth to top of screen (m)	7.92	8.48	4.68	6.32	12.48	15.48
Depth to water level (m)	0	2.1	1.67	0	0	11.9
Saturated thickness (m)	13.1	14.4	11.03	11.5	20.5	11.6
Saturated depth to screen top (m)	7.42	5.88	2.51	5.82	11.98	3.08

Appendix 6 Hydraulic tests at the Jinja station on the shores of Lake Victoria